ORNL-1649
Progress

AIRCRAFT NUCLEAR PROPULSION PROJECT

QUARTERLY PROGRESS REPORT

FOR PERIOD ENDING DECEMBER 10, 1953

OAK RIDGE NATIONAL LABORATORY
OPERATED BY
CARBIDE AND CARBON CHEMICALS COMPANY
A DIVISION OF UNION CARBIDE AND CARBON CORPORATION
UCC
POST OFFICE BOX P
OAK RIDGE, TENNESSEE

ORNL-1649

This document consists of 152 pages.
Copy 91 of 266 copies. Series A.

Contract No. W-7405-eng-26

AIRCRAFT NUCLEAR PROPULSION PROJECT
QUARTERLY PROGRESS REPORT
For Period Ending December 10, 1953

R. C. Briant, Director
A. J. Miller, Assistant Director
W. B. Cottrell, Editor

DATE ISSUED

JAN 18 1954

OAK RIDGE NATIONAL LABORATORY
Operated by
CARBIDE AND CARBON CHEMICALS COMPANY
A Division of Union Carbide and Carbon Corporation
Post Office Box P
Oak Ridge, Tennessee

INTERNAL DISTRIBUTION

1. G. M. Adamson
2. R. G. Affel
3. C. R. Baldock
4. C. J. Barton
5. E. S. Bettis
6. D. S. Billington
7. F. F. Blankenship
8. E. P. Blizard
9. M. A. Bredig
10. R. C. Briant
11. F. R. Bruce
12. A. D. Callihan
13. D. W. Cardwell
14. J. V. Cathcart
15. C. E. Center
16. R. A. Charpie
17. J. M. Cisar
18. G. H. Clewett
19. C. E. Clifford
20. W. B. Cottrell
21. R. G. Cochran
22. D. D. Cowen
23. F. L. Culler
24. W. K. Eister
25. L. B. Emlet (Y-12)
26. W. K. Ergen
27. A. P. Fraas
28. W. W. Grigorieff (consultant)
29. W. R. Grimes
30. A. Hollaender
31. A. S. Householder
32. J. T. Howe
33. W. B. Humes (K-25)
34. R. W. Johnson
35. G. W. Keilholtz
36. C. P. Keim
37. M. T. Kelley
38. F. Kertesz
39. E. M. King
40. J. A. Lane
41. C. E. Larson
42. R. S. Livingston
43. R. N. Lyon
44. W. D. Manly
45. L. A. Mann
46. W. B. McDonald
47. J. L. Meem
48. A. J. Miller
49. K. Z. Morgan
50. E. J. Murphy
51. G. J. Nessle
52. H. F. Poppendiek
53. P. M. Reyling
54. H. W. Savage
55. A. W. Savolainen
56. E. D. Shipley
57. O. Sisman
58. L. P. Smith (consultant)
59. A. H. Snell
60. C. L. Storrs
61. C. D. Susano
62. J. A. Swartout
63. E. H. Taylor
64. J. B. Trice
65. E. R. Van Artsdalen
66. F. C. VonderLage
67. J. M. Warde
68. A. M. Weinberg
69. J. C. White
70. G. D. Whitman
71. E. P. Wigner (consultant)
72. G. C. Williams
73. J. C. Wilson
74. C. E. Winters
75-84. ANP Library
85. Biology Library

86-90. Laboratory Records Department
91. Laboratory Records, ORNL R.C.
92. Health Physics Library
93. Metallurgy Library
94. Reactor Experimental Engineering Library
95-97. Central Research Library

EXTERNAL DISTRIBUTION

98-100. Air Force Engineering Office, Oak Ridge
101. Air Force Plant Representative, Burbank
102. Air Force Plant Representative, Seattle
103. Air Force Plant Representative, Wood-Ridge
104. ANP Project Office, Fort Worth
105-116. Argonne National Laboratory (1 copy to Kermit Anderson)
117. Armed Forces Special Weapons Project (Sandia)
118-126. Atomic Energy Commission, Washington (Lt. Col. M. J. Nielsen)
127. Battelle Memorial Institute
128-133. Brookhaven National Laboratory
134. Bureau of Aeronautics (Grant)
135. Bureau of Ships
136-137. California Research and Development Company
138-145. Carbide and Carbon Chemicals Company (Y-12 Plant)
146. Chicago Patent Group
147. Chief of Naval Research
148. Commonwealth Edison Company
149. Convair, San Diego (C. H. Helms)
150. Department of the Navy – Op-362
151. Detroit Edison Company
152-155. duPont Company, Augusta
156. duPont Company, Wilmington
157. Foster Wheeler Corporation
158-160. General Electric Company, ANPP
161-164. General Electric Company, Richland
165. Glen L. Martin Co. (T. F. Nagey)
166. Hanford Operations Office
167. Iowa State College
168-175. Knolls Atomic Power Laboratory
176-177. Lockland Area Office
178-179. Los Alamos Scientific Laboratory
180. Massachusetts Institute of Technology (Kaufmann)
181. Materials Laboratory (WADC) (Col. P. L. Hill)
182. Monsanto Chemical Company
183-185. Mound Laboratory

186-189. National Advisory Committee for Aeronautics, Cleveland (3 copies to A. Silverstein)
190. National Advisory Committee for Aeronautics, Washington
191. Naval Research Laboratory
192-193. New York Operations Office
194-195. North American Aviation, Inc.
196-201. Nuclear Development Associates, Inc.
202. Patent Branch, Washington
203-210. Phillips Petroleum Company
211-220. Pratt and Whitney Aircraft Division (Fox Project)
221-232. Powerplant Laboratory (WADC) (2copies to B. Beaman)
233-234. Rand Corporation (1 copy to V. G. Henning)
235. San Francisco Operations Office
236. Sylvania Electric Products, Inc.
237. U. S. Naval Radiological Defense Laboratory
238. USAF Headquarters
239-240. University of California Radiation Laboratory, Berkeley
241-242. University of California Radiation Laboratory, Livermore
243. Walter Kidde Nuclear Laboratories, Inc.
244-249. Westinghouse Electric Corporation
250-264. Technical Information Service, Oak Ridge, Tennessee
265. Curtiss-Wright Corp., Wright Aeronautical Division (K. Campbell)
266. Armed Forces Special Weapons Project, Washington

Reports previously issued in this series are as follows:

ORNL-528	Period Ending November 30, 1949
ORNL-629	Period Ending February 28, 1950
ORNL-768	Period Ending May 31, 1950
ORNL-858	Period Ending August 31, 1950
ORNL-919	Period Ending December 10, 1950
ANP-60	Period Ending March 10, 1951
ANP-65	Period Ending June 10, 1951
ORNL-1154	Period Ending September 10, 1951
ORNL-1170	Period Ending December 10, 1951
ORNL-1227	Period Ending March 10, 1952
ORNL-1294	Period Ending June 10, 1952
ORNL-1375	Period Ending September 10, 1952
ORNL-1439	Period Ending December 10, 1952
ORNL-1515	Period Ending March 10, 1953
ORNL-1556	Period Ending June 10, 1953
ORNL-1609	Period Ending September 10, 1953

CONTENTS

ANP PROJECT QUARTERLY PROGRESS REPORT

FOREWORD

This quarterly progress report of the Aircraft Nuclear Propulsion Project at ORNL records the technical progress of the research on the circulating-fuel reactor and all other ANP research at the Laboratory under its Contract W-7405-eng-26. The report is divided into three major parts: I. Reactor Theory and Design, II. Materials Research, and III. Shielding Research. Each part has a separate introduction and summary.

The ANP Project is comprised of about 300 technical and scientific personnel engaged in many phases of research directed toward the achievement of nuclear propulsion of aircraft. A considerable portion of this research is performed in support of the work of other organizations participating in the national ANP effort. However, the bulk of the ANP research at ORNL is directed toward the development of a circulating-fuel type of reactor.

The nucleus of the effort on circulating-fuel reactors is now centered upon the Aircraft Reactor Experiment – a high-temperature prototype of a circulating-fuel reactor for the propulsion of aircraft. The equipment for this reactor experiment is now being assembled; the current status of the experiment is summarized in Section 1 of Part I. The supporting research on materials and problems peculiar to the ARE – previously included in the subject sections – is now included in this ARE section, where convenient. The few exceptions are referenced to the specific section of the report where more detailed information may be found.

The ANP research, in addition to that for the Aircraft Reactor Experiment, falls into three general categories: (1) studies of aircraft-size circulating-fuel reactors, (2) materials problems associated with advanced reactor designs, and (3) studies of shields for nuclear aircraft. These three phases of research are covered in Parts I, II, and III, respectively, of this report.

Part I

REACTOR THEORY AND DESIGN

INTRODUCTION AND SUMMARY

Assembly of the Aircraft Reactor Experiment (sec. 1) is nearing completion; all but a few of the components have been received and installed. The items still missing include the new control rod sleeves and parts of the fuel and sodium gas-sealed pumps. As the installation progresses, various auxiliary systems, such as the helium, water, and hydraulic off-gas systems, are being subjected to operational tests. Tests of a prototype pump have established the design criteria for the pump cooling and lubricating systems, as well as the operating characteristics of the pump. The new control rod sleeves will effect a reduction in the structural poison in the core and hence reduce the critical mass. Recent physics calculations indicate that the uranium requirement inside the pressure shell will be well under 40 lb of U^{235}. Other physics calculations on reactor kinetics reveal that reactor operation and control will not be adversely affected by either xenon poisoning or the loss of delayed neutrons in the circulating fuel. The fuel, which will be obtained by the addition of a concentrate, Na_2UF_6, to a solvent mixture, $NaZrF_5$, has been shown to be reasonably compatible with the Inconel container metal for the temperatures and times required. Production of both the solvent and concentrate are essentially complete and the impurities in each are well below acceptable levels. Procedures have been established to assure that the fuel and sodium systems in the experiment will be adequately cleaned prior to being filled with the solvent and sodium, respectively. Additional studies of the fuel recovery and processing problem have established dissolution rates for both molten and solid fuel in batches containing 4 kg of U^{235}.

With the near-completion of the Aircraft Reactor Experiment the emphasis of the experimental work has shifted to the development of components for general aircraft reactor application and supporting research. Valves, pumps, bearings and other components of high-temperature fluoride and liquid metal systems are being developed for these studies (sec. 2). Satisfactory, short, frozen-sodium shaft seals, with length-to-inside-diameter ratios of 1 to 5, have been developed for sodium pumps. A small gas-sealed pump for an in-pile loop and a canned magnetic-torque transmitter for a high-temperature aircraft pump are being developed. Packed seals for fluoride pumps and valves have achieved limited success under controlled conditions, but none of the seals are sufficiently reliable for service conditions. Equipment for high-temperature bearing tests is being assembled, and a number of potential bearing materials are being screened on the basis of wear. A fluoride-to-sodium heat exchange tube bundle and a high-velocity forced-convection corrosion loop are being operated, but results are not yet available on either test.

The designs of a family of 50- to 300-megawatt reflector-moderated reactors have been prepared to permit an Air Force evaluation of over-all aircraft performance (sec. 3). The four reactors considered for 50-, 100-, 200-, and 300-megawatt power outputs are all of the same general species, having all been extrapolated from the same base. The designs are based upon presumed fuel and were made with insufficient physics information for the establishment of over-all design limitations. In other respects, however, the designs are on a firmer basis, since considerable shielding and heat exchanger data are available and the hydrodynamics of the fuel circuit and fuel pump have been confirmed by hydraulic mockups. The gas-sealed centrifugal pump is designed with special baffling above the impeller so that it will operate continuously with its shaft 80 deg from the vertical, and it will even operate for 1 min when inverted without "gassing" the pump. Other aspects of the aircraft reactor, including moderator cooling, assembly of the reactor, control, and fuel filling and draining, are discussed.

The Critical Experiment Facility was used during this quarter to determine the static physics characteristics of a mockup of an air-cooled water-moderated reactor for the General Electric Aircraft Nuclear Propulsion Project (sec. 4). At the same time, preparations were made for measurements of a mockup of a Pratt and Whitney supercritical-water reactor and a Nuclear Development Associates sodium-cooled reactor, as well as the Laboratory's reflector-moderated reactor.

1. CIRCULATING-FUEL AIRCRAFT REACTOR EXPERIMENT

E. S. Bettis J. L. Meem
ANP Division

There were no modifications in the ARE design or critical developments in the ARE program during the quarter, and therefore installation of equipment received maximum attention. The installation is proceeding satisfactorily, and there was no major holdup occasioned by lack of components. For the first time since the project began, it is not necessary to explain either the cause for some delay or some change in plan, and this is the most significant remark that can be made to indicate the status the project attained during this quarter. It is fairly clear now that completion of the installation of the ARE can be effected in an uneventful manner.

One fuel pump sump tank and one sodium pump sump tank were received, and therefore the installation of piping for the fuel and sodium circuits could proceed in a relatively uninhibited manner, even though the spare fuel and spare sodium tanks have not yet been received. Tests on a prototype pump have established the requirements of the auxiliary systems for the pumps, as well as the pump's operating characteristics and performance.

Since all major components of the experiment are now on hand, all crafts have been able to proceed with relatively little interference. Installation of electrical heaters and insulation is progressing rapidly. The heaters are approximately 65% installed, but, since the locations for the remaining heaters are more accessible, the job is 75% complete with regard to man-hours. Insulation work is following closely behind heater installation. The most difficult insulating job, that of insulating tanks and lines in the dump tank pit, is 95% finished, and about 15% of the other insulation has been installed.

Additional data have been obtained from calculations of the reactor statics and dynamics. An evaluation of the effects of xenon poisoning and of the loss of delayed neutrons indicated that neither will be of much consequence to reactor operation. Calculations of the critical mass by two different methods gave values which show that the uranium requirement in the pressure shell will be well below the 40 lb permissible from the viewpoint of uranium allocation and ARE technology. A saving in mass of about 4 lb was realized by a reduction in the poisoning from the control rod sleeves.

The new Inconel-clad control rod sleeves, which will replace the three concentric rod sleeves that were to be used around each rod, have been fabricated. The space outside each new sleeve will be filled with beryllium oxide strips. The reactor, which is complete except for installation of the new rod sleeves and the beryllium oxide strips, has been subjected to preliminary cleaning tests. Tests with simulated reactor fuel tubes indicate that fully established turbulent flow will be realized at a Reynolds number of 5000, which is well under the ARE design value of 14,000.

The ultimate fuel will be obtained by the addition of sufficient fuel concentrate, Na_2UF_6, to the fuel solvent, $NaZrF_5$, to make the reactor critical. The production of the 3300 lb of solvent was completed some time ago, and conversion of the 115 kg of U^{235} into Na_2UF_6 is nearing completion. Initial tests of the concentrate show that, with the exception of one batch which was rejected, the impurities in the concentrate are gratifyingly low. Density and viscosity data have been obtained for the concentrate.

Methods for recovering and reprocessing the fuel after completion of the experiment have received increased attention. It now appears that the used fuel may be transported from the experiment to the reprocessing area in aluminum containers containing 4 kg of U^{235} and that about 20 such transfers will be required. While the reprocessing procedures had been established previously, additional data have been obtained on dissolution rates for the fuel in both liquid and molten states.

THE EXPERIMENTAL REACTOR

The reactor is completely assembled (Fig. 1.1) except for the Inconel-clad stainless steel control rod sleeves, which have not yet been received, and the beryllium oxide strips that will be placed around these sleeves. The fuel tubes have been cleaned according to the established cleaning procedures. Additional measurements of flow phenomena in glass mockups of the fuel tube indicate that fully developed turbulent flow is realized at Reynolds numbers above 5000, that is, well under the reactor design value of 14,000.

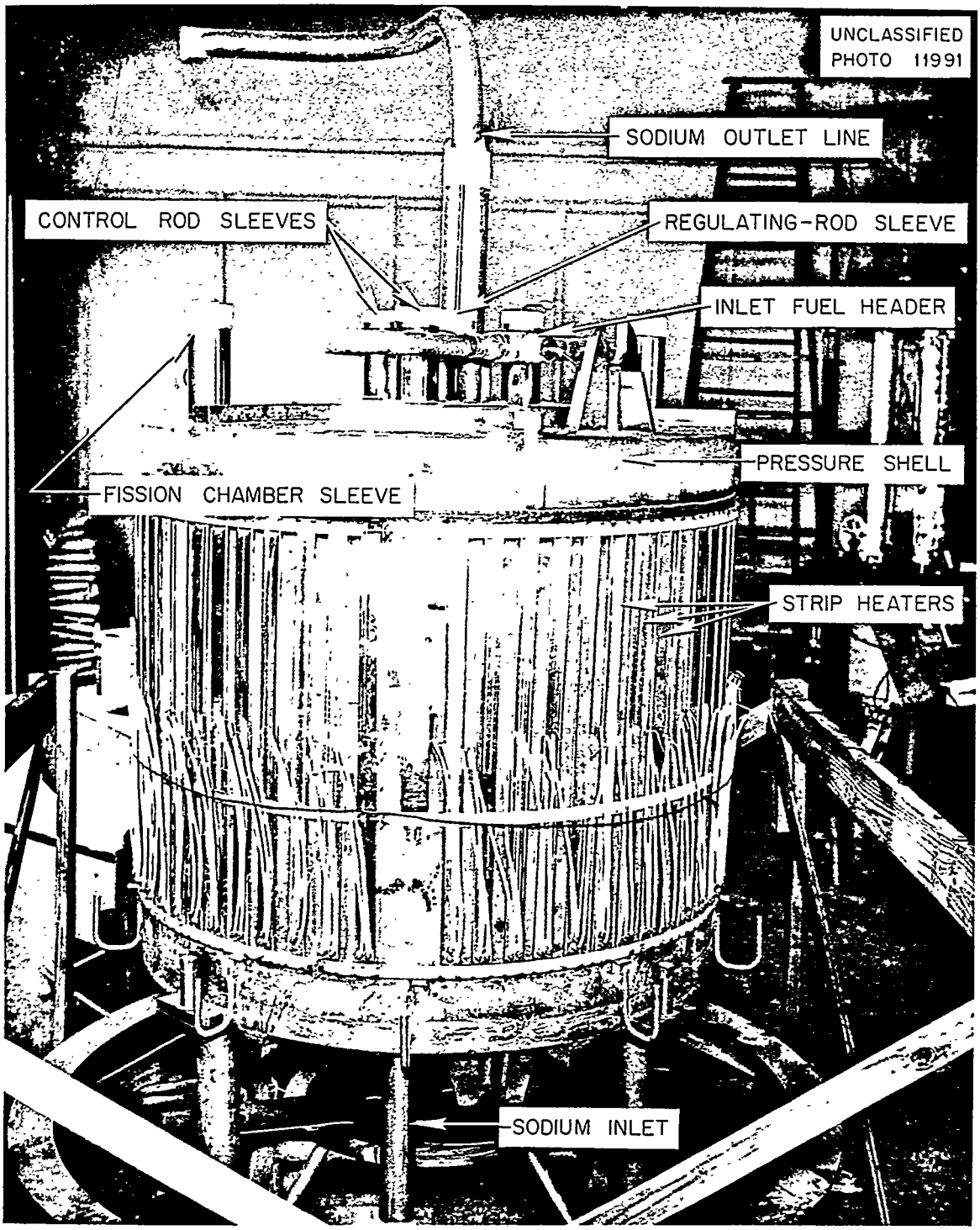

Fig. 1.1. Photograph of the Experimental Reactor.

Control Rod Sleeves

In order to reduce the structural poisons in the reactor, it was decided to replace the three concentric Inconel sleeves around each of the four control rods (one regulating and three safety) with a single Inconel-clad stainless steel sleeve in each hole. Fabrication of the new control rod sleeves has been finished by the International Nickel Company, but they have not yet been delivered.

To further reduce the critical mass of the reactor, the volume outside the rod sleeve was to be packed with beryllium oxide pellets. However, since the beryllium oxide pellets would occupy only about 50% of the volume, it was recently decided to fill this volume with strips from unused beryllium oxide moderator blocks. It is anticipated that approximately 90% of the void volume can be filled with the beryllium oxide strips.

Reactor Control

A. L. Southern J. K. Leslie
ANP Division

There has been only one change (an addition) to the reactor control equipment. An auxiliary low-speed drive has been designed for the regulating rod. This addition was made to provide a means of manually operating the regulating rod when the reactor is operating at zero power during rod calibration.

In the event of fission chamber failure or inadequate Δk in the regulating rod, it may be necessary to change these components during the course of the experiment. Consequently, some of the drive mechanism has been relocated to facilitate replacement of both the regulating rod and the fission chambers. No other changes have been made in the reactor controls and this phase of the work is complete insofar as preliminary checking can determine completeness.

Flow in Fuel Tubes

J. Lang G. M. Winn
Reactor Experimental Engineering Division

The experimental relationship between the friction factor and the Reynolds modulus obtained in a glass replica of the reactor fuel tube system[1] indicated that the transition region (that region which lies between laminar and fully developed turbulent flow) lies approximately between Reynolds moduli of 2000 and 5000. Recent photographs, Figs. 1.2, 1.3, and 1.4, show the diffusion of dye filaments in the second 180-deg return bend in a fuel tube under three Reynolds number flow conditions: 600, 1300, and 2000, respectively. Unfortunately, there was more than one dye source present in the entrance region of the fuel tube system, and thus several filament trajectories were superimposed. In general, the sharp, distinct filaments shown in Figs. 1.2 and 1.3 are characteristic of laminar flow, whereas the diffuse filaments indicate some turbulence, Fig. 1.4.

Fuel Tube Cleaning

G. D. Whitman, ANP Division

The cleaning procedures for the fuel and sodium systems inside and outside the reactor are described in a following subsection (cf., "Reactor and Fluid Circuit Cleaning"). However, a description of the application of these procedures to the actual cleaning of the reactor fuel tubes follows.

The six parallel fuel circuits in the reactor were first rinsed, individually, with tap water. This flushing was accomplished by valving off the outlets of all but one circuit and passing water at a pressure of 60 psi into the fuel inlet header. Following this pressure flushing, each circuit was flushed with distilled water, and the water was blown out as completely as possible with helium. After the water that could be blown out had been removed, a vacuum system was connected through a dry-ice cold trap to the fuel tubes, and the remaining water was evaporated from the fuel circuit at room temperature. During the evaporation process 2 cfh of helium was bled into the system inlet to sweep out all moisture. The residual moisture was determined by the Karl Fisher and dew-point methods.

The reactor will be complete when the control rod sleeves and the bottom fuel outlet manifold have been installed, and it will then be ready for inclusion in the system.

---

[1] ORNL-1609, *ANP Quar. Prog. Rep. Sept. 19, 1953*, J. I. Lang and G. M. Winn.

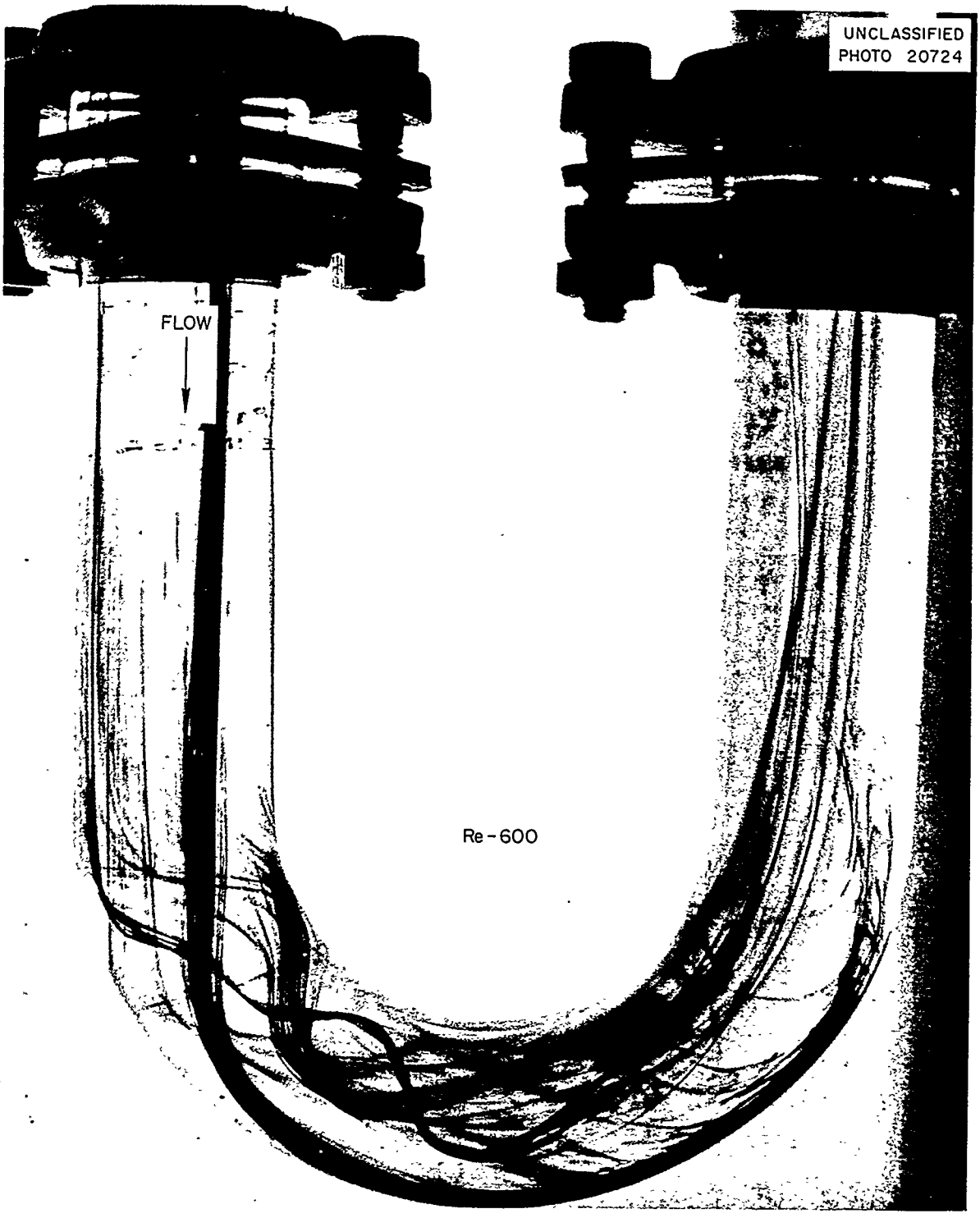

Fig. 1.2. Diffusion of Dye Filaments in a Mockup of a Fuel Tube at a Reynolds Number of 600 (Second 180-deg Bend).

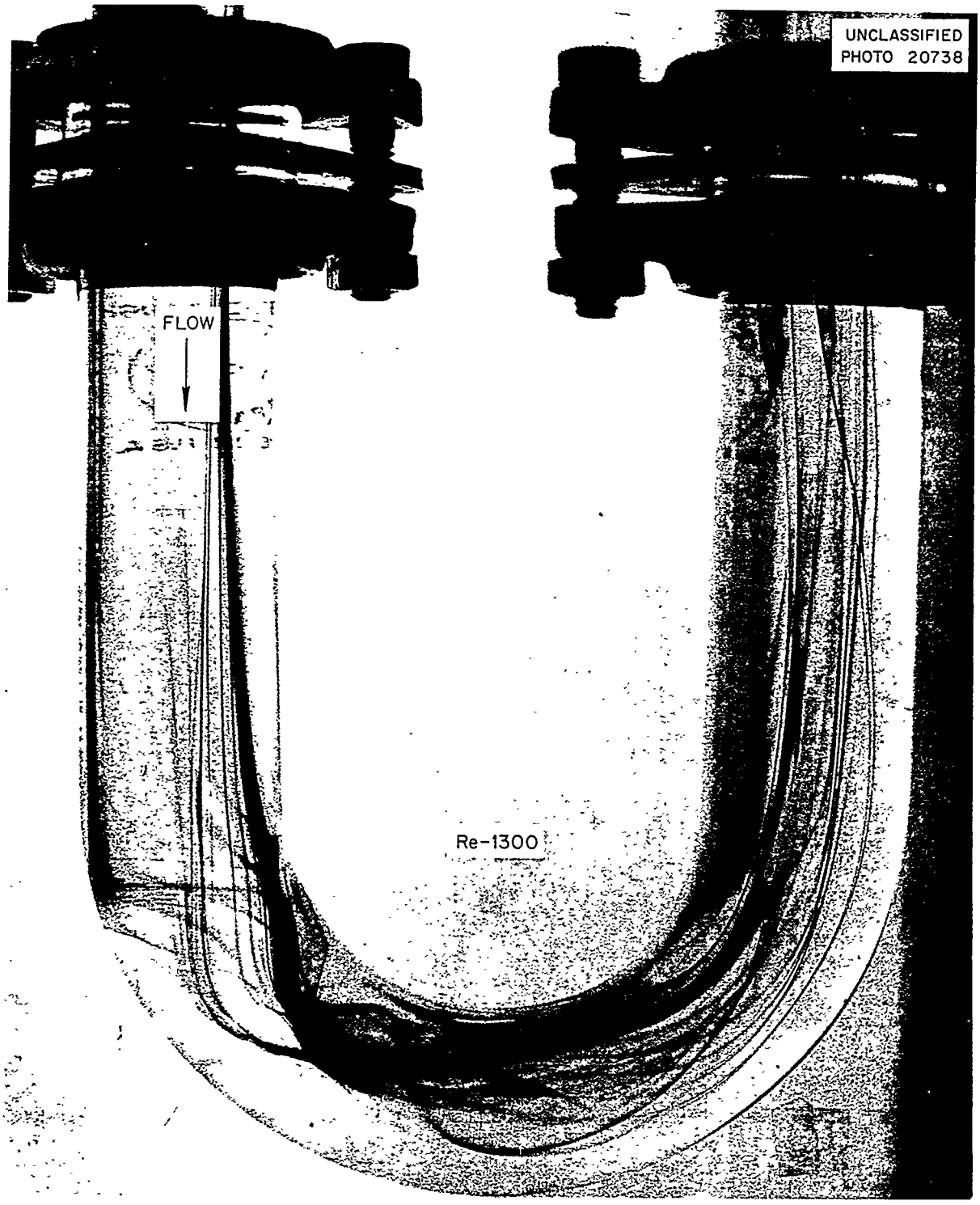

Fig. 1.3. Diffusion of Dye Filaments in a Mockup of a Fuel Tube at a Reynolds Number of 1300 (Second 180-deg Bend).

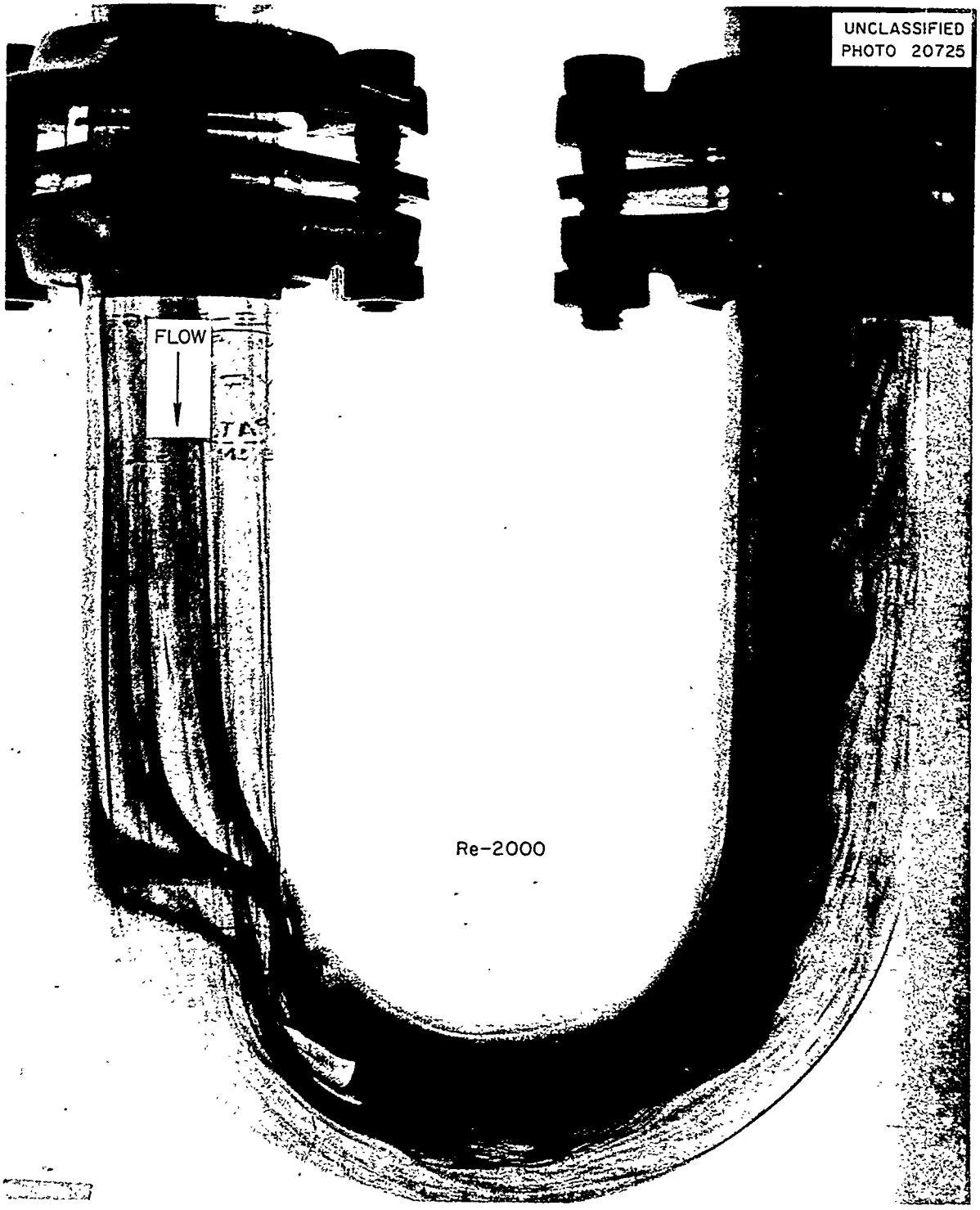

Fig. 1.4. Diffusion of Dye Filaments in a Mockup of a Fuel Tube at a Reynolds Number of 2000 (Second 180-deg Bend).

REACTOR PHYSICS

W. K. Ergen J. Bengston
C. B. Mills, ANP Division

The UNIVAC multigroup calculations and the locally performed two-group calculations gave values which show that the reduction of the poisoning by the control rod sleeves has brought the ARE uranium requirement in the pressure shell to well below the 40 lb permissible from the viewpoint of uranium allocation and ARE technology. The delayed neutrons lost from the reactor by fuel circulation are predominantly those of long decay constants, and hence a small amount of excess reactivity makes it unnecessary for the reactor to wait for the long-delayed neutrons. Small excess reactivities will bring the reactor to relatively short-time constants (10 sec or so), but when the reactor is at such a time constant it is still substantially below the prompt-critical condition because the short-delayed neutrons are not appreciably reduced by fuel circulation. Speculation as to the xenon poisoning shows that the poisoning effect would be easily observable if the xenon were not lost from the fuel and if the xenon cross section were as large for the ARE as it is for low-temperature reactors. Failure to observe the poisoning might mean that Xe^{135} or its parent iodine had evaporated from the fuel, or it might mean that the effective xenon cross section was reduced by the high moderator and neutron temperature. In the latter case, xenon poisoning would still be a problem in high-powered reactors of the ARE type.

Critical Mass

The multigroup calculations made by using the UNIVAC at New York University and essentially the method previously employed[2] by the ANP Physics Group have now yielded fairly reliable, though not yet final, data regarding the uranium requirement of the ARE. These data are in agreement with data obtained by the two-group method. They indicate that the elimination of much of the poison originally incorporated into the control rod sleeves has brought the mass requirement to about 15% below the 40 lb which would be permissible from the viewpoint of phase diagrams, corrosion, and allocation.

[2]Report of the *Technical Advisory Board to the Technical Committee of the Aircraft Nuclear Propulsion Program*, ANP-52 (Aug. 4, 1950).

[3]S. Glasstone and M. C. Edlund, *The Elements of Nuclear Reactor Theory*, p. 329 ff., Van Nostrand, New York, 1952.

Effect of Delayed Neutrons

About one half the delayed neutrons are given off outside the reactor and lost from the chain reaction. These delayed neutrons are predominantly those with long-lived precursors. Most of the short-lived precursors decay before they are swept out of the reactor, and their delayed neutrons are hence not appreciably reduced by the fuel circulation. Since the neutrons with the long delay times are not very effective, it will take only a small excess reactivity to allow the chain reaction to proceed without "waiting" for these neutrons. A small excess reactivity will hence bring the reactor to a relatively short time constant of about 10 seconds. When the reactor is operating at full power, it will probably exhibit small reactivity fluctuations, and this may temporarily bring the reactor from just critical (infinite period) to a period as low as 10 seconds. Hence, it might be difficult to keep the reactor steadily at a period longer than 10 seconds. It should be noted that reactivity fluctuations are not expected at low power operation so that it should be possible to operate the reactor on a 30-sec period during the preliminary, low-power experiments. Because of the only slightly reduced effectiveness of neutrons with short delay times, the amount of additional reactivity required to bring the reactor from a 10-sec period to prompt critical is quite substantial, and the fuel circulation of the ARE does not appreciably reduce this safety feature below its value familiar in stationary-fuel reactors.

Xenon Poisoning

Renewed consideration was given to the problem of xenon poisoning of the ARE. There is reason to believe that the Xe^{135}, and probably also its parent iodine, will evaporate from the fuel so that the xenon poisoning effect will not occur in a reactor of the circulating-fluoride-fuel type. Confirmation of this would be a major accomplishment of the ARE. To investigate the problem experimentally, the reactor would have to be run for a time somewhat shorter than the half life of I^{135} at full power and then reduced to very low power. If the xenon poisoning is appreciable, the reactivity will exhibit the characteristic behavior of first dropping because of xenon formation by I^{135} decay and of then increasing because of Xe^{135} decay. Calculations performed by standard methods[3] show that this behavior should be easily detectable if the iodine and xenon do not evaporate from the fuel. If the behavior is not found it could mean

that the poison is given off. However, it could also mean that the xenon poisoning is largely reduced by the high moderator and neutron temperature and that the xenon cross section is rather low for neutrons that are somewhat faster than room-temperature thermal neutrons. If the latter explanation were correct, xenon, even with reduced cross section, would be a poison for reactors of higher power than the ARE.

There is the interesting possibility that the xenon, and maybe the iodine, is released from the fuel at a rate comparable to the rate of radioactive decay. If so, the build-up and decay of the xenon poisoning could still be observed, but the time constants would be different. A quantitative analysis of the reactivity following a full-power run would disclose this situation. There is also the theoretical possibility that other fission fragments have large absorption resonances at neutron energies above those corresponding to the xenon resonance. In high-temperature reactors such as the ARE, these poisons might conceivably be observable.

THE NaF-ZrF_4-UF_4 FUEL

The reactor fuel will be obtained by the addition of a sufficient amount of the fuel concentrate, Na_2UF_6, to the fuel solvent, $NaZrF_5$, to make the reactor critical. It is expected that the final fuel composition will contain approximately 5.5 mole % UF_4. In lieu of more precise knowledge of the ultimate fuel composition, extensive material research and physical property measurements have been conducted on the fuel composition with 4 and with 6.5 mole % UF_4, as well as on the carrier and solvent. About 3300 lb of the carrier has been produced and is being held under helium pending its use in the experiment. The batch production of the fuel concentrate is nearing completion. The impurities in all but one of these batches were exceptionally low, averaging (not including the one poor batch) 48 ppm of Fe, 16 ppm of Cr, and 46 ppm of Ni.

Physical Properties

H. F. Poppendiek
Reactor Experimental Engineering Division

The densities and viscosities of the fuel solvent, $NaZrF_5$, and of the fuel concentrate, Na_2UF_6, are being measured; these properties of the fuel with 6.5 mole % UF_4 were reported previously.[4] Preliminary density and viscosity values for Na_2UF_4 are: viscosity, 17.5 cp at 725°C, 9.9 cp at 975°C; density, $5.598 - 0.00119\ T$ g/cm^3, where 660°C < T < 1000°C.

Fuel Production

G. J. Nessle J. E. Eorgan
F. A. Doss
Materials Chemistry Division

Production of the required 3300 lb of $NaZrF_5$ is now complete, and the material is being held under helium pending its use in the ARE. Processing of the 253 lb of U^{235} to produce the fuel concentrate, Na_2UF_6, is nearing completion.

The fuel concentrate is being produced by the Y-12 Production Division to permit control of the large quantities of enriched uranium (93.5% U^{235}) involved. Several weeks were spent training operators in the handling of the equipment, as well as in testing the equipment. A few necessary changes and repairs were made at that time. The production equipment and the processing technique are essentially the same as those previously described[5] for fuel solvent production.

The concentrate will be produced in 15 batches of approximately 30 lb each. It has proved possible, after some simple operational changes, to process three batches of material per week. However, three weeks of down-time have been necessary during this period because of analytical difficulties and lack of approval of an additional uranium allotment. To date, 10 of the required 15 batches have been processed, and it is estimated that the production operation will be completed before December 1.

As the material was produced by the Y-12 Production Division for use in the ARE, analyses of the material were made by both the Y-12 and the ORNL groups involved. Any differences in these analyses were to be explained and corrected by using, if necessary, the triplicate sample originally taken before production operations proceeded. The analytical situation appears quite satisfactory at present, insofar as production control and fissionable material accountability is concerned. Some discrepancies between the two laboratories have occurred in determinations of the uranium content of the UF_4; these difficulties have

[4] *ANP Quar. Prog. Rep. Sept. 10, 1953*, ORNL-1609, p. 15.

[5] *Ibid.*, p. 15.

been shown to be due to faulty sampling of some poorly milled UF_4. Agreement between the laboratories on uranium content of the Na_2UF_6 has been excellent; tentative plans call for accountability transfer of the material on the basis of these analyses.

A comparison of the analytical data for eight of the ten batches for which results are available is shown in Table 1.1. It should be noted here that the Y-12 laboratory used spectrographic analysis for determining the metallic impurities, while the ANP laboratory used chemical methods of analysis. In general, the agreement is exceptionally good. One batch (AREU-4) must, on the basis of these figures, be reprocessed to lower the impurities to an acceptable level.

Corrosion of Inconel

G. M. Adamson W. D. Manly
Metallurgy Division

The corrosion of Inconel by fluoride fuels has been discussed at length in this and preceding quarterly reports. In loop tests in which the fluoride is circulated at 4 gpm by thermal convection, the maximum depth of attack is less than 10 mils after 500 hr at 1500°F. The recent corrosion data emphasize the value of minimizing the impurities in the fluoride and, to a lesser extent,

TABLE 1.1. COMPARISON OF ANALYTICAL RESULTS FOR SAMPLES OF ARE FUEL CONCENTRATE

BATCH NO.	LABORATORY	COMPOSITION ANALYSIS						
		Weight Fraction (g/g)			Impurities (ppm)			
		U	Na	F	Fe	Cr	Ni	B
AREU-1	Y-12*	0.59534	0.1142	0.2881	25	25	35	1
(310423)	ANP**	0.59521	0.1225	0.2830		20	20	
AREU-2	Y-12	0.59529	0.1158	0.2865	23	11	53	0.2
(310430)	ANP	0.59598			80	20	90	
AREU-3	Y-12	0.59702	0.1168	0.2879	30	20	50	0.2
(310431)	ANP	0.59661			75	20	20	
AREU-4	Y-12	0.59470	0.1160	0.2876	150	12	7400	0.2
(310432)	ANP	0.59577			220	25	475	
AREU-5	Y-12	0.59637	0.1171	0.2883	14	6	21	0.2
(310433)	ANP	0.59649			60	20	35	
AREU-6	Y-12	0.59548	0.1174	0.2905	21	9	42	0.2
(310434)	ANP	0.59582			60	20	45	
AREU-7	Y-12	0.59513			35	6	67	0.2
(310435)	ANP	0.59583			100	20	65	
AREU-8	Y-12	0.59530			32	6	56	0.2
(310437)	ANP	0.59544			75	20	50	

*Fe, Cr, and Ni contents were obtained by spectrographic analysis.
**ANP analyses were made by wet chemical means.

the value of clean container systems. Additives to the fluoride, such as ZrH_2, which would serve to reduce the impurities in the fluoride mixtures and hence the fluoride corrosion, are being evaluated. For a detailed report of the investigation of the effect of various parameters on corrosion in the fluoride-Inconel system, as well as of the postulated mechanism, see sec. 6, "Corrosion Research."

PUMPS

H. W. Savage W. R. Huntley
W. G. Cobb A. G. Grindell
ANP Division

Developmental work on the gas-sealed pumps and auxiliaries for the ARE has progressed to the point where acceptance tests of the pumps for the ARE and the mockup reliability test of a spare pump and auxiliaries are being performed.

Parts for the two fuel and two sodium gas-sealed sump-type pumps are being received; one pump has been completely assembled and two others are almost complete. The pumps for the two systems will be identical except for minor differences in the impeller designs and the volumes of the sump tanks, since the fuel pump sump tank must provide volume for the addition of the fuel concentrate, as well as for the thermal expansion of the fuel. The operating characteristics of these pumps, as well as of the components, and the design of the pump auxiliary systems for oil and dibutylcarbitol distribution are being determined on a prototype sodium pump. The fuel pump auxiliary system design will be the same as that determined for the sodium pump, since the requirements of the latter will be the more severe.

Prototype Sodium Pump Test

The tests of the gas-sealed sump pump with NaF-ZrF_4-UF_4 (50-46-4 mole %) were reported previously.[6] This pump is a prototype of those being assembled for the ARE. The termination of these tests was caused by bearing noises which were determined to be the result of slippage of the inner bearing race on the shaft. The bearing race and the shaft were altered to give a 0.0002- to 0.0004-in. interference fit between them in an attempt to eliminate the slippage. Subsequent operation of the pump with sodium was terminated after more than 300 hr at 1200°F, because a gasket leak at the parting face of the pump casing allowed sodium to jet against the top flange near the primary gas seal. No further bearing trouble was experienced during the tests, and postrun examination revealed no bearing or shaft wear. It is therefore concluded that altering the interference fit between the bearing and the shaft did successfully eliminate the slippage that occurred in the previous tests.

Postrun examination showed that sodium vapor had no deleterious effect on the silver-impregnated graphite seal material. To confirm this, silver-impregnated graphite was immersed in sodium at 300°F for 150 hr in a laboratory test, and again no harmful effects could be observed. The test to determine the reliability of the secondary gas seal at high system pressure (50 psig) was not completed because of the gasket leak which brought about early termination of pump operation. This test is now being made without sodium in the pump.

It was found that gas entrained during pump start-up could be rejected in ½ min at a pumping rate of 35 gpm and in 4 min at a pumping rate of 125 gpm. Since there is no apparent demand for higher pumping rates during startup, the degassing characteristic appears to be satisfactory.

Pump Auxiliaries

The auxiliary systems for the ARE pumps are (1) a system for circulating light spindle oil as shaft coolant and seal lubricant and (2) a system for circulating dibutylcarbitol, which acts as a heat barrier between the sump tank liquid and the gas seal. With the prototype sodium pump operating at 1500°F, heat loads of 11,000 Btu/hr in the dibutylcarbitol from the seal-cavity cooling annulus and 7,000 Btu/hr in the light spindle oil used as shaft and bearing lubricant were found. This heat was removed by water in external heat exchangers.

The tests conducted with the prototype pump to determine heat loads of the shaft- and seal-cooling circuits showed the need for redesign of these circuits to eliminate the rotary union in the shaft-cooling circuit at the upper end of the pump shaft. The cooling circuits have been modified, and the cooling and lubricating oil now enters the bearing housing between the upper bearing and the lubricant-to-air face seal. Upon entry, the oil is divided; some of it trickles over the bearings for lubrication

[6] *ANP Quar. Prog. Rep. Sept. 10, 1953*, ORNL-1609, p. 21.

and heat removal and the other portion passes into the hollow shaft for heat removal. All the oil collects below the bottom bearing in a cavity outside the primary face seal. It flows from the cavity by gravity through nine ¼-in.-dia connections at the bottom of the bearing housing to the lubricant reservoir for cooling and recirculation.

Heat exchanger tests indicate that eight pumps will be required for the pump lubrication (oil) system, that is, one operating and one spare pump for each of the sodium and fuel pumps. One pump and its spare will suffice for the dibutylcarbitol system for all sodium and fuel pumps. These auxiliary lubrication and coolant pumps have been checked and found to be satisfactory.

Impeller Fabrication

All the Inconel impeller castings made by the vendor have been rejected because of imperfections such as sand inclusions, cold shots in the cast metal, and porosity. Each of these imperfections could result in pump failure because of structural failure of the impeller vanes or because the removal of sand inclusions and metal particles in the cold shots would cause intolerable unbalance of the impeller. As a consequence of these rejections, impellers for ARE pumps are being fabricated from Inconel plate stock. Impellers for the sodium pumps (high flow) will have curved vanes to provide heat and flow characteristics similar to those of the cast impellers. Impellers for the fuel pumps (low flow) will be drilled, and, although somewhat less efficient than the curved-vane impellers, they will be easier to fabricate.

Acceptance Tests

Test equipment has been designed and some of it has been placed in operation for running acceptance tests on all ARE pumps. These tests will include (1) water tests to determine head, flow, and efficiency of each pump, (2) short-time, cold, run-in tests of seals at 65 psig, and (3) hot tests at ARE temperature, flow, and pressure conditions. The water test equipment is now in operation, and an all-Inconel loop is being fabricated for the hot tests. The hot test loop will include an ARE-type gas control system and the cooling and lubricating circuits described above. One ARE pump has been assembled and checked with cold water. The performance of the pump in this preliminary test was acceptable.

FLUID CIRCUITS

G. D. Whitman
ANP Division

G. A. Cristy
Engineering and Maintenance Division

Except for the installation of the pumps, the external fuel and sodium systems are essentially completed. Installation of heaters and insulation on these systems is about 65% complete. Additional tests of the bellows-seal and the frangible-disk valves have demonstrated the reliability of each under ARE operating conditions. A flow diagram showing the major fluid circuits and design-point operating conditions is presented in Fig. 1.5.

Fuel System

One fuel pump casing has been received and installed in the fuel system; the other is expected early in December. Only seven welds remain to be made before the system, including the spare pump, is completed; some operational tests may be undertaken before installation of the spare pump. The fuel fill-and-flush tanks have been thoroughly cleaned by hot-water flushing and dried by prolonged evacuation at slightly elevated temperatures (around 200°C).

Sodium System

The status of the sodium system is comparable to that of the fuel system. Assembly of the sodium piping is essentially complete, except for 17 welds that are in the vicinity of either the pump casings or of the reactor.

Valves

The valve tests reported previously indicated that the valves to be used in the ARE would give satisfactory performance if held at a temperature of 1200°F or below. The only additional information on bellows-seal valves involves operational tests at 1100 to 1275°F after the valve had first been held for some time at 1300°F in contact with the fluoride NaF-ZrF_4-UF_4 (50-46-4 mole %). In these latter tests, there was no leakage but some sticking; the operation at 1300°F apparently softened the sealing surfaces. The pressure required to open the stuck valves increased rapidly and then leveled off as the valve-closed time was increased; at no time, however, did the pressure exceed 30 psig.

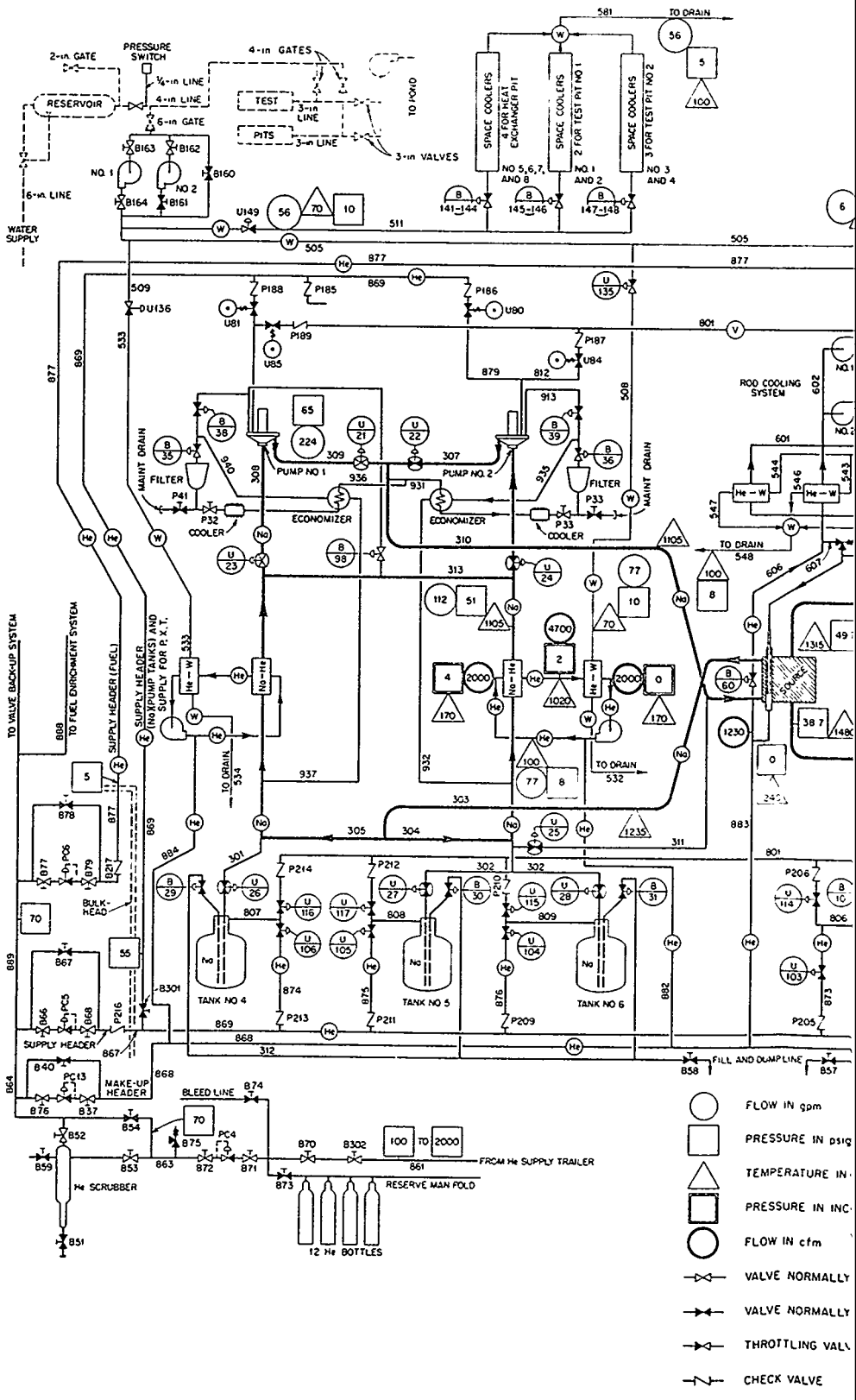

Fig. 1.5. Aircraft Reac

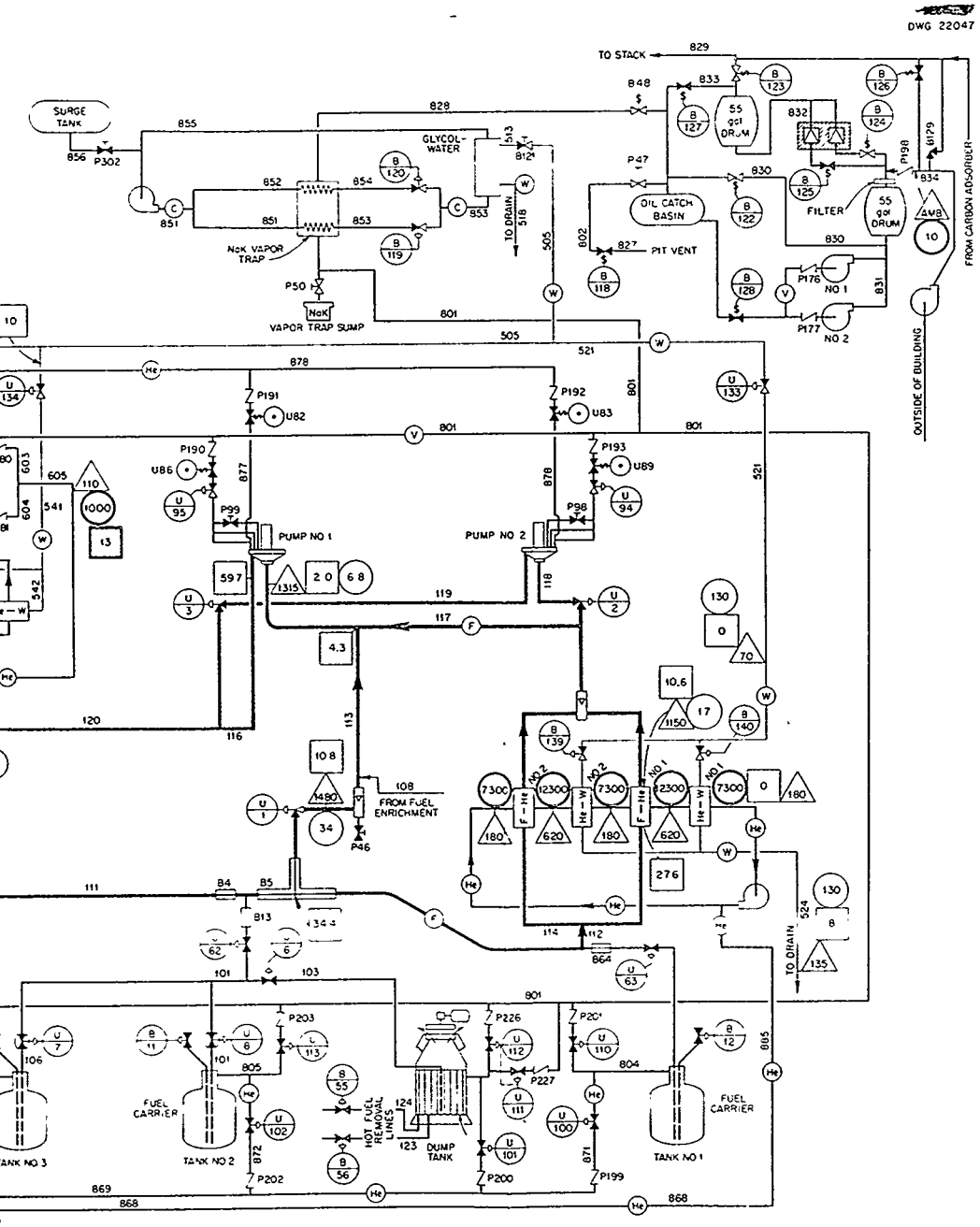

- (F) FUEL
- (Na) REFLECTOR COOLANT
- (He) HELIUM
- (W) WATER
- (C) COOLANT
- (V) VENT SYSTEM
- REMOTE MANUAL VALVE
- REMOTE MANUAL ANGLE VALVE
- MANUAL VALVE
- SOLENOID VALVE
- RELIEF VALVE
- FREEZE VALVE
- PUSH-BUTTON CONTROL

FLOW CONDITIONS ARE BASED ON THE ASSUMPTION THAT THE COOLANT HAS THE FOLLOWING PROPERTIES:

ρ = 210 lb/ft^3
$\mu \cong$ 7 TO 13 cp AT OPERATING CONDITIONS
Cp = 0.23 Btu/lb °F

APPROXIMATE VOLUME OF MAIN SYSTEM:

INTERNAL	1.3 ft^3
INITIAL-EXTERNAL	3.5 ft^3
ENRICHING FLUID	1.7 ft^3 MAX.
TOTAL	6.5 ft^3 MAX

r Experiment Flow Diagram.

Additional data are also available from tests of the frangible-disk valves operated in the fluoride fuel. The frangible-disk valve was held in contact with molten fuel at a temperature of about 1300°F for 160 hr and was opened immediately by the actuator at the end of this period. The valve operation was normal in every way. These tests on ARE-type valves in fluoride mixtures have produced confidence in the valves that are to be used in the ARE, and no serious valve problems are anticipated in the operation of the experiment. All frangible-disk valves have been completely fabricated, tested, and installed. All the Fulton-Sylphon valves were thoroughly flushed and tested with helium for leak tightness across the valve seat.

Auxiliary Systems

The helium heat exchanger loops and the associated hydraulic systems have been completed and tested in air. These tests have shown that the systems have lower pressure drop than calculated, which will result in lower operational speeds and consequently greater factors of safety (or greater heat transfer capacity).

The pit for the secondary off-gas system has been completed, and about 75% of the piping for the system has been installed. The planned program for inspecting and testing of individual systems is being put into operation as rapidly as the installations are completed.

INSTRUMENTATION

R. G. Affel
ANP Division

The detailing of all instrumentation is essentially complete. System changes have necessitated the ordering of several small components which will arrive soon. Approximately two man-weeks of labor will be required before the control room is ready for complete testing. The flux servo system was installed and tested with simulated error signals. Ninety per cent of the needed copper tubing (12,000± ft) is installed. All this tubing is to be checked for leaks. The major jobs remaining to be done are checking and testing.

REACTOR AND FLUID CIRCUIT CLEANING

L. A. Mann
ANP Division

F. F. Blankenship
Materials Chemistry Division

G. A. Adamson
Metallurgy Division

G. A. Cristy
Engineering and Maintenance Division

Corrosion tests have repeatedly demonstrated the deleterious effects of surface contamination of container metals and of impurities in the fluoride mixture on the corrosive attack on the container. Accordingly, both the sodium and the fuel systems will be cleaned. The methods and procedures to be followed in cleaning these systems have been established by a group consisting of representatives from the ANP chemical, metallurgical, engineering, and ARE groups. The complete, final report of this committee has been issued, and a brief outline of the procedures is given below in the order in which they will be used.

TEST	TEMPERATURE	PURPOSE
Reactor Fuel Tubes		
1. Helium pressure test	Room	Leak test
2. Flush with hot, high-velocity water	150 to 180°F	Remove foreign material
3. Flush with distilled water	Room	Replace dirty water
4. Purge with helium	Room	Remove water
5. Dry by evacuation	Room	Complete removal of water
Fuel System Without Reactor		
1. Flush components with hot water	150 to 180°F	Remove foreign material
2. Rinse with distilled water	Room	Replace dirty water
3. Helium pressure test	Room	Leak test
4. Circulate hot water with detergent[7]	150 to 180°F	Remove grease
5. Drain and evacuate	Room	Remove dirty water

[7]The detergent to be used is "Kon Kleen;" active ingredient, sodium metasilicate.

TEST	TEMPERATURE	PURPOSE
Sodium System Without Reactor		
1. Flush components with hot water	150 to 180°F	Remove foreign material
2. Rinse with distilled water	Room	Replace dirty water
3. Helium pressure test	Room	Leak test
4. Circulate hot water with detergent[7]	150 to 180°F	Remove grease
5. Drain	Room	Remove dirty water
6. Rinse with distilled water	Room	Remove all traces of dirt
7. Alternate evacuation and helium purging	Up to 600°F	Remove moisture
Fuel System with Reactor, Part I[8]		
1. Pressure test	Room	Leak test
2. Circulate hot water with detergent[7]	150 to 180°F	Remove grease
3. Rinse with tap water	Room	Remove cleaning water
4. Rinse with distilled water	Room	Remove all contamination
5. Alternate evacuation and helium purging	Up to 600°F	Remove moisture
6. Vacuum rate of rise	Up to 600°F	Leak test
7. Hot gas test: argon in fuel tubes, helium in annulus	Up to 600°F	Leak test
Sodium System with Reactor		
1. Alternate evacuation and helium purging	Up to 600°F	Remove moisture
2. Circulate sodium	600°F	Clean and leak test
Fuel System with Reactor, Part II[8]		
1. Heat reactor and fuel piping	1200°F	Above fluoride mixture melting point
2. Evacuate	1200°F	To fill system
3. Circulate solvent, $NaZrF_5$	1100°F	Clean and leak test
4. Replace with clean solvent	1100°F	Ready for operation

FUEL RECOVERY AND REPROCESSING

D. E. Ferguson F. N. Browder
G. I. Cathers
Chemical Technology Division

Transportation of Fuel

Although the basic outline of an aqueous processing method to be used for ARE fuel recovery has been established,[9] the method of transporting the fuel from the reactor to the processing site will somewhat affect the details of the dissolution procedure. A comparative study indicated that the most satisfactory method would be transportation of the solid fuel in partially filled open-top aluminum cans. A measured amount of the molten fuel would be poured into the cans and allowed to solidify, and the cans would be transported one at a time to the Metal Recovery Building where both can and contents would be dissolved. The use of open-top instead of sealed cans would simplify the remote-filling operation and decrease the dissolution time. None of the valuable material should be lost as a result of fragmentation of the charge if there is sufficient freeboard in the aluminum container.

To illustrate the feasibility of canning molten fluorides in metallic aluminum, three 10-kg batches

[8] Cleaning of the "Fuel System with Reactor" is divided into two parts because the high-temperature phase is dependent upon preheating the reactor with sodium.

[9] D. E. Ferguson, G. I. Cathers, and O. K. Tallent, *ANP Quar. Prog. Rep. June 10, 1953*, ORNL-1556, p. 102.

of $NaF-ZrF_4-UF_4$ (50-46-4 mole %) were transferred to air-cooled aluminum containers. Each of the cans, two with 0.065-in. walls and one with a 0.25-in. wall, withstood the test in which the fluoride temperature was 600°C. It was discovered that the thin-walled cans should not be subjected to more than 5-in. vacuum or 5-psig pressure.

Previously, cans approximately 5 in. in diameter for transporting 6.6 kg of fuel plus flush material, which would contain 0.5 kg of U^{235} if the mixture were homogeneous (or a maximum of 1 kg of U^{235} if the mixture were not homogeneous), were considered.[10] This amount of fuel would dissolve to give about 35 gal of solution.

The process appears to be most attractive if 4 kg of uranium per container, which amounts to 53 kg of fuel plus flush (assuming a homogeneous mixture), can be transported and charged to the 500-gal dissolver to make one 265-gal batch of solution. For this size batch, the containers would be about 9 in. in diameter and 18 in. long. This quantity would be more compatible with the size of the Metal Recovery Building equipment, and the number of containers required to transport the 80 to 100 kg of U^{235} would be reduced from 100 to about 25. Processing of 4 kg of U^{235} per batch in the existing dissolver is subject to approval by the Criticality Hazards Committee.

Another method of dissolving the fuel involves introducing it to the dissolver in the molten state. If this method were used, the fuel could be transported in a special can that would hold about 25 kg of U^{235}. The advantages of this method are the rapidity of the dissolution and the decrease in the number of truck trips required for the transportation. The disadvantages are the difficulty of providing shielding suitable for use in the handling of the molten material and the excessive development work required on equipment that would have to be built into the cans, for example, heaters for remelting the fuel if it solidified before the dissolution was carried out, temperature-measuring instruments, and devices for controlling flow. Construction of the dissolver at the ARE site would eliminate the need for constructing transportable shielding and would permit the use of less rugged heaters, but it would require too large a capital expenditure. It would also split the locations of the chemical operations, and additional operators would be required.

[10] *Ibid.*, p. 103.

Rate of Dissolution of ARE Fuel

Based on the results of laboratory dissolution experiments, a dissolution time of 6 to 12 hr is estimated for a 53-kg charge of ARE fuel. For a 6.6-kg batch, a dissolution time of 3 to 6 hr is estimated. A reliable value for the dissolution time cannot be calculated from the data obtained in these small-scale experiments, since the dissolution rate is not constant throughout the dissolving.

With a 1-in.-dia cylindrical charge weighing approximately 50 g, an initial penetration rate of 0.003 in./min was observed over a 4-min period (Table 1.2). Over the next 3 min, the penetration rate increased to 0.006 in./min, based on the initial dimensions. This increased rate is due to uneven penetration and cracking, which exposes

TABLE 1.2. DISSOLUTION RATE OF SOLID ARE FUEL

Cylindrical samples 1 in. in diameter tested in boiling 4 *M* nitric acid plus 0.67 *M* aluminum nitrate solution

	INITIAL AREA OF SAMPLE ($in.^2$)	TIME IN DISSOLVANT (min)	AMOUNT DISSOLVED (wt %)	CALCULATED PENETRATION RATE (in./min)
First immersion	3.5	4	8.7	0.003
Second immersion	3.5	3	23	0.006
First immersion	5.2	5	13	0.005
First immersion*	3.9	2	2.2	0.002

*Solution already contained the normal complement of dissolved fuel.

more surface area. In a second experiment, a penetration rate of 0.005 in./min was observed over a 5-min interval. After the 5-min period, the sample had broken up into several smaller pieces. Another fresh sample tested in a solution that already contained a normal complement of dissolved fuel gave a penetration rate of 0.002 in./min; however, in the final stage of an actual dissolution, the charge would probably have broken up to expose a very large surface area per unit weight. Based on these results, the average penetration rate will probably exceed 0.006 in./min.

The sample charges for these experiments were prepared by pouring molten fuel (NaF-ZrF_4-UF_4, 50-48-2 mole %) into a split graphite mold and cooling. The pit formed by contraction on cooling was removed by pressing the cylinder against a hot metal plate. The sample was placed in the dissolvant (boiling 4 *M* nitric acid and 0.67 *M* aluminum nitrate solution) and then removed and weighed after a measured interval to determine the amount dissolved.

Since the scale-up of these laboratory data is inconclusive, three charges will be poured into aluminum cans, 6 in. in diameter and 9 in. long, and dissolved to establish the dissolution time more accurately.

Molten Fuel Dissolution

No excessive violence was observed in several preliminary tests in which molten ARE fuel, at temperatures of over 550°C, was poured into the aqueous solvent (4 *M* nitric acid plus 0.67 *M* aluminum nitrate). On contact with the aqueous phase, the fuel solidified in the form of small irregular particles 1 to 2 mm in diameter and then dissolved at a rate of about 50 g in 10 min, which is comparable with the rate of 50 g in 5 min that had been observed with finely ground fuel. Apparently the only precaution required is to make sure that the addition is slow enough to prevent excessive overheating and overboiling. However, colloidal material has been present in all dissolver solutions prepared to date from molten fuel, possibly as a result of the instability or hydrolysis of zirconium compounds in aqueous solutions at high temperatures. Some modification of the dissolver solution to prevent formation of this material would probably be required if molten fuel dissolution were to be used.

---

2. EXPERIMENTAL REACTOR ENGINEERING

H. W. Savage, ANP Division

The completion of the developmental work on the gas-sealed sump pumps for the ARE has made possible a change in emphasis of the experimental work, and increased effort has been devoted to the development of a hydrodynamic type of bearing and a heat exchanger for the reflector-moderated reactor.

The developmental work on the frozen-sodium-sealed pump for sodium during this quarter included tests of a frozen-sodium shaft seal with a single $\frac{1}{2}$-in.-long frozen-sodium sealing region backed up with helium pressure in the sealing cavity. The short seal is being developed in an effort to lower the power consumption of the seal and yet maintain the low leakage obtained with the $5\frac{13}{16}$-in.-long seal previously described. In tests, the new short seal dissipated approximately $\frac{3}{4}$ hp, with no power fluctuations, and it was found that the sodium leakage could be made negligible if back-up pressure was used to reduce the pressure differential across the seal. Water tests on the gas-sealed sump pump for the in-pile loop showed fluid gassing to be a problem, and, accordingly, changes are being made in an effort to eliminate this condition. In other tests, the problems associated with developing a canned magnetic-torque-transmitter for a high-temperature pump for aircraft application are being explored.

Since the adoption of the gas-sealed sump pump for ARE operation, seal developmental work has been carried on at a reduced rate; however, tests for rotary shaft and valve stem seals have continued with materials which showed promise in earlier tests. These include graphite packed around a spiral-grooved shaft, graphite and BeF_2 mixtures, a V-ring type seal, and a bronze-wool, graphite, and MoS_2 mixture. Although each of these seals

has performed well under laboratory controlled conditions, none has demonstrated sufficient reliability to warrant adoption in a pump for reactor operation. Also, none of the packing materials tested thus far for valve-stem seals has demonstrated sufficient reliability to replace the bellows as a valve-stem seal.

A hydrodynamic type of bearing which will operate in liquid metals, fused salts, or other fluids at temperatures of up to 1500°F is being developed. Materials for this application are being screened in a compatibility testing device, and a test program is being planned for obtaining the bearing characteristics, which are usually represented as friction factor vs. Sommerfeld number.

A heat exchanger incorporating some design features proposed for the reflector-moderated reactor is currently being tested. The fluoride system has operated at above 1200°F for over 600 hr, but performance data are not yet available.

A small forced-convection loop is being operated to test corrosion of Inconel in circulating fluoride mixture NaF-ZrF_4-UF_4 at high fluid velocities and high temperature differences. The fluid velocities obtained in this loop are a factor of 50 or 60 greater than those of thermal-convection loops, but the Reynolds modulus remains in the laminar region at approximately 1700.

PUMPS FOR HIGH TEMPERATURE LIQUIDS

W. G. Cobb
A. G. Grindell
W. R. Huntley
W. B. McDonald
D. R. Ward
ANP Division

Frozen-Sodium-Sealed Pump for Sodium

A frozen-sodium shaft seal with a ½-in.-long frozen-sodium region backed up with helium pressure in the sealing cavity was tested. This seal differed from the previously tested[1] short seal in that only one ½-in.-long sealing region was used and the blanket gas was under pressure. The short seal is being developed in an effort to lower the power consumption of the seal and yet maintain the low leakage obtained with the $5\frac{13}{16}$-in.-long seal previously described.[2]

For the first 168 hr of operation with the new short seal, the sodium temperature at the pump was 960°F, the suction pressure was 20 psig, and the back-up pressure was 15 psig. The total sodium leakage past the seal during this period was 32 cm^3 or an average of 4.8 cm^3 per day. Approximately ¾ hp was dissipated in the seal and the power trace was smooth.

The Buna N rubber O ring used to seal the back-up gas was destroyed during the application of heat to remove the sodium leakage at the end of 168 hr, and the remainder of the testing was accomplished without the use of back-up pressure. Operation was continued for a total of 980 hr with a shaft speed of 1800 rpm, a sodium temperature of 960°F, and a suction pressure of 12 psig. A slight flow of helium was maintained across the back of the seal. The increase in the pressure differential across the seal from 5 psig during the first part of the test to approximately 12 psig during the remainder of the test resulted in an increase in sodium leakage past the seal to approximately 20 cm^3 per day.

Erratic power fluctuations caused by sodium oxide migrating to the cold section of the seal became negligible when a standard, cold-trap, bypass filter was installed in the loop. The filter bypasses approximately 0.25 gpm of sodium. Excessive heat loss in the filter (approximately 3 kw) necessitated its redesign to incorporate a heat economizer designed to waste only 0.3 kw. Transit time through the new filter is approximately 6 minutes.

The results of these tests, together with the previously reported results of tests with longer frozen-sodium seals, have led to the conclusion that a frozen-sodium shaft seal is manageable for a sodium pump. A satisfactory length-to-diameter ratio for such a seal is approximately 1 to 5. Leakage of sodium past the seal can be made negligible by using back-up pressure to reduce the pressure differential across the seal. Water cooling is an efficient means of freezing the seal, and several thousand hours of operation have demonstrated that the hazard in using water with a properly designed seal is trivial.

Gas-Sealed Sump Pump for In-Pile Loop Test

A pump is being developed for in-pile loop tests which is similar to the laboratory-sized gas-sealed pump[3] but which has been scaled down to reduce

[1] *ANP Quar. Prog. Rep. Sept. 10, 1953*, ORNL-1609, p. 20.
[2] *ANP Quar. Prog. Rep. June 10, 1953*, ORNL-1556, p. 11.
[3] *Ibid.*, p. 17.

the fluid holdup in the pump. Water tests of the first pump constructed show that the pump head and flow are within design specifications; however, a fluid gassing problem exists which indicates that some design changes will be necessary.

While some gassing of the fluid is evident under all operating conditions, its magnitude increases rapidly as the height of the free fluid surface above the suction is decreased or the shaft speed is increased. This indicates that the difficulty is caused by vortexing of the free fluid surface because of shaft rotation. As an initial attempt to suppress vortexing, changes are being made in the antiswirl baffles in the pump, and the opening through which the rotating shaft enters the suction chamber is being moved to a point well below the free surface of the fluid.

Magnetic-Torque-Transmitter Pump

High-temperature pumps for aircraft application may include a canned magnetic-torque-transmitter pump with the external shaft driven by suitable means, for example, a gas turbine. The problems encountered in building such a torque transmitter are being investigated. Reduced-scale tests have been conducted for determining the expected efficiency of a magnetic torque transmitter at elevated temperatures, the geometry of such a transmitter, and to what extent slippage occurs as a function of temperature.

The first transmitter tested consisted of a permanent magnet outer rotor and a squirrel cage (from a $\frac{1}{40}$-hp motor) inner rotor. A nonmagnetic stainless steel can separated the driving and driven rotors. The entire assembly (excluding the outboard bearings) was heated to above 1100°F, and the slippage rate was appreciable in the temperature range of 600 to 1100°F. However, the full $\frac{1}{40}$-hp torque was transmitted from room temperature to 600°F, but the efficiency then dropped off rapidly at higher temperatures. It is yet to be determined whether the drop in efficiency is due to the drop of the flux of the permanent magnet or to lowered resistance of the windings of the rotor. A permanent magnet inner rotor is presently being constructed which will resolve this question.

ROTARY-SHAFT AND VALVE-STEM SEALS FOR FLUORIDES

R. N. Mason P. G. Smith
W. C. Tunnell
ANP Division

Graphite-Packed Seal for Spiral-Grooved Shaft

Operation of the spiral-grooved shaft with a powdered-graphite-packed seal[4] has continued for over 3000 hr with no detectable leakage of fused fluorides. During this period of operation, heater failure occurred on two occasions and caused the shaft rotation to stop. When repairs were made, operation was resumed with no difficulty.

Graphite-BeF_2 Packed Seal

The previously reported[5] test of a seal packed with a mixture of 80% graphite powder and 20% BeF_2 has now operated for over 3700 hours. The leakage for the past 3500 hr was less than 15 in.^{3}. Power fluctuations have occurred, and some of them were accompanied by squeaking, which indicated possible metal-to-metal contact between the shaft and the gland.

When this packing material was installed in a tester having a $2\frac{1}{4}$-in.-dia shaft, excessive graphite and BeF_2 leakage occurred. Investigation disclosed that the temperature during pretreatment was insufficient to fuse the BeF_2, and thus the seal contained loosely packed material rather than the solidly fused material desired. For the second test, the pretreatment temperature was raised to 1800°F, and the BeF_2-graphite mixture fused solidly. During the dry run of this seal, there was no leakage of powder. The seal region has been operated at a higher temperature (above 975°F) in this test than in previous tests to reduce power fluctuations. There has been some fluoride leakage.

V-Ring Seal

Operation of the V-ring seal test[6] was continued, and a heater was installed inside the $2\frac{1}{2}$-in.-dia rotating shaft. During an extended dry run in which the seal was gradually heated to about 1200°F, satisfactory sealing of helium was attained. The inert gas blanket and seal gas supply was inadvertently shut off for about 20 min during operation, and, since some damage to the seal rings occurred, satisfactory sealing could no longer be obtained. Examination of the rings after disassembly of the seal showed that the outside

[4] *ANP Quar. Prog. Rep. Sept. 10, 1953*, ORNL-1609, p. 23.

[5] *Ibid.*, p. 24.

[6] *ANP Quar. Prog. Rep. June 10, 1953*, ORNL-1556, p. 19.

ring was 75% destroyed and the other rings had either oxidized or worn about 0.0005 to 0.0015 in. on the inside diameter; the shaft was undamaged. The outside ring has been replaced and another dry run will be made in an attempt to seal helium at above 1000°F before fluorides are introduced.

Bronze-Wool, Graphite, and MoS_2-Packed Frozen Seal

The test[7] of the bronze-wool, graphite, and MoS_2-packed frozen seal continued until operation was terminated at the end of 1198 hr because of leakage of the fluoride mixture $NaF-ZrF_4-UF_4$ from a flange. The leakage rate was less than 1 cm^3 per day with the fluoride pot at 1175°F and pressurized to 10 psi.

An additional test was made with the packing annulus reduced from $\frac{3}{4}$ to $\frac{3}{8}$ inch. This test was unsuccessful and was terminated at the end of 211 hours. The failure was attributed to faulty alignment between the shaft and the packing housing.

Packed Seals for Valve Stems

A series of tests is in progress to determine whether the packing materials which sealed well in the packing penetration tests[8] will seal high-temperature fused salts under simulated valve operating conditions. None of the materials tested has demonstrated sufficient reliability to replace the bellows as a valve-stem seal.

The test apparatus consists of a standard valve stem and bonnet placed in a vertical position with the stem down. The pot in which the molten fluoride mixture is pressurized against the packing in the bonnet is welded to the top of the bonnet. The stem is rotated at frequent intervals to simulate valve operation. Three tests have been completed in which the valve stem was cycled once every 24 hr, and the pressure on the packing was 5 psi. The packings tested were Asbury graphite 805 at 1100°F, 90% Asbury graphite 805 plus 10% BaF_2 at 1100°F, and 50% graphite (from the Y-12 Carbon Shop) plus 50% BeF_2 at 1350°F. Each of these tests was terminated because of fluoride leakage.

[7] *ANP Quar. Prog. Rep. Sept. 10, 1953*, ORNL-1609, p. 25.

[8] *Ibid.*, p. 28.

HIGH-TEMPERATURE BEARING DEVELOPMENT

R. N. Mason P. G. Smith
W. C. Tunnell W. K. Stair
ANP Division

Developmental work is under way on a hydrodynamic type of bearing which will operate in liquid metals, fused salts, or other fluids at temperatures of up to 1500°F. This developmental program will probably be carried out in three phases: (1) test programs to find materials which have low wear and low corrosion rates in the fluids of interest at 1500°F, (2) a test program to establish the bearing characteristics, which are usually represented as friction factor vs. Sommerfeld number, and (3) the design and test of a bearing for a particular application using the information obtained in phases 1 and 2. Effort to date has been confined to materials compatibility tests and to an evaluation of the accuracy which may be expected in carrying out the program for obtaining bearing characteristics.

Materials Compatibility Tests

Initial screening tests for finding materials that possess satisfactorily low wear and low corrosion rates are being made in apparatus in which a $2\frac{3}{4}$-in.-dia, $\frac{1}{2}$-in.-thick plate specimen of one material rotates against a $\frac{1}{2}$-in.-dia stationary pin of another or the same material. The end surface of the pin is ground to a $\frac{1}{2}$-in.-radius cylinder to approximate line contact along a radial line of the rotating plate at a mean radius of 1 in. from its center (Fig. 2.1). Contact pressure between the plate and pin is maintained by means of an external coil spring and a sliding shaft.

A test was run of the equipment made with a Graphitar plate and an Inconel pin. A Hertz stress (estimated stress in the line of contact) of about 10,000 psi, or a 5-lb force load between the plate and pin, was used. With the test specimens submerged in acetylene tetrabromide to simulate the fluoride melt, it was found that the 5-lb load was insufficient for breaking through the hydrodynamic film and that the film persisted until a load of about 10 lb was applied to give a Hertz stress of about 15,000 psi. The rate of rotation was 850 rpm, which gave a sliding speed of about 7.4 fps. Having determined the load requirement, a series of correlation tests was conducted with plates of type 416 stainless steel rotating against stationary

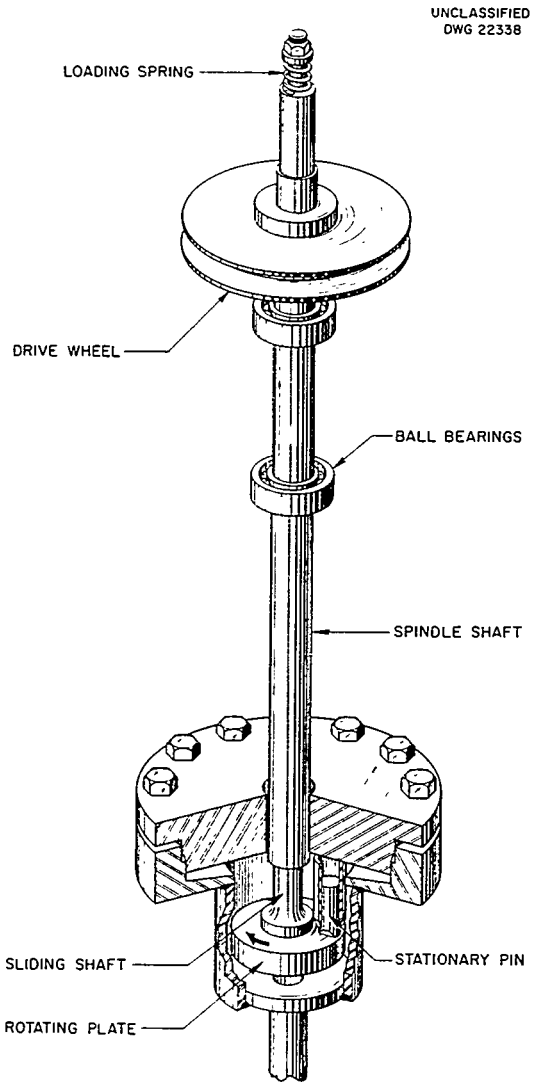

Fig. 2.1. Bearing Materials Compatibility Tester.

pins made of babbit, a die steel, a high-speed tool steel, Stellite 6, Stellite Star J, and Superoilite. In each case, the stationary pin and the rotating plate were submerged in a regular-grade, Texaco, Regal "A" oil, without additives, that has a viscosity of SUS 40-44 at 210°F. The results of this series of tests conformed with those obtained earlier at KAPL.[9]

The first test at a high temperature was made with Graphitar rotating against Inconel in NaF-ZrF_4-UF_4 at 1200°F for 2 hours. The Graphitar appeared to be scratched lightly and it was warped, while the Inconel specimen appeared to be burred and built up at the rubbing surface.

The following materials are being screened in seesaw corrosion tests: B, ZrC + Fe, MgO + Ni, BeO + Ni, BeO, hot-pressed Al_2O_3, high-density graphite, TiC + Ni, TiC + Co, CrC, B_4C, WC + Co, and WC + Ni. Plates and pins of most of the above materials either have been ordered or will be fabricated.

Combinations of materials which possess both satisfactorily low wear and low corrosion rates based on the qualitative results of the screening tests will subsequently be tested in equipment which simulates a conventional journal and bearing.

Bearing Characteristics

An evaluation has been made of the accuracy of the data which will be obtained in the test program for determining bearing characteristics. Two experimental approaches for obtaining the data have been reviewed. First, the test may be simply a load-life experimental study to establish reliability of a single bearing design in fluoride melts. Information gained from this approach might or might not be useful in predicting the behavior of other bearings; certainly, the information could be used only with limited assurance. On the other hand, the experimental study may be a performance test in which an effort is made to establish parameters which will describe the bearing characteristics in such a way that they may be employed to determine design configurations other than the one tested.

The information to be obtained by using the second approach is usually presented as a plot of f_b vs. S_n, where f_b is the bearing friction factor (dimensionless) and S_n is the Sommerfeld variable (dimensionless):

$$S_n = \frac{\mu N}{P}\left(\frac{r}{c}\right)^2 \qquad (1)$$

and

$$f_b = f\left(\frac{r}{c}\right) \quad , \qquad (2)$$

where

μ = absolute viscosity of lubricating fluid, lb_f-sec/in.^{2},

[9] D. B. Vail, *Compatibility of Materials in Liquid Metals*, KAPL-589 (Aug. 18, 1951).

N = journal speed, rps,
P = unit bearing load, psi,
r = journal radius, in.,
c = radial clearance, in.,
f = coefficient of bearing friction.

The significance of these relationships in design work will depend on their accuracy, which can be defined in terms of the accuracy to be associated with each of the variables. The fractional precision of S_n will depend upon the fractional precision of μ, P, N, r, and c, and it may be shown that

$$(3)\quad P_{S_n}^2 = \left(\frac{\partial S_n}{\partial \mu}\right)^2 P_\mu^2 + \left(\frac{\partial S_n}{\partial N}\right)^2 P_N^2 + \left(\frac{\partial S_n}{\partial P}\right)^2 P_P^2 + \left(\frac{\partial S_n}{\partial r}\right)^2 P_r^2 + \left(\frac{\partial S_n}{\partial c}\right)^2 P_c^2 ,$$

where P_{S_n}, P_μ, . . . represent the probable errors of S_n, μ, ... Taking the partial derivative of S_n with respect to μ, N, . . . and substituting in Eq. 3 gives

$$(4)\quad P_{S_n}^2 = \left(\frac{S_n}{\mu}\right)^2 P_\mu^2 + \left(\frac{S_n}{N}\right)^2 P_N^2 + \left(\frac{S_n}{P}\right)^2 P_P^2 + 4\left(\frac{S_n}{r}\right)^2 P_r^2 + 4\left(\frac{S_n}{c}\right)^2 P_c^2 ,$$

and dividing both sides by S_n^2 gives

$$(5)\quad \left(\frac{P_{S_n}}{S_n}\right)^2 = \left(\frac{P_\mu}{\mu}\right)^2 + \left(\frac{P_N}{N}\right)^2 + \left(\frac{P_P}{P}\right)^2 + 4\left(\frac{P_r}{r}\right)^2 + 4\left(\frac{P_c}{c}\right)^2 .$$

As an example, suppose that it is desired to evaluate S_n with a precision of ±10%. If it is assumed, for the first approximation, that each of the quantities μ, N, P, r, and c may be measured with the same precision, then

$$\frac{P_x}{x} = \sqrt{\frac{1}{11}\left(\frac{P_{S_n}}{S_n}\right)^2} = \sqrt{\frac{1}{11}}\,(0.1) = 0.0302 ,$$

and P_x/x is the fractional precision of μ, N, P, r, or c. The variables N, P, and r can be measured to even greater precision than that required for the example given above, but it is doubtful whether μ or c can be measured to even this fractional precision. In this case, it may be assumed that N, P, and r are measured without error, and P_μ/μ and P_c/c are then found to have a fractional precision of

$$\frac{P_x}{x} = \sqrt{\frac{1}{5}(0.1)^2} = 0.0447 .$$

It is possible to measure c with this degree of precision, but μ is likely to involve a much larger error; thus, if it were necessary to evaluate S_n to ±10%, the measuring technique for μ would have to be much refined.

Equation 5 may be used to indicate the resulting precision of S_n for the case in which the probable errors in μ, N, P, r, and c are known. As an example, a journal bearing in a fluoride mixture under the following typical operating conditions will be considered: speed, 1800 rpm; unit load, 20 psi; journal radius, 1 in.; fluoride temperature, 1200°F; radial clearance between bearing and sleeve, 0.0015 inch. At 1200°F, the viscosity of the fluoride mixture $NaF\text{-}ZrF_4\text{-}UF_4$ is reported to be 11.8 cp plus or minus approximately 30%, or $\mu = 11.8 \times 1.45 \times 10^{-7} = 1.72 \times 10^{-6}$ (lb_f-sec/in.^{2}) ± 30%. The expected fractional precisions for the variables are then:

	P_x/x	$(P_x/x)^2$
μ	0.3	0.09
N	0.0025	0.0000063
P	0.025	0.00063
r	0.001	0.000001
c	0.067	0.00449

and

$$\frac{P_{S_n}}{S_n} = \sqrt{(0.09) + (0.0000063) + (0.00063) + (0.000004) + (0.01796)}$$

$$= \sqrt{0.1086} = 0.3296 \text{ or } 32.96\%$$

and

$$S_n = \frac{1.72 \times 10^{-6} \times 30}{2} \left(\frac{1}{0.0015}\right)^2$$

$$= 1.146 \pm 33\% \ .$$

If f_b (bearing friction factor) is considered in a similar manner,

$$f_b = \frac{Fr^2}{RWc} \ ,$$

where

r = radius of journal, in.,
F = frictional force of torque arm length, R, lb_f,
R = torque arm length, in.,
W = total bearing load, lb_f,
c = radial clearance between bearing and sleeve, in.

The expression for obtaining the fractional precision can then be written as

$$\left(\frac{P_{f_b}}{f_b}\right)^2 = \left(\frac{P_F}{F}\right)^2 + 4\left(\frac{P_r}{r}\right)^2 + \left(\frac{P_W}{W}\right)^2 + \left(\frac{P_R}{R}\right)^2 + \left(\frac{P_c}{c}\right)^2 \ .$$

For the assumed operating conditions stated above, the estimated values of the quantities measured for evaluating f_b are: r, 1 in.; R = 6 in.; W, 180 lb_f; c, 0.0015 in.; F, 0.5 lb_f. The expected fractional precisions for the variables are then

	P_x/x	$(P_x/x)^2$
F	0.20	0.04
R	0.10	0.01
r	0.001	0.000001
W	0.1	0.01
c	0.067	0.0049

and

$$\frac{P_{f_b}}{f_b} = \sqrt{(0.04) + (0.000004) + (0.01) + (0.01) + (0.0049)} = \sqrt{0.0649} = 0.255 \text{ or } 25.5\%$$

and

$$f_b = \frac{0.5 \times 1^2}{180 \times 6 \times 0.0015} = 0.308 \pm 25.5\% \ .$$

Thus it appears that the precision of the experimental effort on bearing characteristics is limited by the precision of the data available for the viscosity of the fluoride and the ability to accurately measure the radial clearance and frictional force. If consideration is given to the fact that the $\Delta\mu/\Delta T$ for the fluoride is quite large and that the lubricant film temperature is extremely difficult to accurately measure, the precision of the experimental results will be even lower. Because errors of this type are usually cumulative and the derivations represent ideal conditions, reality may result in errors in the relationships as high as 75 or 100%, which would indicate that refinements in measuring all critical parameters may be needed.

HEAT EXCHANGER TEST

R. E. MacPherson H. J. Stumpf
ANP Division

A heat exchanger incorporating some design features proposed for the reflector-moderated reactor is currently being tested. This exchanger, which is enclosed in a 5-in. tube furnace for preheating, has the molten fluoride mixture NaF-ZrF_4 (53-47 mole %) circulating in the shell and high-

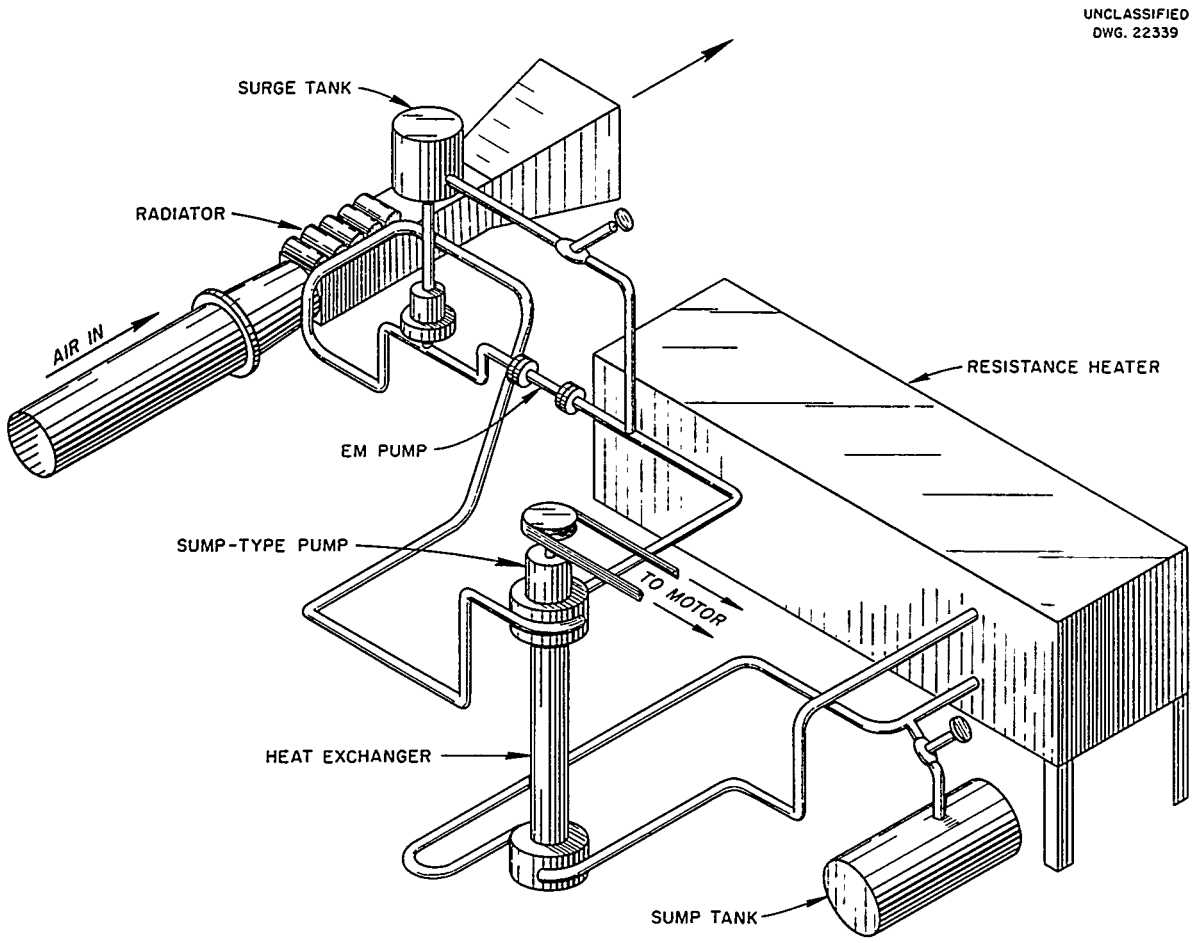

Fig. 2.2. Heat Exchanger Test Apparatus.

temperature sodium circulating through the tube bundles (Fig. 2.2). A sump-type pump continuously circulates the fluoride mixture; the sodium flow is maintained by an electromagnetic pump. The sodium is resistance heated, and it enters the tubes in one half the exchanger to heat the fluorides. It is then cooled in a sodium-to-air radiator (100 kw, interrupted-fin type) from which it enters the tubes in the other half of the heat exchanger to cool the fluorides and then returns to the sodium heating coil. Thus both the fluoride mixture and the sodium are alternately cooled and heated. The heat exchanger is designed to transfer 1.5 megawatts, but performance to date has been limited by an inability to supply sufficient power to the resistance heater for the sodium. The fluoride system has been in operation at above 1200°F for over 600 hr, and the completed bifluid system has been operating at 1200 to 1400°F for 300 hours. Performance data are not yet available.

FORCED-CIRCULATION CORROSION LOOP

D. F. Salmon
ANP Division

A small forced-circulation corrosion loop was operated with NaF-ZrF_4-UF_4 to extend the corrosion data being obtained from low-velocity thermal convection loops. The aim is to eventually obtain a fluid velocity of 5 fps or greater with a temperature difference of 200°F. Circulation is obtained with an Eastern Industries, E-100, centrifugal pump that was redesigned for sump-type operation and fabricated of Inconel. A gas seal is maintained in a water-cooled, Teflon-packed gland on

the shaft. The loop was fabricated of 0.1-in.-OD, 0.025-in.-wall Inconel tubing. Heating is accomplished by passing an electric current through 17 ft of the tubing, and cooling is by natural convection to air from 9 ft of tubing. The tubing is coiled to reduce the space requirement.

The fluid velocities obtained in this loop are a factor of 50 or 60 greater than those of thermal convection loops, but the Reynolds modulus remains in the laminar region at approximately 1700. The loop operated approximately 200 hr with a gradual slowing down of flow, which indicated possible plugging. A summary of the results is presented graphically in Fig. 2.3, which shows velocity and temperature difference as a function of elapsed time. The speed of the pump, which was checked periodically, did not vary appreciably. The velocity of the fluoride mixture was calculated, rather than measured, from heat balance data on the loop heating section. The loop was terminated because of the indicated plugging and is being examined metallurgically. A second loop is being constructed.

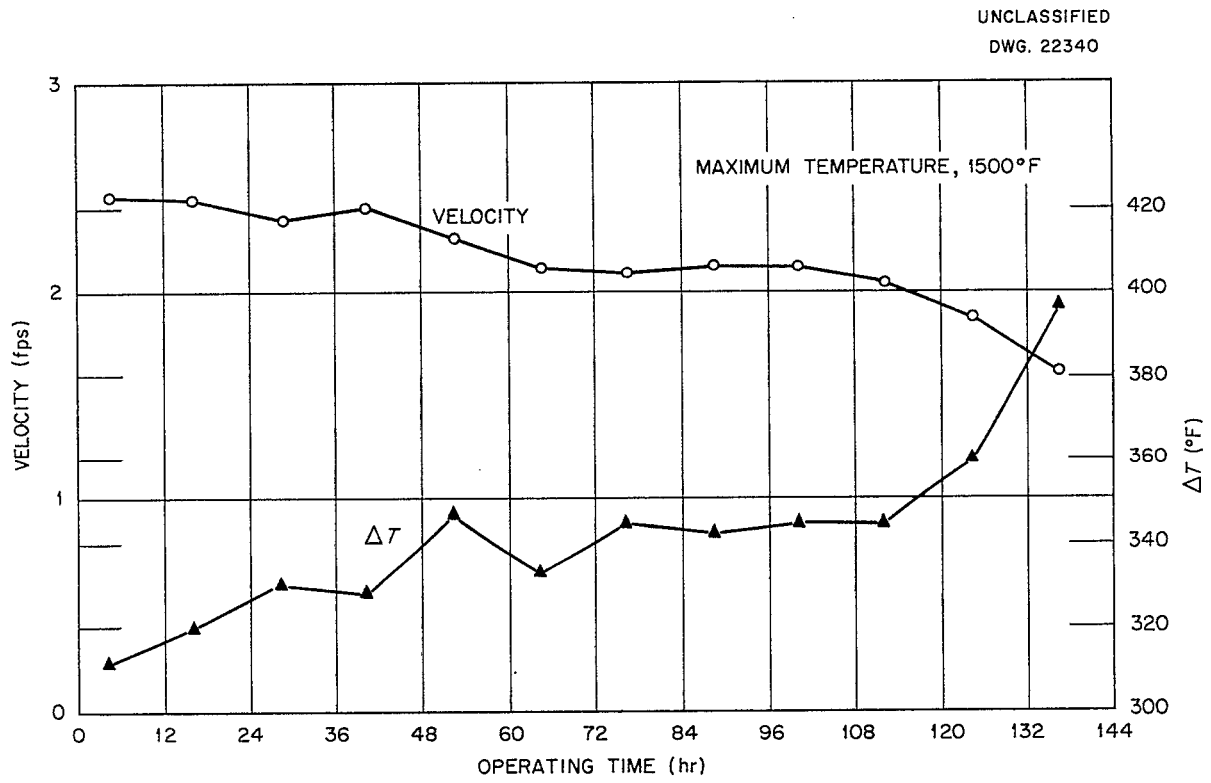

Fig. 2.3. Velocity and Temperature Difference as a Function of Operating Time for $NaF-ZrF_4-UF_4$ in an Inconel Forced-Circulation Corrosion Loop.

3. REFLECTOR-MODERATED REACTOR DESIGN STUDIES

R. W. Bussard A. P. Fraas
ANP Division

In May 1953, the U. S. Air Force requested that a series of design studies be prepared to outline the characteristics of 100-, 300-, and 600-megawatt circulating-fuel reactors. Unfortunately, the reactor physics work essential for establishing the over-all design limitations has lagged far behind schedule, and many materials questions are not yet solved. However, even though detailed designs cannot be prepared at this time, it has been recognized that design information is urgently needed, and therefore the preliminary layouts presented in this report were prepared to give the best estimate of preliminary designs that can be made now. While interest was expressed in reactor power outputs of as much as 600 megawatts, a careful examination of the basic limiting factors indicated that it would not be prudent to extrapolate the information currently available beyond a reactor size of 300 megawatts. The design for the 600-megawatt reactor was therefore dropped, and studies for 50- and 200-megawatt reactors, in addition to the 100- and 300-megawatt reactor designs requested, were prepared.

The more important parameters for the designs are presented in Tables 3.1 and 3.2. Layouts for 50-, 100-, and 300-megawatt reactors are presented in Figs. 3.1, 3.2, and 3.3, respectively. Detail drawings for the main heat exchanger, pumps, and core shells have been prepared for the 50-megawatt reactor. The designs for the 50- and 100-megawatt reactors appear to be quite conservative so that it seems probable that their ratings could be increased to 75 and 150 megawatts, respectively. Parameters such as flow rates and temperature drops would, of course, increase accordingly.

An explanation and qualification of the more important features of the principal components and the considerations that determined them has been prepared to supplement the drawings. The static physics, moderator cooling, pumps, hydrodynamics, heat exchangers, pressure shell, control, and fuel addition and drainage systems are each discussed, in turn. An effort has been made to include in these discussions an indication of the status of the design at this time and of the experimental work planned to provide badly needed design data. A familiarity with information published previously is presumed.[1,2]

REACTOR PHYSICS

A wide variety of reactor types and geometries has been considered for circulating fluoride fuels. Of these, the most promising at this time appears to be a reflector-moderated reactor with a central island. Sodium-cooled beryllium seems to be the best choice as the moderating material. However, the picture is very incomplete because calculations for only about 25 reflector-moderated reactors had been completed until recently because of lack of computing facilities. Calculations for approximately 100 two-region reactors have just been completed, and the results are being analyzed; calculations for about 200 three- to nine-region reactors have been started. By April 1954, this work should be far enough along to give a more complete picture of the effects of reactor geometry and materials of construction on parameters such as critical mass and power distribution for every type of circulating-fuel reactor that has appeared promising. A particular effort will be made to find an arrangement that will give the most rugged, reliable, and simple reactor construction consistent with limitations imposed by corrosion and gamma-heating effects.

Five critical assemblies have been run to date on reflector-moderated reactors. All these have been rather rough approximations to what currently appears to be a promising full-scale aircraft reactor. The weakest element in all of these approximations has been the fuel region composition. In the first critical assembly, the fuel region was simulated with cans of sodium interspersed with disks of metallic uranium, while in the subsequent assemblies, cans of powdered $NaF\text{-}ZrF_4\text{-}UO_2$ were employed. The first assembly suffered from severe inhomogeneity and self-shielding of the fuel, and the subsequent assemblies had the shortcoming

[1] A. P. Fraas, C. B. Mills, and A. D. Callihan, *ANP Quar. Prog. Rep. March 10, 1953*, ORNL-1515, p. 41.

[2] A. P. Fraas, *ANP Quar. Prog. Rep. Sept. 10, 1953*, ORNL-1609, p. 31.

TABLE 3.1. PRINCIPAL DIMENSIONS OF A SERIES OF REFLECTOR-MODERATED CIRCULATING-FUEL REACTORS

Power, megawatts	50	100	200	300
Core diameter, in.	18	18	20	23
Power density in fuel, kw/cm^3	1.35	2.7	3.9	3.9
Pressure shell outside diameter, in.	48.5	50.6	56.4	62.0
Fuel System				
Fuel volume in core, ft^3	1.3	1.3	1.8	2.7
Core inlet outside diameter, in.	10	10	11	12.8
Core inlet inside diameter, in.	7	7	7.7	9
Core inlet area, in.^{2}	40	40	49	67
Fuel volume in inlet and outlet ducts, ft^3	0.4	0.4	0.5	0.7
Fuel volume in heat exchanger, ft^3	1.25	2.5	5	7.5
Fuel volume in pump and plenum, ft^3	0.3	0.3	0.5	1.0
Total fuel volume circulating, ft^3	3.25	4.5	7.8	11.9
Fuel expansion tank volume, ft^3 (8% of system volume)	0.26	0.36	0.62	0.95
Fuel Pumps				
Fuel pump impeller diameter, in.	5.75	7	8.5	10
Fuel pump impeller inlet diameter, in.	3.5	4.5	5.5	6.75
Fuel pump impeller discharge height, in.	1.1	1.5	1.8	3.2
Fuel pump shaft center line to center line spacing, in.	20	21	22.5	27
Plenum chamber width, in.	14.5	15	15.5	17.5
Plenum and volute chamber length, in.	30	31	33	37
Plenum and volute chamber height, in.	2.0	2.0	2.4	3.0
Impeller rpm	2700	2700	2500	2300
Estimated impeller weight, lb	8	12	17	24
Impeller shaft diameter, in.	1.5	1.75	2	2.25
Impeller overhang, in.	12	13	14	15
Critical speed, rpm	6000	6000	5200	5000
Sodium Pump				
Na pump impeller diameter, in.	3.4	4.1	5.0	5.9
Na pump impeller inlet diameter, in.	2.4	2.9	3.5	4.2
Na pump impeller discharge height, in.	0.75	0.9	1.1	1.2
Na expansion tank volume, ft^3 (10% of system volume)	0.08	0.09		
Na in Be passages, ft^3	0.43	0.47		
Na in pressure shell, ft^3	0.15	0.15		
Na in pump and heat exchanger, ft^3	0.20	0.25		
Fuel-to-NaK Heat Exchanger				
Heat exchanger thickness, in.	1.7	2.75	4.65	5.9
Heat exchanger inside diameter, in.	42	42	44	47
Heat exchanger outside diameter, in.	45.4	47.5	53.3	58.8
Heat exchanger volume, ft^3	6	10	20	30
Angle between tubes and equatorial plane, deg	27	27	27	27
Number of tubes	2304	3744	6600	9072
Tube diameter, in.	0.1875	0.1875	0.1875	0.1875
Tube spacing, in.	0.2097	0.2097	0.2119	0.2094
Number of tube bundles	12	12	12	12
Tube arrangement in each bundle	8 × 24	13 × 24	22 × 25	28 × 27

TABLE 3.1. (continued)

Moderator Region				
Volume of Be plus fuel, ft^3	22.4	22.4	25.8	31.5
Volume of Be only, ft^3	21.1	21.1	24.0	28.8
No. of coolant holes in reflector	208	208	554	554
No. of coolant holes in island	86	86	210	210
Na coolant tube inside diameter, in.	0.155	0.187	0.187	0.218
Na coolant tube wall thickness, in.	0.016	0.016	0.016	0.016
Na pressure shell annulus thickness, in.	0.125	0.125	0.187	0.200

that the atomic density in the fuel region was only about 33% of that of liquid fluoride fuel. These shortcomings will be largely eliminated in a new critical experiment that is being planned. Sheet Teflon and 0.002-in.-thick uranium foil will be stacked in laminae to simulate the fluoride fuel, both from the standpoint of atomic density and of neutron-scattering and absorption cross sections.

Another weak point in the critical assemblies that have been run has been that the geometric approximation left much to be desired. It is planned that the sheet Teflon and the uranium foil will be cut to appropriate lengths to permit the construction of a configuration essentially the same as that envisioned for the full-scale reactor.

FUEL COMPOSITION AND PROPERTIES

It was assumed in the design work that the physical properties of the fluoride fuel at 1500°F would be similar to those of NaF-KF-LiF-UF_4 (10.9-43.5-44.5-1.1 mole %), which are, approximately, the following: heat capacity, 0.45 Btu/lb·°F; thermal conductivity, 2.6 Btu/hr·ft·°F; viscosity, 3 cp; density 2.0 g/cm^3. Heat transfer considerations show that such a fuel would be much better than the sodium-zirconium fuel that has been prepared for the ARE. If such a fuel were not developed, it would be necessary to increase the heat exchanger size given in the accompanying designs by a factor of 2 or 3. This would mean an increase in shield weight of about 6% and a serious increase in heat exchanger header complexity.

There are two possible ways of obtaining a satisfactory fuel. The first is to use the above-mentioned fluoride, or some modification of it, in a container fabricated of an alloy that has no chromium. This should eliminate the serious shortcoming of this particular fluoride mixture, that is, its tendency to form low-conductivity films of a highly insoluble potassium-chromium-fluoride mixture on surfaces in Inconel systems. Initial tests show Hastelloy B (80% Ni–20% Mo) to be a possible container material for this fluoride, and it will be tested in the coming months.

A second way to obtain a fuel with satisfactory physical properties is to test various melts that have compositions that seem promising, and such a program is now under way. Melts of seven different compositions containing lithium, sodium, rubidium, and beryllium are being prepared, and their physical properties are being determined. The best of these melts will be selected for corrosion test work.

MODERATOR REGIONS

Heat transfer analyses indicate that a sodium-cooled beryllium moderator is superior from the heat transfer standpoint to any other arrangement considered thus far.[3] Static and seesaw Inconel capsule tests show virtually no signs of corrosion or mass transfer at 1500°F for beryllium specimens immersed in sodium. However, it is felt that mass transfer in a larger-scale test loop operating with a substantial temperature differential and with the beryllium presenting the hottest surface in the system (as in a full-scale reactor) is very likely to be serious. A test loop to investigate this possibility has been designed, and it is scheduled to operate about February 1954. Should mass transfer prove to be serious, canned beryllium will be tested.

It is expected that the results of the multigroup reactor calculations will indicate what further moderator designs should be prepared and analyzed from the heat transfer standpoint to investigate the possibilities of exploiting lead and bismuth as moderator coolants. Lead and bismuth are

[3] R. W. Bussard *et al.*, *The Moderator Cooling System for the Reflector-Moderated Reactor*, ORNL-1517 (to be published).

interesting because of their high densities. Some metallurgical work is currently under way in an attempt to find a system that is satisfactory with respect to corrosion and mass transfer.

Some structural problems exist in designing the support of the reflector and the island. At first glance, it would appear that these assemblies hang from the flat decks that span the pump region. This would not be the case when the fluoride system had been filled, however, because the beryllium density (1.84 g/cm^3) would be somewhat less than the expected fuel density (about 2.0 g/cm^3) and hence the moderator region would tend to float in the fuel. With the moderator region

TABLE 3.2. HEAT TRANSFER SYSTEM CHARACTERISTICS FOR A SERIES OF REFLECTOR-MODERATED CIRCULATING-FUEL REACTORS

REACTOR POWER, megawatts	50	100	200	300
Fuel-to-Nak Heat Exchanger and Related Systems				
Fuel temperature drop, °F	400	400	400	400
NaK temperature rise, °F	400	400	400	400
Fuel ΔP in heat exchanger, psi	35	51	61	75
NaK ΔP in heat exchanger, psi	40	58	69	85
Fuel flow rate, lb/sec	263	527	1,053	1,580
NaK flow rate, lb/sec	474	948	1,896	2,844
Fuel flow rate, cfs	2.1	4.2	8.4	12.6
NaK flow rate, cfs	10.5	21.0	42.0	63.0
Fuel velocity in heat exchanger, fps	8.0	9.9	11.2	12.2
Fuel flow Reynolds number in heat exchanger	4,600	5,700	6,700	7,000
NaK velocity in heat exchanger, fps	36.4	44.9	50.9	55.4
Over-all heat transfer coefficient, Btu/hr·ft^2·°F	3,150	3,500	3,700	3,850
Fuel-NaK temperature difference, °F	95	100	110	115
Sodium-to-Nak Heat Exchanger and Related Systems				
Na temperature drop in heat exchanger, °F	100	150	150	150
NaK temperature rise in heat exchanger, °F	100	150	150	150
Na ΔP in heat exchanger, psi	7	7	7	7
NaK ΔP in heat exchanger, psi	7	7	7	7
Power generated in island, kw	500	1,000	2,000	3,000
Power generated in reflector, kw	1,700	3,400	7,500	11,200
Power generated in pressure shell, kw	190	350	500	620
Na flow rate in reflector, lb/sec	53	72	154	234
Na flow rate in island and pressure shell, lb/sec	22	28	51	76
Total Na flow rate, lb/sec	75	100	205	310
Na temperature rise in pressure shell, °F	28	39	30	26
Na ΔP in pressure shell, psi	4	6	6	6
Na temperature rise in island, °F	72	111	120	124
Na ΔP in island, psi	32	21	12	12
Na temperature rise in reflector, °F	100	150	150	150
Na ΔP in reflector, psi	36	27	18	18
Na-Nak temperature difference, °F	43			
Shield Cooling System				
Power generated in 6-in. lead layer, kw	110	210	300	350
Power generated in 24-in. H_2O layer, kw	<3	<6	<12	<18

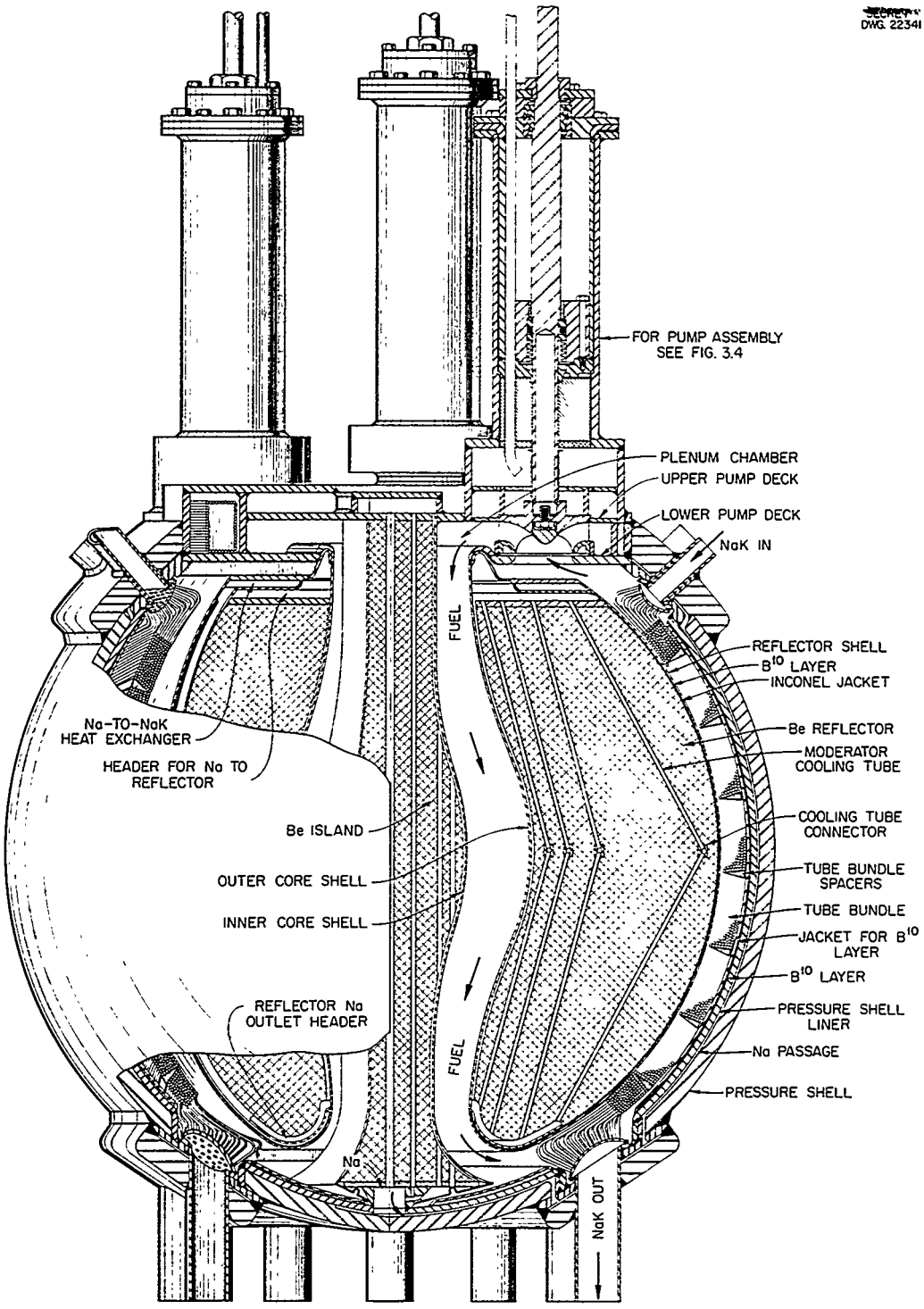

Fig. 3.1. 50-Megawatt Reflector-Moderated Reactor.

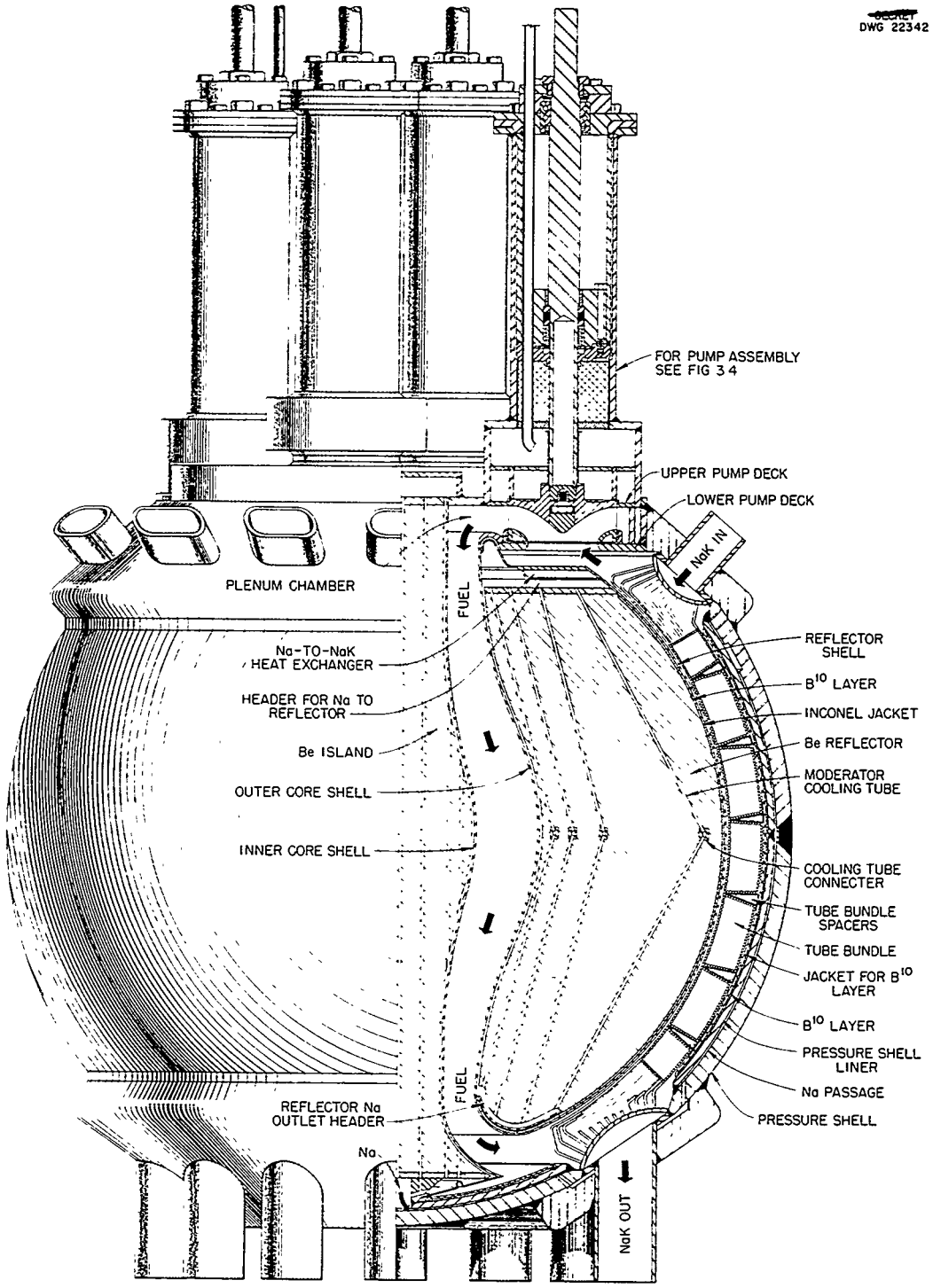

Fig. 3.2. 100-Megawatt Reflector-Moderated Reactor.

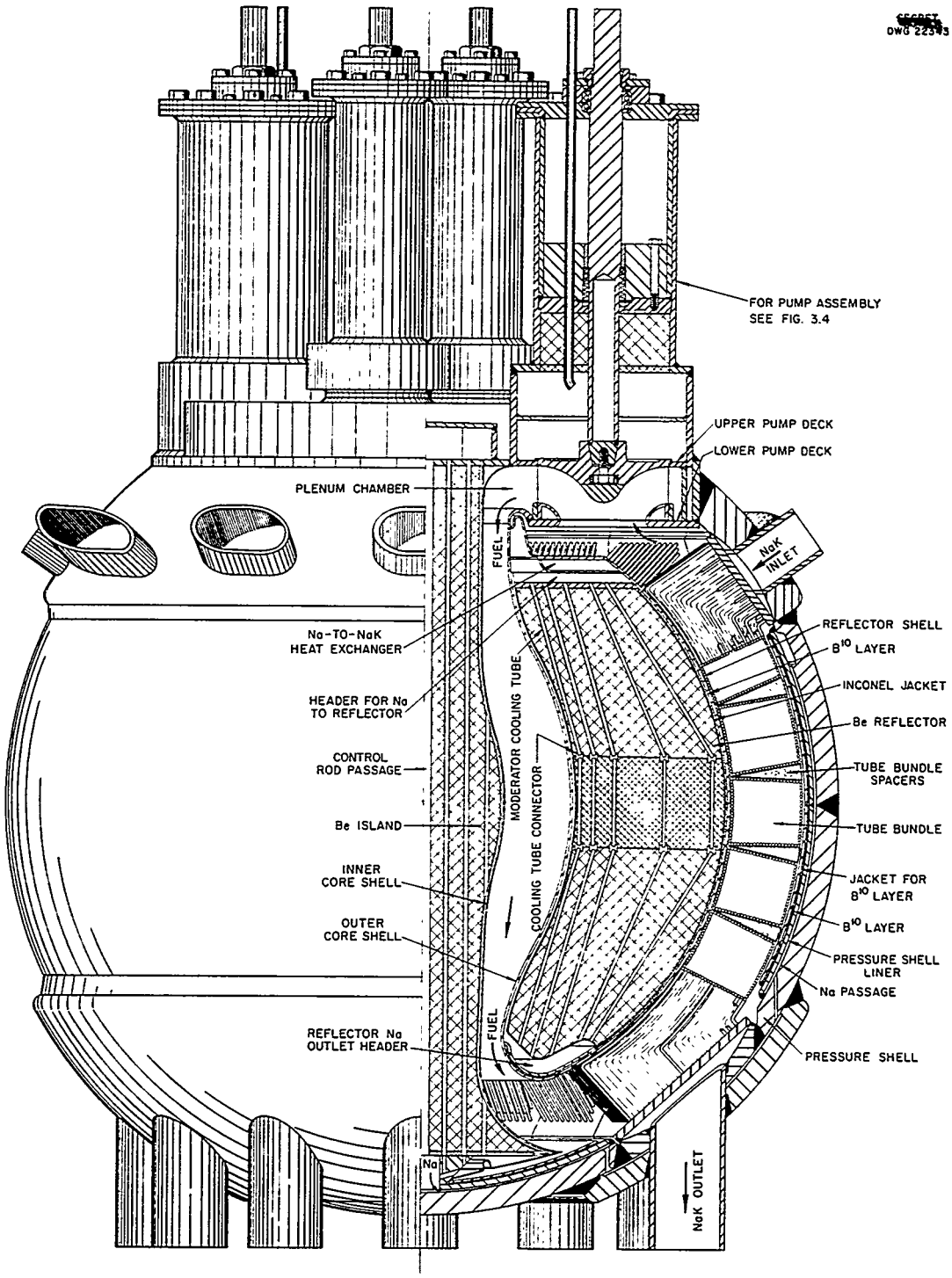

Fig. 3.3. 300-Megawatt Reflector-Moderated Reactor.

buoyed up by the fuel in an almost ideal "shock mounting," accelerations that would occur under crash landing conditions (in which vertical accelerations of as much as 10 g should be anticipated) would yield a net upward force on the reflector assembly that would be about equal to its weight. In the designs illustrated, the reflector assemblies are attached to the lower deck of the pump region by welds to the walls of the sodium return passages.

The sodium pump and heat exchanger subassemblies are positioned around the top edge of the upper pump deck. The pipe from the sodium pump discharge makes a slip fit into the reflector sodium inlet tube. The leakage through this slip fit into the sodium return passage simply recirculates with no penalty other than a small increase in the required pump capacity. The two sodium pump and heat exchanger assemblies could be welded in place by passing a bead around the lower edge at the outer periphery and up and across the top where they adjoin the plenum chamber between the two fuel pumps.

The reactor designs illustrated in Figs. 3.1, 3.2, and 3.3 presume that canning of the beryllium will be required but that trace leaks in the Inconel-to-can connections can be tolerated. Therefore the tubes passing through the rifle-drilled holes in the reflector are designed to be driven into tapered bores in the fittings shown at the equator, and the outer ends of these same tubes are to be rolled into their respective header sheets at the top and bottom. The tube connecting fittings at the equator also serve as dowels to locate the two beryllium hemispheres relative to each other.

HYDRODYNAMICS OF THE FUEL CIRCUIT

Hydrodynamic considerations impose a number of restraints on the geometry of the fuel passages in the reactor fuel circuit. These restraints are not sharply defined, but they are sufficiently rigid that they limit the fuel circuit proportions for a well-balanced design to a considerably narrower range than would at first be expected. The pressure drop through the heat exchanger goes up very rapidly with fuel flow rate – so much so that there is little to be gained by going to fuel velocities which correspond to pressure drops in the heat exchanger of greater than 80 psi. This is particularly true if an effort is made to keep the stresses in the core shells and heat exchanger tube walls to 500 psi or less. If the rest of the fuel system is examined carefully, it is evident that it should involve a pressure drop very much less than that across the heat exchanger in a well-balanced design. Thus, since a bleed-off-air turbine-pump-drive arrangement seems to be at once the lightest, simplest, and most flexible and since such a pump drive system should be designed to require less than 3% air bleed-off from the compressors, there seems to be a strong incentive to limit the pressure drop through the pump inlet and discharge passages and the core inlet and outlet ducts to not more than 15 psi.

If it is assumed that the reactor core diameter is determined by a compromise between shielding and other considerations and that the island diameter will be determined by fission density distribution considerations, it becomes evident that these two basic dimensions for the fuel circuit may be taken as a base for determining the proportions for the rest of the system. The inlet and outlet duct passage arrangements should be as small as possible to simplify the shielding problem and to reduce shield weight. However, it is of paramount importance that boundary-layer thickening and flow separation be avoided in the diffuser region at the inlet to the core. This, in turn, imposes a lower limit on the flow passage area that may be used at the core inlet. An asymmetric design might be employed in that this flow limitation would not apply to the outlet duct, particularly since a diffuser giving a reasonably high efficiency can probably be provided between that duct and the inlet to the heat exchanger. It is quite evident from this standpoint alone that further shielding tests should be made to investigate the effect of fuel duct size on over-all shield weight. While the problem is not clearly defined, it does appear from flow test work, as well as from analyses of the adverse pressure gradients along the diffuser walls in the core inlet region, that the outer diameter of the core inlet duct should be roughly 60% of the core diameter, while the inner diameter of that duct should be between 60 and 70% of the outer diameter.

The plenum chamber between the volute discharges and the core inlet ducts should provide for smooth transition and uniform velocity distribution at the inlet to the core. One promising way of accomplishing this would be to provide a plenum chamber having a height somewhat greater than the

thickness of the core inlet duct and a diameter at least half again as large as that of the inlet duct. The pump volutes could then be designed to give a fluid velocity entering the plenum chamber about equal to that in the core inlet duct. This would mean that for high power density reactors, for example, a 200-megawatt reactor with an 18-in.-dia core, the discharge annulus of a mixed flow impeller should be made as wide as possible so that it would approach the height of the plenum chamber. For low power density reactors, for example, a 50-megawatt reactor with an 18-in.-dia core, the disparity in these dimensions is inherently large. A careful examination of the magnitude of the eddy losses to be expected at the pump inlet, through the impeller, in the pump volute, and in the plenum chamber leads to the conclusion that the pump should be designed for an inlet velocity of not much more than about 30 fps, that is, a velocity giving a dynamic head of about 12 psi.

On the basis of these considerations, it is possible to specify dimensions for the principal fuel flow passages for a wide range of reactor power outputs. While the dimensions are given in Table 3.2, it should be noted that there is some latitude in the selection of these dimensions. Furthermore, it is clear that passages of larger size would require substantially heavier shields, while passages of substantially smaller size would be likely to give some sort of difficulty from the hydrodynamic standpoint.

Some preliminary flow tests were carried out a year ago,[4] and the results were encouraging. Additional flow tests are being made to determine whether the proportions indicated in Table 3.2 lead to a satisfactory configuration for a reactor designed for an output of 50 to 100 megawatts.

PUMP DESIGN

In examining the over-all system requirements, it becomes evident that it would be very desirable if the fuel pumps could perform several functions in addition to that of pumping the fuel. It seems likely that most of the xenon and possibly some of the other fission-product poisons might be removed from the fluoride mixture if helium could be bubbled through the fuel while it was being thoroughly agitated. Furthermore, it would be advantageous to have the pumps serve as mixing chambers in which high-uranium-content fuel could be added to the main fuel stream to enrich the mixture and compensate for burnup. Finally, it is essential that an expansion tank be provided so that entrainment of bubbles would not prove to be a problem in maneuvers or in "bumpy" flight.

The pump arrangement shown in Fig. 3.4 was worked out to provide for all the points mentioned above. The pump design embodies a variation of an idea tested three years ago.[5] The back of the impeller is used to centrifuge out the gas bubbles. The design also uses the overhung impeller, the bearing arrangement, and the face-type gas seal of the previous pump, along with several features that have proved to be successful in sump pump test work during the past year. The principles of operation are quite simple and have been demonstrated with a plastic model. The fuel in the expansion tank above the impeller tends to swirl in the same direction as the impeller (but at a lower speed) so that it forms a vortex with a roughly conical free surface. A relatively large amount of fluid leaks from the high-pressure region at the impeller outlet through the labyrinth seal at the periphery of the impeller into the swirl chamber immediately above the impeller. Since this swirl chamber is connected through a bypass line to the impeller inlet, the leakage is simply recirculated at no cost other than an increase in pumping power. Some fluid leaks upward through the clearance between the top lip of the swirl chamber and the outside of the centrifuge cup on the back face of the impeller, but this leakage rate is small because there is little pressure differential across this gap. The leakage that does occur is made up by bleed flow from small holes in the periphery of the centrifuge cup on the back of the impeller. Thus there is a small, continuous flow from the fluid vortex in the expansion tank into the centrifuge cup and thence into the swirl chamber. The fluid region close to the surface of the vortex in the expansion tank is highly turbulent and full of bubbles so that it should be effective in degassing the fuel.

In initial tests of a water pump with the above-mentioned features, the pump continued to pump when it was inverted for as much as a minute before the liquid supply in the centrifuge cup and

[4] R. E. Ball, *Investigation of the Fluid Flow Pattern in a Model of the "Fireball" Reactor*, ORNL Y-F15-11 (Sept. 4, 1952).

[5] A. P. Fraas, *Progress Report on Stainless Steel Acid Pump Reworked to Test Special Features for Operation with Liquid Metals*, ORNL Y-F15-6 (Feb. 1, 1951).

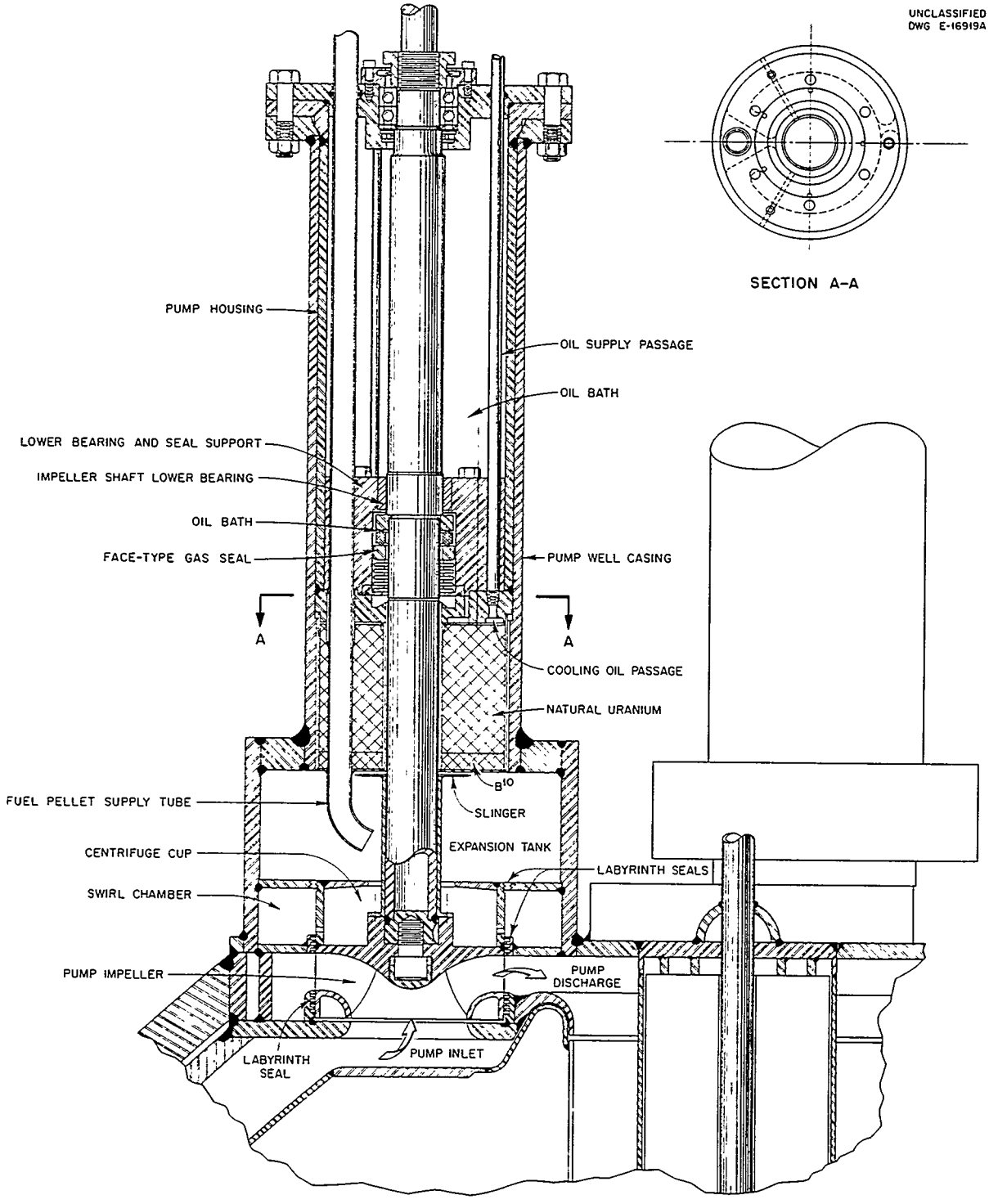

Fig. 3.4. Gas-Sealed Aircraft Pump.

swirl chamber was depleted by fluid leakage from the swirl chamber into the expansion tank. The slinger ring on the impeller shaft at the top of the expansion tank acts to throw the fluid away from the shaft when the pump is inverted and thus prevent flow into the clearance around the shaft between the slinger and the face-type gas seal.

A number of other special features have been included in the pump design to adapt it to the full-scale reactor shield. The pump has been designed so that it can be removed or installed as a subassembly with the impeller, shaft, seals, and bearings in a single compact unit. As can be seen from Figs. 3.1 and 3.4, this assembly fits into the bore of a cylindrical casing welded to the top of the reactor pressure shell. A 3-in. layer of uranium just above a ½-in. layer of B^{10} around the lower part of the impeller shaft is at the same level as the reactor gamma shield just outside the pressure shell. The steel seal and bearing support above the layer of uranium gives additional gamma shielding, while the oil-filled cavity between the bearings acts as neutron shielding. An air-driven turbine and gear box could be mounted on the flange at the upper end of the pump casing. Since the outer surface of this casing was designed to be about 8 in. inside the outer surface of the shield, there need be no protuberances from the shield surface in the final installation. The long, slender, "pill supply" tube for fuel enrichment is sufficiently small that it should not permit much gamma leakage.

The large amount of impeller shaft overhang inherent in the design of the pump could be avoided if a journal bearing could be operated with the molten fluoride mixture acting as the lubricant. The pump impeller and volute could be designed so that the radial load on such a bearing would be very small, perhaps not more than 25 psi. Since the viscosity of the fluoride mixture is greater than that of water, the arrangement should be completely satisfactory after the pump was started. Pickup and scuffing of the bearing or shaft during startup or shutdown might prove to be problems. A test rig for investigating the compatibility of different materials in sodium at high temperature has been built and is being used to evaluate the compatibility of various material combinations in fluorides (cf., sec. 2). Preliminary results are encouraging.

PRESSURE SHELL

As much as ½% of the reactor output may go into gamma heating of the pressure shell. The provision for the removal of this heat presents several design choices, none of which is entirely satisfactory. If no provision is made for cooling the pressure shell, it will be much hotter than the fluoride mixture that contacts its inner surface. Unfortunately, this would give the highest pressure shell temperatures in precisely the zone in which the stresses are the highest, that is, in the ligaments between the NaK ducts in the lower header region. The pressure shell might be cooled with the coolant system that serves the lead gamma shield, but this would make temperature control difficult over a wide range of power outputs because of the inherently large temperature differential. Furthermore, it would make necessary the dumping of large amounts of heat at a low temperature level through the shield coolant radiator – a costly matter in an airplane. Cooling of the pressure shell with sodium from the island moderator cooling system has the disadvantage of complicating the pressure shell construction, but it has many advantages. It provides a simple way of returning the sodium that has passed through the island cooling passages to the sodium-to-NaK heat exchanger. It not only serves to cool the pressure shell in the critically stressed fuel discharge end of the reactor so that the creep strength of the Inconel there becomes more than adequate, but it makes it possible to maintain the entire pressure shell at an essentially uniform temperature. This should markedly reduce both thermal distortion and clearance buildups resulting from differential thermal expansion between the pressure shell, heat exchanger tube bundles, and the reflector.

The construction envisioned is shown in Figs. 3.1, 3.2, and 3.3. The inner liner assembly consists of a ⅜-in.-thick Inconel shell, a ⅛-in. hot-pressed B^{10} layer, and an inner 0.062-in.-thick Inconel can. Inconel is also used to cover the interior of the pressure shell between the two end headers. Closely spaced grooves, ⅛ in. deep and 2 in. wide, milled into the outer surface of the liner provide ample flow passage area for the sodium to flow upward. Four transfer tubes carry the sodium from the top of the pressure shell to the outer face of the pressure shell at the sodium-to-NaK heat exchanger inlets. The hot-pressed

boron blocks are diamond-shaped, with 60-deg angles at their vertexes, and they have rabbeted edges. This design permits the covering of a spherical surface with a single block size and shape.

The construction in the vicinity of the end header regions was deliberately varied in Figs. 3.1, 3.2, and 3.3 to show three different ways in which the detail design may be handled. Another design would involve the use of a pressure shell with forged annular protuberances to receive the headers, while yet another possibility would be a shell sufficiently thick (about 2.5 in.) to permit machining annular grooves for the headers. This latter arrangement would have the advantage of a more regular exterior surface on the pressure shell.

FUEL-TO-NaK HEAT EXCHANGER

The heat exchanger envisioned for the reflector-moderated reactors is similar to that described previously.[6] The major unknowns in the fuel-to-NaK heat exchanger are concerned with fabrication. It is presumed that the tube-to-header connections would be heliarc welded by hand, as in the 210-tube six-tube-bundle fluoride-to-NaK heat exchanger presently being tested. It is expected that a large amount of welding research and component testing will be required to obtain a satisfactory solution to this tube-to-header welding problem.

The tube bundles are separated by long cans that are triangular in cross section and parallel the tubes. The cans would be filled with hot-pressed B^{10} to assist in inhibiting the low-energy neutron flux in the heat exchanger region.

REACTOR CONTROLS

One of the salient features of the circulating-fuel reactor is its inherent stability. It appears that no fast-moving control rods will be required to cope with fast transients. No large amounts of shim control are required to compensate for burnup, because a uranium-rich fluoride can be added at intervals during the course of operation. The only important control needed is a means of varying the mean operating temperature. In examining over-all power plant considerations, it appeared that provision for effecting a temperature change of 200°F should be included in the design (that is, about 3% $\Delta k/k$). It appears from critical experiments that this could be provided by a $\frac{3}{8}$-in.-OD tube filled with B^{10} and placed to give a 27-in. stroke from the pump deck down through the center of the island. While the rod and its actuating mechanism are not shown in designs illustrated, a 0.50-in.-ID tube has been provided through the center of the island to receive the rod. In the design contemplated, the rod would be machined from a thick-walled tube to give three equally spaced $\frac{1}{16}$-in.-high ridges along its entire length. These ridges would serve to center the rod in the passage provided and thus give uniform flow of sodium coolant around the rod periphery. The ridges would also engage a grooved guide at the upper end to prevent rotation. A short length of $\frac{5}{8}$-in.,-10 thread at the top of the rod would be engaged by an internally threaded tube enclosed in a casing extending up through the shield. The tube would be rotated by a drive at the top end through a bellows seal. This seal would be brazed to the center of a bar with three spherical bearings, one at each end and one in the center. This bar would be inclined at an angle of about 15 deg to the axis of the control rod drive tube. The center bearing would be fixed relative to the rod casing, while a crank attached to the upper end of the control rod drive tube would be attached to the lower spherical bearing. As the rod drive tube rotated, the axis of the drive bar would generate a cone, with the centers of the spherical bearings at its upper and lower ends generating circles. The drive actuator would be an electric motor and gear box connected to the upper spherical bearing. The closed end of the bellows at the center bearing would describe a wobble-plate type of motion.

The fuel enrichment system that appears most attractive is based on the use of cold-pressed disks of Na_2UF_6 about $\frac{1}{2}$ in. in diameter and $\frac{1}{4}$ in. high. These disks could be fed to the tops of the fuel addition tubes in the pumps by means of a relatively simple "pill vending" machine. Several promising detail designs of such machines have been prepared from which it appears that this phase of the development should not prove to be a serious problem. However, it may be difficult to prevent the fuel in the expansion tank from entering, freezing, and blocking the fuel enrichment tube during inadvertent inverted flight. The pump design has been worked out so that this should not happen,

[6] A. P. Fraas and M. E. LaVerne, *Heat Exchanger Design Charts*, ORNL-1330 (Dec. 7, 1952).

but the effectiveness of this feature of the swirl expansion tank design has not yet been checked.

SHIELDING

A substantial amount of fundamental work on the shielding problems of the reflector-moderated reactor has been covered in other reports.[2,7,8] Three important factors remain undetermined: namely, the energy spectrum of the short half-lived fission-product gammas, the effect of variations in end duct and in fuel pump and header tank geometry, and the possibilities in the use of unusual materials such as lithium hydride. Tests have been carefully planned to provide the essential design data necessary for determining the first two of these factors during the coming months, and a long-range program is contemplated for investigating unusual materials. It is hoped that a shielding experiment that is to be carried out in conjunction with a critical experiment will yield data that will validate the use of multigroup, multiregion calculations as an aid in shield analysis.

Analyses of the effects of the neutron-to-gamma dose ratio and of varying proportions of gamma shielding on shield weight are being made. The strength of lead and bismuth alloys at temperatures of 250 to 350°F, shield design for jet fuels in place of water, shield heat removal, and the dose from the shield after shutdown are also subjects currently being investigated.

FILLING AND DRAINING OF THE REACTOR

After 100 hr or more of full-power operation, the fuel charge will require roughly 10 in. of lead shielding to bring the radiation from it down to a level of 1 r/hr at 5 feet. This will mean that a tank to contain the roughly 4 ft^3 of fuel required for a 50-megawatt reactor will require about 10 tons of lead shielding. This could be mounted on a heavily constructed dolly or on an elevator designed to raise it up from a pit under the runway. A cooling system to remove the afterheat from the fuel will also be required. Preliminary estimates indicate that the afterheat can be removed most readily by circulating a liquid metal through a coiled tube in the fluoride drain tank and then through a radiator to dump the heat to air forced through the radiator by a blower. Such a system should be reasonably light, compact, and mobile.

The filling and draining operation could be carried out by carefully positioning the airplane over the tank after removing a vertical plug, perhaps 5 in. in diameter, from the bottom of the reactor shield. The shielded tank assembly with a pipe extending vertically upward from it could be raised so that the pipe would project into the hole in the shield. A coupling at the upper end of the pipe would engage a corresponding coupling at the bottom of the reactor pressure shell. The space between the drain valve at the bottom of the reactor and the valve at the top of the pipe from the drain tank could then be evacuated, the drain tank valve and the reactor drain valve opened, and the fuel drained. A blast of helium directed through appropriate fittings could be used to blow out the fuel droplets between the valves. The valves could then be closed, the tank disconnected, lowered, and dropped into its pit or removed to a suitable location. The reverse procedure could be followed in the filling operation. Helium pressure on the liquid in the shielded tank would serve to force the fuel up into the reactor.

The biggest problem in the design of a system of this sort is the detail design of the valves and the remotely operated coupling to get the high degree of leak tightness and exceptional reliability required. Several rough preliminary layouts have been sketched and work is proceeding in an effort to develop valves and couplings that could be used for routine filling and draining operations in current ORNL experimental laboratory work.

---

[7] *Report of the 1953 Summer Shielding Session*, ORNL-1575 (to be published).

[8] F. H. Abernathy *et al.*, *Lid Tank Shielding Tests of the Reflector-Moderated Reactor*, ORNL-1616 (to be published).

4. CRITICAL EXPERIMENTS

A. D. Callihan D. V. P. Williams H. Lynn
Physics Division
J. W. Noaks, Pratt and Whitney Aircraft Division

The Critical Experiment Facility at the Oak Ridge National Laboratory may be used to determine the static physics characteristics of a wide variety of reactor mockups. During the past quarter, measurements were completed on a mockup of an air-cooled, water-moderated reactor (AC-1) for the General Electric Aircraft Nuclear Propulsion Project, and preparations were made for measurements on a mockup of a Pratt and Whitney supercritical-water reactor, a Nuclear Development Associates sodium-cooled reactor, and the ORNL's reflector-moderated reactor (cf., sec. 3, "The Reflector-Moderated Reactor").

The air-cycle reactor (AC-1) mockup was an approximated cylinder 27 in. in length, 30 in. in diameter, surrounded by a $7\frac{1}{2}$-ft-thick beryllium reflector. The fuel elements and the uranium distribution were simulated by properly spaced uranium disks sandwiched between mild steel which represented the structural materials of the reactor. Each fuel element was surrounded by a 1-in.-thick layer of Plexiglas to simulate the water moderator. The originally designed assembly was an octagonal array of 37 fuel channels. This system, however, could not be made critical with the 7.5-in.-thick beryllium reflector until the number of fuel channels had been increased to 43 and five channels had been loaded with twice the uranium prescribed. The critical loading was then 29.8 kg of U^{235} with 98.9 kg of steel. Flux and power distributions have been determined throughout the core and reflector. The data will be reported in detail in a topical report to be issued by ORNL when the experiment is complete and are discussed in General Electric's Engineering Progress Reports.

Part II

MATERIALS RESEARCH

INTRODUCTION AND SUMMARY

The research on high-temperature liquids for reactors has been primarily concerned with the determination of phase diagrams of fluoride and chloride systems with and without fissionable material, although a substantial effort has been devoted to the production and purification of halides and hydroxides (sec. 5). Detailed study of the $NaF-ZrF_4-UF_4$ system has continued because of its intended application in the Aircraft Reactor Experiment, wherein Na_2UF_6 will be added to $NaZrF_5$ to produce a suitable fuel. Techniques such as quenching, petrographic and x-ray analysis, differential thermal analysis, and high-temperature filtration, as well as the customary thermal analyses, have been applied to the binary and ternary systems $NaF-ZrF_4$ and $NaF-ZrF_4-UF_4$. Spectrophotometric measurements of fused salts containing UF_4 show only two absorption-spectrum patterns in the $NaF-ZrF_4-UF_4$ system. Some physical property data substantiate the concept that the fused salts are essentially totally ionized. A number of fluoride samples were purified in the laboratory for various tests while the facilities for the routine production of these fluoride mixtures are being constructed. In an examination of various phases of fluoride purification techniques, it was found that the reduction rate of Na_2UF_6 by hydrogen increases with temperature. The reducing power of NaH when added to $NaZrF_5$ is being studied, as well as the kinetics of the H_2 reduction of Ni^{++} in $NaZrF_5$. Chemical studies of hydroxides were limited to the purification of NaOH and $Sr(OH)_2$ and the determination of the carbonaceous content of NaOH at 700°C.

The recent corrosion studies have been devoted almost entirely to the effects of various parameters on the corrosion of Inconel by fluorides, although some work with hydroxides and liquid metals was continued (sec. 6). Studies of the corrosion of Inconel by the fluoride fuel $NaF-ZrF_4-UF_4$ (50-46-4 mole %) have substantiated earlier conclusions that the total attack in 500 hr is independent of temperature from 1500 to 1650°F and that the attack rate is time dependent. The value of having purified fluoride melts in clean container systems has been investigated not only with regard to the metallic fluoride impurities in the melt, the concentration of which may be directly correlated with corrosive attack, but also with regard to contamination of the container surface, which has a less deleterious effect. Pretreatments of the fuel with chromium and Inconel, as well as the precirculation of fuel, have each been effective in reducing attack, and an observed correlation between depth of attack and surface-to-volume ratio of the Inconel and fluoride also indicates that the impurities in the fluorides are the major factor in corrosion. The attack by fluorides on Inconel at 1500°F apparently increases in intensity, although not in maximum depth, as the UF_4 content of the melt is increased from 0 to 6.5 mole %. Static tests of various combinations of metals in fluorides at 1500°F have shown that one of the metals is attacked to a greater extent than the other, even though the heavily attacked metal may be relatively unattacked when alone in the fluoride. The fluoride fuel $NaF-ZrF_4-UF_4$ (50-46-4 mole %) has also been circulated in nickel and type 430 stainless steel loops for 500 hr at 1500°F; no plugging occurred, but some mass transfer was observed in the stainless steel loop. A number of metal specimens were tested in circulating lead in quartz thermal convection loops. Of the metals tested, oxidized types 347 and 304 stainless steel and molybdenum-nickel alloy produced the least mass transfer. Other liquid metal studies included tests of Inconel, stainless steels, and potential bearing materials in lithium, sodium, and lead. The more fundamental corrosion studies included the determination of the equilibrium pressure of hydrogen in hydroxide metal systems and an attempt to determine the chemical equilibria for the postulated fluoride corrosion which results in the selective leaching of chromium from Inconel.

The fabrication of high-performance radiators and high-conductivity radiator fins represents the major undertaking of the metallurgical research program, which also included stress-rupture tests of Inconel, the forming of special alloys, the fabrication of solid fuel elements, and the development of ceramic materials (sec. 7). Although Inconel-clad copper fins are inadequate because of diffusion of nickel into the copper, a copper-aluminum bronze fin and types 310 or 346 stainless steel clad copper fins have been fabricated and satisfactorily brazed to Inconel or stainless steel tubing with a number of special brazing alloys. The technique of "backing-up" the heliarc-welded

radiator joints with a brazing alloy produces sound, leak-tight radiators. The stress-rupture life of Inconel under various combinations of temperature, stress, and environment is being measured; the tests at 3500 psi and 1500°F show that, as far as rupture life is concerned, air is the most beneficial environment and hydrogen the most deleterious. Stress-rupture data are also being obtained for Inconel tubes and for fine- and coarse-grained Inconel sheet. The limited effort on solid fuel elements has been confined to the drawing of tubular fuel elements and the plug welding of stainless steel-clad fuel plates, both of which were effected with some success. Inconel tubing for experimental equipment is being drawn satisfactorily with reductions as high as 36%. The rolling of various metals and alloys was effected: columbium sheet after an 87.5% reduction at 1100°F showed complete recrystallization.

The physical properties of several fluorides and metal alloys have been measured at temperatures of up to 1000°C, and the heat transfer characteristics of reactor coolants are being studied in various systems (sec. 8). The viscosity and density of the ARE fuel concentrate, Na_2UF_6, and the vapor pressure of the fuel solvent, $NaZrF_5$, have been measured. All these values are in line with those anticipated for these materials. Other heat capacity, thermal conductivity, density, and vapor pressure data for fluoride compositions of interest have been obtained. Measurements of the velocity in a thermal convection loop indicate that the radial temperature gradients cause turbulence in the liquid flow at Reynolds numbers above 100; the laminar flow solutions for flow in this regime are thus in serious error. Forced-convection heat transfer data with the NaF-KF-LiF eutectic in nickel and in Inconel tubes have been confirmed; the heat transfer in Inconel is less than that in nickel because of film formation. Preliminary data are available on a forced-flow heat transfer experiment in the laminar flow regime, and apparatus is being prepared for measurements of fluid flow in an annulus and for studies of surface-boiling phenomena.

The radiation damage program included studies of the stability of fluoride mixtures in Inconel and determinations of the creep of metals under irradiation, as well as the construction of the in-pile circulating loop (sec. 9). Although Inconel capsules containing fluorides show more tendency toward intergranular corrosion under irradiation than they do in out-of-pile control tests, there is no definite trend in corrosion behavior that can be correlated with either irradiation time (from 53 to 810 hr) or irradiation level (from 230 to 8000 watts/cm^3). There were no in-pile creep tests made in the LITR or in the MTR during this quarter, because more reliable apparatus for creep measurements in both these irradiation facilities was being developed and constructed. The in-pile circulating loop, types of which will be used for forced-convection corrosion tests in the LITR and in the MTR, is being fabricated and assembled.

The analytical studies of reactor materials included chemical, spectrometric, and petrographic analyses of fuel composition and corrosion products (sec. 10). The chemical analyses were primarily concerned with the oxidation states of the constituents and the metallic corrosion products in the various fluoride mixtures. Techniques were established for determining the amounts of FeF_2, CrF_2, and UF_3 in fluoride fuel mixtures, as well as the reducing power of $NaZrF_5$. None of a number of solvents tested were as effective for dissolving the proposed fluoride fuels from the walls of metal containers as the nitric and boric acid mixtures which are currently used. Petrographic examination of a number of irradiated and unirradiated fuel samples did not reveal any differences in the two species. A technique has been developed by which the mass spectrometer may provide a measurement of the uranium burnup (due to irradiation), as well as a quantitative analysis of the uranium in the fuel.

5. CHEMISTRY OF HIGH-TEMPERATURE LIQUIDS

W. R. Grimes
Materials Chemistry Division

Exploratory investigations of phase equilibria in fused salt systems by the simple thermal analysis technique have been extended to a number of chloride systems containing UCl_4 and UCl_3 as the fissionable components, as well as to examination of several fluoride systems with and without uranium that are of possible interest as fuels, fuel solvents, or coolants. In addition, the thermal analysis technique has been applied to a number of previously studied systems in attempts to verify some doubtful values in various regions or to amplify data for regions in which previous experimentation was limited.

During the past several months, other techniques useful for more refined studies of systems previously shown to be valuable have been developed and perfected. These techniques, especially quenching, with petrographic and x-ray examination of the solids, differential thermal analysis, and high-temperature filtration, have been applied, in general, to the binary and ternary systems $NaF\text{-}ZrF_4$ and $NaF\text{-}ZrF_4\text{-}UF_4$. While it is not yet possible to interpret even the binary system uniquely, it appears that combining the data obtained by these techniques and the thermal analysis data will permit rapid progress to be made.

Spectrophotometric measurements of the absorption spectra of UF_4 and UF_3 in fused salts were made. Only two absorption spectrum patterns were found for glasses from the $NaF\text{-}ZrF_4\text{-}UF_4$ system. Glasses were obtained with compositions of between 16.65 and 50 mole % UF_3 in the $ZrF_4\text{-}UF_3$ binary system.

Additional electrolyses of various solutions of metal chlorides in potassium chloride were made. Erratic results obtained with chromium anodes have been ascribed tentatively to oxidation of the chromium. When a thin plate of nickel was used to protect zirconium electrodes from oxidation, reproducible emf's were observed.

Measurements of the density and electrical conductivity of the fused salt system LiCl-KCl are indicative of considerable short-range order persisting in these high-temperature fluids; these and other measurements substantiate the concept that fused salts are essentially totally ionized.

Facilities for the production of a variety of fluoride compositions are being prepared and laboratory-scale production is to be discontinued, except for the preparation of small enriched-uranium-bearing specimens for radiation stability tests. A number of small fluoride samples were purified for phase equilibria studies, plans were made for producing the enriched material for the in-pile loop experiments, and various simple structural metal fluorides were prepared for corrosion studies.

In a study of the reduction of Na_2UF_6 by hydrogen it was found that the rate of reduction increased as a function of temperature. A further check on the possibility of retaining reducing species in $NaZrF_5$ melts was attempted by treating $NaZrF_5$ with NaH, and the kinetics of the reduction of Ni^{++} in $NaZrF_5$ by H_2 at 800°C was studied because of the importance of this reduction in fluoride purification procedures. Studies of the reaction of sodium hydroxide with carbonaceous matter suggest that it would not be possible to maintain sodium hydroxide free from carbonate at high temperatures in metals which contain appreciable quantities of carbon.

THERMAL ANALYSIS OF FLUORIDE SYSTEMS

C. J. Barton L. M. Bratcher
J. Truitt
Materials Chemistry Division

Additional data that are believed to be more reliable than some obtained early in the phase study program were obtained on a number of binary and ternary fluoride systems. Revised diagrams will be published in topical reports when the studies are completed. Although some data for compositions in the $NaF\text{-}ZrF_4\text{-}UF_4$ system were obtained by the thermal analysis technique, it is expected that the major emphasis will be placed upon other techniques for study of this system.

$NaF\text{-}ZrF_4\text{-}UF_4$

The probable existence of a ternary eutectic $NaF\text{-}ZrF_4\text{-}UF_4$ (63.5-19.0-17.5 mole %) with a melting point of 600°C was mentioned in the previous report. Closer study of this region has

shown that this composition is probably near the bottom of a very narrow valley extending down toward the Na_2ZrF_6-$NaZrF_5$ eutectic. Additional data between the 40 to 50 mole % NaF lines at several uranium concentration levels essentially confirmed the location of the isotherms in this region that are shown in the published diagram for the system.[1] Data for the 75% NaF mixtures are shown in Fig. 5.1. These data indicate solid solution formation between Na_3ZrF_7 and Na_3UF_7 over a wide range of compositions, and they have been confirmed by other methods (cf., subsection on "Filtration Analysis of the NaF-ZrF_4-UF_4 System"). Thermal data obtained from sealed capsules of ternary mixtures containing more than 75% NaF have, in general, indicated melting points that were lower than had been anticipated for this region and lower than had been indicated by the few runs made previously. Further study of this system by other methods is planned.

[1] L. M. Bratcher, R. E. Traber, Jr., and C. J. Barton, *ANP Quar. Prog. Rep. Sept. 10, 1952*, ORNL-1375, Fig. 41, p. 78.

RbF-LiF-UF_4

Data for the system RbF-LiF-UF_4 were published in a previous report.[2] Additional data obtained during this quarter confirmed the existence of two low-melting-point regions in the ternary system, one close to the RbF-LiF binary eutectic and the other in the vicinity of the LiF-UF_4 eutectic. These data indicate that revision of the isotherms shown in the published diagram is needed. It appears to be rather difficult to obtain reproducible thermal data in this system, possibly because of the oxygen introduced into the mixtures by the hygroscopic alkali fluorides.

NaF-ThF_4

Thermal analysis of the system NaF-ThF_4, supplemented by petrographic study of a number of slowly cooled compositions, continued during this quarter. It seems to be a difficult matter to prepare

[2] J. P. Blakely *et al.*, *ANP Quar. Prog. Rep. Sept. 10, 1951*, ORNL-1154, Fig. 13.3, p. 159.

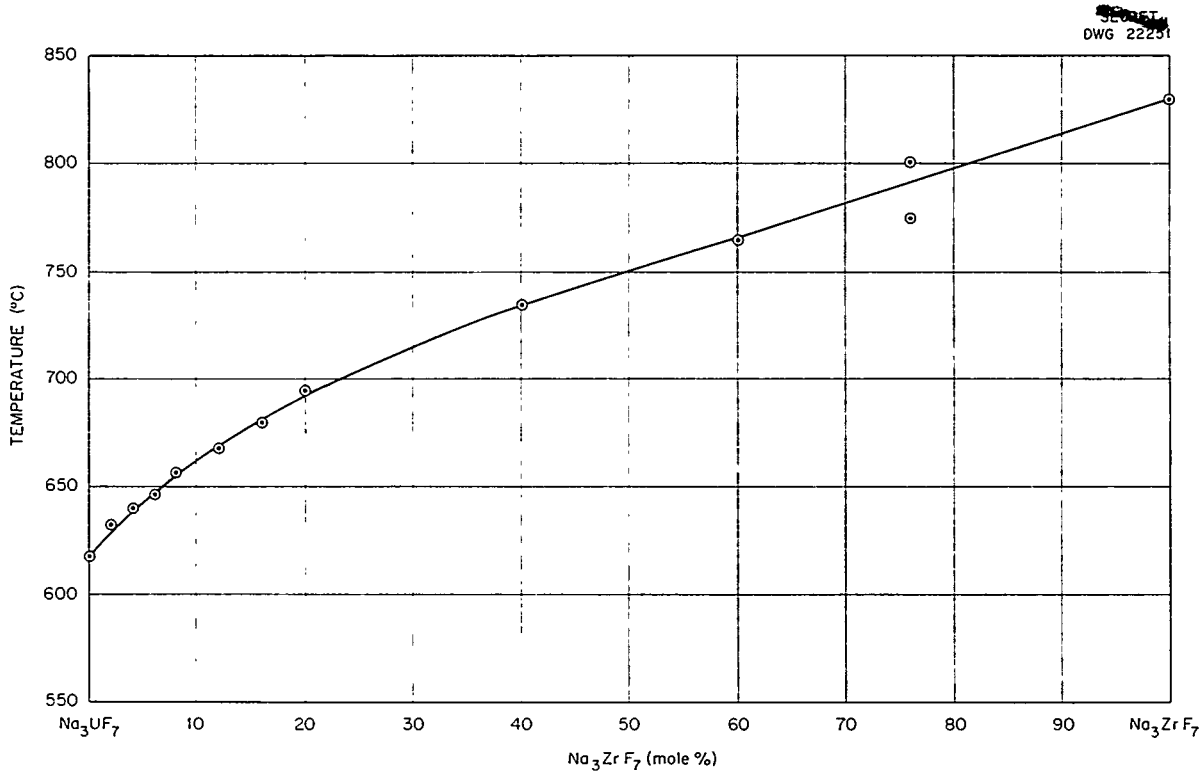

Fig. 5.1. The System Na_3UF_7-Na_3ZrF_7.

compounds in this system in the pure, well-crystallized condition needed for petrographic identification. Two crystalline phases have been observed, and one of them is believed to be Na_2ThF_6, the identity of the other is still uncertain. Further study will be required before a satisfactory equilibrium diagram for the system can be prepared.

LiF-RbF-BeF_2

Thermal data were obtained in the system LiF-RbF-BeF_2 for 50 compositions with up to a BeF_2 concentration of 60 mole %. The lowest melting point observed with these mixtures was 345°C for material containing (in mole %) 37% LiF, 8% RbF, and 55% BeF_2. The composition of this material is close to that of the LiF-BeF_2 binary eutectic reported to melt at 356°C.[3] It appears unlikely that compositions with melting points substantially lower than 350°C exist in this system, except possibly in the high BeF_2 region which is not amenable to thermal analysis; materials with such high BeF_2 concentration would probably be of little interest in the reactor program because of their probable high viscosity. These results are similar to those reported previously for the KF-LiF-Be_2 system.[4]

RbF-BeF_2-ZrF_4

The system RbF-BeF_2-ZrF_4 was investigated with ZrF_4 concentrations of up to 50 mole % and with BeF_2 concentrations of up to 60 mole %. Halts in the cooling curves at temperatures near 300°C were observed for several compositions in this system. It is likely that the lowest thermal effects observed can be attributed to a solid-phase transition, since the RbF-BeF_2 and RbF-ZrF_4 binary systems showed thermal effects in the 300 to 350°C temperature range which were almost certainly due to such transition. No liquidus temperatures significantly lower than 380°C (the minimum melting point in the RbF-BeF_2 system) were observed with the compositions tested.

THERMAL ANALYSIS OF CHLORIDE SYSTEMS

C. J. Barton S. A. Boyer
Materials Chemistry Division

The UCl_3 used for most of the phase studies of chloride systems made this quarter was prepared by the Y-12 Chemical Division by hydrogenation of UCl_4. The melting point (840°C) obtained for this material agrees well with the melting point of 842 ± 5°C reported by Kraus.[5] Uranium and chloride analyses of the as-received material checked with the theoretical values very closely; however, slight hydrolysis of the material occurs on heating, even when considerable precaution is taken to avoid exposure.

LiCl-UCl_3

Thermal data obtained with a number of compositions in the system LiCl-UCl_3 are shown in Fig. 5.2. The only eutectic in the system contains approximately 25 mole % UCl_3 and melts at 495 ± 5°C. This is apparently the lowest melting alkali chloride–UCl_3 binary eutectic. The thermal data gave no indication of compound formation in this system, but, since the solid phases have not yet been studied, the absence of incongruently melting compounds is not completely demonstrated.

NaCl-UCl_3

An equilibrium diagram for the system NaCl-UCl_3 was reported by Kraus,[5] who stated that there were no compounds formed by these components. Thermal data obtained with nine mixtures containing 33 to 85 mole % UCl_3 are in reasonable agreement with Kraus' data. However, the absence of the eutectic break in the cooling curves for the mixtures containing 65 mole % UCl_3 or more seems to indicate the possibility of compound formation in the high UCl_3 region. A thermal effect at 415 ± 5°C throughout the region studied here, which was not reported by Kraus, could be due to a solid transition of a compound in the system.

KCl-UCl_3

Kraus also published an equilibrium diagram for the system KCl-UCl_3.[5] Thermal analysis of the system in this laboratory with mixtures containing 12 to 65 mole % UCl_3 has essentially verified Kraus' data. The maximum difference in liquidus temperatures in the two studies was about 15°C.

[3] D. M. Roy, R. Roy, and E. F. Osborn, *J. Am. Ceramic Soc.* 33, 85 (1950).

[4] L. M. Bratcher and C. J. Barton, *ANP Quar. Prog. Rep. March 10, 1953*, ORNL-1515, p. 113.

[5] C. A. Kraus, *Phase Diagrams of Some Complex Salts of Uranium with Halides of the Alkali and Alkaline Earth Metals*, M-251 (July 1, 1943).

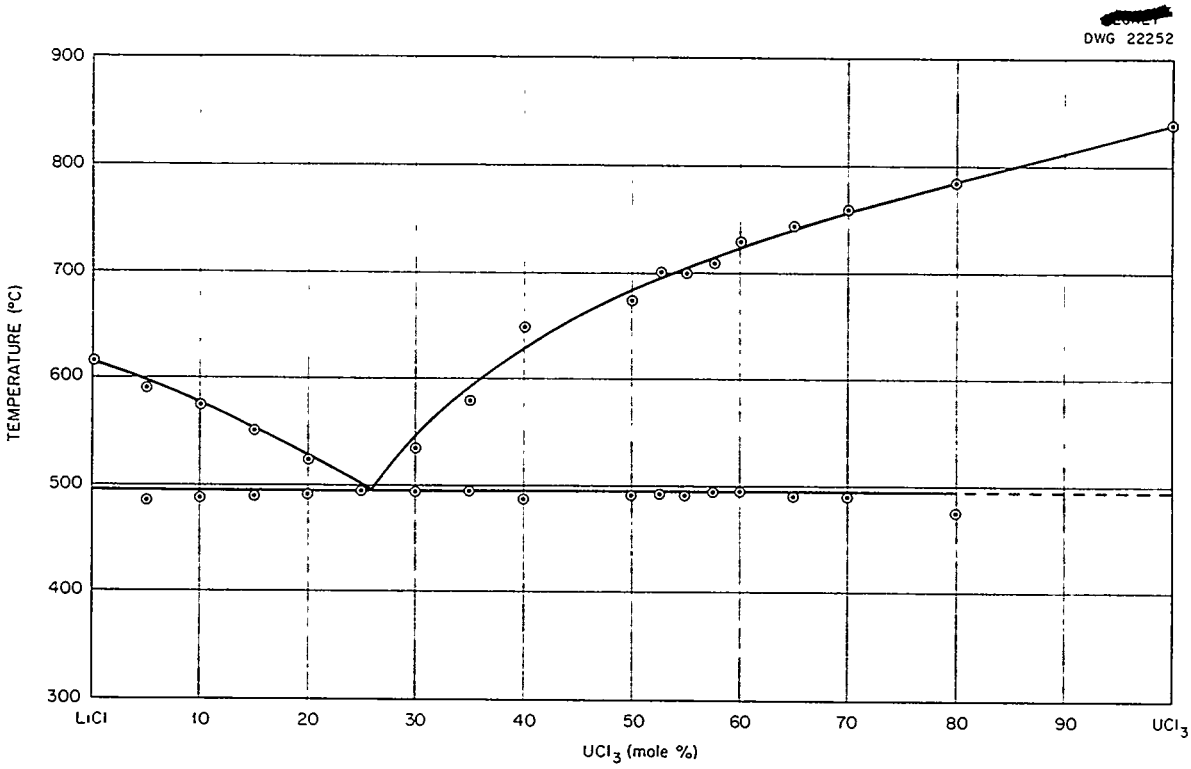

Fig. 5.2. The System LiCl-UCl_3.

RbCl-UCl_3

Preliminary data indicate that there are two eutectics in the system RbCl-UCl_3, one at about 15 mole % UCl_3 that melts at 605 ± 5°C and another lying between 40 and 50 mole % UCl_3 that melts at 515 ± 5°C. The compound Rb_3UCl_6 melts congruently at about 730°C, while Rb_2UCl_5 appears to melt incongruently at approximately 565°C.

CsCl-UCl_3

Only a few thermal measurements have been made on the system CsCl-UCl_3, but there is indication that there are probably only two eutectics in this system. One eutectic has a high CsCl content and melts at 580°C, and the other contains approximately 47 mole % UCl_3 and melts at about 540°C.

KCl-LiCl-UCl_3

The few studies that have been made on the system KCl-LiCl-UCl_3 indicate that the addition of about 4 mole % UCl_3 to the KCl-LiCl eutectic lowers the melting point from 355 to 345°C, but further additions of UCl_3 result in a sharp increase in melting point that is probably due to formation of the high-melting-point K_2UCl_5 complex. Study of this system will be resumed at a later date.

RbCl-UCl_4

Preliminary data for the system RbCl-UCl_4 indicate that Rb_2UCl_6 melts congruently at about 630°C and that the eutectic in the 40 to 50 mole % region melts at approximately 340°C.

CsCl-UCl_4

Preliminary data for the system CsCl-UCl_4 were presented in the previous report.[6] A tentative equilibrium diagram for this system, based on the available thermal data, is shown in Fig. 5.3. The compound Cs_2UCl_6, with a melting point of 657 ± 5°C, is believed to be the only congruently melting compound in this system. There is some evidence for a compound such as CsU_2Cl_9 or

[6] R. J. Sheil, S. A. Boyer, and C. J. Barton, *ANP Quar. Prog. Rep. Sept. 10, 1953*, ORNL-1609, p. 59.

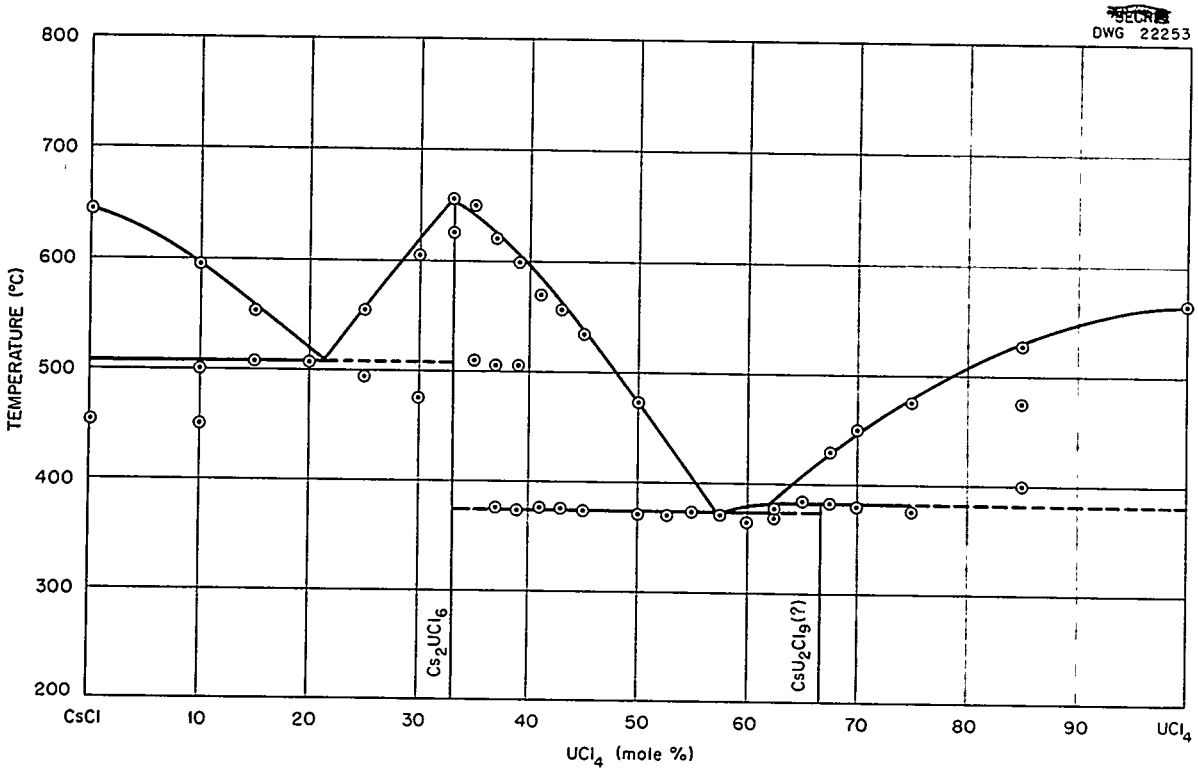

Fig. 5.3. The System CsCl-UCl_4.

CsU_3Cl_{13} that would melt incongruently at about 382°C, which is only a few degrees above the melting point of the eutectic containing approximately 58 mole % UCl_4.

KCl-LiCl-UCl_4

Preliminary data reported[7] for the system KCl-LiCl-UCl_4 indicated a eutectic of unknown composition that melts at approximately 275°C. Further investigation of the system during this quarter confirmed the existence of the low-melting-point eutectic, which appears to contain (in mole %) approximately 45% KCl, 20% LiCl, and 35% UCl_4. However, a more complete study of the system will be required for determining the eutectic composition with more certainty.

[7] R. J. Sheil and C. J. Barton, *ANP Quar. Prog. Rep. June 10, 1953*, ORNL-1556, p. 42.

NaCl-LiCl-UCl_4

The very complete investigation of the system NaCl-LiCl-UCl_4 made during this quarter failed to show a ternary eutectic with a melting point significantly lower than that of the lowest melting NaCl-UCl_4 binary eutectic (375°C). Since this investigation covered the region where low melting compositions are believed most likely to occur, no further work with this system is contemplated at the present. It is interesting to note that when small amounts of UCl_4 (2 to 10 mole %) were added to the NaCl-LiCl binary eutectic, the resulting ternary mixtures had lower melting points than those of the binary mixtures. The smallest addition of UCl_4 (1 mole %) to the KCl-LiCl eutectic resulted in a higher melting point. This difference in behavior probably can be attributed to the higher melting point of the K_2UCl_6 complex as compared with that of the Na_2UCl_6 complex.

QUENCHING EXPERIMENTS WITH THE $NaF\text{-}ZrF_4$ SYSTEM

C. J. Barton
R. E. Moore
R. E. Thoma
J. Truitt
G. D. White
Materials Chemistry Division

Recent improvements in previously described[8] techniques and equipment for quenching small samples of fused fluorides have greatly improved the reproducibility of results. The technique of determining equilibrium conditions in solid phases by quenching a composition to glass and then heating to the temperature of interest to grow crystalline phases in the glass gives promise of solving some of the more difficult problems in the $NaF\text{-}ZrF_4$ system. Only preliminary results with this technique have been obtained.

It is apparent that very accurate temperature control is necessary to establish phase relationships in the 40 to 60 mole % ZrF_4 region of the $NaF\text{-}ZrF_4$ binary system in which most of the quenching work has been done. The improved equipment in use at present controls and measures temperatures to ±0.5°C. The two furnaces now in operation make possible the quenching of about 40 samples a day.

Oil has proved to be as effective a quenching medium as mercury and it is much more convenient because it eliminates the necessity of having to attach it to the capsules. The formation of crystals during quenching has been kept to a minimum through the use of small samples (about 3 mg) and by severe pressing of the portion of the capsule that contains the sample to decrease the sample thickness. However, quench growth is still sometimes troublesome in the $NaF\text{-}ZrF_4$ system. Another problem that is not yet completely solved is the presence in most quench samples of small amounts of an unidentified phase believed to be a complex sodium zirconium oxyfluoride. However, the practice of hydrofluorination of small samples (cf., subsection on "Production of Purified Fluorides") and the handling of the finely ground samples in vacuum dry boxes have been of value in keeping these phases at a minimum.

Quenching of specimens containing 33 to 46 mole % ZrF_4 reveals a cubic crystalline phase. Because the phase is isotropic, petrographic identification is difficult; x-ray diffraction techniques will be required to establish the liquidus temperatures. The cubic material is believed to be a form of Na_2ZrF_6, but the possibility that it is $Na_3Zr_2F_{11}$ has not yet been eliminated.

Material containing 46 mole % ZrF_4 shows $NaZrF_5$ as the primary phase. The liquidus temperature is 512 to 515°C, and the solidus temperature is 510°C. Devitrification at 506°C of glass of this composition gave $NaZrF_5$ and a small amount of the cubic material.

Material containing 48 mole % ZrF_4 shows as its primary phase an easily crystallized species believed to be a high-temperature form of $Na_3Zr_4F_{19}$ (designated R3).

In the mixture containing 50 mole % ZrF_4 the primary phase is R3; the liquidus temperature is near 518°C; and the solidus temperature is slightly above 510°C. Slow cooling of mixtures with this composition invariably gives a phase referred to as $NaZrF_5$ and $Na_3Zr_4F_{19}$. However, devitrification of the glass of 506°C provided only crystalline $NaZrF_5$ with some glass residue. It now appears that solid solutions of Na_2ZrF_6 in $NaZrF_5$ exist which show optical properties that differ only slightly from those of $NaZrF_5$. The devitrification experiments seem to indicate that $NaZrF_5$ is the stable solid phase at this concentration.

Material containing 53.8 mole % ZrF_4 shows R3 as the primary phase; the liquidus temperature has not been established, but it is above 517°C; the solidus temperature is about 511°C. Both $Na_3Zr_4F_{19}$ and $NaZrF_5$ are present below the solidus temperature.

Mixtures containing 57.2 mole % ZrF_4 correspond to the formula $Na_3Zr_4F_{19}$. A glass devitrification experiment produced an almost pure crystalline phase with this composition. Although this single experiment apparently confirms the formula, further experimentation at this and neighboring compositions will be required to establish beyond doubt the composition of the compound.

DIFFERENTIAL THERMOANALYSIS OF THE $NaF\text{-}ZrF_4$ SYSTEM

R. A. Bolomey
Materials Chemistry Division

The equipment used for differential thermoanalysis was modified during this quarter by replacing the capsules that had thermocouples

[8] R. E. Moore and C. J. Barton, *ANP Quar. Prog. Rep. Sept. 10, 1953*, ORNL-1609, p. 59.

welded to the side with small capsules that have center thermocouple wells. With the new capsules, much better agreement is obtained between heating and cooling curves, and, for most samples, the break for the liquidus transition is sharper and better defined. Heating and cooling rates of 1°C per minute can now be employed satisfactorily for most samples. Data have been obtained with these capsules for mixtures in the system NaF-ZrF_4 that were hydrofluorinated before use. A break at about 512°C for samples containing 57 to 60 mole % ZrF_4 suggests that the composition of the phase which precipitates from 50 mole % material is probably above 57 mole %. It is possible, however, that the existence of the 512°C break in this region is due to a solid transition; this point will be established by combining the data obtained from differential analysis with that obtained by using quenching techniques. Data are being collected in the 40 to 50 mole % ZrF_4 range, and, when extended to higher ZrF_4 concentrations, a complete phase diagram will be presented.

FILTRATION ANALYSIS OF FLUORIDES

C. J. Barton R. J. Sheil
Materials Chemistry Division

The high-temperature filtration method of studying phase equilibria mentioned in the previous report[9] was applied mainly to NaF-ZrF_4-UF_4 compositions during this quarter. Two attempts to filter UF_4-ZrF_4 mixtures were unsuccessful because the high vapor pressure of ZrF_4 resulted in separation by sublimation rather than liquid-solid separation. In the NaF-ZrF_4-UF_4 system, the filtration method provided useful information about an important fuel composition in addition to data for fundamental studies of phase relationships in this system.

Mixtures with 53 mole % NaF

The melting point of a mixture containing (in mole %) 53.5% NaF, 40.0% ZrF_4, and 6.5% UF_4 has been reported as 545°C. However, in a previous filtration at 560°C of a 7 mole % UF_4 mixture, analysis of the residue and of the filtrate indicated some segregation of a high-uranium-content material. This experiment has been repeated carefully with a mixture containing (in mole %) 53.0% NaF, 40.0% ZrF_4, and 7.0% UF_4, which was filtered at 604, 575, and 560°C. At the two higher temperatures, there was no detectable difference between the filtrate and the residue, when examined either petrographically or by x-ray diffraction. At 560°C, more than 99% of the charge material passed through the filter, but examination of the residue indicated that it was a higher uranium solid solution than the filtrate. There was not enough residue obtained in this experiment for a chemical analysis, and therefore the significance of the apparent phase separation is not clear. In one filtration carried out at 525°C with the same composition, 63 wt % of the material filtered. Both filtrate and residue were found to be solid solutions of the type $Na(U)ZrF_5$, with the residue having the higher uranium content. It is considered significant that no trace of free UF_4 was detected in the solid phases.

Mixtures with 50 mole % NaF

Thermal data for NaF-ZrF_4-UF_4 mixtures[10] containing 50 mole % NaF seemed to indicate that $NaUF_5$ and $NaZrF_5$ form solid solutions. Petrographic and x-ray diffraction studies have shown that solid solutions do occur in this system but that UF_4 is probably the primary phase that separates from the mixture containing 50% NaF, 25% UF_4, and 25% ZrF_4. Filtration experiments with 50% NaF mixtures containing 10, 12.5, 25, 31, and 37.5 mole % UF_4 showed that UF_4 separated in significant amounts from the 12.5, 25, and 31% UF_4 compositions, with the maximum separation occurring at 25%. Trace amounts of UF_4 were found in several of the other solid phases. Because of the UF_4 separation, chemical analysis of the filtrate and residue did not give a reliable indication of the liquidus and solidus temperatures for most of the 50% NaF join.

Mixtures with 75 mole % NaF

The thermal data for the 75% NaF compositions in the NaF-ZrF_4-UF_4 system showed evidence of more or less complete solid solution formation between Na_3UF_7 and Na_3ZrF_7. Since Na_3UF_7 melts incongruently, it was expected that the solid solutions would break down near the uranium end of the series. However, preliminary data indicate

[9] R. J. Sheil and C. J. Barton, *ANP Quar. Prog. Rep. Sept. 10, 1953*, ORNL-1609, p. 61.

[10] L. M. Bratcher and C. J. Barton, *ANP Quar. Prog. Rep. Dec. 10, 1952*, ORNL-1439, Fig. 10.2, p. 108.

that a comparatively small amount of ZrF_4 (1.5 mole %) stabilizes the Na_3UF_7 structure.

Filtrations with mixtures containing $8\frac{1}{3}$, $12\frac{1}{2}$, and $16\frac{2}{3}$ mole % UF_4 (equivalent to 25, 50, and 75 mole % Na_3UF_7) gave evidence of complete solid solution formation within this range. The x-ray diffraction pattern for all six samples from these filtrations showed only the Na_3ZrF_7 and Na_3UF_7 lines with the maximums shifted to varying extents. Petrographic examination, which is capable of detecting trace amounts of crystalline phases not shown by x-ray diffraction, showed the presence in some samples of other phases, such as Na_2ZrF_6 and $NaZrF_5$, that contained dissolved uranium and, in one case, a small amount of UO_2. An unidentified yellow-brown phase, which appears to be characteristic of NaF-ZrF_4-UF_4 mixtures containing more than 75 mole % NaF, was reported to be present in both the filtrate and the residue from the filtration of the $8\frac{1}{3}$ and $12\frac{1}{2}$ mole % UF_4 mixtures. Since this phase did not appear in hydrofluorinated mixtures, it seems probable that it is an oxygen-containing complex.

The data shown in Table 5.1 indicate that, within the range of compositions and temperatures covered in these experiments, the system NaF-ZrF_4-UF_4 is a true binary system, since the phase separation resulted in mixtures of very nearly the same NaF content as the starting material. The liquidus temperatures determined by the filtration method agreed well with the thermal data shown in Fig. 5.1 (cf., subsection on "Thermal Analysis of Fluoride Systems"). Since cooling curves for these compositions failed to indicate solidus temperatures, the data in Table 5.1 give the first indication of the temperature spread between liquidus and solidus lines for this system. Further filtrations with compositions approaching that of the pure compounds are planned for the near future in an attempt to determine whether limits of solid solution exist in this system.

FUNDAMENTAL CHEMISTRY

Spectrophotometry of Supercooled Fused Salts

H. A. Friedman
Materials Chemistry Division

Measurements of the absorption spectra for UF_4 and UF_3 in quenched fluoride melts with a Beckman DU spectrophotometer and the procedure described by Friedman and Hill[11] have been continued. More efficient quenching was obtained by flattening the sealed samples in a hydraulic press to give larger surface areas and thinner melts.

With glasses from the NaF-ZrF_4-UF_4 system, only two absorption spectrum patterns have been found. One of these superficially resembles that of crystalline UF_4; the other more closely resembles crystalline Na_2UF_6. The Na_2UF_6 type of pattern was found only in a localized region near the Na_2UF_6 composition. Glasses of the ZrF_4-UF_4 system were prepared with compositions in the range from 30 to 70 mole % UF_4 in 10 mole % intervals. Outside this region, no glasses were obtained; within this region, Beer's law was closely followed by the UF_4 type of pattern. Samples along the Na_2UF_6-Na_2ZrF_6 join that contained less than 60% Na_2UF_6 were not studied because of quench growth; the Na_2UF_6 type of pattern was found in samples that contained from 60 to 100 mole % Na_2UF_6. Nine mixtures were prepared in which the ZrF_4 content was held at 41 mole %, but the NaF-to-UF_4 ratios were adjusted to cover the

[11] H. A. Friedman and D. G. Hill, *ANP Quar. Prog. Rep. Sept. 10, 1953*, ORNL-1609, p. 62.

TABLE 5.1. LIQUIDUS-SOLIDUS EQUILIBRIA OBTAINED BY FILTRATION

INITIAL COMPOSITION (mole %)		FILTRATION TEMPERATURE (°C)	FRACTION OF CHARGE IN FILTRATE (wt %)	ANALYSIS OF FRACTIONS (mole %)					
				Filtrate			Residue		
Na_3UF_7	Na_3ZrF_7			NaF	ZrF_4	UF_4	NaF	ZrF_4	UF_4
75	25	695	63	74.9	5.1	20.0	74.9	8.4	16.7
50	50	742	29	75.0	10.5	14.5	75.1	13.8	11.1
25	75	786	60	74.9	17.4	7.8	75.6	20.6	3.8

region from 6 to 59 mole % UF_4; all nine mixtures formed glasses and exhibited the UF_4 type of absorption in conformity with Beer's law. The $NaUF_5$-$NaZrF_5$ system is currently being investigated.

Glasses were obtained with compositions of between 16.67 and 50 mole % UF_3 in the ZrF_4-UF_3 binary system. At higher concentrations, crystallization of UF_3 could not be avoided. No shift in pattern occurred in the glass region to indicate a change in the nature of the UF_3 species in the liquid melt at concentrations below 50 mole % UF_3. The color of the glasses was rust-olive. A typical spectrum is shown in Fig. 5.4.

EMF Measurements in Fused Salts

L. E. Topol
Materials Chemistry Division

The techniques described previously have been used for additional electrolyses of various solutions of metal chlorides in potassium chloride. Containers of morganite, graphite anodes, and platinum or nickel cathodes are used, and the electrolyses are carried out at a temperature of 850°C. Potassium chloride solutions containing 1 wt % of $NiCl_2$ (theoretical $E^0 = 0.82$ volt) gave decomposition potentials at 1.20 to 1.26 volts, while solutions containing 10 wt % $NiCl_2$ yielded values in the range 1.0 to 1.06 volts. Solutions

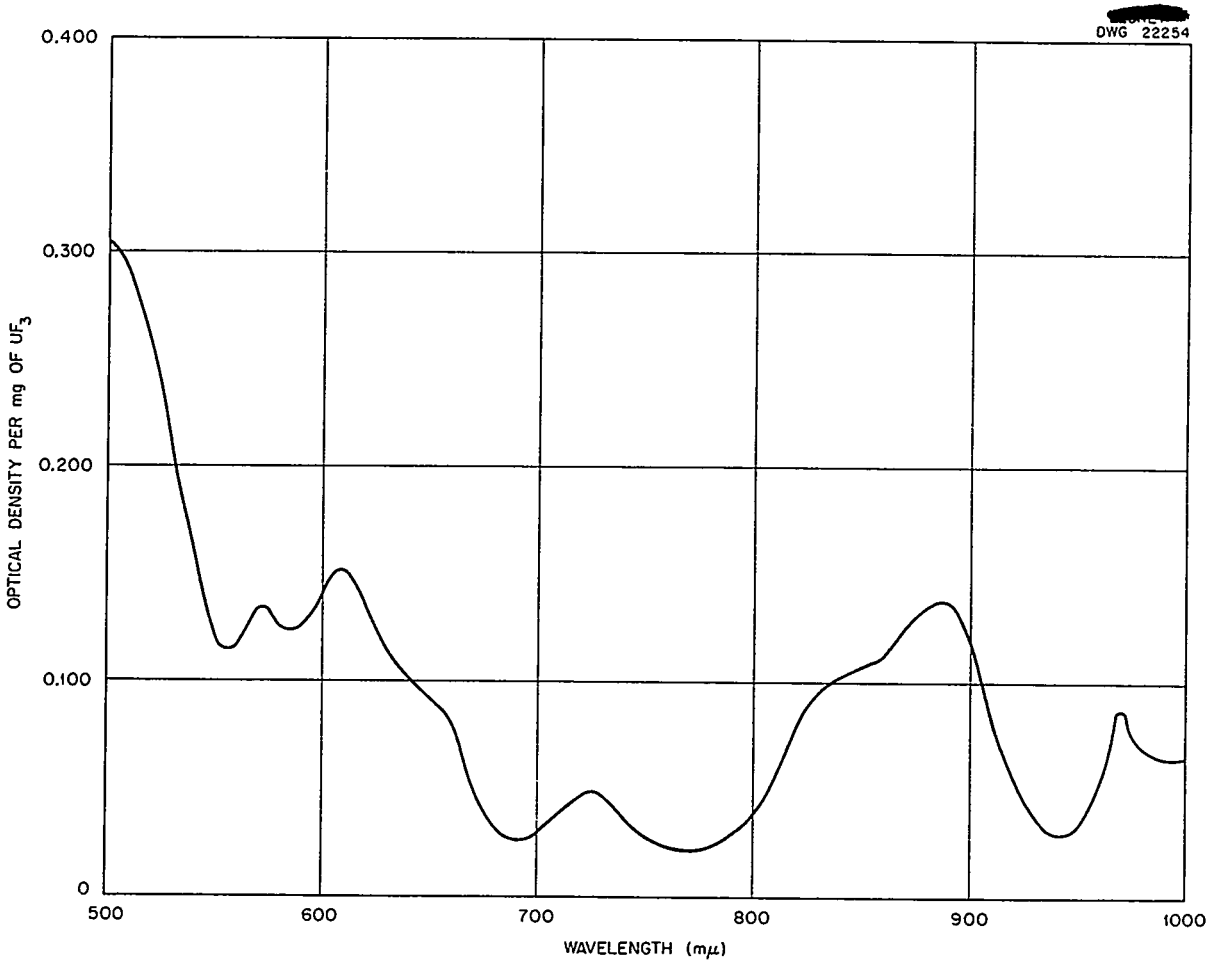

Fig. 5.4. Absorption Spectrum of the ZrF_4-UF_3 System Containing 33.3 mole % UF_3.

containing 1 to 2 and 10 wt % of $FeCl_2$ (theoretical E^0 = 1.11 volts) yielded decomposition potentials at 1.50 to 1.55 and 1.20 volts, respectively. A mixture containing 2 wt % of $NiCl_2$ and 2 wt % of $FeCl_2$ in KCl yielded two distinct breaks in the *I-E* curve at 1.18 and 1.56 volts, as shown in Fig. 5.5.

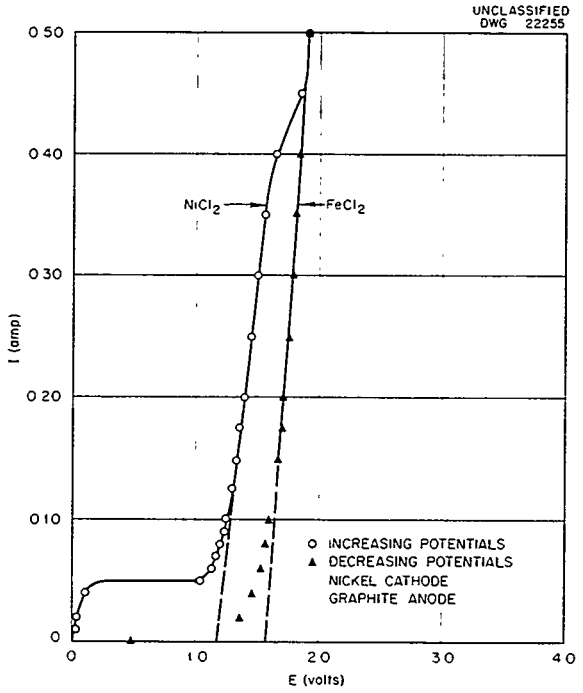

Fig. 5.5. Electrolysis at 850°C of Mixture Containing 2 wt % of $NiCl_2$ and 2 wt % of $FeCl_2$ in KCl.

Attempts to electrolyze CrF_3 in KCl in similar experiments have yielded decomposition potentials at about 1.15 to 1.30 and 1.50 to 1.75 volts, but reproducibility of the results has been rather poor. Electrolyses of KCl with chromium anodes have shown erratic results that are tentatively ascribed to oxidation of the chromium, even though attempts are made to maintain an inert atmosphere. Rather erratic changes of slope at about 1.2 and 1.9 volts are observed.

When a thin plate of nickel was used to protect zirconium electrodes from oxidation, reproducible emf's at 1.06 to 1.12 volts were observed in electrolyses of KCl. Since nickel is not dissolved in KCl at potentials below 1.8 volts, the emf's obtained are considered to be characteristic of the zirconium. Based on the value for zirconium and the decomposition potential for KCl (3.1 volts), the potential for the reaction

$$ZrCl_4 \longrightarrow Zr + 2Cl_2$$

appears to be 2.0 volts. When a hydrogen atmosphere is used over the zirconium electrode system, the decomposition potential rises to 1.12 to 1.18 volts. Whether this may be due to formation of hydrides of zirconium is not certain.

Physical Chemistry of Fused Salts

E. R. Van Artsdalen
Chemistry Division

Some insight into the fundamental physical chemistry of fused salt systems may be realized from the physical properties of these systems. Accordingly, the depression of the freezing point of sodium nitrate by a wide variety of solutes was determined, and measurements were made of the density and electrical conductivity of the LiCl-KCl system and the heat capacity of CdI_2. The molten NaCl-KCl system is also being investigated in the hope that it will yield not only practical data, but will also contribute to the understanding of short-range order and the nature of electrical conductivity of fused salt systems. This work is reviewed briefly below and is reported in detail in the Chemistry Division semiannual report.[12]

Detailed, highly reproducible measurements of the density and the electrical conductivity of the fused salt system LiCl-KCl were completed for the entire composition field over wide temperature ranges. An exact linear relation between molar volume and composition at any specified temperature indicates that no complex formation occurs in this molten system. On a molar basis, lithium chloride is a considerably better electrical conductor than potassium chloride. It was therefore significant to discover that substitution of lithium chloride for some of the potassium chloride actually lowered the equivalent conductance of the solution below that of pure potassium chloride. This phenomenon was interpreted to be indicative of considerable short-range order persisting in these high-temperature fluids. A further tentative explanation of this

[12] A. S. Dworkin, D. J. Sasmor, and E. R. Van Artsdalen, *Chem. Div. Semiann. Prog. Rep. June 20, 1953*, ORNL-1587, p. 19-25.

behavior was based on the consideration of the relative sizes of the ions. Substitution of small Li^+ ions for some of the much larger K^+ ions will shrink the short-range chloride semilattice of the fluid and make transport by K^+ appreciably more difficult. As more and more Li^+ is substituted for K^+, the conductivity will pass through a minimum and again increase until, finally, pure LiCl is present.

The depression of the freezing point of sodium nitrate was investigated with a wide variety of solutes. The results significantly substantiate the concept that fused salts are essentially totally ionized and behave as nearly ideal electrolytes, even at relatively high concentrations of the solute. Thus, calcium, strontium, barium, and lead chlorides, for example, are completely dissociated, as is $LaCl_3$. $FeCl_3$ seems to form two particles only, apparently $FeCl_2^+$ and Cl^-. Chromate, dichromate, and bromate ions are stable in liquid sodium nitrate, but the metaperiodate ion, IO_4^-, decomposes to yield oxygen and the iodate ion.

The heat capacity of high-purity crystalline cadmium iodide has been measured from 15°K to room temperature. It remains necessary to determine c_p in the range well below 15°K because of the observed high heat capacity at this temperature. The heat capacity shows approximately a 1.4-power temperature dependence at the lowest measured range and, therefore, does not yet fit either the usual Debye T^3 law or the T^2 law observed here for boron nitride. At 298.16°K, the following thermodynamic values have been found for cadmium iodide: $c_p = 19.12$ cal/mole, $S° = 38.5_0$, $-(F° - H°_0)/T = 23.19$, $(H° - H°_0)/T = 15.31$. The $S°$ value has an uncertainty of about ±0.5 because of the high heat capacity value at 15°K and its attendant inherent difficulty of extrapolation to 0°K. This uncertainty is, of course, reflected in the two derived quantities.

PRODUCTION OF PURIFIED FLUORIDES

F. F. Blankenship G. J. Nessle
Materials Chemistry Division

Laboratory-Scale Production of Molten Fluorides

F. F. Blankenship F. P. Boody
C. M. Blood G. M. Watson
Materials Chemistry Division

Twenty-eight batches totaling 55 kg of molten fluorides and including one batch containing 15 g of enriched uranium were prepared and distributed to various laboratories for testing. When the experimental production facilities have been expanded (cf., subsection on "Experimental Production Facilities"), production of materials in this laboratory will be terminated, except for the preparation of small enriched-uranium-bearing specimens for radiation stability tests.

Purification of Small Fluoride Samples for Phase Studies

F. F. Blankenship C. M. Blood
F. P. Boody
Materials Chemistry Division

Studies of phase equilibria in the $NaF-ZrF_4$ and $NaF-ZrF_4-UF_4$ systems by the quenching technique have been hampered by contamination of the materials with traces of water which caused hydrolysis of the tetravalent halides during the heating period and consequent contamination of the quenched melt with oxide or oxyfluoride phases. Materials for this and similar phase equilibrium studies that are essentially free from water and oxygenated compounds are now routinely prepared by a modification of the hydrofluorination-hydrogenation pretreatment method used for larger specimens.

In this process a number (up to 28) of small (~25 g) samples are placed in nickel or platinum crucibles on a nickel rack inside a 4-in.-diameter nickel reactor for processing. A typical processing cycle of 2 hr of treatment with HF at 800°C followed by stripping with H_2 at 600°C for 18 hr has been shown to produce material satisfactory for these purposes. To date, a total of six batches comprising 67 samples has been prepared. It appears, however, that handling of the specimens in a vacuum dry box may be required if freedom from oxygenated phases is to be maintained.

Production of Enriched Material for In-Pile Loop Experiment

G. J. Nessle
Materials Chemistry Division

Plans for preparation of the enriched fuel for a miniature in-pile loop facility and for charging of the material into it have been prepared in accordance with the necessary technical and accountability considerations. It is planned that this loop will be charged with a uranium-free mixture for preliminary testing before the enriched concentrate is added for final testing.

The processing equipment for this production operation has been fabricated. When production of the ARE enriched concentrate has been completed, the new process equipment will be installed in Building 9212 in the area now occupied by the ARE facilities. The enriched fluorides for the in-pile loop will be transferred to the X-10 site where the loop will be filled.

Experimental Production Facilities

J. P. Blakely C. R. Croft
Materials Chemistry Division

D. E. McCarty R. Reid
R. G. Wiley
ANP Division

A total of 329.2 kg of mixed fluorides was processed and dispensed to various requestors during this quarter. Included in this total were 14 batches of approximately 2.5 kg each, 3 batches of approximately 10 kg each, and 10 batches of approximately 27 kg each.

Although the quantity of fluorides processed decreased, the variety of demand increased sharply. This tendency is becoming more pronounced, and it appears that production of large quantities of a few materials will be of considerably less importance; versatility and adaptability of equipment will be primary requirements. Consequently, an installation is being planned for producing a variety of fluoride compositions with a minimum loss of time and equipment.

Reduction of Na_2UF_6 by Hydrogen

F. F. Blankenship F. P. Boody
Materials Chemistry Division

The Na_2UF_6 which had previously been hydrofluorinated and stripped with hydrogen so that the structural metal content should have been reduced to less than 30 ppm was bubbled with hydrogen gas in the original nickel reactor for considerable periods of time at 692, 785, and 882°C. It was found that the rate of reduction of the uranium according to the equation

$$UF_4 + \tfrac{1}{2}H_2 = UF_3 + HF$$

increased with temperature, as shown in Table 5.2. When the data given in Table 5.2 are plotted on a semilogarithmic scale as reaction rate vs. $(1/T) \times 10^4$ the straight line shown in Fig. 5.6 is obtained. From the slope of this curve, the activation energy of the reduction can be calculated to be 33,700 ± 2600 cal/mole.

Treatment of Molten $NaZrF_5$ with Strong Reducing Agents

F. F. Blankenship C. M. Blood
G. M. Watson
Materials Chemistry Division

It was previously reported[13] that zirconium bars suspended in molten $NaZrF_5$ contained at 800°C in graphite-lined reactors and stirred by bubbling argon undergo weight losses far in excess of the amount required to reduce structural metal ions. This observation was further confirmed by additional experiments that involved the treatment of $NaZrF_5$ in graphite-lined nickel at 800°C with zirconium chips; the unrecovered zirconium metal amounted to at least 20 g per kilogram of fused salt. However, it has since been observed that little if any loss of weight occurred when zirconium metal chips were exposed in a parallel experiment without the graphite liner. The difference might be due to the formation of zirconium carbide, but the available data are insufficient to show it. The possibility that a portion of the zirconium enters the melt as the trifluoride or as dissolved zirconium metal has not been ruled out.

[13] C. M. Blood *et al.*, *ANP Quar. Prog. Rep. Sept. 10, 1953*, ORNL-1609, p. 69.

TABLE 5.2. RATE OF REDUCTION OF Na_2UF_6 WITH H_2 AS A FUNCTION OF TEMPERATURE

TEMPERATURE		$\frac{1}{T(°K)} \times 10^4$	REACTION RATE AS MOLES OF HF PER LITER OF H_2 BUBBLED
°C	°K		
692	965	10.36	8.8×10^{-6}
785	1058	9.45	3.7×10^{-5}
882	1155	8.65	1.58×10^{-4}

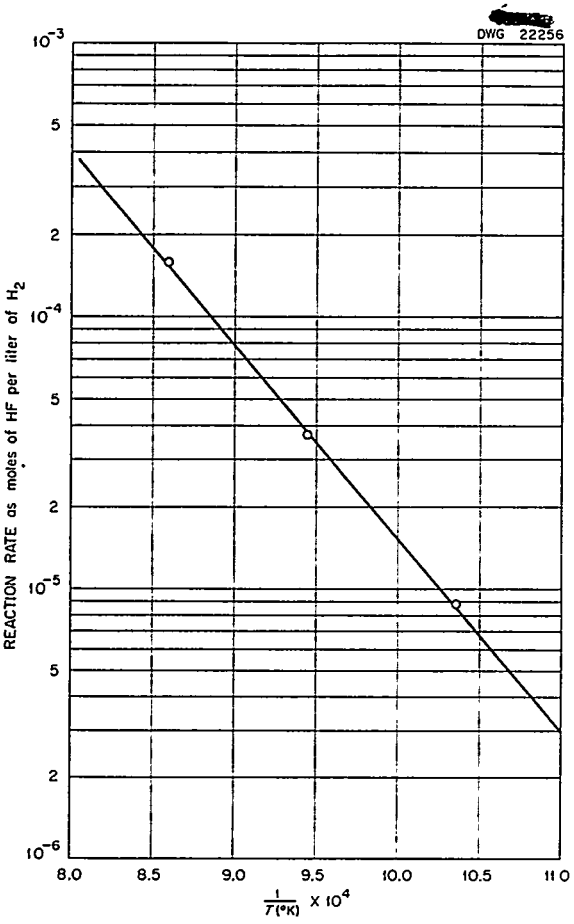

Fig. 5.6. Reaction Rate vs. Reciprocal Temperature According to the Equation $UF_4 + \frac{1}{2} H_2 = UF_3 + HF$.

The effect of uranium metal on $NaZrF_5$ was studied by adding 5.5 wt % of uranium chips to the material in a graphite-lined reactor. Unlike the previous experiments, the mixture was treated with hydrogen for 2 hr at 800°C, and the material was subsequently filtered at 700°C. The filtrate started freezing at about 540°C and contained five phases typically found in fuels which are reduced to the extent that orange-red $UF_3 \cdot 2ZrF_4$ and purple UF_3 appear. The uranium content of the filtrate was 5.00 wt %, and apparently about 90% of the uranium reacted. If it is considered that the dissolved uranium is present as UF_3 and that all other reduced phases are insoluble, a reducing power of 210 meq per kilogram of melt should have resulted; if all reduced phases remained in solution, the theoretical reducing power would be 840 meq/kg. Chemical analysis by H_2 evolution showed 550 meq of reducing power per kilogram of filtrate, which indicated the presence of soluble reduced phases in addition to the UF_3. Less than 20 ppm of nickel and chromium and 85 ppm of iron were found. The unfiltered residue in the reactor contained black opaque material which liberated gas readily when treated with dilute acids. X-ray analysis of the residue revealed the presence of ZrH, UF_3, and uranium metal, along with occluded melt. Thus it appears that the uranium did not react quite completely and that some zirconium tetrafluoride was reduced to the metal by the uranium. Since ZrH_2 is decomposed to the extent of about 25% at 800°C under 1 atm of H_2,[14] most of the zirconium appears as ZrH.

A further check on the possibility of retaining reducing species such as Zr°, ZrF_3, ZrC, ZrH, and ZrH_2 in $NaZrF_5$ melts was attempted by treating $NaZrF_5$ with NaH (2 moles per kilogram of melt). The mixture was sparged with hydrogen in a graphite liner for 24 hr at 800°C and then filtered. The reactor heel contained a dark-black residue which was tentatively identified as ZrH mixed with the melt. Chemical analysis of the white filtrate showed 106.5 meq of reducing power per kilogram or about 5% of that expected if all reduced species were soluble. Efforts to learn more about the nature of this apparent reducing power will be continued.

Reduction of NiF_2 by Hydrogen

F. F. Blankenship C. M. Blood
G. M. Watson
Materials Chemistry Division

Considerable attention has been given to the kinetics of the reduction of Ni^{++} in $NaZrF_5$ by H_2 at 800°C because of the importance of this reduction in fluoride purification procedures. The use of graphite liners in the nickel reactors for handling molten salts is a great convenience in loading and unloading and in avoiding excessive contamination with NiF_2 during the HF treatment. Accordingly, for most of the kinetic studies, graphite-lined reactors have been used. Early suspicions that graphite might reduce Ni^{++} were allayed by the large, positive, standard free energy estimated for

[14] M. N. A. Hall, *Trans. Faraday Soc.* 41, 306 (1945).

6. CORROSION RESEARCH

W. D. Manly
Metallurgy Division

W. R. Grimes F. Kertesz
Materials Chemistry Division

H. W. Savage
ANP Division

The static and the seesaw corrosion testing facilities have been used to study the corrosion of Inconel, cermets, and some special alloys in the fluoride fuel NaF-ZrF_4-UF_4 (50-46-4 mole %). The effects of improper degreasing of metals and of contaminants in the fluorides were studied. Several tests of bearing materials and hard-facing alloys have been completed in which the molten fluorides were used as the corroding agent. The materials tested are of considerable interest because of their prospective uses as high-temperature bearings and valve facings. Various cermets have also been tested in the fluorides to determine their fitness for these same applications. Static tests in graphite capsules of Inconel specimens exposed to fluoride fuel to which FeF_3, FeF_2, or NiF_2 additions were made gave anomalous results that were presumably due to the reduction of the added metal fluorides by the graphite. Static tests of two dissimilar metals indicated that one metal is usually preferentially attacked.

Fluoride corrosion tests were made in Inconel thermal convection loops to supplement and extend the data obtained in the above-mentioned and previous static tests. Although the thermal convection loops normally operate with a hot-leg temperature of 1500°F, the temperatures were varied to determine the effects of both time and temperature. Additional tests have substantiated the earlier conclusion that attack by NaF-ZrF_4-UF_4 (50-46-4 mole %) on Inconel is independent of temperature, at least in the range of 1500 to 1650°F, and dependent on exposure time. The purity of the fluoride mixture was shown to be important when the attack depth was increased by a factor of 3 in a loop operated with a low-purity batch of fuel. Reductions in attack, in comparison with that found in the standard loop, that is, a loop operated for 500 hr at 1500°F, were achieved by (1) precirculating the fluorides, (2) pretreating the fluorides with chromium metal flakes, and (3) holding the fluorides in contact with Inconel turnings before circulation in the loop. While pretreatment of the fluorides with metallic chromium was beneficial, a chromium plate on the pipe wall was not. Increasing the UF_4 content in the fluoride mixture from 4 to 6.5 mole % caused an increase in mass transfer in the loops and possibly a slight increase in corrosion. The maximum depth of attack by the purified ARE fuel solvent, $NaZrF_5$, was comparable to that of the purified fuel mixture (with 4 mole % UF_4), although the intensity of the $NaZrF_5$ attack was much less and the same mass transfer was noted.

Additional studies were performed in an attempt to establish the chemical equilibria of the postulated corrosion reaction which results in the selective leaching of chromium from Inconel. Preliminary values have been obtained for the equilibrium constants involved, but the data are not yet sufficiently reliable.

Nickel and type 430 stainless steel thermal convection loops were also operated with the fluoride NaF-ZrF_4-UF_4 (50-46-4 mole %). There was no measurable mass transfer in the nickel loop, and the hot-leg surface had a polished finish. The hot leg of the type 430 stainless steel loop showed a small amount of smooth, even removal, with no subsurface voids or intergranular attack; metal crystals were deposited in the cold leg.

A number of tests, both static and dynamic, were performed with the liquid metals lithium, sodium, and lead. Tests have been completed on beryllium oxide and a number of bearing materials and cermets.

The investigation of the mass transfer and corrosion of metals and alloys in quartz thermal convection loops containing liquid lead have continued. The metals tested during this quarter included a molybdenum-nickel (25% Mo–75% Ni) alloy, a chromium-iron-silicon (14% Cr–84% Fe–2% Si) alloy, and types 304 and 347 stainless steel specimens which were oxidized prior to contact with the lead. The most significant result from

this study was the marked improvement in the resistance to mass transfer of these metals because of the oxide film. Some static tests on the corrosion and mass transfer characteristics of various alloys in contact with lithium were completed.

Static tests on a number of solid fuel elements were performed in sodium and sodium hydroxide. While there was no evidence of attack in any of the sodium tests, all the fuel elements were severely attacked in the hydroxide. In connection with a study of hydroxide containment, the equilibrium pressures of hydrogen over a number of hydroxide-metal systems are being determined.

FLUORIDE CORROSION IN STATIC AND SEESAW TESTS

E. E. Hoffman L. R. Trotter
J. E. Pope D. C. Vreeland
Metallurgy Division

H. J. Buttram R. E. Meadows
N. V. Smith
Materials Chemistry Division

Both the static capsule and the seesaw tests provide relatively cheap and simple means of investigating the many parameters which affect fluoride corrosion. The seesaw tests in which the capsule containing the fluoride is rocked in a furnace were operated at 4 cps with the hot end of the capsule at 815°C and the cold end at 700°C. The static tests in which the fluoride mixture is sealed in a capsule were usually conducted for 100 hr at 816°C. In order to permit testing of material which could not be readily fabricated into capsules or to permit variation of the surface-to-volume ratio of fluoride to metal, a number of tests were performed in which the fluoride and metal specimens were contained in graphite capsules. All capsules are filled in a helium dry box, and therefore oxidation or hydrolysis of the contents of the capsules is improbable.

Inconel Corrosion by Fluorides with Metal Fluoride Additives

In general, corrosion of Inconel specimens by several fluoride preparations in graphite capsules was similar to that obtained when Inconel capsules were used in static tests. Some carburization of the specimens was obtained, but no other special effects were observed.

However, when fluorides to which had been added considerable quantities of FeF_3, FeF_2, or NiF_2 were tested in graphite capsules containing Inconel specimens, rather surprising results were obtained. In each case, tests at 800°C showed extensive deposition of iron or nickel, usually in films on the graphite capsule and on the specimen. When FeF_3 was the additive (in amounts up to 5 wt %), the corrosion of the Inconel specimen, as observed by metallographic examination and by analysis of the final melt for chromium, was much less than expected. In similar tests with FeF_2, corrosion of the Inconel was virtually undetectable by either technique. In this case, the precipitated film of metal appeared to be protective.

When NiF_2 was the added material, however, no protection of the specimen by the film resulted. In these experiments, extremely heavy subsurface void formation to a depth of 9 mils was observed. There is evidence that corrosion by fluoride mixtures with NiF_2 added is more severe at 600 than at 800°C.

These experiments suggest that graphite or some unknown contaminant in the graphite is responsible for reduction of the added metal fluoride. While reduction of FeF_2, for example, by graphite should have an extremely low equilibrium constant, it is possible that the volatile reaction product (CF_4) escapes from the system and permits the reaction to proceed. It is also possible that there is sufficient oxygen or water adsorbed in or on the graphite so that reduction of oxide by carbon (a reaction with an appreciable equilibrium constant at these temperatures) is responsible for these effects. Further study of this and similar reactions is in progress.

Corrosion of Various Metal Combinations

A series of experiments in which various metals, either alone or in combination, were tested in molten fluorides in graphite capsules have yielded the following results. (1) Nickel alone shows no attack. (2) Chromium-plated Inconel shows heavy subsurface void formation at all temperatures above 600°C; the voids were 3 to 4 mils deep at 700°C and above. (3) Chromium metal yielded high values for chromium content of the melt; it is possible, however, that slight surface oxidation of the chromium pellets used was responsible for this dissolved material. (4) When Inconel and chromium specimens were exposed together, the chromium

test piece was nearly completely dissolved, while the Inconel specimen, which was covered with a thin metal layer, was almost completely unattacked. (5) However, when Inconel and nickel were exposed together, the nickel appeared unaffected, while the Inconel was badly attacked; at 700°C, for example, the heavy subsurface void formation reached a depth of 3 to 4 mils.

Corrosion of Cermets

Several cermets which were considered for bearings and hard-facing applications were tested for resistance to fluoride corrosion. Three of these ceramic-metal materials were subjected to static tests. The materials consisted of heavy metal carbides bonded by nickel and were obtained from the Firth Sterling Company. Table 6.1 presents results obtained when the cermets were exposed to two fluoride mixtures in graphite capsules. The results indicate fair resistance to the two fluoride mixtures under the conditions of the test, and there was no apparent change in the appearance of the specimens after testing.

Another set of specimens was subjected to seesaw tests in Inconel capsules for 100 hr, with the specimens restricted to the hot zone of the Inconel tube. The hot-zone temperature was 816°C, and the cold-zone temperature was 730°C. Results of these tests are presented in Table 6.2. Some of these specimens contained chromium as a binding

TABLE 6.1. RESISTANCE OF CERMETS TO TWO FLUORIDE MIXTURES

Static tests at 800°C for 100 hr in graphite containers

CERMET (wt %)	FLUORIDE COMPOSITION (mole %)	WEIGHT CHANGE (%)
TiC-Cr_3C_2-Ni (42.9-7.1-50.0)*	NaF-ZrF_4 (50-50)	+1.12
	NaF-ZrF_4-UF_4 (53-43-4)	+1.27
TiC-Mo_2C-Ni (72-5-23)	NaF-ZrF_4 (50-50)	+0.047
	NaF-ZrF_4-UF_4 (53-43-4)	−0.005
Cr_3C-Ni (89-11)	NaF-ZrF_4 (50-50)	+0.152
	NaF-ZrF_4-UF_4 (53-43-4)	+0.153

*Firth Sterling 27.

TABLE 6.2. RESULTS OF SEESAW TESTS OF VARIOUS CERMET MATERIALS TESTED IN NaF-ZrF_4-UF_4 (50-46-4 mole %)

MATERIAL	COMPOSITION (wt %)	METALLOGRAPHIC NOTES
Metamic LT-1 (not heat treated)	Cr-Al_2O_3 (77-23)	Specimen completely penetrated
Metamic LT-1 (heat treated)	Cr-Al_2O_3 (77-23)	Specimen completely penetrated
Firth Sterling 27	TiC_2 with Ni-Cr binder*	Attack zone 2 to 5 mils deep, 3 mils in most places
Kenametal 151A	TiC_2 with 20% Ni	Slightly affected zone 1 to 2 mils deep

*Cf., Table 6.1.

agent, and, as expected, these materials were attacked by the fluorides. Metamic LT-1, in both the heat-treated and unheat-treated conditions, was attacked severely. While the attack on the Firth Sterling 27 and on the Kenametal 151A in the seesaw tests was only moderate, the increased severity of attack in the seesaw tests compared with that in the static tests is evidenced by the test data on Firth Sterling 27.

Inconel with Oil and Trichloroethylene Additives

Several thermal convection loops had more than average depths of attack which were thought to be due to improper degreasing of the loops prior to filling. Therefore, a static test was run in which six drops of oil and six drops of trichloroethylene were added to an Inconel capsule containing an Inconel specimen and the solution was allowed to evaporate in an attempt to duplicate improper degreasing. This capsule was then loaded with the fluoride mixture NaF-ZrF_4-UF_4 (50-46-4 mole %) and tested for 100 hr at 816°C under static conditions, along with a control capsule for comparison. The specimen in the control capsule had greater weight loss and depth of attack than the specimen contaminated by the evaporation of the trichloroethylene-oil solution. It appears that under the conditions of this test, the contamination was not detrimental and might even have been beneficial.

Inconel Corrosion by Fluorides with MoS_2 Additive

Molybdenum disulfide is being used as a Swagelok lubricant in fluoride production systems, and therefore it was pertinent to determine whether increased corrosion of the Inconel tubing would result if some of the MoS_2 were to contaminate the fluoride. Accordingly, two seesaw tests of the fluoride mixture NaF-ZrF_4-UF_4 (50-46-4 mole %) in Inconel tubing were run for 100 hr. In one of these tests, an addition of 3 wt % MoS_2 was made to the fluoride; the other test was run with no addition to fluoride.

Metallographic examination of sections of tubing from hot and cold zones of both tests showed that more severe attack had taken place in the test with the MoS_2 addition. The cause of this increased corrosion is not known. The type and extent of attack both with and without MoS_2 additions is shown in Fig. 6.1.

Screening Tests of Metallic Bearing Materials

Several tests have been completed in the screening program on materials for potential use in bearing and hard-facing applications. Materials for these uses must be resistant to corrosion by molten fluorides. One set of specimens consisted of Hastelloys B, C, and D, and Stellites 1, 6, 12, 21, 25, 40, and 41 deposited on pieces of type 347 stainless steel. These composite specimens were tested in the fluoride mixture NaF-ZrF_4-UF_4 (50-46-4 mole %) for 100 hr at 816°C under static conditions. In these tests, it appeared that Hastelloys B, C, and D and Stellites 21, 25, and 40 satisfactorily resisted attack by this fluoride mixture. Stellites 1, 6, 12, and 41 appeared to be attacked severely. The appearance of Stellite 40 after the test is shown in Fig. 6.2; the attack is limited to a depth of 4 or 5 mils. As reported previously, it is apparently the carbides in the Stellites which are preferentially attacked by the fused fluoride salts, and it appears that the Stellites of low carbon content are not so severely attacked. The results of these tests are presented in Table 6.3.

FLUORIDE CORROSION OF INCONEL IN THERMAL CONVECTION LOOPS

G. M. Adamson
Metallurgy Division

The use of thermal convection loops for determining dynamic corrosion by liquids has been previously described.[1] Unless otherwise stated for the tests described in the following sections, the temperature of the hot leg of the loop was maintained at 1500°F and the temperature of the uninsulated cold leg was approximately 1300°F. With the fluoride salts, this temperature difference results in a fluid velocity of about 6 to 8 fpm. The usual testing period is 500 hours.

Effect of Fluoride Batch Purity

Pilot-plant batches of the fluoride fuel mixture NaF-ZrF_4-UF_4 (50-46-4 mole %) which received a 24-hr gas purification instead of the customary 8 hr or less are now available for thermal convection loop work. The longer gas purification results in a reduction of the hydrogen fluoride content of the melt. Corrosion results from three

[1] D. C. Vreeland *et al.*, *ANP Quar. Prog. Rep. March 10, 1953*, ORNL-1515, p. 121.

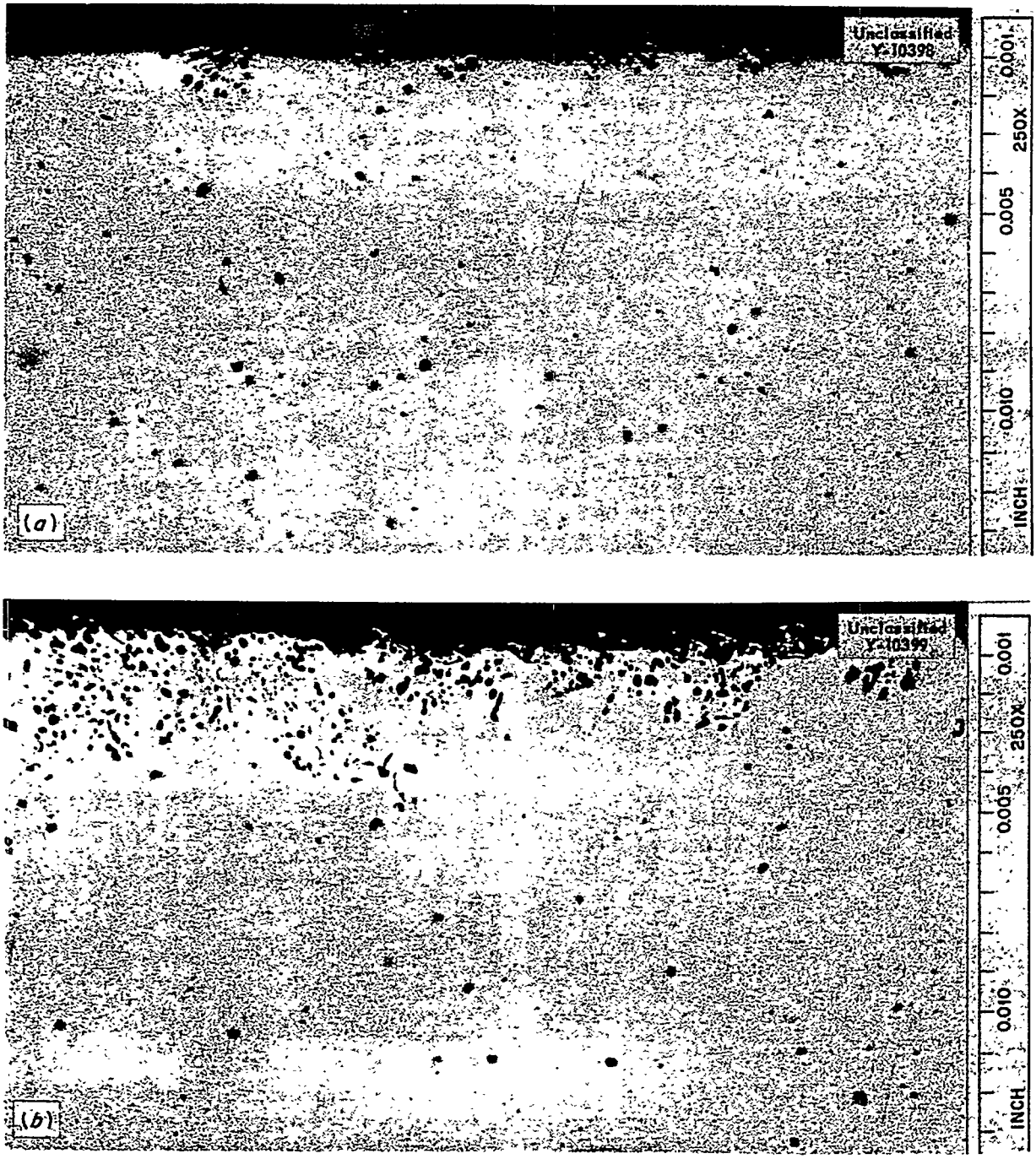

Fig. 6.1. Corrosion of Inconel after a 100-hr Seesaw Test at 815°C in the Fluoride NaF-ZrF_4-UF_4 (50-46-4 mole %) with and Without 3 wt % MoS_2 Additive. *a*. Tested with no additive. 250X. *b*. Tested with 3 wt % MoS_2 added. 250X.

TABLE 6.3. CORROSION OF HARD-FACED TYPE 347 STAINLESS STEEL SPECIMENS EXPOSED TO $NaF-ZrF_4-UF_4$ FOR 100 hr AT 816°C UNDER STATIC CONDITIONS

HARD-FACING MATERIAL	COMPOSITION (wt %)	METALLOGRAPHIC NOTES
Hastelloy B	Mo, 26 to 30 Fe, 4 to 7 C, 0.12 max Ni, balance	A few voids to a depth of 0.5 mil
C	Mo, 16 to 18 Fe, 4.5 to 7 C, 0.15 max Cr, 15.5 to 17.5 W, 3.75 to 5.25 Ni, balance	A little spalling and a few voids to a maximum depth of 1 mil
D	Cu, 3 Al, 1 Si, 10 Mn, 1 Ni, balance C, ?	Subsurface voids to a depth of 1.5 mils
Stellite 1	Cr, 30.5 W, 12.5 Fe, 3 max C, 2.5 Ni, 1 Co, balance	Many voids to a depth of 5 to 10 mils
6	Cr, 27.5 W, 4 Fe, 2 to 3 max C, 1 Co, balance	Erratic attack up to 15 mils deep along carbides in grain boundaries
12	Cr, 29.5 W, 8.25 Fe, 2 to 3 max C, 1.4 Ni, 1 Co, balance	Erratic intergranular attack 0 to 13 mils deep
21	Cr, 25 to 30 Ni, 1.5 to 3.5 Mo, 4.5 to 6.5 Fe, 2 max Co, balance C, 0.2 to 0.35	A few voids to a depth of 0.5 mil

TABLE 6.3. (continued)

HARD-FACING MATERIAL	COMPOSITION (wt %)	METALLOGRAPHIC NOTES
Stellite 25	Cr, 19 to 21 C, 0.15 Ni, 9 to 11 W, 14 to 16 Si, 1 Mn, 1 to 2 Fe, 2 Co, balance	A few voids to a depth of 0.5 mil
40	Composition not available	Voids to a depth of 3 to 5 mils
41	Composition not available	Heavy, erratic intergranular attack 4 to 23 mils deep

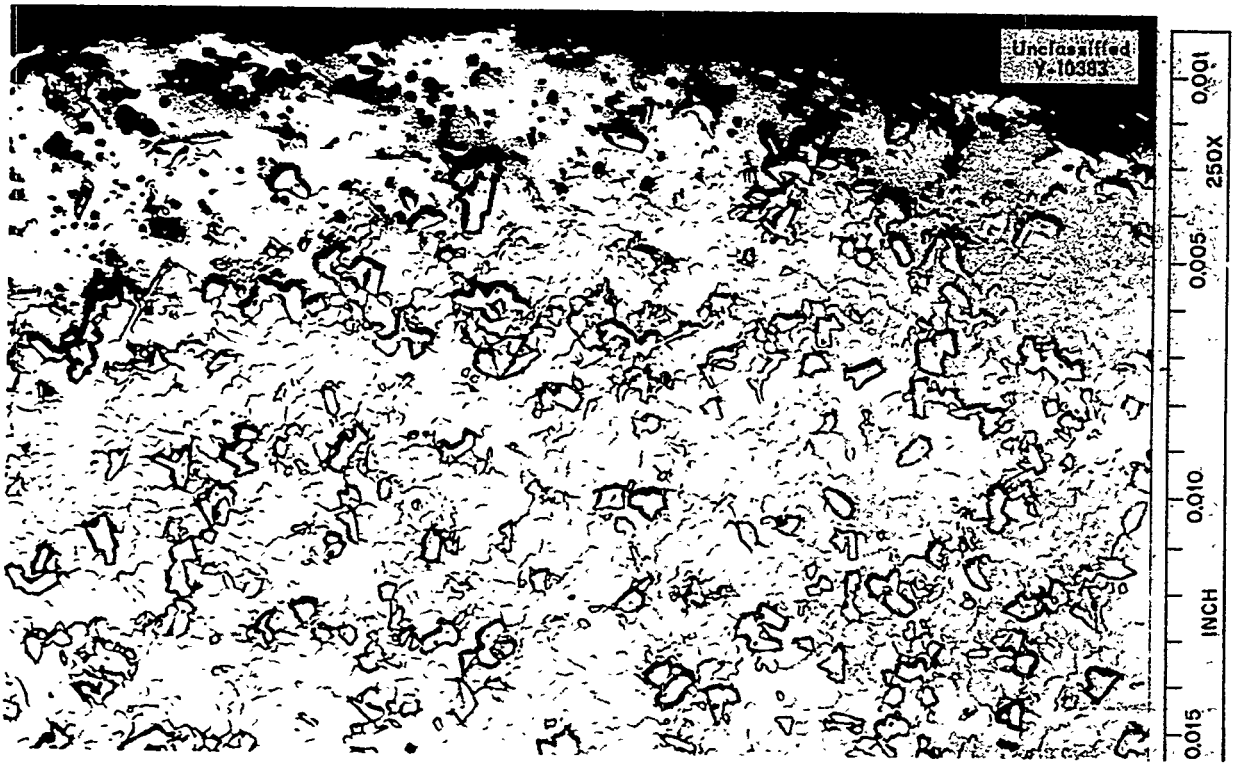

Fig. 6.2. Stellite 40 After Static Testing in $NaF-ZrF_4-UF_4$ (50-46-4 mole %) for 100 hr at 816°C.

Inconel loops operated with this material showed general attack to a depth of 3 mils and some intergranular penetration to a depth of 6 mils. The importance of purity of the materials is evident from these tests, since the average maximum penetration in standard production batches has been 9 mils. The reduction in attack, shown on Fig. 6.3, was also reflected in the chromium pickup, which was down to 450 to 600 ppm, that is, less than one half the previous contamination. Some reduction was also obtained in the amount of iron present.

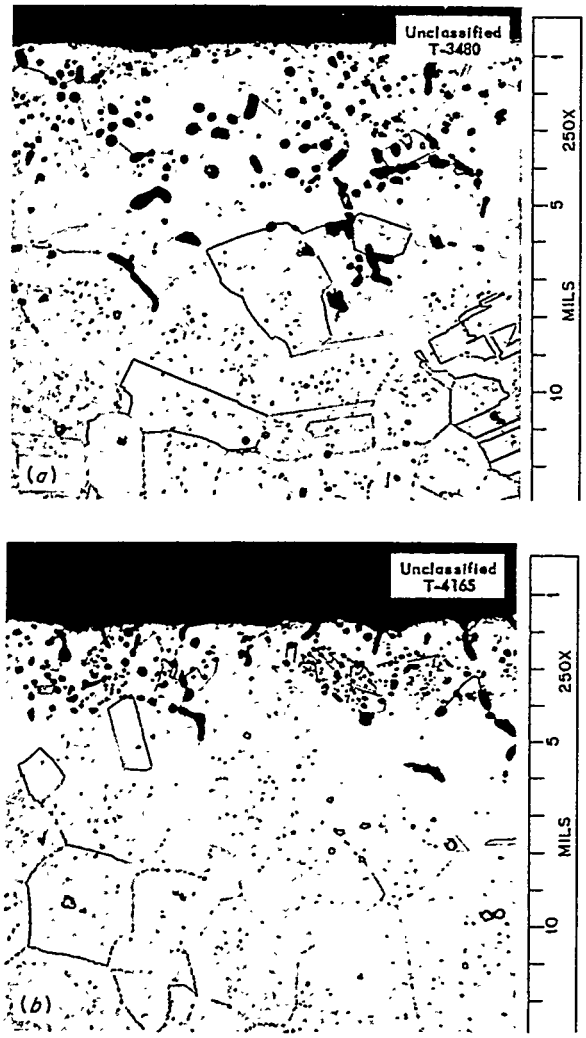

Fig. 6.3. Effect of Fluoride Batch Purity on the Corrosion of Inconel Exposed in Thermal Convection Loops to NaF-ZrF_4-UF_4 (50-46-4 mole %) for 500 hr at 1500°F. *a.* Exposed to standard production batch. 250X. *b.* Exposed to high-purity batch. 250X. Reduced 17%.

Fluoride fuel mixtures with high hydrogen fluoride content were circulated in a number of loops. Increased corrosion, as indicated by heavy attack and maximum penetrations of 14 and 15 mils, was found under standard operating conditions.

Effect of Chromium Additives

Data were presented previously[2] which indicated doubtful improvement in corrosion characteristics when chromium powder was added to the fluoride mixtures. However, in a new test, in which the chromium was added in the form of coarse metallic flakes, a reduction in the depth of attack was found. The fluoride mixture was held in contact with the chromium flakes overnight at a temperature of 1300°F before being charged into the loop. Examination subsequent to operation of the loop showed a maximum penetration of only 4 mils, as compared with penetration of the control loop to a depth of 15 mils. As in previous tests with chromium additions, a thin, continuous, metallic deposit was found in the cold leg of the loop.

One thermal convection test was run in which the chromium was added in the form of an electroplated layer on the inner surface of a 6-in. length of Inconel pipe. This pipe was welded into the top of the hot leg of a standard loop. After operation of the loop, no trace of the chromium could be found in the hot leg by metallographic examination. Typical subsurface void attack was found in the Inconel, with a maximum penetration of 10 mils. No data are available on the hydrogen fluoride content of the batch circulated in this loop. The 10 mils of attack is slightly higher than the average, but no change in attack could be seen on opposite sides of the hot leg where the section was welded into the loop. Scattered metallic particles were found on the cold-leg wall. This test confirms the earlier finding that, while a direct chromium addition to the fuel may result in a beneficial effect, a chromium plate on the pipe wall does not offer any protection in a dynamic system.

Although large additions of chromium were made to the fluoride mixtures in both these loops, the chromium concentration in the fluoride mixtures after circulation in both loops was uniform and was only 1600 ppm. A study of the chemical analyses of fluoride mixtures from other loops showed this concentration to be the maximum reported. Attempts have been made by the Materials Chemistry Division to obtain apparent solubilities of chromium of over 1% at 800°C in this fluoride mixture, but it is speculated that 1600 ppm is an equilibrium concentration. Attempts to obtain this concentration in the laboratory have not yet been successful.

[2] G. M. Adamson, *ANP Quar. Prog. Rep. June 10, 1953*, ORNL-1556, p. 60.

Pretreatment of Fluoride with Inconel

Some reduction in corrosive attack was obtained by first holding the fluorides in contact with Inconel turnings for 100 hr at 1300°F. After subsequent operation of the convection loop, examination revealed the maximum depth of attack of the Inconel to be 11 mils, as compared with a maximum depth of 14 mils in the control tests. This pretreatment, although it apparently does not have as beneficial an effect on the corrosion properties as does the chromium addition, has the advantage that it prevents the formation of a layer on the cold-leg wall. It is likely that larger reductions in attack would be obtained with higher treatment temperatures, although it is not convenient to do this with existing equipment.

Effect of Exposure Time

Two series of Inconel loops have been filled and are now being operated to determine the effect of time on corrosion and mass transfer. One series is circulating the fluoride fuel NaF-ZrF_4-UF_4 (50-46-4 mole %), and the other is circulating the fuel solvent $NaZrF_5$; periods of operation have ranged from 500 to 5000 hours. Both series of loops were filled with especially purified fluorides. Metallographic results are now available for the loops which circulated fuel for 500 and 1000 hours.

Moderate to heavy subsurface void formation with a maximum penetration of 8 mils was found in the hot leg of a loop that operated for 1000 hours. The voids tended to concentrate more in the grain boundaries than they do in standard loops. An intermittent very thin layer that appeared to be metallic was noted in the cold leg, and a thin, metallic ring of chromium metal was visible in the cold trap. This is the first Inconel loop circulating the NaF-ZrF_4-UF_4 fuel in which a definite cold-leg layer has been found.

The standard loop that operated for 500 hr showed moderate to heavy attack with a maximum penetration of 6 mils. No metallic deposit was visible in the cold leg or in the trap of this loop. A dark layer was found in the trap, but it was not metallic. Comparison of the results from these two loops helps to confirm the previous observation that a decrease in rate of attack is apparent with longer operating times; however, the attack does not stop completely. The increase in the metallic deposit on the cold leg and in the trap points to mass transfer as the cause of the continuing attack.

Effect of Temperature

Additional confirmation of the conclusion presented in the previous report[3] that attack is independent of hot-leg temperature from 1400 to 1650°F has been obtained. A loop operated for 1000 hr with a hot-leg temperature of 1650°F showed attack comparable to that of another loop which operated for 1000 hr at 1500°F. Both loops were filled with fluoride fuel of comparable purity, and the attack in both was moderate, with a maximum penetration of 8 mils. Furthermore, the voids in both loops were similar, although they were larger and more concentrated at the grain boundaries than they were in similar loops operated for only 500 hours.

Effect of Surface-to-Volume Ratio

Large differences have always been observed between the corrosion results obtained in seesaw tests and those obtained in convection loops. One of the main variations is in the surface-to-volume ratios. To determine the effect of this variable, a loop was constructed from 1-in. tubing instead of from the standard ½-in.-IPS pipe. The loop with the 1-in. tubing has a surface-to-volume ratio of 4.5 $in.^2/in.^3$, while that of a standard loop is 6.5 $in.^2/in.^3$. The attack in the hot-leg of the loop with 1-in. tubing was light to moderate, with a maximum penetration of 9 mils. A standard loop filled from the same fuel batch showed similar attack, with a maximum penetration of 5.5 mils. The percentage increase in attack depth was about the same as that for the decrease in the surface-to-volume ratios. This increase in attack depth with a decrease in surface-to-volume ratio again points to impurities in the fluorides as the major factor in corrosion.

Fluoride with 6.5 mole % UF_4

Tests have been completed on two Inconel loops circulating the fluoride fuel mixture with the highest UF_4 concentration contemplated for use in the ARE, that is, NaF-ZrF_4-UF_4 (53.3-40.0-6.5 mole %). For the first test, which was run to provide preliminary data, the loop was not thoroughly

[3] G. M. Adamson, *ANP Quar. Prog. Rep. Sept. 10, 1953*, ORNL-1609, p. 77.

cleaned, and the fuel preparation was not of optimum purity. The preliminary test loop was operated for 350 hr at 1500°F, and, upon examination, was found to have moderate to heavy attack in the form of subsurface voids to a maximum depth of 12.5 mils. A very thin metallic deposit was found in the cold leg. The second test loop was cleaned by circulating $NaF\text{-}ZrF_4$, and it was charged with high-purity fuel. After 500 hr of operation, this loop showed heavy attack to a maximum penetration of 7 mils, as shown in Fig. 6.4. Again, a thin, metallic layer was found in the cold leg. Two more standard Inconel loops are now being operated with this high-purity fuel mixture. The preliminary tests indicate that the higher uranium content of this fuel may cause a small increase in the depth of attack, but additional tests are needed for confirmation. The higher uranium content also causes an increased amount of mass transfer, as shown by the thin, metallic layer in the cold leg.

The Fluoride $NaZrF_5$

One batch of $NaZrF_5$, the ARE fuel solvent, was tested in a series of six Inconel loops. Upon examination, the loops showed light to moderate attack, with maximum penetration ranging from 4 to 8 mils, and the fluoride was found to contain average impurities, that is, 230 ppm of Cr, 55 ppm of Fe, and less than 20 ppm of Ni. A typical corrosion specimen taken from the hot leg of one of these loops is shown in Fig. 6.5. The voids are larger, and they are more definitely concentrated in the grain boundaries than they were in the tests with the uranium-bearing fluoride mixture. The low chromium content of the fluoride after circulation in these loops is not understood because, even though the attack was less, it was not decreased so much as was the chromium content. There was a gray layer above the freezing line in the trap of each of these loops that was about $\frac{1}{8}$ to $\frac{1}{4}$ in. in thickness. This material was identified petrographically as fine, needle-like, metallic crystals of chromium metal dispersed in the fluoride. Some mass transfer had, therefore, taken place even with the low chromium concentrations found in these loops.

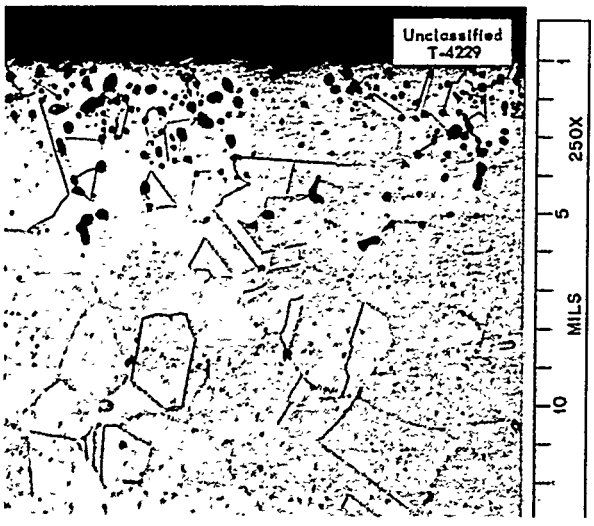

Fig. 6.4. Corrosion of Inconel Thermal Convection Loop by High-Purity $NaF\text{-}ZrF_4\text{-}UF_4$ (53.5-40.0-6.5 mole %) After 500 hr at 1500°F. 250X. Reduced 15%.

FLUORIDE CORROSION OF NICKEL AND STAINLESS STEEL LOOPS

G. M. Adamson
Metallurgy Division

A small amount of mass transfer was previously observed[4] in a nickel loop in which the fuel $NaF\text{-}ZrF_4\text{-}UF_4$ (50-46-4 mole %) was circulated. To confirm this single test, another nickel loop was

[4] G. M. Adamson, *ANP Quar. Prog. Rep. June 10, 1953*, ORNL-1556, p. 63-64.

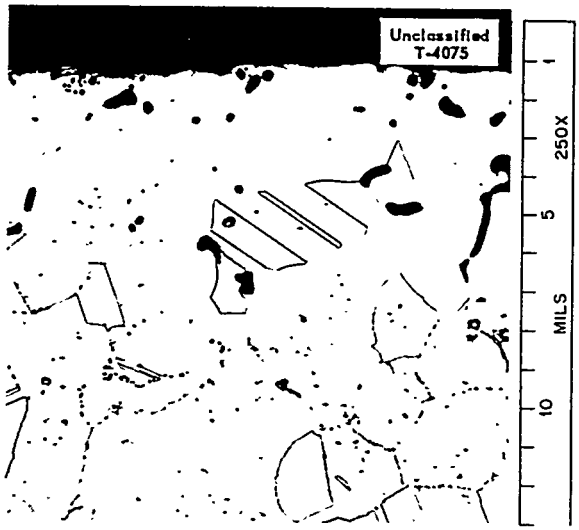

Fig. 6.5. Corrosion of Inconel Thermal Convection Loop by $NaZrF_5$ After 500 hr at 1500°F. 250X. Reduced 12%.

cleaned with $NaZrF_5$ and operated with high-purity fuel. After circulation of the fuel, no metallic crystals were found in the fluorides in the cold leg or in the trap nor could any layer be identified on the cold-leg surface. The surface of the hot leg was bright and polished, and there was no evidence of subsurface voids or intergranular attack. The wall thickness was within commercial tolerances, but it was again on the low side. It seems likely that a small amount of even removal had taken place, since the surface was polished; however, this seems to be the smallest amount of mass transfer yet found.

One type 430 stainless steel loop operated with the fuel $NaF-ZrF_4-UF_4$ (50-46-4 mole %) for 500 hr at 1500°F with no sign of plugging. However, a preliminary metallographic examination revealed unexpected even surface removal in the hot leg rather than the subsurface voids in the grain boundaries that were found in the type 316 stainless steel loop. The hot-leg surface was smooth, with no subsurface voids or intergranular type of attack. Carbides appear to have been leached (or possibly to have gone back into solution) from a zone about 2 mils wide on the surface, and considerable grain growth had taken place in this zone. The outer surface of the pipe was quite rough, and therefore the wall thickness measurements are questionable. Variations in thickness of from 0.106 to 0.109 in. were found. Since the specified thickness of the wall was 0.109 in., it is evident, at least, that no large amount of even removal occurred. However, some removal had taken place, as shown by the scattered metallic crystals adhering to the cold-leg surface.

LIQUID METAL CORROSION

W. H. Bridges
J. V. Cathcart
E. E. Hoffman
J. E. Pope
G. P. Smith
L. R. Trotter
D. C. Vreeland
Metallurgy Division

Mass Transfer in Liquid Lead

Investigations of mass transfer and corrosion of various metal specimens in small, quartz, thermal convection loops containing liquid lead have been continued. Details of the construction and operation of the loops and the results obtained for Inconel, columbium, molybdenum, types 304, 347, 410, and 446 stainless steel, Armco iron, nickel, chromium, Nichrome V, and a nickel-iron (30% Ni–70% Fe) alloy were reported previously.[5] The metals tested during this quarter included a molybdenum-nickel (25% Mo–75% Ni) alloy, a chromium-iron-silicon (14% Cr–84% Fe–27% Si) alloy, and types 304 and 347 stainless steel specimens which were oxidized prior to contact with the lead.

The molybdenum-nickel alloy loop was operated for 672 hr with hot- and cold-leg temperatures of 820 and 480°C, respectively. Plugging did not occur, but a small amount of mass-transferred material was found in the bottom of the cold leg. The extent of the corrosive attack may be seen in Fig. 6.6. A spectroscopic analysis showed that the mass-transferred material consisted almost entirely of nickel, the concentration of molybdenum being less than 0.01%. The results for this loop were comparable to those previously obtained for the 400 series stainless steels.

The loop containing chromium-iron-silicon alloy specimens was operated for 550 hr with hot- and cold-leg temperatures of 805 and 490°C, respectively. Again, the mass transfer which occurred was not sufficient to stop circulation, but a plug was starting to form in the cold leg. The amount of mass-transferred material was slightly greater than that found in loops containing the 400 series stainless steels. Rather severe intergranular attack to a depth of 12 mils was found.

The effect of an oxide coating on the metal specimens was also studied. Sections of types 347 and 304 stainless steel tubing were oxidized until they showed interference colors corresponding to oxide thicknesses of 500 to 1000 Å. These test specimens were then tested in quartz loops, and marked improvement in resistance to mass transfer was noted with both metals. A loop containing oxidized, tubular, type 347 stainless steel specimens was operated for 550 hr with hot- and cold-leg temperatures of 815 and 510°C, respectively. The loop was terminated on schedule and only a small amount of mass-transferred material was found in the cold leg. When the type 347 stainless steel specimens were used in the as-received condition, a plug formed in the loop within 140 hours. Although uniform intergranular attack was observed on the inner surface of the oxidized

[5] *ANP Quar. Prog. Rep.*, ORNL-1515, p. 128; *op. cit.*, ORNL-1556, p. 64; *op. cit.*, ORNL-1609, p. 80; *Met. Div. Semiann. Apr. 10, 1953*, ORNL-1551, p. 17.

Fig. 6.6. Corrosion of a Molybdenum-Nickel (25% Mo–75% Ni) Alloy Specimen in a Quartz Thermal Convection Loop After Circulation of Lead for 672 hr at 820°C. 500X.

tubular specimen, much less corrosion was observed on the outer surface. The attack appeared to have started on the outer surface of the specimen at isolated points along the surface, perhaps corresponding to breaks in the oxide film, and to have spread out in fan-like fashion (Fig. 6.7). Corrosion of the specimen in the cold leg of the loop was much less pronounced.

A type 304 stainless steel loop containing previously oxidized specimens was also operated for 550 hr without the formation of a plug large enough to stop circulation. The hot- and cold-leg temperatures were 800 and 550°C, respectively. Metallographic examination of this loop is incomplete. In previous tests with type 304 stainless steel specimens in the as-received condition, the loops had to be terminated within 100 hr because of plug formation.

Static Tests of Beryllium Oxide in Sodium, Lithium, and Lead

Specimens of beryllium oxide, approximately ½ by ¼ by ¼ in., cut from 2-in. hexagonal blocks hot pressed by the Norton Company were tested in sodium, lithium, and lead. One half the specimens were tested as cut from the original block, and one half were tested after having been refired for 2 hr at 1800°C. The refired specimens had higher density and lower apparent porosity than those specimens which were not refired. The sodium was contained in Inconel tubes, and the lithium and the lead were contained in Armco iron tubes. The test time was 100 hr, and the temperature was 538°C. The weight and dimension changes after test were less than 1.5%. The weight gains in sodium and lithium were presumed to be due to absorption of these metals. The specimens tested in lead appeared to be affected the least. Edges of the specimens appeared to be just as sharp after test as before. The refired beryllium oxide specimens apparently had greater resistance to attack than did the specimens that were not refired. The one exception appeared in the sodium test, and, even in this test, the refired specimen was more dimensionally stable.

Spinner Tests of Inconel and Type 405 Stainless Steel in Sodium

A spinner test was run with Inconel-X in sodium, but the apparatus was not rotated. This test was run to check the possibility that attack noted in a previous spinner test might be due to impurities in the sodium or in the atmosphere rather than to the velocity of test. However, much lighter attack and less weight change was noted on these specimens than on the Inconel-X specimens previously tested at fluid velocities of 405 fpm; therefore it is evident that most of the attack in spinner tests is due to velocity effects.

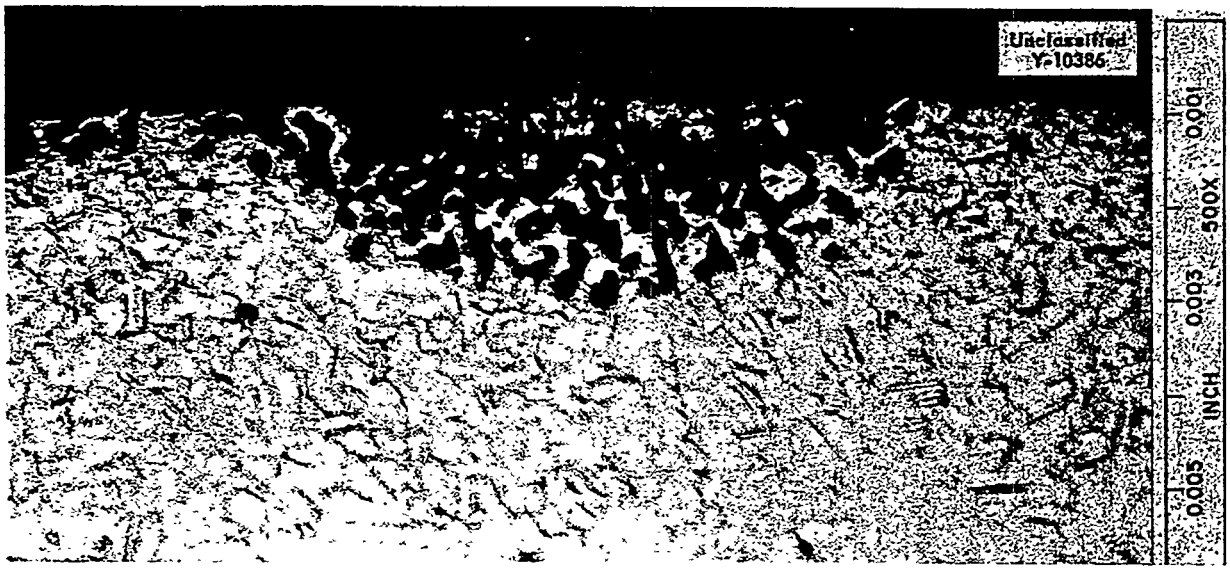

Fig. 6.7. Corrosion on Outer Surface of a Tubular Type 347 Stainless Steel Specimen Exposed to Circulating Lead in a Quartz Convection Loop for 550 hr at 815°C. 500X.

A spinner test with type 405 stainless steel (12% Cr) has also been run at a velocity of 405 fpm. These tests were conducted at a temperature of 816°C for 100 hr in sodium. The weight change was of the order of +0.5%, and the attack was intergranular to a maximum depth of 3 mils, with surface roughness to approximately 1 mil.

Static Tests of Bearing Materials in Sodium, Lithium, and Lead

A number of metal alloys of potential value in bearing and hard-facing applications in liquid metals have been tested in sodium, lead, and lithium under static conditions for 100 hr at 816°C. The results of these screening tests are given in Table 6.4.

Static Tests of Stainless Steels in Lithium

A series of static tests of various stainless steels in two types of lithium (helium packed and oil packed) have been run for 100 hr at 816°C. In this group of tests, types 310 and 446 stainless steel showed the least resistance to attack by lithium, while type 347 stainless steel showed the best resistance. Types 304, 309, 316, and 347 stainless steel showed very little or no subsurface attack. Crystals of what were identified by x-ray diffraction as a chromium carbide phase (DPH 1000 to 1100) were detected on the exposed surface of all the austenitic stainless steel specimens, as shown in Fig. 6.8. These crystals were more numerous and slightly larger on the specimens tested in the oil-packed lithium, as would be expected because of the higher carbon content of this material. Chemical analyses of the lithium baths after testing revealed no significant changes in the iron, nickel, and chromium contents of the oil-packed and helium-packed lithium. In the tests in which weight changes were noted, the weight changes of the specimens in helium-packed lithium were less than those of the specimens in oil-packed lithium, possibly because of the higher purity of the gas-packed lithium. Results of these tests are summarized in Table 6.5.

Static Tests of Solid Fuel Elements in Sodium and Sodium Hydroxide

Core materials (UO_2) that had been clad with nickel, copper, and types 304, 316, and 347 stainless steel were tested in sodium and sodium hydroxide for 100 hr at 816°C under static conditions. These specimens were prepared to the specifications given in Table 6.6.

Specimens clad with nickel and types 304, 316, and 347 stainless steel were annealed for 15 min at 1000°C in hydrogen; copper-clad specimens were annealed for 15 min at 450°C in hydrogen. These specimens were approximately 1 by 0.35

TABLE 6.4. STATIC TESTS OF VARIOUS ALLOYS IN SODIUM, LITHIUM, AND LEAD FOR 100 hr AT 816°C

MATERIAL	COMPOSITION	CORRODANT	METALLOGRAPHIC NOTES
Hastelloy			
B	Mo, 26 to 30 Fe, 4.7 C, 0.12 max Ni, balance	Sodium	Some voids to 0.5 mil in a few places
		Lead	0 to 5 mils of erratic alloying type of attack
		Lithium	5 mils of subsurface voids
C	Mo, 16 to 18 Fe, 4.5 to 7 C, 0.15 max Cr, 15.5 to 17.5 W, 3.75 to 5.25 Ni, balance	Sodium	Some voids in a few places to 0.5 mil
		Lead	Erratic attack; practically complete penetration in some places, very little in others
		Lithium	4 to 8 mils of subsurface voids
D	Cu, 3 Al, 1 Si, 10 Mn, 1 Ni, balance C, ?	Sodium	Layer of subsurface voids 1 to 2 mils deep on some portions of specimen
		Lead	Specimen appeared to be completely penetrated
		Lithium	4 to 6 mils of subsurface voids
Stellite			
1	Cr, 30.5 W, 12.5 Fe, 3 max C, 2.5 Ni, 1 Co, balance	Sodium	Apparently no attack
		Lead	2 mils of voids and intergranular attack
		Lithium	0.5 to 1 mil subsurface voids where carbides were attacked
6	Cr, 27.5 W, 4 Fe, 2 to 3 max C, 1 Co, balance	Sodium	Very slight intergranular penetration, less than 0.5 mil
		Lead	Intergranular attack 1 to 2 mils deep
		Lithium	4 to 6 mils of subsurface voids where carbides were attacked
12	Cr, 29.5 W, 8.25 Fe, 2 to 3 max C, 1.4 Ni, 1 Co, balance	Sodium	Very slight intergranular penetration, less than 0.5 mil
		Lead	Apparently no attack
		Lithium	Less than 0.5 mil of attack on carbide phase
21	Cr, 25 to 30 Ni, 1.5 to 3.5 Fe, 2 max Mo, 4.5 to 6.5 C, 0.2 to 0.35 Co, balance	Sodium	Apparently no attack
		Lead	A slight roughening and intergranular penetration to about 0.5 mil
		Lithium	0.5 mil of small subsurface voids

TABLE 6.4 (continued)

MATERIAL	COMPOSITION	CORRODANT	METALLOGRAPHIC NOTES
Stellite 25	Cr, 19 to 21 C, 0.15 Ni, 9 to 11 W, 14 to 16 Si, 1 Mn, 1 to 2 Fe, 2 Co, balance	Sodium	Some voids and intergranular attack to 1 mil maximum in a few places
		Lead	Voids to about 0.5 mil
		Lithium	2 mils of subsurface voids in most places, 10 to 12 mils in several places
40	Composition not available	Sodium	
		Lead	Very heavy penetration to about 50 mils
		Lithium	Subsurface voids to a depth of 10 mils
41	Composition not available	Sodium	Apparently no attack
		Lead	Apparently complete penetration
		Lithium	Subsurface voids to a depth of 10 to 15 mils

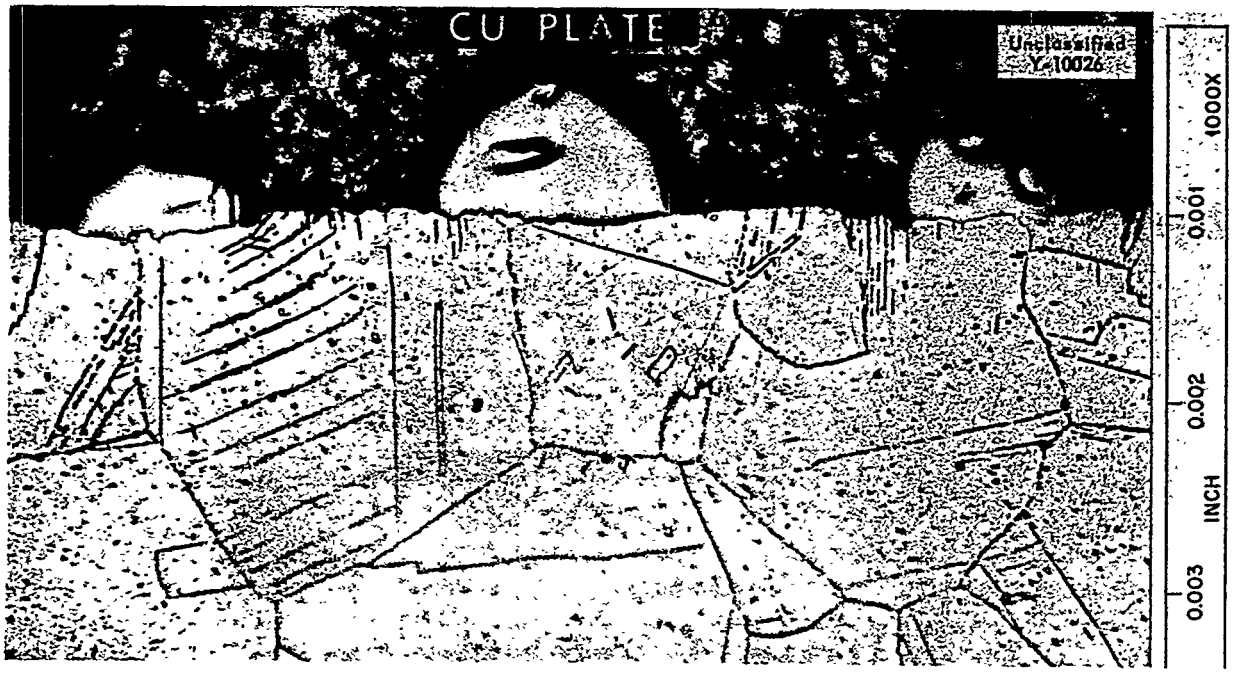

Fig. 6.8. Type 316 Stainless Steel After Static Testing in Lithium for 100 hr at 816°C. Note crystals attached to surface. 1000X. Specimen copper plated to preserve edge during polishing.

by 0.050 inch. The thickness of the core and of each of the cladding layers was approximately 16 mils.

In sodium, the specimens clad with nickel and types 304, 347, and 316 stainless steel showed no evidence of attack. The sample clad with copper had a slightly irregular edge and showed weight and dimensional increases after testing. The many, copper, mass-transferred crystals attached to this specimen were probably caused by temperature gradients during the test. In the tests in sodium hydroxide, the copper- and nickel-clad specimens were unattacked, and the types 304, 316, and 347 stainless steel-clad materials were attacked more or less severely, that is, from 5 to 18 mils. The type 347 stainless steel-clad specimen tested in sodium hydroxide is shown in Fig. 6.9.

TABLE 6.5. STATIC CORROSION OF STAINLESS STEELS TESTED IN TWO TYPES OF LITHIUM FOR 100 hr AT 816°C

TYPE OF STAINLESS STEEL	WEIGHT CHANGE ($g/in.^2$)	ANALYSIS (wt %)	METALLOGRAPHIC NOTES
304 (a)*	0	Fe, 0.024 Ni, 0.017 Cr, <0.001	Small crystals (0.5 mil thick) attached to surface; some of this same phase concentrated in grain boundaries near surface
(b)**	0	Fe, 0.026 Ni, 0.021 Cr, 0.002	Same as above, with surface of specimen slightly irregular, 0.5 mil of attack
309 (a)	−0.0010	Fe, 0.017 Ni, 0.034 Cr, 0.018	Specimen attacked to 4 mils in one area; several small crystals attached to surface
(b)	−0.0013	Fe, 0.017 Ni, 0.040 Cr, 0.011	No attack on specimen; crystals (0.25 mil thick) attached to surface in some areas
310 (a)	−0.0007	Fe, 0.012 Ni, 0.032 Cr, 0.028	Grain boundaries of specimen exuded moisture to a depth of 6 to 7 mils, which indicated penetration by lithium to this depth; crystals attached to surface in some areas
(b)	−0.0007	Fe, 0.018 Ni, 0.030 Cr, 0.046	Grain boundaries of specimen exuded moisture to a depth of 6 to 8 mils, as above; surface layer on part of specimen approximately 0.25 mil in thickness
316 (a)	0	Fe, 0.007 Ni, 0.037 Cr, 0.01	Grain boundaries exuded moisture to a depth of 5 mils in some areas; specimen heavily attacked to 0.5 mil in one area; crystals attached to surface
(b)	+0.0009	Fe, 0.006 Ni, 0.038 Cr, 0.01	Approximately 0.5 mil of grain boundary attack; 1-mil-thick crystals attached to surface

*Tested in helium-packed lithium.

**Tested in oil-packed lithium.

TABLE 6.5 (continued)

TYPE OF STAINLESS STEEL	WEIGHT CHANGE ($g/in.^2$)	ANALYSIS (wt %)	METALLOGRAPHIC NOTES
317 (a)	+0.0007	Fe, 0.009 Ni, 0.028 Cr, 0.008	No attack except for surface layer 0.1 to 0.2 mil thick
(b)	+0.0009	Fe, 0.004 Ni, 0.009 Cr, 0.035	Same as above, with crystals to a maximum thickness of 0.7 mil
347 (a)	−0.0003	Fe, 0.11 Ni, 0.038 Cr, 0.003	No attack except for 0.25-mil-thick crystals attached to surface in some areas
(b)	+0.0003	Fe, 0.015 Ni, 0.039 Cr, 0.002	Same as above
446 (b)	+0.0026		Grain boundary voids to a depth of 10 mils

TABLE 6.6. SPECIFICATIONS OF SOLID FUEL ELEMENTS

CLADDING	CORE	ROLLING TEMPERATURE (°C)	HOT REDUCTION (%)
Type 304 stainless steel	Type 302 stainless steel–UO_2	1225	60
Type 316 stainless steel	Type 302 stainless steel–UO_2	1225	60
Type 347 stainless steel	Type 302 stainless steel–UO_2	1225	60
Nickel	Nickel-UO_2	1100	60
Copper	Copper-UO_2	1000	60

FUNDAMENTAL CORROSION RESEARCH

J. V. Cathcart G. P. Smith
Metallurgy Division

Oxidizing Power of Hydroxide Corrosion Products

The work on trivalent nickel compounds formed in hydroxides was continued. The compound $NaNiO_2$ was found to undergo a change in crystal structure at about 225°C, and the structure of the high-temperature form has been determined. The existing evidence indicates that the transformation may be of the martensitic type.

Equilibrium Pressure of Hydrogen in Hydroxide-Metal Systems

F. Kertesz F. A. Knox
Materials Chemistry Division

During this quarter, equilibrium pressures of hydrogen over the KOH-Ni system were partially determined, and values previously reported for NaOH-Cu and NaOH-Au systems were redetermined by using a modified form of the apparatus previously described.[6]

The modified apparatus includes a long nickel tube which serves as a reaction chamber in place of the metal crucible previously used. This tube is surrounded by a quartz tube to which it is

[6] *ANP Quar. Prog. Rep. Sept. 10, 1953*, ORNL-1609, p. 84.

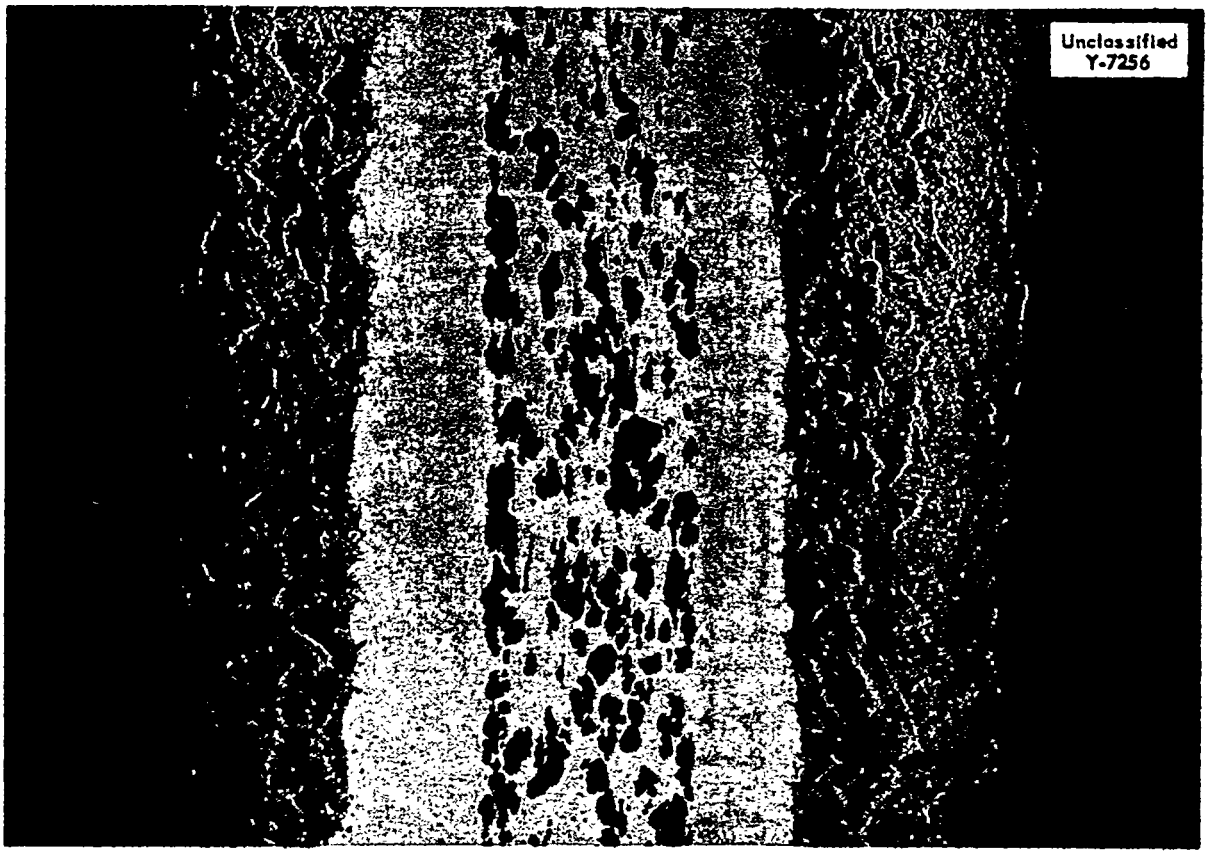

Fig. 6.9. Static Test of a Type 347 Stainless Steel-Clad Fuel Plate After 100 hr at 816°C in Sodium Hydroxide. 80X.

sealed by means of a Kovar seal. The pressures established inside the nickel tube and in its quartz jacket (nickel being permeable to hydrogen at the temperatures utilized in these experiments) are measured by two mercury manometers connected to the system by seals; therefore the pressure built up by the hydrogen that diffuses through the nickel can be determined independently from the pressure inside the tube. This apparatus utilizes both the passivity of nickel to sodium hydroxide and the nonpermeability of quartz to hydrogen. Equilibrium pressures may be established more rapidly by adding hydrogen to the quartz-nickel cavity to bring its pressure close to that inside the nickel tube.

The hydrogen pressure of the KOH-Ni system, as determined in the above-described apparatus, was found to be less than 1 mm at 600°C, while it is in the range of 8 to 12 mm at 700°C. Measurements at higher temperatures are being made.

The NaOH-Cu and NaOH-Au hydrogen equilibrium pressures were redetermined, and the results agreed closely with those previously reported:[6] for the NaOH-Au system at 900°C, 3.5 mm compared with 3.0; at 1000°C, 7.5 compared with 6.0 mm. The results for the NaOH-Cu system show reasonable agreement at 700°C (2.2 mm compared with 3.0 mm); however, the more recent determination at 800°C shows a thus far unexplained time dependence of the hydrogen pressure. An initial pressure of 14 mm gradually fell to about 10 mm after a few hours; the 10-mm pressure then remained constant.

Mass Transfer of Chromium in Inconel-Fluoride Systems

L. G. Overholser J. D. Redman
C. F. Weaver
Materials Chemistry Division

When Inconel is exposed to molten fluorides at elevated temperatures, chromium is selectively leached from the alloy. While a considerable fraction of this corrosion may be ascribed to oxidizing impurities in the molten material or on the capsule walls, reactions of UF_4 with the container metals to yield UF_3 and complex metal fluorides could well be responsible. The reaction

$$Cr + 2UF_4 \rightleftharpoons 2UF_3 + CrF_2$$

has at 600°C a standard free energy change of −7 kcal and should, if the ionic species were soluble and showed activities proportional to their concentrations, proceed nearly to completion. That such is not the case, or at least that the reaction does not equilibrate at a reasonable rate, is well demonstrated in a large number of corrosion tests.

If the assumption that the physical solubility of chromium as metal in fused $NaZrF_5$ is quite low is permissible, then equilibration of UF_4 dissolved in $NaZrF_5$ with chromium metal followed by separation of the phases and analysis of the filtrate would permit evaluation of the equilibrium constant of the reaction. For these studies, the purest $NaZrF_5$ available was used, along with chromium metal hydrogen fired at 2000°F in nickel equipment of the type previously described. All handling of the materials before testing was performed in an inert-atmosphere dry box. The filtrates obtained were submitted for chemical analysis, and the results shown in Table 6.7 were obtained.

These data indicate that equilibration is rapid because the values obtained after 5 hr at temperature are not distinguishable from those obtained for a shorter exposure. It is obvious from the exposure of the nonuranium-bearing material that the chromium contains some oxide and that hydrogen firing of the nickel equipment is not sufficiently complete. (Subsequent experiments, not sufficiently complete to report, in which the chromium was fired under dry hydrogen directly in the nickel reaction vessel demonstrate that it is possible to have less than 200 ppm of Cr in the nonuranium-bearing material.) The chromium concentration increase resulting from the reduction of UF_4 to UF_3 was obtained by subtracting the chromium content of the nonuranium-bearing material from the total chromium found, and this value was used for obtaining the UF_3 concentration, since the methods for determining UF_3 in the presence of divalent chromium are not sufficiently accurate to permit a direct determination of UF_3.

If unit activity is assumed for the chromium and activities equal to concentrations (in moles per mole of solvent) are assumed for the uranium and chromium species, these data indicate that the equilibrium constant at 600°C is 1.2 by 10^{-3}, and, at 800°C, it is 1.7 by 10^{-3}. The data are certainly not sufficient in amount or in precision for an evaluation of this small difference. It does

TABLE 6.7. ANALYSES OF FILTRATES FROM EQUILIBRATION OF CHROMIUM WITH NaF-ZrF_4-UF_4 MELTS

CONDITIONS OF EQUILIBRATION		FILTRATE ANALYSIS			
Time (hr)	Temperature (°C)	Total Uranium (%)	Chromium (ppm)	Nickel (ppm)	Iron (ppm)
5	800	0	935	355	75
		0	930	200	40
3	800	8.47	3420	30	65
		8.80	3330	40	60
3	600	8.80	3200	130	50
		8.65	3100	125	50
5	600	8.65	3100	130	70
		8.88	3200	130	60

appear, however, that the standard free energy change for the reaction at 600°C is about +11.5 kcal. The discrepancy between this measured value and the value of −7 kcal calculated for the reaction by assuming no complexing is probably to be ascribed to solvation of the UF_4.

These experiments are being refined, insofar as purity of the materials and improvement of techniques are concerned, and additional experiments will be conducted at considerably lower reagent concentrations so that the assumptions regarding activities will have more validity.

---

7. METALLURGY AND CERAMICS

W. D. Manly J. M. Warde
Metallurgy Division

A sodium-to-air radiator was fabricated by brazing the tube-to-fin joints and backing up the previously heliarc-welded tube-to-header and manifold joints with brazing alloy G-E No. 62, a nickel-chromium-silicon alloy. The radiator assembly was welded and then dry-hydrogen brazed at 2100°F for approximately 30 minutes. Subsequent testing after slow cooling showed all the welded and brazed joints to be satisfactorily leak and pressure tight. The duplex fabrication technique, that is, the combination of heliarc welding and high-temperature brazing, apparently produces satisfactory, sound, leak-tight radiators and minimizes many of the problems encountered in brazing operations. The use of the G-E No. 62 brazing alloy eliminates many of the deleterious effects of the Nicrobraz alloy that was formerly used.

The investigation of the fabrication of high-conductivity fin materials included a study of diffusion barriers for use between Inconel and copper, electroplating copper to obtain oxidation resistance, and the fabrication of clad-copper fin material in sufficient quantities for experimental radiators. Furthermore, several new high-conductivity fin materials were studied because it was found that diffusion of nickel and copper made the brazing of Inconel-clad copper fins to Inconel tubing less satisfactory than it was previously thought to be. Each clad-copper and copper-aluminum bronze fin material was tested by brazing to either Inconel or stainless steel tubing with each of the following brazing alloys: low-melting-point Nicrobraz (LMNB), "electroless" nickel-phosphorus, LMNB plus 10 wt % "electroless" nickel-phosphorus, and nickel-phosphorus-chromium alloys. A summary of the results of this study is given. A series of one hundred 3 × 3 in. nickel fins is being "electroless" preplated with nickel-phosphorus alloy for brazing into a radiator assembly. In a preliminary test, good-quality brazes were obtained with this material at-tube-to-fin joints.

The assembly of stainless steel-clad fuel plates into fuel elements is being studied, and it appears that inert-arc plug welding may be a feasible method of fabrication. The configuration investigated consisted basically of a 0.026-in.-thick type 304 stainless steel-clad type 304 stainless steel sheet 24 in. long that was to be joined on the edge at 2-in. intervals to a 0.041-in.-thick type 304 stainless steel side plate.

Stress-rupture tests of coarse- and fine-grained Inconel in argon and in fluoride fuel $NaF\text{-}ZrF_4\text{-}UF_4$ at temperatures of 1300, 1500, and 1650°F are being made. The tests completed at 1500°F show that hydrogen is the most detrimental environment and that air is the most beneficial, as far as rupture life is concerned, and that increased ductility in air and in sodium is probably the result of decarburization. Tube-burst tests of triaxially stressed Inconel tubes are being made with fluoride fuel $NaF\text{-}ZrF_4\text{-}UF_4$ inside the tube and purified argon outside. Comparison of the data obtained with creep data shows that the tube-burst time is about the same as the time for 2% elongation in the tensile creep tests.

Several special alloys for the corrosion testing program were melted in the high-vacuum melting furnace and extruded into a draw blank. The draw blank was drawn into tubing by the Superior Tube Company. Columbium cold worked to a reduction of 87.5% has been shown to have a recrystallization temperature of between 1000 and 1100°C.

Tubular fuel elements are being produced by using plug drawing techniques. The drawing schedule was found to be too severe in that it caused premature failure during drawing. However, even this severe working schedule produced tubing that had excellent inside and outside finishes and there was no evidence of rippling or folding in the core region.

Ten test rings of a beryllium fluoride glass were prepared for determining their suitability as high-temperature pump seals. A ceramic container for use in the investigation of the electrical resistivity of fluoride fuels is being prepared by isostatically pressing and sintering beryllium oxide. High-density graphite (Graph-i-tite) is being tested for compatibility with fluorides and other molten salts and molten metals.

Studies of the flammability of jets of sodium alloyed with numerous metals have been made. Sodium-mercury alloys containing less than 34 mole % sodium and sodium-bismuth alloys containing less than 40 mole % sodium did not burn; all other alloys tested burned.

WELDING AND BRAZING RESEARCH

P. Patriarca G. M. Slaughter
Metallurgy Division

J. M. Cisar, ANP Division

Brazing of Radiator Assemblies

It was stated in the previous report that the G-E No. 62 brazing alloy (69% Ni–20% Cr–11% Si) might be suitable for use on ANP-type sodium-to-air radiators. Stainless steel joints brazed with this alloy were considered to possess adequate resistance to cracking. This alloy was also shown to exhibit excellent resistance to high-temperature oxidation. A metallographic section of a joint of an Inconel tube brazed to a type 304 stainless steel fin and exposed in static air for 1200 hr at 1500°F is shown in Fig. 7.1. It can be seen that

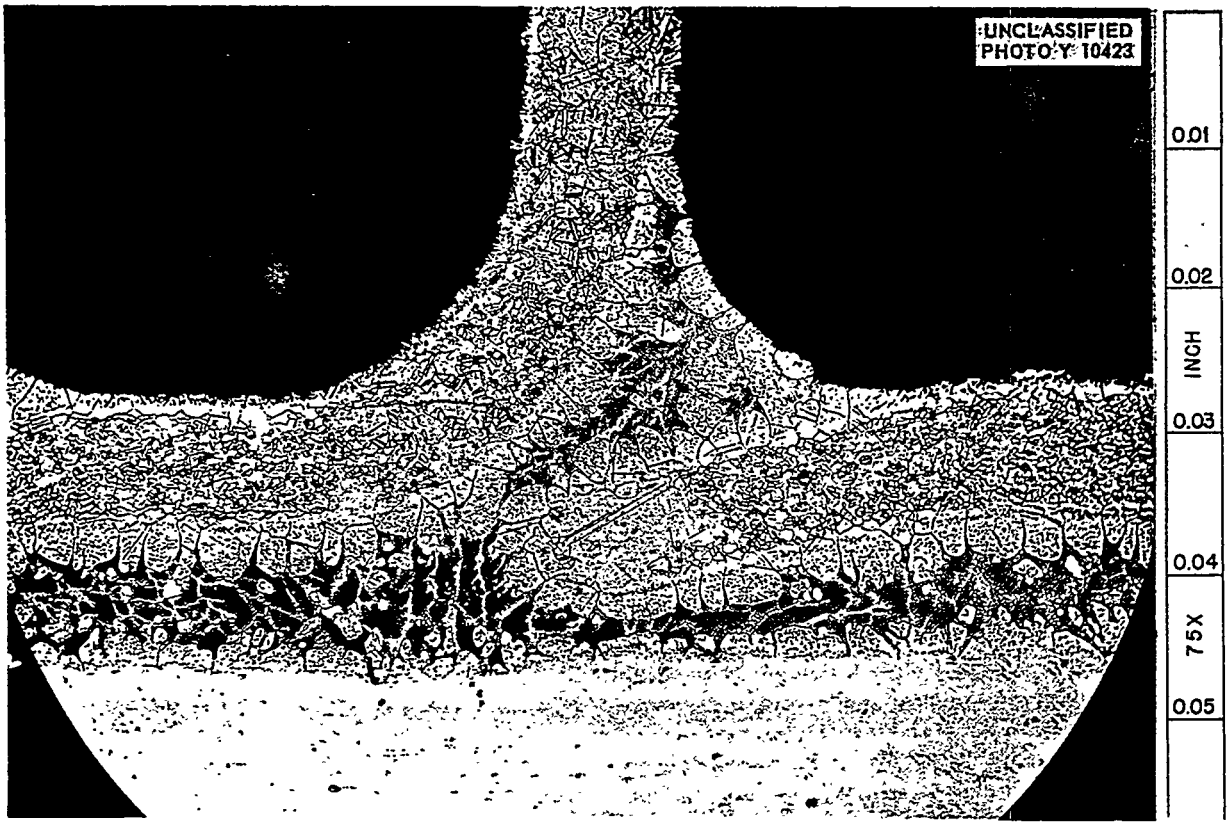

Fig. 7.1. Section of Joint of Inconel Tube Brazed to a Type 304 Stainless Steel Fin with G-E No. 62 Brazing Alloy and Exposed to Static Air at 1500°F for 1200 Hours. Etchant: glyceria regia. 75X

the extent of attack is minor. Previous tests had also shown that this alloy was attacked by molten sodium only slightly at 1500°F in a 100-hr test.

Therefore the sodium-to-air radiator shown in Fig. 7.2 was fabricated by brazing the tube-to-fin joints and backing up the previously heliarc-welded tube-to-header and manifold joints with brazing alloy. This method of fabrication is thought to be the most reliable for obtaining a pressure-tight system with one brazing operation.

The tube-to-header welds were manually inert-gas tungsten-arc welded with argon as the shielding gas and helium as the back-up gas. The header caps and the manifold were also heliarc welded by using suitable joint designs to permit complete penetration.

The sequence of manifold and header cap welding was such that the nickel-chromium-silicon alloy could always be applied to the underside of the joint after welding. Each tube-to-header weld was also backed up with this brazing alloy. A typical heliarc-welded joint backed up with the nickel-chromium-silicon braze is shown in Fig. 7.3. It can be seen that the probability of obtaining a leak-tight joint is very good.

The completed assembly was then dry-hydrogen brazed by using the thermal cycle shown in Fig. 7.4. A preheat at 1600°F was utilized to permit an equilization of temperatures over the assembly. The thermocouple, which was placed directly on the radiator, also indicated that a maximum temperature of 2150°F was attained and that the unit was held above 2100°F for approximately 30 minutes. The brazing technique used for this fabrication ensures a relatively slow cooling rate so that cracking upon cooling as a result of uneven thermal contractions should not be a major problem.

Helium leak testing at less than 0.03-μ vacuum revealed that all welded and brazed joints in the radiator were leak tight. The assembly was also pressure tight to a 20-psi helium pressure when it was immersed in water.

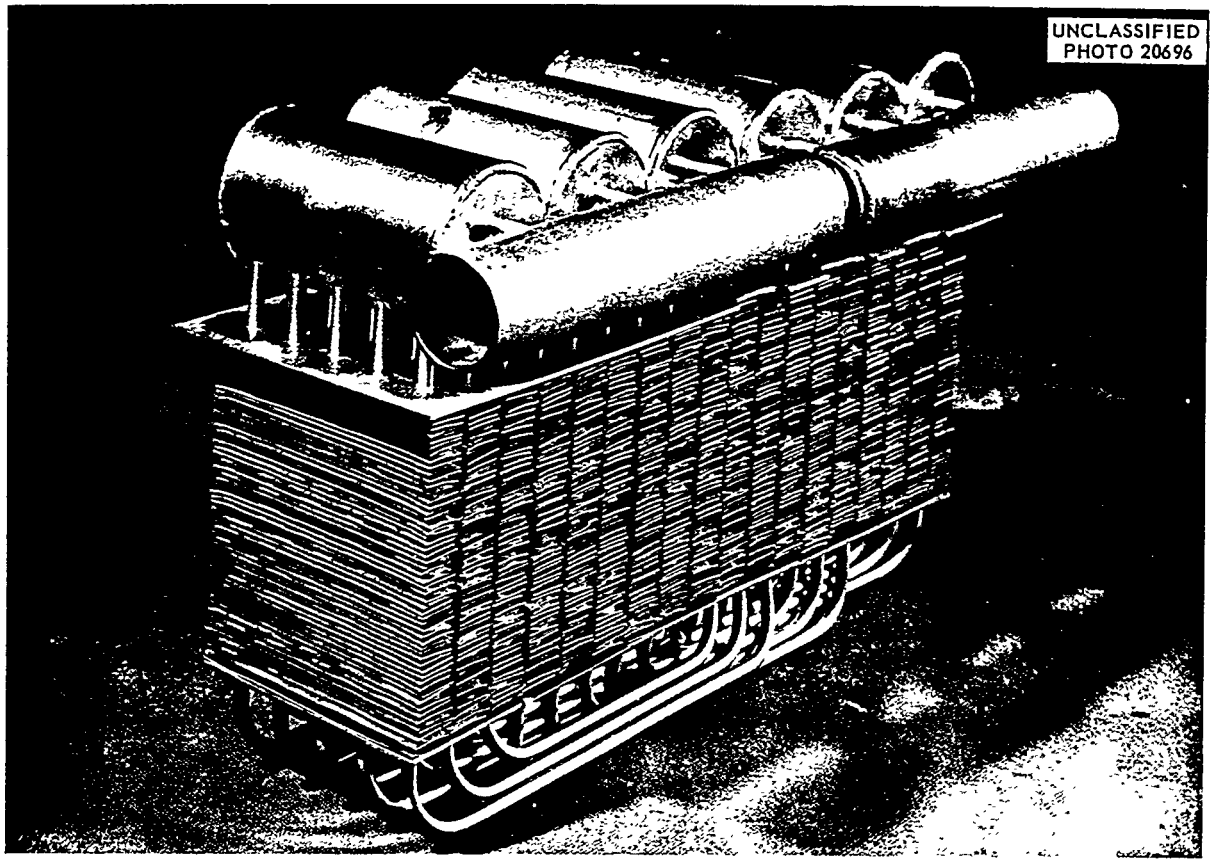

Fig. 7.2. Sodium-to-Air Radiator Fabricated by the Combined Welding and Brazing Technique.

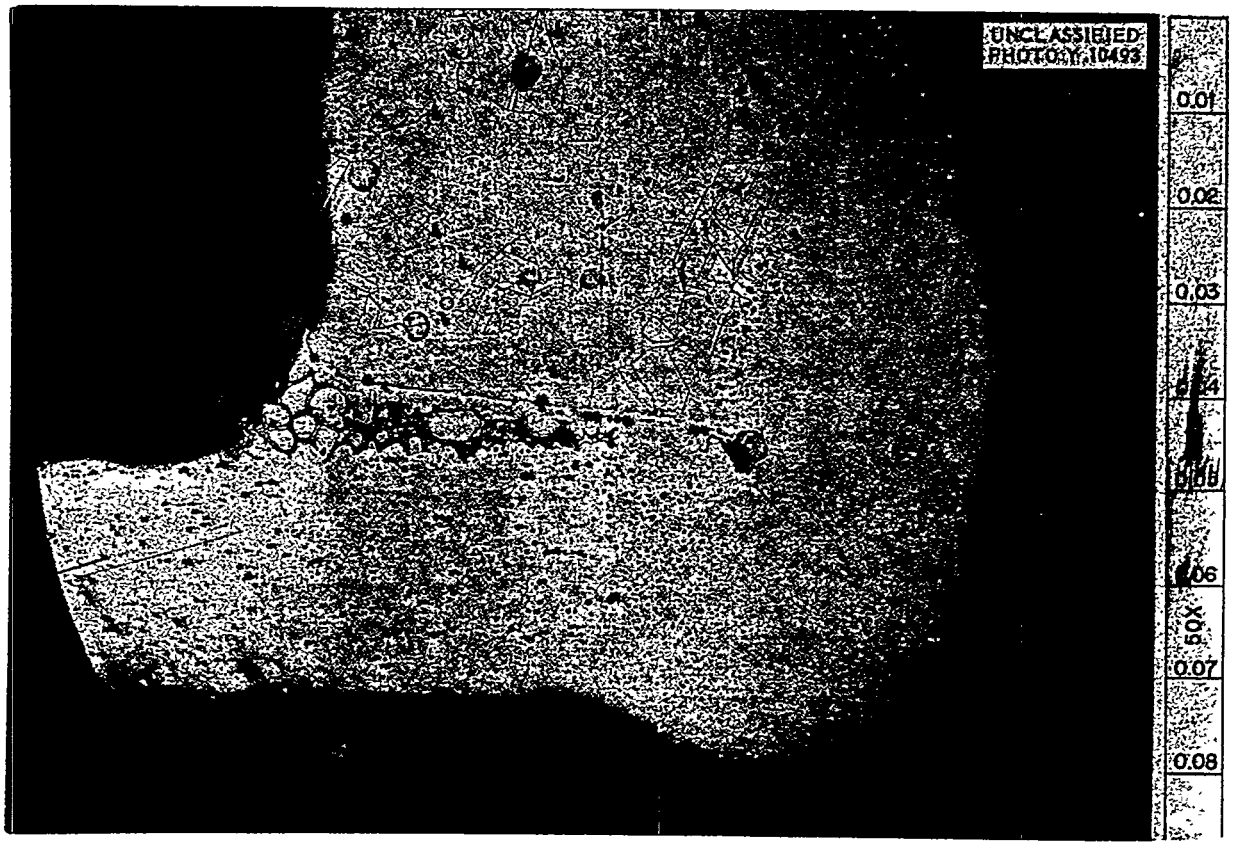

Fig. 7.3. Inconel Tube-to-Header Heliarc Welded Joint Backed Up with G-E No. 62 Brazing Alloy. Etchant: glyceria regia. 50X

It is thus believed that a combination heliarc-welding and high-temperature-brazing procedure is satisfactory for fabricating sound leak-tight radiators. This duplex technique has been shown to minimize many of the problems and difficulties usually encountered in brazing operations. The use of the G-E No. 62 brazing alloy also seems to minimize or completely eliminate many of the deleterious effects of the Nicrobraz alloy that was formerly used.

Brazing of High-Conductivity Radiator Fins

Although the problem of brazing Inconel-clad copper high-conductivity fin material to Inconel tubing was satisfactorily resolved, as described in the previous report,[1] the subsequent determination of the detrimental effects of diffusion of nickel and copper has proved to be a limitation of the method. Accordingly, a group of other high-conductivity fin materials was fabricated for brazing tests.

The high-conductivity fin materials studied during the current investigation were types 446 and 310 stainless steel-clad copper and a copper-aluminum (94% Cu–6% Al) bronze. The fabrication of these materials is described below under "High-Conductivity Metals for Radiator Fins." The brazing alloys investigated were low-melting-point Nicrobraz (LMNB), "electroless" nickel-phosphorus (90% Ni–10% P) alloy, low-melting-point Nicrobraz plus 10 wt % "electroless" nickel-phosphorus alloy, and nickel-phosphorus-chromium (80% Ni–10% P–10% Cr) alloy. Each of the brazing alloys was used in conjunction with each of the high-conductivity fin materials against Inconel tubing, as well as against tubing of the same nominal composition as that of the stainless steel component of the fin material.

The test specimens were designed to simulate T flowability specimens. A sheet and a tube were

[1] E. S. Bomar *et al.*, *ANP Quar. Prog. Rep. Sept. 10, 1953*, ORNL-1609, p. 95.

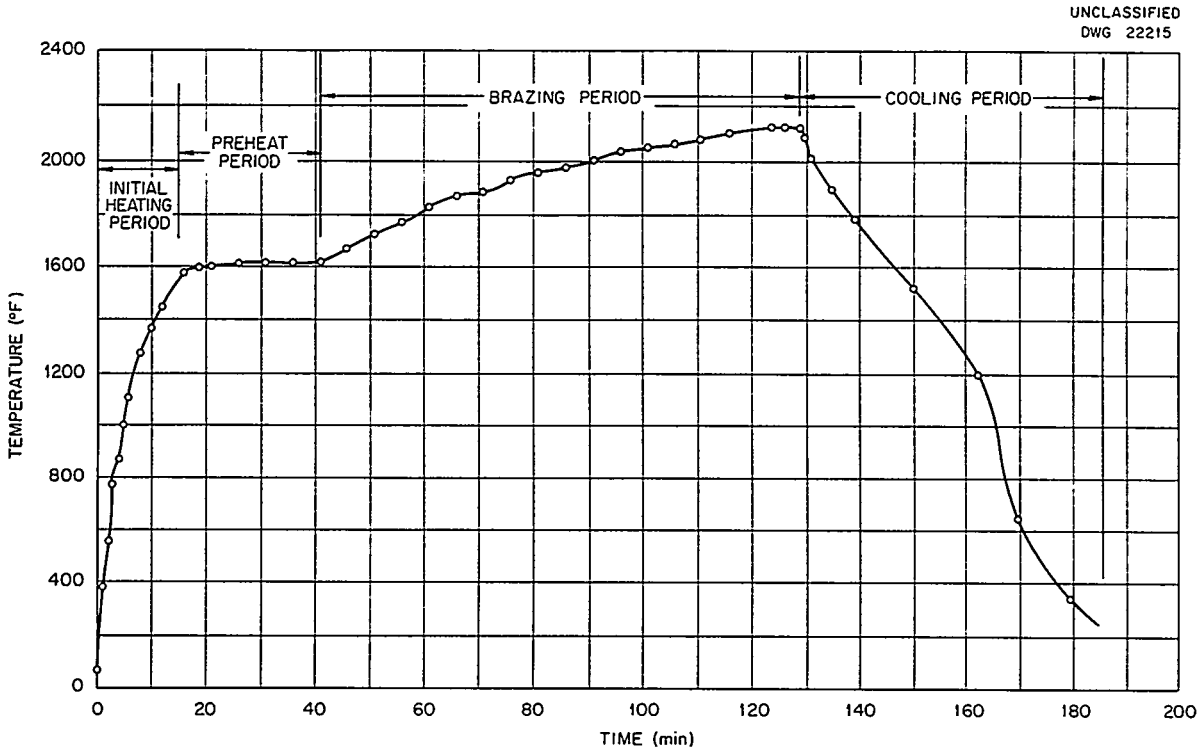

Fig. 7.4. Thermal Cycle Employed in Furnace Brazing a Heat Exchanger with G-E No. 62 Alloy. Temperatures were obtained with a chromel-alumel thermocouple secured to the heat exchanger.

placed side by side, and the brazing alloy was applied initially to one end of the specimen. All test specimens were brazed in –70°F dew-point hydrogen for 10 minutes. A summary of the data and the results of this study are presented in Table 7.1, along with an evaluation of the flowability of of the braze material based on visual observations.

The following conclusions have been drawn from these tests:

1. All the brazing alloys investigated, which were chosen because of oxidation resistance and favorable melting temperature, exhibited excellent flow against types 310 and 446 stainless steel-clad copper when used against Inconel tubing. It appears that the Inconel behaved as a "carrier" for the alloys.

2. The oxide films present on the as-received type 310 stainless steel tubing used in this investigation inhibited in varying degrees the flow of all the brazing alloys tested. The removal of this oxide by prebright annealing at 1150°C or by electropolishing improved the observed flow. The most marked effect was the improved flow of LMNB.

3. Removal of oxide films by prebright annealing or by electropolishing the type 446 stainless steel tubing did not markedly improve the flow of the brazing alloys and was particularly ineffective for the LMNB alloy.

4. The addition of 10 wt % nickel-phosphorus (90% Ni–10% P) alloy to the LMNB alloy markedly improved flow against type 446 stainless steel tubing, although this addition was not beneficial against type 310 stainless steel tubing.

5. The oxide film which formed on the copper-aluminum (94% Cu–6% Al) fin material during the brazing cycle impeded flow of all the brazing alloys investigated. Prevention of this oxide formation by preplating with electrolytic nickel permitted excellent wetting and flow of all the brazing alloys investigated.

TABLE 7.1. SUMMARY OF BRAZING STUDIES OF HIGH-CONDUCTIVITY FIN MATERIALS

T SPECIMEN		BRAZING ALLOY	BRAZING TEMPERATURE (°C)	FLOWABILITY (visual observation)
Fin Material	Tubing			
Type 446 stainless steel-clad copper (0.004 in. of copper clad on both sides with 0.002 in. of the steel)	Inconel, as-received	LMNB	1050	Good
		90% Ni–10% P	1000	Excellent
		LMNB + 10% Ni-P*	1050	Excellent
		80% Ni–10% P–10% Cr	1050	Excellent
	Type 446 stainless steel, as-received	LMNB	1050	None
		90% Ni–10% P	1000	Excellent
		LMNB + 10% Ni-P	1050	Good
		80% Ni–10% P–10% Cr	1050	Excellent
	Type 446 stainless steel, prebright annealed in dry H_2 at 1150°C for 15 min	LMNB	1050	None
		90% Ni–10% P	1000	Excellent
		LMNB + 10% Ni-P	1050	Good
		80% Ni–10% P–10% Cr	1050	Excellent
	Type 446 stainless steel, electropolished	LMNB	1050	None
		90% Ni–10% P	1000	Excellent
		LMNB + 10% Ni-P	1050	Excellent
		80% Ni–10% P–10% Cr	1050	Excellent
Type 310 stainless steel-clad copper (0.004 in. of copper clad on both sides with 0.002 in. of the steel)	Inconel, as-received	LMNB	1050	Excellent
		90% Ni–10% P	1000	Excellent
		LMNB + 10% Ni-P	1050	Excellent
		80% Ni–10% P–10% Cr	1050	Excellent
	Type 310 stainless steel, as-received	LMNB	1050	None
		90% Ni–10% P	1000	Good
		LMNB + 10% Ni-P	1050	None
		80% Ni–10% P–10% Cr	1050	Fair
	Type 310 stainless steel, prebright annealed in dry H_2 at 1150°C for 15 min	LMNB	1050	Good
		90% Ni–10% P	1000	Excellent
		LMNB + 10% Ni-P	1050	Excellent
		80% Ni–10% P–10% Cr	1050	Excellent
	Type 310 stainless steel, electropolished	LMNB	1050	Good
		90% Ni–10% P	1000	Excellent
		LMNB + 10% Ni-P	1050	Excellent
		80% Ni–10% P–10% Cr	1050	Excellent
Copper-aluminum (94% Cu–6% Al) alloy electroplated with 0.0002 in. of nickel**	Inconel, as-received	LMNB	1030	Excellent
		90% Ni–10% P	1000	Excellent
		LMNB + 10% Ni-P	1030	Excellent
		80% Ni–10% P–10% Cr	1030	Excellent
	Type 446 stainless steel, prebright annealed	LMNB	1030	Excellent
		90% Ni–10% P	1000	Excellent
		LMNB + 10% Ni-P	1030	Excellent
		80% Ni–10% P–10% Cr	1030	Excellent
	Type 310 stainless steel, prebright annealed	LMNB	1030	Excellent
		90% Ni–10% P	1000	Excellent
		LMNB + 10% Ni-P	1030	Excellent
		80% Ni–10% P–10% Cr	1030	Excellent

*Low-melting-point Nicrobraz plus 10 wt % of nickel-phosphorus (90% Ni–10% P) alloy.

**Without the electroplate, this alloy was not wet by any of the brazing alloys.

"Electroless" Preplating of Brazing Alloys

Work on the "electroless" preplating of nickel-phosphorus brazing alloy, as described previously,[2] has continued, and the method is being applied to practical brazing problems. A commercially available system of plating solutions is now being successfully used to plate the nickel-phosphorus alloy on to-be-brazed specimens. The system, Lustralloy, manufactured by Metal Processing Company, Inc., is cheaper and as satisfactory as the procedure developed by the ORNL Research Shops. A series of approximately one hundred 3 × 3 in. nickel fins is currently being preplated with nickel-phosphorus alloy for brazing into a radiator assembly for the Griscom-Russell Company. As a preliminary test, two of these fins were sheared into ¾-in. sections; nickel tubes were inserted into holes in these fins, and the mock assembly was placed into the hydrogen furnace at 1020°C for approximately 10 minutes. The specimen was then cooled slowly under a hydrogen atmosphere. The finished specimen was bright, and the joints were well brazed. A similarly brazed assembly is shown in Fig. 7.5. As can be seen, the brazing alloy, originally uniformly distributed on the fins and absent on the tubes, was drawn to the capillary. Figure 7.6, a photomicrograph of the tube-to-fin joints, shows the good quality of the braze.

[2] P. Patriarca and G. M. Slaughter, *ANP Quar. Prog. Rep. Sept. 10, 1953*, ORNL-1609, p. 91.

Inert-Arc Plug Welding of Solid Fuel Elements

The assembly of stainless steel-clad fuel plates into fuel elements of the size and configuration of interest presents a problem for which there are several possible solutions. One method that may prove useful in certain applications utilizes inert-

UNCLASSIFIED
PHOTO Y 10200

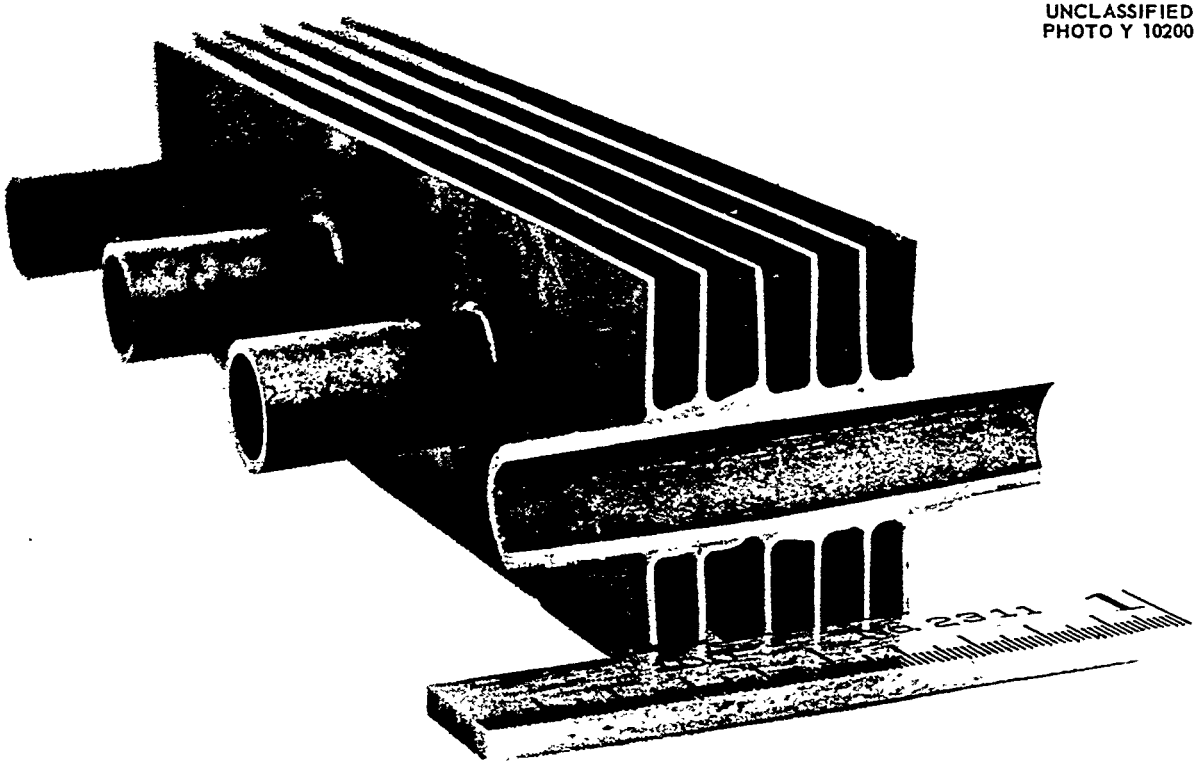

Fig. 7.5. Tube-to-Fin Assembly Brazed with Preplated "Electroless" Nickel-Phosphorus Brazing Alloy.

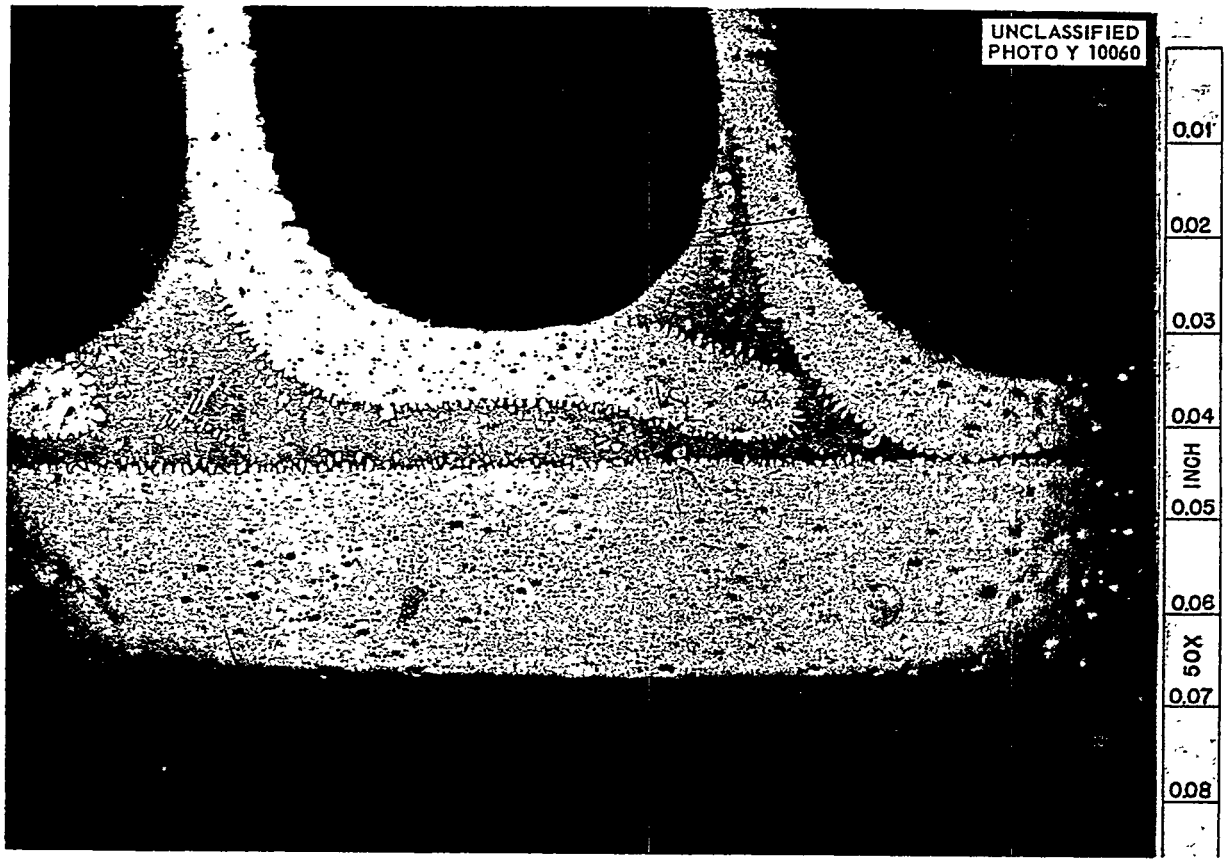

Fig. 7.6. Tube-to-Fin Joints Brazed with Preplated "Electroless" Nickel-Phosphorus Brazing Alloy.

arc plug welding techniques. The configuration investigated in these preliminary experiments consisted basically of a 0.026-in.-thick type 304 stainless steel-clad type 304 stainless steel sheet 24 in. long that was to be joined on the edge at 2-in. intervals to a 0.041-in.-thick type 304 stainless steel side plate.

The joint design considered to be optimum for welding is shown in Fig. 7.7. A hole 0.067 in. in diameter is drilled in a 0.041-in.-thick header sheet to receive a projection 0.062 × 0.026 × 0.125 in. obtained by edge milling the 0.026-in. type 304 stainless steel-clad sheet. The 0.84-in. extension of the projection above the header sheet was predetermined from the following volume considerations: (1) the volume of the 0.067-in.-dia, 0.041-in.-deep header hole was 0.00015 $in.^3$; (2) the volume of the 0.062 × 0.026 × 0.125-in. projection was 0.0002 $in.^3$; (3) the excess of 0.00005 $in.^3$ would ensure adequate weld buildup and could be removed by finish machining.

A series of specimens of the design shown in Fig. 7.7 were welded with variations in arc current, arc time, arc distance, and welding sequence. Since precise control of these variables was required, cone-arc equipment was used throughout the study. The welds were examined metallographically for penetration and flaws.

Examination of test specimens indicated that the most favorable weld geometry could be achieved by two separate inert-arc welding operations. The projection was melted into a "rivet" by an initial choice of arc current, arc time, and arc distance. The arc distance was then reduced, and an additional application of current was used to form the the finished weld, the filler metal being provided by the rivet.

The rivet formed during the first operation by using the optimum welding conditions is shown in Fig. 7.8, which is a section through the weld joint corresponding to section A-A in Fig. 7.7. The plug weld formed in the second operation is shown in

Fig. 7.9. As may be noted, the penetration of the type 304 stainless steel-clad sheet was complete and reasonably uniform, which indicates that an apparently sound weld joint was obtained. It thus appears that inert-arc plug welding may be a feasible method of fabrication of these assemblies.

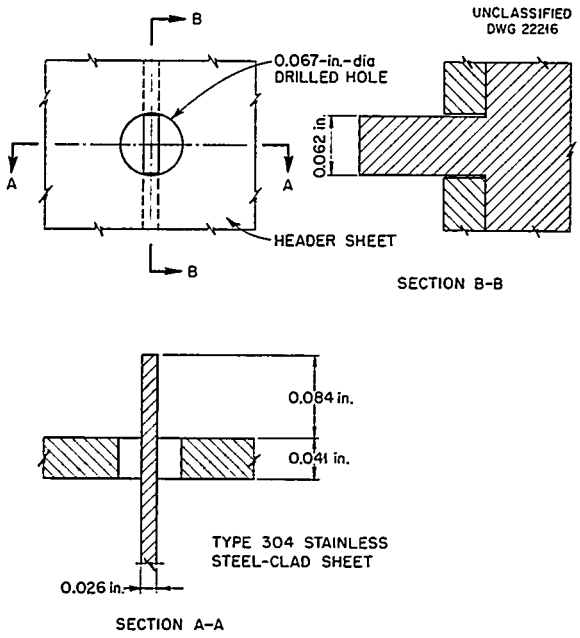

Fig. 7.7. Assembly of Type 304 Stainless Steel Components Prior to Inert-Arc Plug Welding.

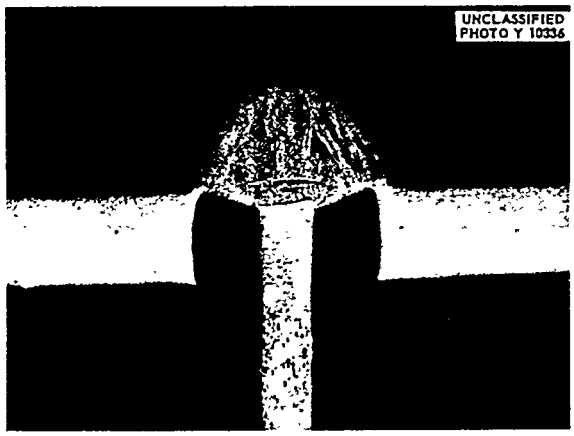

Fig. 7.8. Section of "Rivet" Formed by Initial Application of a 30-amp (DCSP) Arc Current for an Arc Time of 2 sec at an Arc Length of 0.140 in. Etchant: aqua regia. 21X

However, the application of these techniques to the fabrication of a multiweld unit should be investigated further.

MECHANICAL PROPERTIES OF INCONEL

R. B. Oliver D. A. Douglas
K. W. Reber J. M. Woods
Metallurgy Division

Stress-Rupture of Inconel in Fluoride Fuel

Stress-rupture tests of coarse- and fine-grained Inconel in argon and in fluoride fuel NaF-ZrF_4-UF_4 at temperatures of 1300, 1500, and 1650°F are being made. Data for the higher stress ranges are complete, and the tests being made currently are expected to run from three to eight months. Testing in the stress range from 500 to 1500 psi will commence in about six months when the six new units designed for low loads are completed. The results obtained to date for fine-grained Inconel are summarized in Table 7.2.

Tube-Burst Tests of Triaxially Stressed Tubes

In the past, data obtained in the tube-burst tests of triaxially stressed Inconel tubes have shown considerable scatter and interpretation has been difficult. However, data obtained in recent tests have shown reasonable reproducibility, and it is believed that most of the operating difficulties have been overcome. The present procedure is to

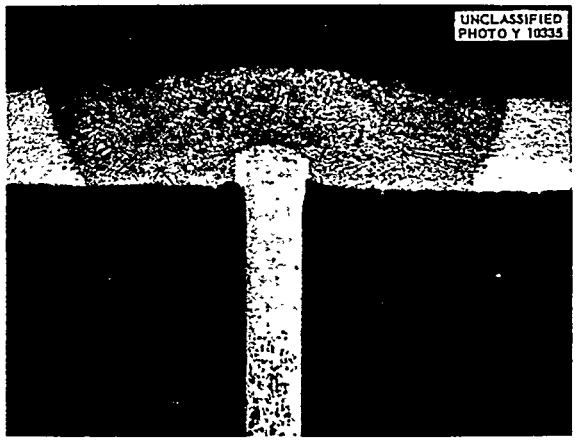

Fig. 7.9. Section of Completed Weld Formed by Application of a 30-amp Arc Current for 4 sec at an Arc Length of 0.060 in. to the "Rivet" Shown in Fig. 7.8. Etchant: aqua regia. 21X

TABLE 7.2. RESULTS OF STRESS-RUPTURE TESTS OF FINE-GRAINED INCONEL IN $NaF\text{-}ZrF_4\text{-}UF_4$

TEMPERATURE (°F)	STRESS (psi)	RUPTURE TIME IN ARGON (hr)	RUPTURE TIME IN FLUORIDES (hr)
1300	10,000	2000	
1500	10,000	50	30
1300	5,000	7000	
1500	5,000	540	260
1650	5,000	25	25
1500	2,500	4000	1200
1650	2,500	450	175

test the tube with the fluoride fuel $NaF\text{-}ZrF_4\text{-}UF_4$ inside and purified argon outside. The stress range from 500 to 3500 psi is currently being investigated and tests have been completed in the upper half of the range. In comparing the data with creep data at the same stresses in the same fuel, it is found that the tube-burst time is about the same as the time for 2% elongation in the tensile creep tests. The tube specimens loaded by internal pressures give an axial-to-tangential stress ratio of $\frac{1}{2}$, which results in minimum ductility; thus the results probably represent the minimum life expectancy, other factors being equal. In the near future, these tube specimens will be tested with the fuel inside the tube and sodium, instead of argon, outside.

Environmental Effects on Creep of Inconel

Creep tests of Inconel specimens in nitrogen and in sodium environments at 1500°F have recently been completed. Thus it is now possible to compare the effects of six types of environments that Inconel structures might encounter. The results of these creep tests are summarized in Table 7.3.

Table 7.3 shows that hydrogen is the most detrimental environment and that air is the most beneficial, as far as rupture life is concerned. It is interesting to note that, with the exception of the tests in air and sodium, all the specimens reached about the same total elongation regardless of the rupture time. The increased ductility in air and in sodium is probably the result of decarburization. Chemical analyses are being made to test this hypothesis. The results presented in Table 7.3 are for Inconel specimens that were annealed at 1650°F before being tested. Specimens annealed at 2050°F and then stressed in hydrogen or $NaF\text{-}ZrF_4\text{-}UF_4$ have shown more resistance to the environmental effect. Tests of this type of specimen in the other environments are now being made.

TABLE 7.3. RESULTS OF CREEP TESTS OF INCONEL ANNEALED AT 1650°F AND TESTED UNDER A STRESS OF 3500 psi at 1500°F IN VARIOUS ENVIRONMENTS

ENVIRONMENT	LIFE RUPTURE (hr)	FINAL ELONGATION (%)
Hydrogen	446	13.0
$NaF\text{-}ZrF_4\text{-}UF_4$	550	12.0
Sodium	1333	35.0
Argon	1467	12.0
Nitrogen	1770	11.6
Air	2567	50.0

HIGH-CONDUCTIVITY METALS FOR RADIATOR FINS

E. S. Bomar J. H. Coobs
H. Inouye, Metallurgy Division

The investigation of the fabrication of high-thermal-conductivity fins was confined during this period to a study of diffusion barriers for use between Inconel and copper, the fabrication of clad-copper fin material in sufficient quantities for the assembly of experimental radiators, and the investigation of special materials.

Diffusion Barriers

Barrier material for use between Inconel and copper was selected on the basis of low solubility of the element or alloy in copper or Inconel. In addition, it was desired to fabricate thin composite clads to determine their rolling characteristics. The barrier materials used were tungsten, molybdenum, titanium, zirconium, tantalum, vanadium, types 310 and 446 stainless steel, and iron plus silver.

Several composites were hot rolled approximately 50% at 1800°F and then finished cold to 0.008 in. total thickness. Bonding was not achieved between molybdenum and Inconel or between vanadium and Inconel, and the following composites could not be successfully rolled: (1) Inconel-Ag-Fe-Cu-Fe-Ag-Inconel and (2) Inconel-W-Cu-W-Inconel. The first of these composites was unsuccessful because of improper design, and the second showed severe stretcher marks. Oxidation and diffusion tests of the other composites are being made.

Some of the earlier tests of Inconel-clad copper showed the absence of diffusion voids, and therefore a few tests are now being made to determine the effect of surface preparation on void formation and diffusion. The composites for this study have been fabricated; they consist of a layer of oxide on Inconel formed by heating in wet hydrogen and in air at 1300°F.

Clad Copper

As reported previously,[3] types 310 and 446 stainless steel are suitable cladding material for copper for use at 1500°F, while Inconel cladding causes severe diffusion. In order to establish which of the claddings is most suitable on copper and also to determine the effect of diffusion on thermal conductivity, approximately 15-ft^2 samples of copper clad with Inconel, type 310 stainless steel, and type 446 stainless steel have been or are being made. The fin material is to be strips 4 in. wide and 0.010 in. total thickness; the copper core will be 0.006 in. thick and the cladding material will be 0.002 in. thick. This material is to be used for the fabrication of experimental heat exchangers.

Electroplated Copper

Plates of chromium plus iron and of iron plus nickel plus chromium to give compositions corresponding to types 446 and 310 stainless steel, respectively, did not protect copper from oxidizing at 1500°F. A composite made entirely by electroforming showed the same results. The inability of these plates to protect copper at 1500°F is ascribed to the lack of a metallurgical bond between the copper and the plate and to the brittleness of the deposits. Although the ductility can be restored by heating to 1600°F, the damaging cracks are present in the as-received or annealed material.

Solid Phase Bonding

An alternate investigation for obtaining uniform thin claddings is being made. A bond between the copper and the cladding can be obtained by seam welding material of the final desired thickness. The Glen L. Martin Company proposed this method and has supplied samples up to 4 in. long which appear satisfactory. Joint efforts have, to date, produced claddings 0.002 and 0.001 in. thick.

The thermal properties of the aluminum bronzes at low temperatures indicate that the conductivity of alloys containing about 6% aluminum is greater than that of the stainless steels or Inconel by a factor of about 6 at 1500°F. To verify this, measurements are now being made on 6 and 8% aluminum bronzes. These alloys are oxidation resistant, and if the expected thermal properties are correct, the need to fabricate composite bodies will be eliminated because these alloys may be suitable for use as radiator fins. This is especially important because difficulties have been experienced in obtaining clad material from commercial suppliers.

FABRICATION OF SPECIAL MATERIALS

E. S. Bomar J. H. Coobs
H. Inouye, Metallurgy Division

Extrusion of Inconel-Type Alloys

Extruded Inconel tubing was redrawn from 1 in. in outside diameter with a 0.125-in. wall to 0.500 in. in outside diameter with a 0.035-in. wall by the Superior Tube Company. These materials were drawn satisfactorily at reductions as high as 36% per pass with annealing after each stage at 1900°F. The properties of the tubing are listed in Table 7.4.

The extrusion of near-Inconel alloys from seven other vacuum melts was attempted with varying degrees of success. Temperatures from 2150 to

[3] E. S. Bomar *et al.*, *ANP Quar. Prog. Rep. Sept. 10, 1953*, ORNL-1609, p. 96.

TABLE 7.4. PROPERTIES OF ANNEALED HIGH-PURITY INCONEL TUBING 0.505 in. IN OUTSIDE DIAMETER WITH A 0.035-in. WALL

MELT NO.*	GRAIN SIZE (mm)	TENSILE STRENGTH (psi)	YIELD STRENGTH (psi)	ELONGATION (%)
DPI-7	0.090/0.130	81,000	35,000	52
DPI-8	0.075	83,400	36,000	50
DPI-9	0.090/0.110	83,500	40,000	48
DPI-10	0.090/0.130	80,400	40,800	46

*Analyses of melts 8, 9, and 10 were given in the *Metallurgy Division Progress Report for the Period Ending April 10, 1953*, ORNL-1551, Table 22, p. 54.

2350°F were employed to produce the tubing (or rod), and, in some instances, extrusion ratios as low as 10:1 were required. All the extruded tubing has been sent to the Superior Tube Company for further reduction. A molybdenum-nickel alloy (20% Mo–80% Ni, nominal composition) did not extrude at a reduction of 13:1 at 2350°F. An attempt will be made to extrude this alloy at a lower reduction ratio.

Rolling of Chromium-Cobalt Alloy

A chromium-cobalt alloy ingot 6 in. long and 1 in. in diameter (45% Cr–55% Co, nominal composition) was cast, and attempts to roll it at 2350°F showed that this alloy was hot-short. Additions of 0.5% manganese and 0.5% aluminum did not improve the hot-rolling properties. A solid rod of this alloy which was precision cast was readily machinable, but it cracked severely. The present plans call for precision casting the alloy tubing. The hardness of the cast alloy is Rockwell C-50.

Rolling of Cobalt

A 1½-in.-dia, 6-in.-long cobalt ingot containing 0.5% manganese and 0.5% aluminum was successfully rolled to ½-in.-dia rod at 2300°F. Previously, it was found that cobalt without the manganese and aluminum additions was hot-short. The alloy containing aluminum and manganese has an as-cast hardness of Rockwell A-49.

Rolling of Iron-Chromium-Nickel Alloy

A 1½-in.-dia, 6-in.-long ingot of iron-chromium-nickel alloy (45% Fe–40% Cr–15% Ni) was rolled to ½-in.-dia rod at 2350°F. This alloy was found to be hot-short at 1850°F, even though it contained 1% of a nickel-manganese-titanium master alloy. Previously, attempts to hot roll this alloy at 1850°F without the alloy addition were unsuccessful because of hot-shortness. The as-cast alloy has a hardness of Rockwell A-62.

Cold-Rolled Columbium

Columbium sheet 0.200 in. thick obtained from the Fansteel Corporation was annealed to a grain size of ASTM 7 at 1100°C in a vacuum. The sheet was cold rolled to 0.025 in., which represented a reduction of 87.5% in thickness. The room-temperature mechanical properties were determined on specimens vacuum annealed for ½ hr at various temperatures and are summarized in Table 7.5.

The microstructure of columbium under these conditions shows partial recrystallization at 1000°C, and, at 1100°C, recrystallization is complete. Vacuums of the order of 10^{-5} mm Hg were obtained in the annealing furnace. The analysis of the sheet shows 0.75 + 0.3% tantalum, and traces of copper, iron, and titanium. Analysis of the oxide content of the sheet is not complete, but it is expected to be greater than 0.3%.

TUBULAR FUEL ELEMENTS

J. H. Coobs, Metallurgy Division

Drawing of tubular fuel elements has been continued. Plans called for the reduction of six tubes on each of two schedules in steps of 15% and 20% reduction per pass, respectively. All tubes were to be reduced from 0.750 in. in diameter with a 0.042-in. wall to a final size of 0.250 in. in diameter with a 0.015-in. wall, or a total reduction of 87%. Plug drawing was used in preference to drawing on a

mandrel, as explained previously.[4] However, because of failure of the tubes at intermediate steps, the drawing schedules could not be carried to completion. Reduction of the tubes was continued as long as was considered practical, that is, until each tube had failed within the core region or near the starting end in such a way as to make further drawing difficult or impossible. The final sizes of the tubes processed on the 15% schedule are given in Table 7.6, along with core composition and total reduction.

Because the results with the 20% schedule were discouraging, only three tubes were processed; all tubes failed on the second pass. Total reduction of these tubes was 36%.

In general, the tubes reduced by both schedules developed excellent finishes on both inner and outer diameters, with no evidence of rippling or folding in the core region. In most cases, failure occurred near the trailing end of the core. The failures were attributed mainly to inability to keep the plugs positioned in the die properly, with the result that the reductions did not conform strictly to the schedule. The reductions were somewhat higher than scheduled on several passes and caused galling in the dies and failure of the tubes because of severe tensile stresses. Samples have been cut from the nine tubes drawn and are now being examined metallographically.

[4] *Ibid.*, p. 99.

TABLE 7.5. MECHANICAL PROPERTIES OF COLUMBIUM COLD ROLLED TO A REDUCTION OF 87.5%

SPECIMEN NO.	ANNEALING TEMPERATURE (°C)	HARDNESS (VPN)	YIELD POINT AT 0.1% OFFSET (psi)	TENSILE STRENGTH (psi)	ELONGATION IN $1\frac{1}{2}$ in. (%)	MODULUS OF ELASTICITY ($\times 10^{-6}$ psi)
1	As rolled	145		76,500	4.0	
2	300	154	69,500	80,700	2.6	17.66
3	600	147	62,300	73,400	6.0	16.60
4	900	136	57,300	63,100	8.3	17.30
5	1000	100	37,500	50,800	12.6	17.88
6	1100	85	23,400	42,200	26.6	19.30
7	1200	86	24,000	45,000	18.6	17.20

TABLE 7.6. FINAL SIZES OF TUBES PROCESSED ON THE 15% SCHEDULE

TUBE NO.	COMPOSITION (BY VOLUME)	NO. OF PASSES	FINAL SIZE (in.)	TOTAL REDUCTION (%)
1	80% type 302 stainless steel–20% UO_2	5	0.562	56
2	70% Ni–30% UO_2	9	0.396	77
3	80% Ni–20% UO_2	9	0.396	77
4	70% type 302 stainless steel–30% UO_2	10	0.355	80
5	80% Fe–20% UO_2	3	0.625	39
6	70% Fe–30% UO_2	5	0.562	56

CERAMIC RESEARCH

L. M. Doney J. A. Griffin
J. R. Johnson, Metallurgy Division

Glass-Type Pump Seals

Work continued on the development of a suitable, viscous, high-temperature pump seal. Ten test rings, $2\frac{1}{2}$ in. ID, $3\frac{1}{2}$ in. OD, $\frac{7}{16}$ in. thick, of a beryllium fluoride glass[5] were prepared by melting the glass batch in a platinum crucible and casting the glass in graphite dies (Fig. 7.10). The rings were cooled slowly in a blanket of glass wool to minimize cracking. The finished rings were sent to the Experimental Engineering Group for testing.

Ceramic Container for Fuel

Further work is being done on the fabrication of a ceramic container for use in the investigation of the electrical resistivity of the fluoride fuels (cf., sec. 8, "Heat Transfer and Physical Properties"). Three specimens, $5\frac{1}{2} \times 1 \times 1$ in., were cut from hot-pressed beryllium oxide blocks (ARE blocks). A hole $\frac{7}{16}$ in. in diameter was drilled $4\frac{1}{2}$ in. deep along the long axis of the specimen and then tapered to 0.158 in. in diameter for the remaining length of the specimen. These specimens were tested and found to be resistant to attack by the fuel; however, they were too short to satisfy the test conditions. Work has commenced on the fabrication of a suitably sized beryllium oxide shape by isostatically pressing and sintering.

[5] L. M. Doney, J. A. Griffin, and J. R. Johnson, *ANP Quar. Prog. Rep. Sept. 10, 1953*, ORNL-1609, p. 98.

Fig. 7.10. Glass-Type Pump Seal. Composition (by weight): BeF_2, 50%; KF, 25%; MgF_2, 16%; AlF_3, 9%.

High-Density Graphite

Specimens of high-density graphite (Graph-i-tite) supplied by the Graphite Specialties Corporation were obtained and sent to the Metallurgy Division's Corrosion Group for compatibility tests with the fluorides and other molten salts and molten metals. Typical properties of this graphite are given by the manufacturer as:

Apparent density, g/cm^3	1.85 to 1.92
Tranverse breaking strength, psi	4000 to 4500
Modulus of elasticity, lb/in.^{2}/in./in.	20×10^5 to 25×10^5
Electrical resistance, ohm-in.	0.00032 to 0.00040
Permeability	
1.85-g/cm^3 density	Impermeable to water at 40 psi and room temperature for 10 min minimum
1.92-g/cm^3 density	Impermeable to air at 40 psi and room temperature for 10 min minimum

COMBUSTION OF SODIUM ALLOYS

G. P. Smith M. E. Steidlitz
Metallurgy Division

Studies of the flammability of jets of sodium alloys in wet and dry air at temperatures of up to 800°C have been continued. Sodium-mercury alloys containing less than 34 mole % sodium and sodium-bismuth alloys containing less than 40 mole % sodium did not burn. All other alloys tested burned in degrees ranging from slight to violent. The combustible alloys tested were: binary alloys containing, in addition to sodium, 90% aluminum, 50 to 60% bismuth, 90% indium, 90% lead, 0.6 to 66% mercury, 90% silver, or 90% zinc; ternary alloys having a 45% sodium–50% bismuth base and containing 5% each of calcium, copper, magnesium, mercury, potassium, or silver; and ternary alloys having a 30% sodium–65% mercury base with 5% each of aluminum, bismuth, calcium, copper, magnesium, potassium, or silver. The humidity of the air was noted to have a very slight effect on the rate of combustion.

8. HEAT TRANSFER AND PHYSICAL PROPERTIES RESEARCH

H. F. Poppendiek
Reactor Experimental Engineering Division

The physical properties of a number of fluorides and other materials of interest to aircraft reactor technology have been measured. Preliminary density and viscosity measurements have been obtained for the ARE fuel concentrate over the temperature range of 660 to 1000°C; the viscosity varied from about 17.5 cp at 725°C to 9.9 cp at 975°C. The vapor pressure equations for two $NaF\text{-}ZrF_4$ mixtures were determined. The thermal conductivity of the solid fluoride mixture $NaF\text{-}KF\text{-}LiF\text{-}UF_4$ (10.9-43.5-44.5-1.1 mole %) was determined to be 1.7 Btu/hr·ft·°F, while that of the solid heat transfer salt $NaNO_2\text{-}NaNO_3\text{-}KNO_3$ (40-7-53 wt %) was only 0.6 Btu/hr·ft·°F. The heat capacity of $NaF\text{-}ZrF_4\text{-}UF_4$ (50-25-25 mole %) was 0.17 cal/g·°C in the solid state and 0.27 cal/g·°C in the liquid state over the temperature range of 610 to 930°C, with a heat of fusion of 42 cal/g. The heat capacities of two special samples of type 310 stainless steel and of G-E No. 62 brazing alloy have also been measured.

Additional forced-convection heat transfer experiments with NaF-KF-LiF eutectic in a nickel tube were made, and the data obtained were found to be in agreement with data from the former experiments. No additional thermal resistance was present and no film deposits on the inner surface of the nickel tube were observed, in contrast to the conditions found with this fluoride mixture in Inconel.

Temperature and velocity measurements were obtained in a glass thermal convection loop over a Grashof modulus range from 2×10^4 to 67×10^4. The experimental velocity data are compared with predicted values which were obtained by the numerical solution of the laminar-flow heat-conduction equation. The measured values diverge radically from the theoretical values, undoubtedly because of the turbulence which was introduced by the radial temperature gradient and which was observed at Reynolds numbers as low as 100.

Forced-laminar-flow volume-heat-source velocity and temperature solutions have been derived for the case in which the fluid viscosity is temperature dependent. These solutions are functions of a new dimensionless modulus which is a measure of the importance of the viscosity variation of the system.

Experimental apparatus is being assembled for measurements of fluid flow in an annulus and for studies of transient surface-boiling phenomena. The annulus flow will be determined by photographing dust particles; the essential photographic technique is being developed. The boiling studies will be conducted on a flat metal filament suspended in water.

HEAT CAPACITY

W. D. Powers G. C. Blalock
Reactor Experimental Engineering Division

The enthalpy and the heat capacity of $NaF\text{-}ZrF_4\text{-}UF_4$ (50-25-25 mole %) were determined[1] in the liquid and the solid state with a Bunsen ice calorimeter. The data can be represented by the following equations:

$$H_T(\text{solid}) - H_{0°C}(\text{solid}) = -18 + 0.17T,$$
$$c_p = 0.17 \pm 0.02, \quad \text{at 280 to 610°C,}$$
$$H_T(\text{liquid}) - H_{0°C}(\text{solid}) = -39 + 0.27T,$$
$$c_p = 0.27 \pm 0.02, \quad \text{at 610 to 930°C,}$$

where H is the enthalpy in cal/g, T is the temperature °C, c_p is the heat capacity in cal/g·°C. The heat of fusion is 42 cal/g at 610°C.

The enthalpy and the heat capacity of two special samples of type 310 stainless steel and of brazing compound G-E No. 62 (69% Ni–20% Cr–11% Si) were determined for the General Electric Company:[2]

1. for type 310 stainless steel (heat 64177) from 238 to 858°C,

$$H_T - H_{0°C} = -7.2 + 0.143T,$$
$$c_p = 0.143 \pm 0.007;$$

[1] W. D. Powers and G. C. Blalock, *Heat Capacity of Fuel Composition No. 33*, ORNL CF 53-11-128 (Nov. 23, 1953).

[2] W. D. Powers and G. C. Blalock, *Heat Capacity of Two Samples of 310 Stainless Steel and of a Brazing Compound*, ORNL CF 53-9-98 (Sept. 18, 1953).

2. for type 310 stainless steel (heat 64270) from 240 to 834°C,

$$H_T - H_{0°C} = -5.5 + 0.139T,$$
$$c_p = 0.139 \pm 0.005;$$

3. for G-E No. 62 brazing alloy from 211 to 840°C,

$$H_T - H_{0°C} = -4.3 + 0.142T,$$
$$c_p = 0.142 \pm 0.012.$$

THERMAL CONDUCTIVITY OF SOLIDIFIED SALTS

W. D. Powers R. M. Burnett
S. J. Claiborne
Reactor Experimental Engineering Division

The thermal conductivities of solid fluorides have been measured by a transient cooling method. A sphere of the material being studied is allowed to remain in a calorimeter until a uniform initial temperature is established. The sphere is then rapidly transferred to a large circulating bath at a lower temperature. A fine-gage thermocouple at the center of the sphere is used to determine the time-temperature curve as the sphere cools. Classical transient temperature solutions in terms of the physical properties of the sphere are available and may be used to extract the thermal conductivity of the sphere from the experimental time-temperature data. In this way the thermal conductivity of the solid fluoride mixture NaF-KF-LiF-UF_4 (10.9-43.5-44.5-1.1 mole %) was found to be 1.7 Btu/hr·ft² (°F/ft), as compared with a value of 2 Btu/hr·ft² (°F/ft) for the same fluoride mixture in the liquid state. The thermal conductivity of a solid heat transfer salt ($NaNO_2$-$NaNO_3$-KNO_3; 40-7-53 wt %) is also being determined by the transient cooling method. Preliminary measurements indicate a value of 0.6 Btu/hr·ft²(°F/ft) over the temperature range 80 to 170°F.

DENSITY AND VISCOSITY OF FLUORIDES

S. I. Cohen T. N. Jones
Reactor Experimental Engineering Division

Preliminary viscosity and density measurements on Na_2UF_6 were made[3] on a Brookfield viscometer and displacement apparatus, respectively. The density, as plotted in Fig. 8.1, is given by the equation

$$\rho = 5.598 - 0.00119T,$$

where ρ is in g/cm³ and 660°C < T < 1000°C. The viscosity varies from about 17.5 cp at 725°C

[3] S. I. Cohen, *Preliminary Measurement of the Density and Viscosity of Composition 43 (Na_2UF_6)*, ORNL CF 53-10-86 (Oct. 14, 1953).

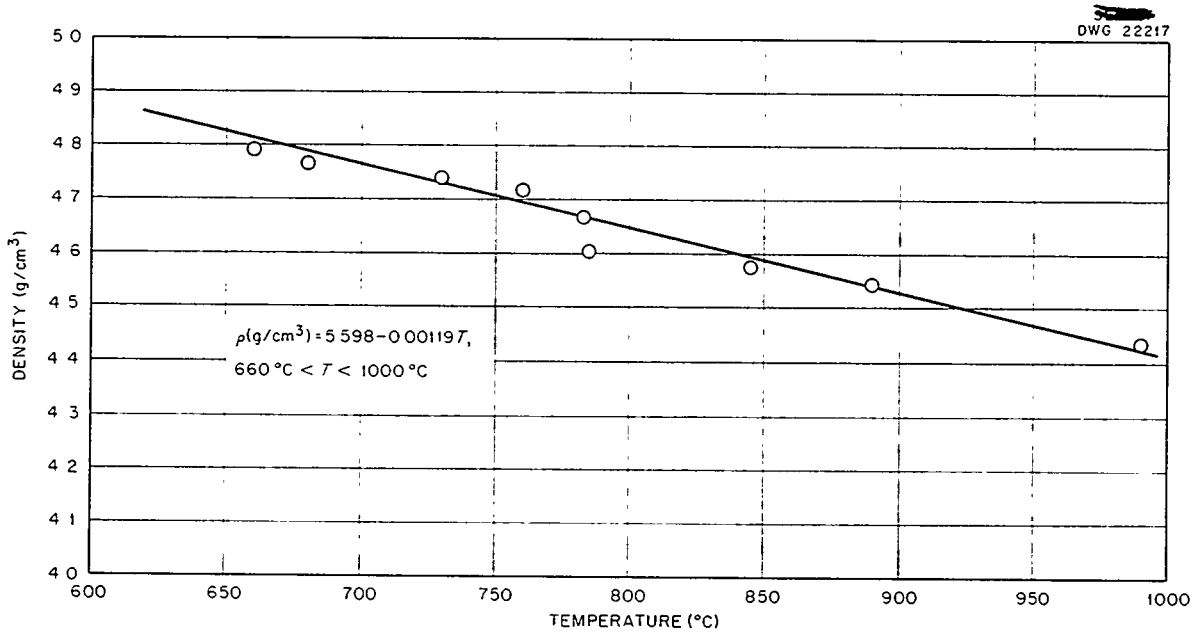

Fig. 8.1. Density of Na_2UF_6 as a Function of Temperature.

to about 9.9 cp at 975°C (Fig. 8.2), and the experimental data are represented by the equation

$$\mu = 0.92\, e^{2936/T},$$

where μ is in centipoises and T is in °K.

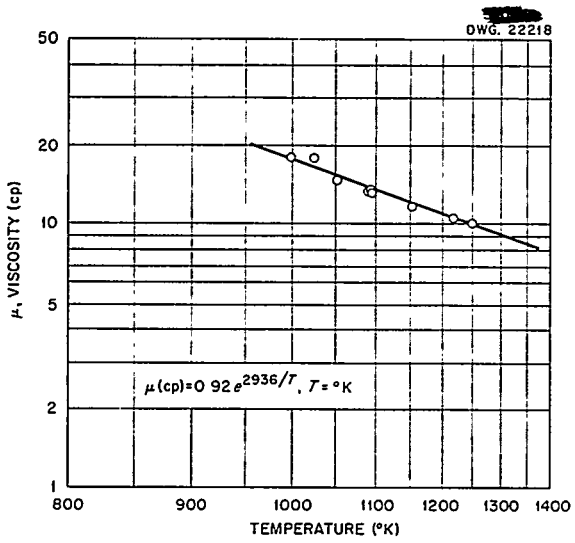

Fig. 8.2. Viscosity of Na_2UF_6 as a Function of Temperature.

The following solid density measurements at room temperature were made on $NaF\text{-}ZrF_4$ mixtures in support of phase studies of these materials:

	DENSITY (g/cm^3)
Batch B-62 (53-47 mole %)	4.00
Batch R-132 (52-48 mole %)	4.103
Batch R-133	4.124

A method for predicting densities of fluoride mixtures have been developed and will be described in a forthcoming report. Plots of liquid densities at any temperature vs. the calculated room-temperature densities have been developed that correlate all the experimental data available to within 2%. Similar plots have been devised for viscosity data, but the correlation is not dependable.

VAPOR PRESSURES OF FLUORIDES

R. E. Traber, Jr. R. E. Moore
C. J. Barton
Materials Chemistry Division

Additional measurements of vapor pressures by the method of Rodebush and Dixon[4] were made. Chemical analysis has shown that the material used for the previously reported[5] measurement of the vapor pressure of $NaF\text{-}ZrF_4$, nominally 50-50 mole %, actually contained 47 mole % ZrF_4. Instead of being the pure compound $NaZrF_5$, it was probably a solid solution of $NaZrF_5$ and Na_2ZrF_6. The vapor pressure equation for this 47 mole % ZrF_4–53 mole % NaF mixture is

$$\log P = -\frac{7213}{T} + 7.635,$$

where P is in mm Hg and T is in °K. The vapor pressure equation for the mixture $NaF\text{-}ZrF_4$ (50-50 mole %) is

$$\log P = -\frac{6827.7}{T} + 7.503$$

over the temperature range 812 to 942°C.

ELECTRICAL CONDUCTIVITY OF FLUORIDES

N. D. Greene
Reactor Experimental Engineering Division

Preliminary electrical conductivity measurements of $NaF\text{-}ZrF_4$ (50-50 mole %) and $NaF\text{-}ZrF_4$ (57-43 mole %) have been obtained for the temperature range 1000 to 1800°F. For these measurements, a thick-walled cylindrical tube of beryllium oxide is mounted vertically in an open Inconel crucible containing the molten fluoride. An electrode is inserted through the tube, and the electrical path is defined from the electrode just under the liquid surface to the Inconel at the bottom of the crucible. However, the beryllia tube was not sufficiently long to prevent nonisothermal regions in the cell, and therefore accurate measurement of the salt temperatures were difficult. A longer tube has been ordered.

An attempt was also made to measure the conductivity of NaF-KF-LiF by using the apparatus described above, but this salt penetrated and eroded the tube so badly that the data obtained were deemed unreliable. A new cell in which only platinum is in direct contact with the salt has been designed and is now being constructed. This cell will be used to measure the conductivities of salts which are not compatible with

[4] W. H. Rodebush and A. L. Dixon, *Phys. Rev.* 26, 851 (1925).

[5] R. E. Moore and R. E. Traber, *ANP Quar. Prog. Rep. Sept. 10, 1953*, ORNL-1609, p. 106.

beryllia. Since slight contamination of the melts occurred as a result of the constituent materials of the crucible going into solution, a more noble material than either Inconel or stainless steel is indicated. Accordingly, a platinum crucible has been designed and constructed for this purpose.

FORCED-CONVECTION HEAT TRANSFER WITH NaF-KF-LiF EUTECTIC

H. W. Hoffman J. Lones
Reactor Experimental Engineering Division

Additional data have been obtained for NaF-KF-LiF eutectic (11.5-42.0-46.5 mole %) flowing through a heated nickel tube. The experimental results are presented in Fig. 8.3 in terms of the Colburn *j*-function. The previously reported results for NaF-KF-LiF in both nickel and Inconel tubes are also shown.

In review, NaF-KF-LiF heat transfer data were first obtained by using a nickel tube. The results (shown by the inverted triangles in Fig. 8.3) indicated that the anticipated heat transfer correlation was followed. The experiment was then repeated with the eutectic flowing through an Inconel tube, and the data (circles in Fig. 8.3) were found to lie approximately 50% below the expected correlation. The discrepancy was believed to be due to the formation of a film of corrosion products at the fluid-metal interface. The heat transfer results and the existence of the film were both definitely verified for NaF-KF-LiF in Inconel tubes in a subsequent experiment (squares in Fig. 8.3). The film was analyzed and found to be K_3CrF_6 plus a small amount of Li_3CrF_6.

The data reported at this time were obtained to establish the validity of the original results for NaF-KF-LiF in nickel tubes. The results (normal triangles in Fig. 8.3) are essentially in agreement with those for nickel tube No. 1; visual observation of the tube showed no film. The experiment was terminated because of fatigue failure of the nickel tube at the high operating temperatures used.

Experimental apparatus is being constructed for studying fluoride films formed on Inconel as a function of time and temperature. Because of the unavailability of pure K_3CrF_6, it has not yet been possible to measure the thermal conductivity of this material. Several other fluoride mixtures are being studied to determine the thermal conductivity of such films because they may form on Inconel tubes.

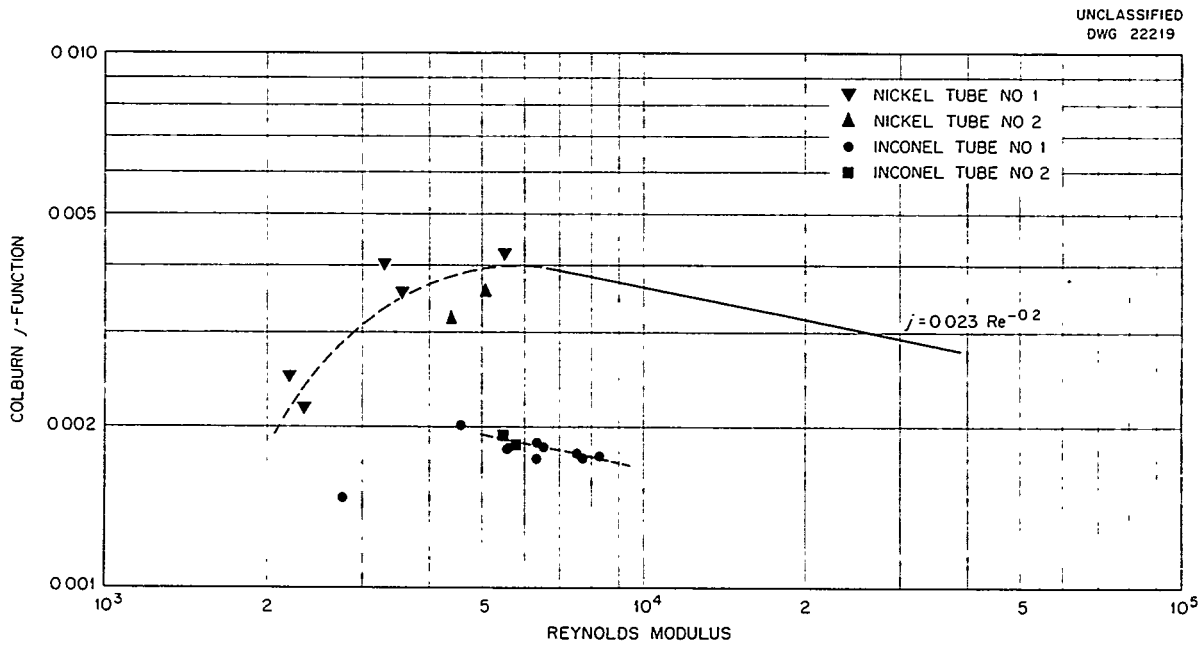

Fig. 8.3. The *j*-Modulus vs. Reynolds Modulus for NaF-KF-LiF (11.5-42.0-46.5 mole %).

FLOW IN THERMAL-CONVECTION LOOPS

D. C. Hamilton F. E. Lynch
L. D. Palmer
Reactor Experimental Engineering Division

Thermal-convection loops have been used for observing the nature of flow of ordinary fluids and to determine the accuracy and range of usefulness of an analytical method for predicting the mean velocity, or Reynolds modulus, from wall temperature measurements. A discussion of the velocity measurements and flow observations was given in a previous report.[6] Additional velocity and wall temperature data have been taken, fluid temperature traverses have been made, the analytical analyses have been completed, and a report of the results is being prepared.[7]

Measurements of temperature and velocity were taken for five specific conditions over the range of Grashof modulus from 2×10^4 to 67×10^4. The corresponding variation of Reynolds modulus was from 50 to 270. The Grashof and Reynolds moduli are, respectively,

$$Gr_d = \frac{d^3 \beta g \theta_w(\max)}{\nu^2}$$

and

$$Re = \frac{u_m d}{\nu},$$

where d is the tube diameter, ν is the kinetic viscosity of the liquid, β is the thermal coefficient of expansion of the liquid, g is the acceleration of gravity, u_m is the mean fluid velocity, and $\theta_w(\max)$ is the maximum variation in wall temperature.

The flow and heat transfer observed in these experiments were characteristic of free convection rather than forced convection, and thus the significant parameter which dictates the character of the flow is the Grashof modulus rather than the Reynolds modulus.

At Reynolds moduli of up to about 100, the flow was essentially laminar. Above this value, the Grashof modulus was supercritical, and the flow was laminar over part of the circuit and turbulent in other parts. As the Grashof modulus (and thus Reynolds modulus) was increased, the length of the circuit in laminar flow decreased. In addition, when the Grashof modulus was high, the radial temperature gradient was sufficient to cause vigorous secondary flow cells in the laminar part of the circuit.

The method for predicting the Reynolds modulus from wall temperature measurements employed the numerical solution of the laminar flow equation for heat conduction. The problem was solved on the ORNL high-speed computer, the ORACLE.

In Fig. 8.4, the predicted and measured values of Reynolds moduli are compared. For the first two sets of data, for which the flow was essentially laminar, the correlation is no worse than 30%; for Reynolds moduli greater than 100, the flow was observed to be partly turbulent, and a laminar flow solution is obviously not applicable. The prediction is satisfactory for the laminar flow regime, but a similar prediction for the turbulent flow regime cannot be made because the turbulent diffusivity is not known for this type of turbulent flow.

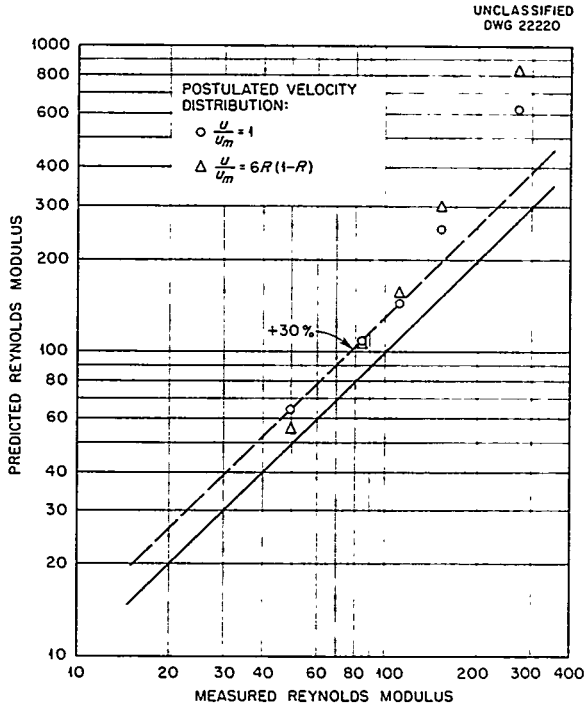

Fig. 8.4. Comparison of Predicted and Measured Reynolds Moduli for a Thermal Convection Loop.

[6] D. C. Hamilton, F. E. Lynch, and L. D. Palmer, *ANP Quar. Prog. Rep. June 10, 1953*, ORNL-1556, p. 89.

[7] D. C. Hamilton, F. E. Lynch, and L. D. Palmer, *The Nature of the Flow of Ordinary Fluids in a Thermal Convection Harp*, ORNL-1624 (to be published).

The method used in the previous work for measuring velocity is not applicable to higher flows. Therefore a velocity measuring device is being developed which will be applicable at higher velocities and which will not offer resistance to the flow.

FLUID FLOW IN AN ANNULUS

J. O. Bradfute
Reactor Experimental Engineering Division

The experiment to be used for measuring fluid velocity profiles in annulus systems was described previously.[8] In essence, the method consists of photographing dust particles which are entrained in air flowing in an annulus. Most of the recent effort on this research was devoted to photographic experimentation to develop a procedure for photographing the grid system and the dust particles with the light available from a single flash of a Strobolume. This has been accomplished.

The problem stemmed from the fact that colimating a beam of light into a sharply defined region in space, a necessary requirement, is extremely inefficient. A pair of parallel slits, each about 2 mm wide and approximately 25 cm apart, with the Strobolume placed immediately behind the last one, produced what seemed to be the optimum combination of intensity and definition in the usable portion of the beam. Although about 700 lumen-seconds per flash of the light energy was dissipated by the light source, the developed image of the grid system obtained by using Kodak Tri-X panchromatic film and a stop opening of f:4.7 was so underexposed that even the doubly accented centimeter lines were barely visible upon careful examination. Several film sensitization and latensification materials, as well as high-speed developers, were tried with varying degrees of success and failure. An f:1.8 lens was obtained, and, by employing this lens and following a complex developing process, negatives were produced which have sufficient contrast for satisfactory printing. Chalk-dust particles were also photographed by applying this procedure.

TRANSIENT SURFACE-BOILING STUDIES

M. W. Rosenthal
Reactor Experimental Engineering Division

In the event a water-cooled reactor suddenly became supercritical, the time required for production of a certain volume of steam would be of importance. Of primary interest would be the effect of generation of heat at rates increasing exponentially with time in vertical plates (such as the fuel plates of an MTR-type reactor) submerged in water that was initially at below the boiling point.

To obtain information on this phenomenon, an experimental study of heat transfer to water under transient conditions has been undertaken. The basic experimental system is a flat metal filament positioned vertically in a tank of water with heat generated electrically in the filament. The research program consists of two phases: a study involving exponential generation of heat, which will be started when the necessary electrical equipment has been developed, and a preliminary general study of boiling from a vertical filament, which will begin immediately.

Arrangements have been made for the Instrumentation and Controls Division to develop and construct equipment to regulate the flow of current in the filament and to produce an exponential heating curve. This equipment will also measure and record instantaneous values of the variables of interest. The filament and the adjacent water will be photographed by using a high-speed motion-picture camera synchronized with the heat generation system.

CIRCULATING-FUEL HEAT TRANSFER

H. F. Poppendiek L. D. Palmer
G. M. Winn
Reactor Experimental Engineering Division

Some preliminary experimental temperature measurements have been obtained in a forced-flow volume-heat-source system under laminar flow conditions. The volume-heat-source is generated within the flowing electrolyte by passing an electric current through it. In general, the experimental results are in agreement with the previously developed laminar flow theory. At low flow rates (Reynolds number of 600 or less), the effect of the free convection which is superimposed on the forced convection was observed. The variable ranges within which theoretical and experimental forced-flow volume-heat-source behavior have been

[8] J. O. Bradfute and J. I. Lang, *ANP Quar. Prog. Rep. March 10, 1953*, ORNL-1515, p. 160.

compared to date are the following:

$$600 < Re < 14{,}000,$$

$$4.6 < Pr < 8.7,$$

$$3 \times 10^{-4} < \frac{\frac{t_0 - t_m}{W\nu_0^2}}{k} < 6 \times 10^{-2} .$$

The next set of experiments is to be made with the test section in a vertical rather than a horizontal position; also, concentrated sulfuric acid is to be used as the electrolyte so that a new Prandtl modulus range can be studied.

Currently, the forced-turbulent-flow temperature solution for the case of fluid flow between parallel plates and annular spaces with volume heat sources in the fluids is being evaluated. This solution will be useful in estimating fluid temperature distributions in reactor systems such as the reflector-moderated reactor.

Forced-laminar-flow volume-heat-source velocity and temperature solutions have been derived for the case in which the fluid viscosity is temperature dependent. A simple, algebraic viscosity-temperature expression which closely approximates experimental viscosity data was substituted into the hydrodynamic equation. A power series with unknown coefficients was substituted into the heat transfer equation, and two integrations were carried out. The resulting temperature solution was then substituted into the hydrodynamic equation, and an integration was carried out. The coefficients of the resulting power series velocity solution were determined by relating them to the initially proposed velocity power series and the integral equation describing the mean fluid velocity. The resulting velocity and temperature solutions are functions of a new dimensionless modulus, as well as radial position. This dimensionless modulus is a measure of the importance of the viscosity variation in the flow system.

---

9. RADIATION DAMAGE

J. B. Trice, Solid State Division
A. J. Miller, ANP Division

Inconel capsules containing the fluoride fuel NaF-ZrF_4-UF_4 were irradiated in the LITR and in the MTR. Examination of the capsule walls showed a tendency toward intergranular corrosion that does not occur in unirradiated static tests. The data on depth of penetration showed considerable scatter, and therefore no correlation with power production rate and exposure time could be made. Design and construction continued on the in-pile circulating-fuel loops and the MTR creep test equipment.

IRRADIATION OF FUEL CAPSULES

G. W. Keilholtz
J. G. Morgan
H. E. Robertson
C. C. Webster
M. T. Robinson
W. R. Willis
W. E. Browning
Solid State Division

Inconel capsules containing various compositions of the fluoride fuel system, NaF-ZrF_4-UF_4, have been irradiated in both the Low-Intensity Test Reactor (LITR) and in the Materials Testing Reactor (MTR). These tests have included irradiation times of from 53 to 800 hr with power production from the 230 watts/cm^3 with a 4 mole % UF_4 fuel in the LITR to the 8000 watts/cm^3 with a 12 mole % UF_4 fuel in the MTR. In general, Inconel surfaces show more tendency toward intergranular corrosion when in contact with irradiated fuel than they do in out-of-pile tests. However, the data so far available indicate no definite trend in corrosion penetration either as a function of rate of power production in the fuel or of irradiation time.

Six Inconel specimens containing the fluoride mixture NaF-ZrF_4-UF_4 (50-46-4 mole %) which were irradiated in the LITR for 53, 140, 270, 565, 685, and 810 hr each are shown in Fig. 9.1. In each case, the power dissipation in the fluoride was 230 watts/cm^3. Out-of-pile control capsules for this series of tests are shown in Fig. 9.2.

Inconel capsules which were irradiated in the MTR with power production in the fluoride mixture of 2500, 3900, and 8000 watts/cm^3 are shown in Figs. 9.3, 9.4, and 9.5, respectively. The NaF-

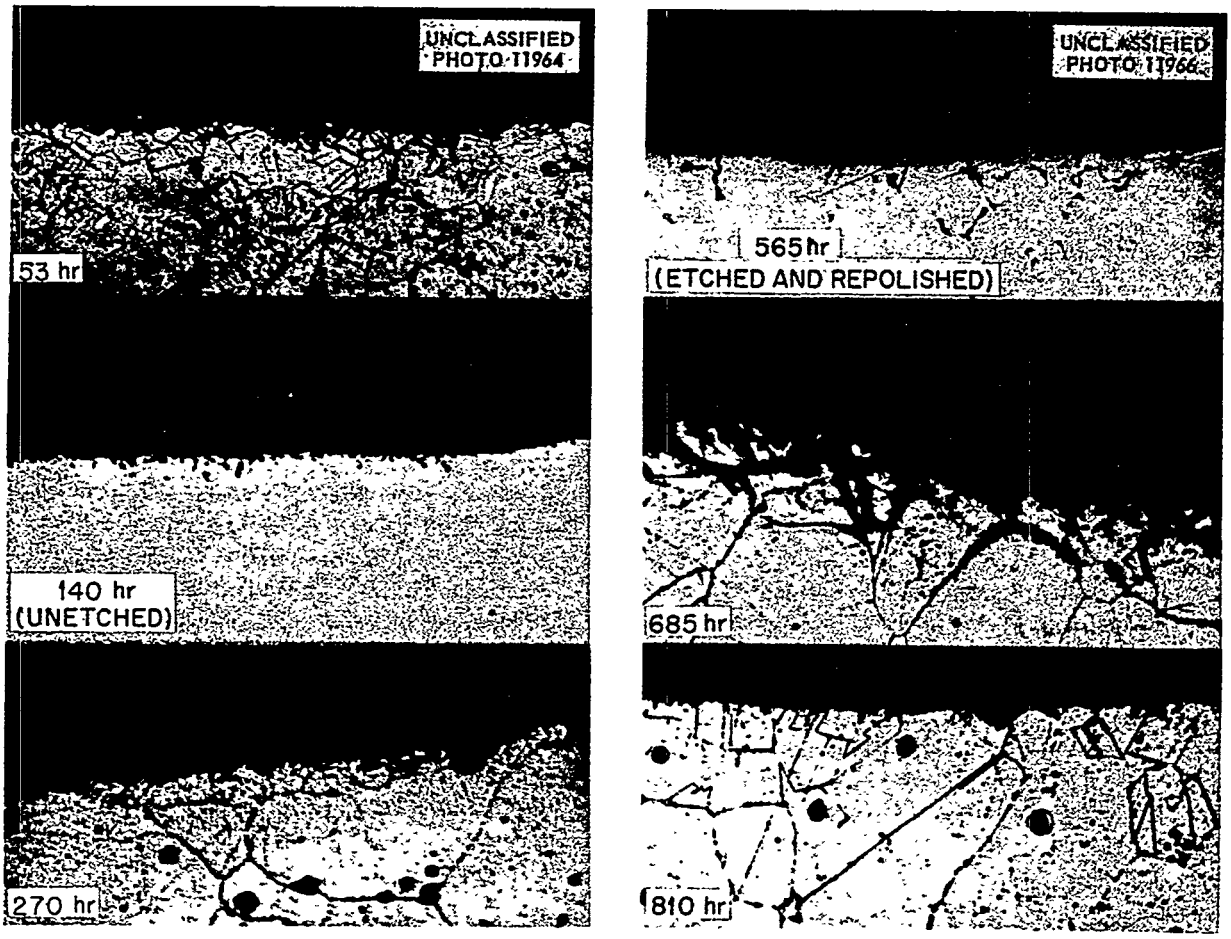

Fig. 9.1. Static Corrosion of Inconel by NaF-ZrF_4-UF_4 (50-46-4 mole %) After Exposure at 1500°F in the LITR to 230 watts/cm^3 for Various Irradiation Times.

ZrF_4-UF_4 system was used in each of these tests, although the composition was varied and the UF_4 content was 4, 6.5, and 12 mole %, respectively, in the three tests. The sample shown in Fig. 9.5, which was contacted for 575 hr in the MTR with fuel producing power at a rate of the order 8000 watts/cm^3, has only 3 or 4 mils of corrosion penetration and is similar to the sample shown in Fig. 9.1, which was exposed at only 230 watts/cm^3. In a few samples in which the Inconel had a very large grain size, occasional penetration to a depth of 12 mils has been observed. This phenomenon appears to be fairly independent of power density or time of irradiation, and, as with the other effects observed, there is no certainty as to how much of the effect is due to radiation.

In confirmation of the analytical work reported previously, petrographic examinations of irradiated fuels showed no decomposition or segregation of the fuel as a result of irradiation.

CREEP UNDER IRRADIATION

W. W. Davis
N. E. Hinkle
J. C. Wilson
J. C. Zukas
Solid State Division

No new creep tests were made during this quarter. The recent increase in power of the LITR causes excessive microformer operating temperatures, and the increasing incidence of microformer failures (which occurred even before the power was increased) prevents reliable strain measurements.

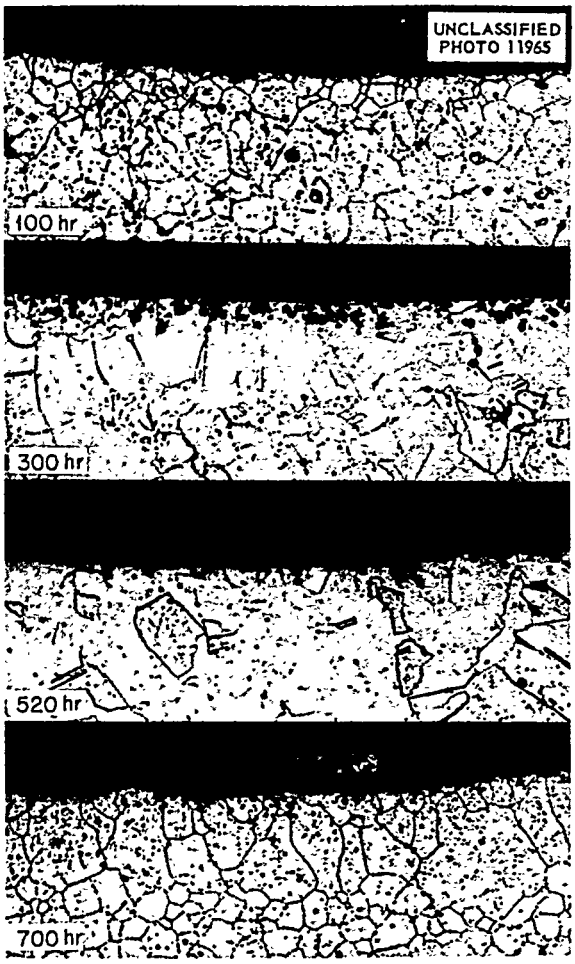

Fig. 9.2. Static Corrosion of Inconel Exposed to NaF-ZrF_4-UF_4 (50-46-4 mole %) at 1500°F for Various Times.

Accordingly, no more creep tests will be operated in the LITR until a suitable strain transducer is found. Both the Bourdon-tube extensometer and a bimetal expansion extensometer now being developed show promise of becoming reliable measuring instruments for use in the LITR and in the MTR.

Several models of an in-pile stress-corrosion apparatus are being built to determine the best system for conducting stress-corrosion tests. The discovery of an effect of straining on the corrosion of Inconel[1] and the recent observation of intergranular corrosion in static, in-pile fuel irradiations

[1]R. B. Oliver *et al., Met. Div. Semiann. Prog. Rep. April 10, 1953,* ORNL-1551, Figs. 43 and 44, p. 52, 53.

Fig. 9.3. Static Corrosion of Inconel by NaF-ZrF_4-UF_4 (50-46-4 mole %) After Irradiation in the MTR at 2500 watts/cm^3 for 575 hr at 1500°F.

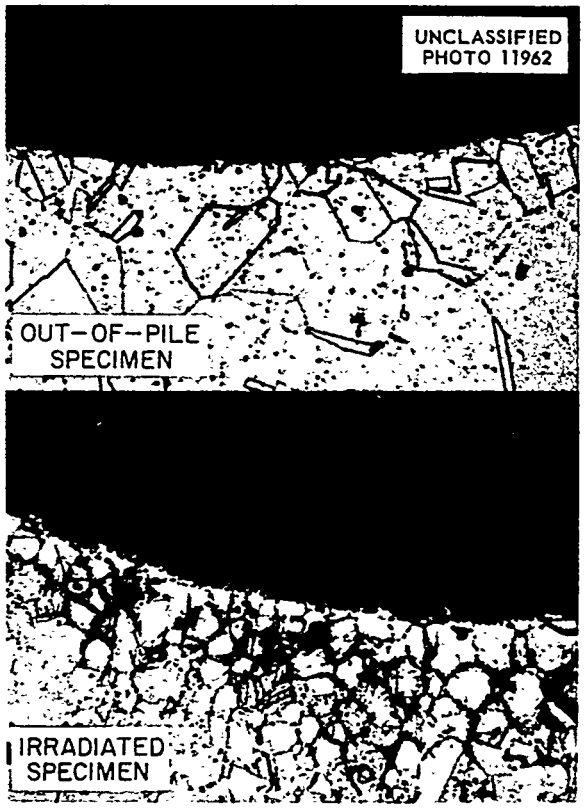

Fig. 9.4. Static Corrosion of Inconel by NaF-ZrF_4-UF_4 (53.5-40-6.5 mole %) After 419 hr at 1500°F With and Without Irradiation in the MTR at 3900 watts/cm^3.

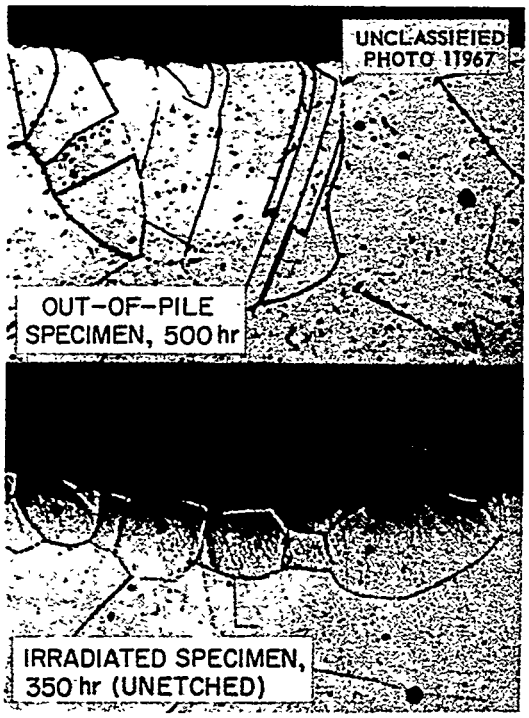

Fig. 9.5. Static Corrosion of Inconel by NaF-ZrF_4-UF_4 (63-25-12 mole %) at 1500°F With and Without Irradiation in the MTR at 8000 watts/cm^3.

have pointed to the need for data on the effects of in-pile stress corrosion.

The MTR creep test rig has been welded shut, but considerable difficulty has been experienced with leaks in the helium supply system and in the seals where the lead wires exit from the pressurized portion of the experimental plug. The complete instrument assembly has been tested and found satisfactory.

IN-PILE CIRCULATING LOOPS

O. Sisman
W. E. Brundage
F. M. Blacksher
C. Ellis
M. T. Morgan
A. S. Olson
W. W. Parkinson
Solid State Division

In-pile circulating loops for studying the corrosion of Inconel by fluoride fuels under dynamic conditions in a neutron flux are being built for insertion in hole HB-2 of the LITR. It is expected that similar loops can be used in the MTR. A loop consists essentially of U-shaped sections of 0.225-in.-OD tubing, which will be in the neutron flux, thick-walled ½-in. tubing that will connect the irradiated section with a Venturi flowmeter and an air-cooled heat exchanger just inside the reactor shield, and a centrifugal sump pump outside the shield. All these components, except the shaft and seal portion of the pump, will be enclosed in a helium atmosphere. All in-pile components, other than the pump, will be surrounded by a water-cooled jacket.

The fabrication of components for the first loop is 80% complete and most of the work remaining to be done on this loop consists of welding or brazing together the finished parts. The components for a second loop are 40% complete. The withdrawal shield is being fabricated, but work on the shield for the pump has not started. The design of the instrumentation is 90% complete, and about 85% of the instruments and controls are on hand.

10. ANALYTICAL STUDIES OF REACTOR MATERIALS

C. D. Susano, Analytical Chemistry Division
J. M. Warde, Metallurgy Division
R. Baldock, Stable Isotope Research and Production Division

Developmental work was mainly concerned with the investigation of methods for the determination of the oxidation states of the constituents and the metallic corrosion products in fluoride fuel mixtures and fuel solvents. Divalent iron fluoride was leached from samples of fluoride mixtures with 0.1 M H_2SO_4, and the iron was determined as the o-phenanthroline complex. Divalent chromium fluoride was found to be complexed by 0.17 M $(NH_4)_2C_2O_4$ and could be distinguished from trivalent chromium fluoride, which is readily complexed with a dilute solution of disodium dihydrogen ethylenediaminetetraacetate (EDTA) at pH 4.0.

Studies were continued on the use of ammonium oxalate for the determination of traces of UF_3 in the presence of UF_4. A separation based on solubility difference is possible but not for low concentrations of UF_3. The absorption spectra of solutions of UF_4 in EDTA and HCl were determined.

The effectiveness of solutions of ammonium oxalate, oxalic acid, and acetic acid as solvents for removing fluoride fuels, which contain zirconium, from metallic thermal convection loops was investigated. Ammonium oxalate proved the most effective solvent tested; however, it was not considered so satisfactory as the nitric and boric acid mixtures which are currently used.

Petrographic examinations were made of irradiated samples of fluoride fuel mixtures. No difference was noted under the petrographic microscope between the irradiated specimens and the comparable control samples.

The mass spectrometer method for quantitative analysis of the uranium content of irradiated fluoride fuel mixtures has recently been extended for use as a measure of uranium burnup during irradiation. A procedure has been developed for calculating the percentage of uranium by weight in both the unirradiated and the irradiated conditions. Hence, the loss in uranium content can be determined to the accuracy that the isotope abundances are known in the original material. The portion of this total uranium loss that is due to burnup is then determined by mathematical analysis.

The activities of the Analytical Service Laboratory have increased markedly during the past quarter. A total of 1,378 samples was received as compared with 878 for the previous quarter, and 1,201 samples involving a total of 11,034 determinations were reported.

ANALYTICAL CHEMISTRY OF REACTOR MATERIALS

J. C. White
Analytical Chemistry Division

The developmental work during this quarter consisted almost entirely of a search for methods for determining the oxidation states of the constituents and the metallic corrosion products in ARE fuels and fuel solvents. Three phases of the problem are currently being studied: the determination of the oxidation states of iron in fuel solvent and in the fuel; the determination of the oxidation states of chromium in similar media; and the determination of the oxidation states of uranium in the fuel. The ultimate aim of these investigations is the determination of each specie in the presence of the other species. The reducing power of specially prepared $NaZrF_5$ with zirconium additive was also determined. The effectiveness of certain solvents for dissolving proposed fuels from the walls of metal containers was investigated. No additional work was conducted on the determination of metallic oxides in reactor fuels because of the urgency of other problems.

Oxidation States of Iron

P. V. Hoffman
Analytical Chemistry Division

A number of samples of the fuel mixture NaF-ZrF_4-UF_4 (50-46-4 mole %) and iron (5 wt %) were heated and filtered. Divalent, trivalent, and total iron contents were determined, in addition to uranium trifluoride. The finely divided samples were leached with 0.1 M H_2SO_4 on the steam bath for 1 hr to remove iron. Ferrous iron in the filtrate

from the leach was determined with o-phenanthroline;[1] iron was determined in the leach filtrate by first reducing the iron present with hydroquinone and then determining it as the o-phenanthroline complex. In order to test the efficiency of the leaching process, a separate sample was dissolved, and the iron was then determined by the o-phenanthroline method.

The results, with a relative standard error of 10%, show that a single acid leach is sufficient to leach iron quantitatively from the fuel mixture. Further evaluation of the data shows that only a small fraction of the added iron reacts with the fuel and passes in solution through the filter. The oxidation state of this iron is predominantly, if not completely, bivalent. It should be recognized, however, that if FeF_3 and UF_3 exist as such in the mixture, reduction of trivalent iron to the bivalent state undoubtedly occurs on contact with sulfuric acid. The absence of UF_3 was indicated by the hydrogen evolution method.[2] However, this method is not sufficiently sensitive to determine the probable small concentration of UF_3 which may be present in these samples. The need for a sensitive method for determining UF_3 in reactor fuels is evident.

Oxidation States of Chromium

D. L. Manning
Analytical Chemistry Division

Work has continued on the determination of the oxidation states of chromium following its reaction with UF_4 in fuel solvent $NaZrF_5$. The formula for the reaction is

$$(1)\quad CrF_3 + 3UF_3 \underset{800°C}{\overset{NaZrF_5}{\rightleftharpoons}} Cr° + UF_4 .$$

It has been shown that chromium trifluoride can be separated from chromium metal by leaching with an acetate-buffered solution (pH, 4.0) of disodium dihydrogen ethylenediaminetetraacetate (EDTA). Chromium metal is insoluble in this medium. Several samples were leached with EDTA at 60 to 70°C for 3 hr to determine the extent of reduction of CrF_3 to metallic chromium during the heating period. No residues indicative of metallic chromium were obtained. This suggests that chromium trifluoride is either not reduced to metallic chromium or that the metal obtained is in such a finely divided and reactive state that it dissolves in the leach solution. However, previous tests would indicate incomplete reduction, probably to divalent chromium fluoride.

Since EDTA solutions complex both di- and trivalent chromium, other complexing agents were studied to distinguish between CrF_2 and CrF_3. Preliminary experiments have indicated that a 0.17 *M* (2.5%) solution of ammonium oxalate will readily dissolve CrF_2 at the refluxing temperature, and a purple complex will form. Metallic chromium, CrF_3, and Cr_2O_3 appear to be insoluble, and they show no tendency to form complexes. The absorption spectrum of the complex formed by divalent chromium fluoride and ammonium oxalate is identical with that of the complex formed by the reaction between trivalent chromium chloride and ammonium oxalate. Further investigation of the nature of this complex is under way.

The work on the determination of the oxidation states of chromium in reactor fuels has shown that (1) divalent chromium fluoride can apparently be selectively leached with 0.17 *M* ammonium oxalate, (2) divalent and trivalent chromium fluoride can be leached simultaneously with EDTA, and (3) the metal and the trivalent oxide are not attacked by either of these solvents.

Determination of UF_3 and UF_4

W. J. Ross
Analytical Chemistry Division

Work on the development of a method for the determination of UF_3 and UF_4 in $NaZrF_5$ has been continued, and the more complete studies show, as reported previously, that EDTA dissolves UF_4 but apparently has little effect on UF_3. The effects of temperature and the concentration and acidity of EDTA on the reaction between UF_4 and EDTA were investigated. Concentration of the reagent was not critical over the range 0.08 to 0.15 *M*; a concentration of 0.1 *M* was used in most of the tests. Solutions of EDTA with acid concentrations of pH 4 were not appreciably more effective in dissolving UF_4 than those with acid concentrations approaching a pH of 7. Use of solutions less acidic than pH 7 resulted in hydrolysis of uranium. Temperature was the most critical condition. The rate of

[1] J. C. White *et al.*, *ANP Quar. Prog. Rep. June 10, 1952*, ORNL-1294, p. 171.

[2] D. L. Manning, W. K. Miller, and R. Rowan, Jr., *Methods of Determination of Uranium Trifluoride*, ORNL-1279 (Apr. 25, 1952).

reaction at 100°C was approximately ten times that at 25°C; however, the data obtained at 25°C were not reproducible because of variations in particle size.

Under various conditions of temperature and acidity, the absorption spectra of UF_4-EDTA are essentially identical with those for UF_4 dissolved in HCl, except that the spectra for the UF_4-EDTA systems are shifted by approximately 20 mμ toward the infrared by the presence of EDTA. The maximum molar extinction coefficients for the four spectra shown are nearly equivalent; they range from 35.7 for UF_4-HCl to 25.0 for UF_4-EDTA at a pH of 6.8 and a temperature of 100°C.

Petrographic and chemical analyses of the three batches of UF_3 used for the study of solubility in 0.1 *M* EDTA showed UF_4 contents of 92.4, 90.4, and 90.7%, respectively. Samples of these batches were treated with 0.2 *M* ammonium oxalate at reflux temperature and filtered, and petrographic examination revealed that the residues were essentially free from UF_4. The data indicate that during the first hour of reflux the greater portion of UF_4 present is removed but that quantitative separation is questionable. The solubility of UF_3 in ammonium oxalate is low; however, UF_3 may oxidize slowly upon contact with this solvent, as indicated by the appreciable concentration of uranium in the solution when allowed to stand overnight. The UF_3 content of the sample which had been treated with oxalate is being determined and is expected to be near 100%.

On the basis of the data obtained thus far, UF_4 and UF_3 can be separated by ammonium oxalate. However, the method is not sufficiently precise for the separation of traces of UF_3 from UF_4. Similar tests are under way to determine the feasibility of using 0.1 *M* EDTA for separating UF_3.

Reducing Power of $NaZrF_5$ with Zirconium Addition

D. L. Manning
Analytical Chemistry Division

The total reducing power of $NaZrF_5$ specially prepared by treatment with metallic zirconium was determined. In the hydrogen evolution method[3] used for this determination, the sample is treated with 0.2 *M* HF to liberate the hydrogen which is formed by the reaction between zirconium and hydrofluoric acid; the gas is collected and measured; and the reducing power is calculated. Essentially no reducing power was observed in these samples. A second method which involved complete dissolution of the sample in standard ceric sulfate solution in 9 *M* H_2SO_4 and back-titration with standard ferrous sulfate solution was used to confirm the results. Further tests by the hydrogen evolution method on synthetic samples of $NaZrF_5$ and zirconium demonstrated that the method is quantitative.

[3] J. C. White and W. J. Ross, *ANP Quar. Prog. Rep. March 10, 1953*, ORNL-1515, p. 173.

Dissolution of Fluoride Mixtures Containing Zirconium

P. V. Hoffman
Analytical Chemistry Division

Nitric and boric acid mixtures have been used successfully as solvents for fluoride mixtures, but, in an effort to find a less-corrosive solvent, small-sized lumps of NaF-ZrF_4-UF_4 (50-46-4 mole %) were contacted with various concentrations of ammonium oxalate, oxalic acid, and acetic acid at 70 to 80°C for various periods of time. The optimum concentration of ammonium oxalate was 1 *M*, which is approximately a saturated solution at 50°C. [One hundred ml of 1 *M* $(NH_4)_2C_2O_4 \cdot H_2O$ will dissolve 1 g of small lumps of fuel in approximately 2 hr.] A 2 *M* solution was the most effective oxalic acid concentration and was approximately equivalent to 1 *M* ammonium oxalate in dissolution effectiveness. The optimum acetic acid concentration was 0.2 *M*, which yielded only 50% of the solubility strength of the oxalates. A comparison of the effectiveness of the three reagents tested is shown in Fig. 10.1. The rate of dissolution with 1 *M* ammonium oxalate is greater than the rate with 2 *M* oxalic acid, although their effectiveness is nearly equivalent. Ammonium oxalate (1.0 *M*), because of its higher pH (6.5), is to be preferred over 2 *M* oxalic acid (pH 0.7), however, with respect to possible corrosiveness. None of these solvents are suitable, however, for dissolving large-sized lumps of NaF-ZrF_4-UF_4 from metallic containers.

PETROGRAPHIC EXAMINATION OF FLUORIDES

G. D. White
Metallurgy Division

T. N. McVay
Consultant, Metallurgy Division

Petrographic examinations were made of fluoride fuel mixtures NaF-ZrF_4-UF_4 (50-46-4 mole %) and

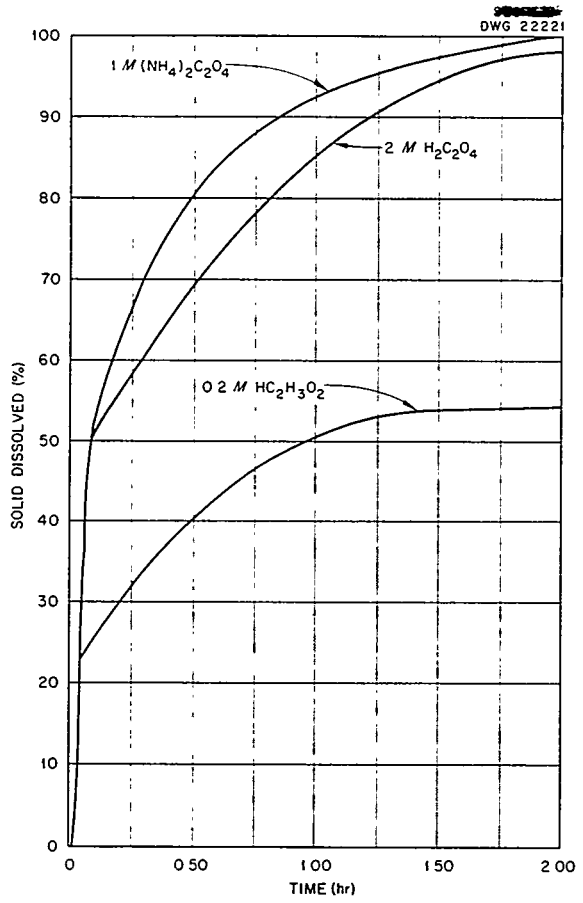

Fig. 10.1. Comparison of Effectiveness of Solutions of Ammonium Oxalate, Oxalic Acid, and Acetic Acid as Solvents for NaF-ZrF_4-UF_4 (50-46-4 mole %).

(53.5-40-6.5 mole %) which had been irradiated a maximum of 492 hr in the MTR. Unirradiated control samples were examined at the same time. These fuels are normally composed of $NaZr(U)F_5$, which is green, and perhaps a very small amount of a lower refractive index complex, which is designated E-2. The irradiated samples were normal, except that the $NaZr(U)F_5$ had a slightly low refractive index and was slightly reduced. There were no differences between the control samples and the irradiated samples which could be observed with a petrographic microscope.

MASS SPECTROMETER INVESTIGATIONS OF IRRADIATED FLUORIDE FUELS

C. R. Baldock
Stable Isotope Research and Production Division

The mass spectrometer has been successfully employed in the quantitative analysis of the uranium content of irradiated fluoride fuel mixtures. Initially, the mass spectrometer method was used to test the validity of chemical analyses, but it was recognized that the method could be extended to obtain an accurate measure of fuel burnup. In addition, by using accepted values of cross sections, an average value of the flux in which the fuel has been irradiated can be determined. This gives an independent check of values predicted from other types of measurements and of the internal consistency of the calculations. The isotope dilution method as applied to the analysis of irradiated fuel has been used extensively with a routine accuracy of ±1%, which is not the ultimate limit of accuracy.

Calculation of UF_4 in Unirradiated Fuels

For the calculation of the percentage of UF_4 (by weight) in unirradiated fluoride fuel samples of known isotopic composition, the exact values for the isotopic masses are used to compute the atomic weight of the uranium in the fuel:

$$(1)\quad \text{At. wt} = 235.12\,A_{235} + 234.12\,A_{234} + 238.12\,A_{238},$$

where A_n denotes abundance of uranium isotope of mass number n. The ratio, R, of U^{235} to U^{238} is obtained from the mass spectrometer measurement, and since the atoms of U^{235} and U^{238} are obtained from both the uranium in the fuel and the natural U_3O_8 spike material added,

$$(2)\quad R = \frac{(\text{atoms of } U^{235} \text{ from fuel}) + (\text{atoms of } U^{235} \text{ from spike})}{(\text{atoms of } U^{238} \text{ from fuel}) + (\text{atoms of } U^{238} \text{ from spike})}.$$

The atomic weight of uranium in the spike is 238.07, and therefore

$$(3) \qquad R = \frac{\frac{W_1F_1YA_{235}}{\text{at. wt}} + \frac{W_2F_2A_{235}}{238.07}}{\frac{W_1F_1YA_{238}}{\text{at. wt}} + \frac{W_2F_2A_{238}}{238.07}},$$

where

W_1 = weight of uranium-bearing fuel,
W_2 = weight of U_3O_8 spike material,
F_1 = U/UF_4 = gravimetric factor for uranium in fuel,
F_2 = $3U/U_3O_8$ = gravimetric factor for uranium in spike,
$Y \times 100$ = percentage of UF_4 (by weight) in fuel.

If Eq. 3 is solved for Y,

$$(4) \quad Y = \frac{\frac{W_2F_2A_{235}}{238.07} - R\,\frac{W_2F_2A_{238}}{238.07}}{R\,\frac{W_1F_1A_{238}}{\text{at. wt}} - \frac{W_1F_1A_{235}}{\text{at. wt}}}$$

$$= \left(\frac{W_2F_2}{W_1F_1}\right)\left(\frac{\text{at. wt}}{238.07}\right)\left(\frac{A_{235} - RA_{238}}{RA_{238} - A_{235}}\right).$$

Calculation of U^{235} Lost from Irradiated Fuel

If C is defined as the number of gram atomic weights of U^{235} in W_1 grams of fuel before irradiation, then

$$(5) \qquad C = \frac{W_1F_1YA_{235}}{\text{at. wt}},$$

and, for the irradiated spiked fuel sample, the following equation must hold:

$$(6) \qquad R = \frac{X + \frac{W_2F_2A_{235}}{238.07}}{\frac{W_1F_1YA_{238}}{\text{at. wt}} + \frac{W_2F_2A_{238}}{238.07}},$$

where X is the gram atomic weight of the U^{235} present in W_1 grams of fuel after irradiation. Solving Eq. 6 for X gives

$$(7) \quad X = R\,\frac{W_1F_1YA_{238}}{\text{at. wt}} + R\,\frac{W_2F_2A_{238}}{238.07} - \frac{W_2F_2A_{235}}{238.07}.$$

Then, the gram atomic weight of the U^{235} lost from W_1 grams of fuel, from Eqs. 5 and 7, is

$$(8) \quad C - X = (A_{235} - RA_{238})\,\frac{W_1F_1Y}{\text{at. wt}} + \frac{W_2F_2}{238.07},$$

and the percentage of U^{235} lost from the fuel follows as

$$\frac{C - X}{C} \times 100.$$

Determination of U^{235} Burnup

Equation 6 gives only the total percentage of U^{235} lost from the fuel. However, this loss may be due to several factors, including burnup, radiation damage, and replacement of chromium leached from the Inconel walls. A graphical method has been developed to test this loss to determine whether it can be completely ascribed to the capture of neutrons to produce fission products and U^{236}, that is, to burnup.

The solution of the differential equation for the first-order rate expression for burnup is found to be

$$(9) \qquad \log \frac{U_0^{235}}{U_t^{235}} = \frac{(\alpha_1 + \alpha_2)\,\phi t}{2.303},$$

where

α_1 = fission cross section = 580 barns,
α_2 = capture cross section = 105 barns,
ϕ = neutron flux density = 2.17×10^{14} n/cm^2·sec,
t = irradiation time, sec,

and the slope is

$$(10) \qquad \frac{(\alpha_1 + \alpha_2)\,\phi}{2.303} = 6.4544 \times 10^{-8}.$$

Therefore

$$(11) \qquad \log \frac{U_0^{235}}{U_t^{235}} = 6.4544 \times 10^{-8} t .$$

If a plot is made of Eq. 11, which might be called the theoretical curve, it is possible to compare the experimental results on burnup with the results predicted by theory. In addition, Eq. 11 can be used to check the product of the three constants α_1, α_2, and ϕ. Or, if the $(\alpha_1 + \alpha_2)$ values are assumed to be correct, Eq. 11 can be used as a check on ϕ, the average flux density.

The values of $\alpha_1 = 580$ barns and $\alpha_2 = 105$ barns are rather well established. The value of $\phi = 2.17 \times 10^{14}$ n/cm^2·sec has been tentatively chosen because it gives the best fit to the data based on samples from four test capsules and it is consistent with values determined by other means.

SUMMARY OF SERVICE CHEMICAL ANALYSES

J. C. White A. F. Roemer
C. R. Williams
Analytical Chemistry Division

Sixty-four samples of UF_4 and ten samples of Na_2UF_6 (the ARE fuel concentrate) have been analyzed to date. The UF_4 samples were analyzed for uranium only, but complete analyses were made of the fuel concentrates, including determinations of iron, nickel, and chromium. The cooperative program with the Laboratory Division of Y-12 was continued on the determination of uranium, as described in the previous report.[4] The relative difference between laboratories on the determination of uranium in the fuel concentrate was 0.04%, and the difference on the UF_4 analyses was 0.18%. The larger difference was attributed mainly to the heterogeneity of the samples of UF_4, which contained black particles and comparatively large hard pieces of a lighter hue than that of the powdered salt; the large pieces were probably UO_2F_2. Uranium metal that was considered to be 99.94% pure was used as the standard. The relative standard error of 12 samples at a 95% confidence level was 0.02%.

Some specimens of Inconel metal used in corrosion tests were analyzed for uranium, zirconium, sodium, and fluoride and the major constituents nickel, iron, and chromium. Traces of sodium carbonate in the range of 0.05% and less in sodium hydroxide were determined.

The major portion of the work was concerned with the analysis of fluoride fuel mixtures. A decided increase occurred in the number of samples received during the quarter. A total of 1,378 samples was received, 1,201 were reported, and 11,034 determinations were made (Table 10.1).

[4] J. C. White *et al.*, *ANP Quar. Prog. Rep. June 10, 1953*, ORNL-1609, p. 121.

TABLE 10.1. SUMMARY OF SERVICE ANALYSES REPORTED

	NUMBER OF SAMPLES	NUMBER OF DETERMINATIONS
Experimental Engineering	596	6,411
Corrosion Studies	271	3,247
Reactor Chemistry	256	1,000
ARE Fluid Circuit	74	328
Heat Transfer and Physical Properties Studies	4	48
	1,201	11,034

Part III

SHIELDING RESEARCH

INTRODUCTION AND SUMMARY

E. P. Blizard, Physics Division

The spectra of gamma rays and of fast neutrons from the Bulk Shielding Reactor were measured (sec. 11). The neutron spectrometer was altered for this work to improve the sensitivity at some sacrifice in energy resolution; however, thicker water shields can now be studied. The gamma-ray spectrum of the Bulk Shielding Reactor without a shield showed the usual broad peaks at 2.2 Mev that are due to water capture and those at 7 to 8 Mev that are due to capture in aluminum and possibly other materials. The fast-neutron leakage spectra of the BSR were obtained from proton-recoil measurements for the water-reflected reactor loading No. 22. Data obtained with the nuclear plate camera have been used to extend the spectrometer data from 1.3 Mev down to 0.5 Mev. A measurement of the angular distribution of fast neutrons in water was also made. At neutron energies above 8 Mev, the intensities at various angles converge.

The Lid Tank Facility was used for studying the slant penetration of fission neutrons in a hydrogenous shield (sec. 12). This problem is encountered in specifying a crew-shield side-wall thickness. The uncertainty lay in the importance of the short circuiting of the shield by scattering into paths more nearly normal to the shield surfaces. For the shield thicknesses which have been measured, it appears that this short circuiting is unimportant, and the attenuation is characteristic of the slant thickness. This is not unexpected for the thin shields (< 7.5 cm) which have been measured to date. There is as yet nothing conclusive about the behavior of very thick shields with slant-incidence radiation, but it will be advantageous if the slant thickness gives the attenuation for the thicker shields.

The Lid Tank Facility was also used for air duct experiments designed to give some insight into the interaction between parallel ducts (sec. 12). Data from three sources, (1) a duct consisting of three sections, 22 in. long and $3\frac{15}{16}$ in. in diameter, joined at angles of 45 deg, (2) a second duct consisting of two such sections, and (3) the slant penetration experiments, were put into the Simon-Clifford formula, and the formula was solved for the reflection factor. The values obtained were in agreement with those obtained from previous thermal measurements and thus constituted an important confirmation of those measurements. It is now felt that engineering designs based on the Simon-Clifford theory are on a sound basis when applied to a single duct, especially when the dimensions are similar to those studied. Since it was observed that the peak values of dose measured at the end of the 19-duct array were a factor of approximately 10 higher than those observed with the single duct, a study of interference between adjacent ducts has been started. Tests are planned to give more quantitative information on the interaction between neighboring ducts and possibly to improve the formula for streaming through ducts.

The effective removal cross section work for which the Lid Tank Facility is used was continued, and old experiments have been reviewed. A new set of values is reported (sec. 12).

A summary of the first 50 Lid Tank experiments is being prepared (sec. 12). The summary will be useful because of the large role the Lid Tank Facility has had in the development of various reactor shield designs and because of the constant need for reference to the data.

The steel structure of the Tower Shielding Facility has been erected, and the ground structures are approximately 75% complete (sec. 13). The optimistic date for completion of the facility is January 15.

Some basic shielding research which is not reported here because it is supported by another activity is, nevertheless, of vital interest to ANP. The development of a scintillating fast-neutron spectrometer has received considerable impetus recently with the growth of a few clear europium-activated lithium iodide crystals. These crystals have been tested on the ORNL Van de Graaff generator and show encouraging energy sensitivity, but an anomalous lack of energy resolution indicates that the development is far from complete. Most of the theoretical shielding work has been reported in the Physics Division Semiannual Report with the exception of a few problems which originated in the experimental program (sec. 14). An unusual calculation has been made of the visible light to be expected from divided-shield aircraft. An estimate of the neutron reflection coefficient for water was obtained by using a simple model with a coincident source and a nondirectional receiver located above the water surface.

11. BULK SHIELDING REACTOR

R. G. Cochran
F. C. Maienschein

J. D. Flynn
M. P. Haydon
K. M. Henry
J. L. Hull
H. E. Hungerford
E. B. Johnson
T. A. Love
G. M. McCammon

Physics Division

During this quarter, the main effort at the Bulk Shielding Facility was directed toward obtaining neutron and gamma-ray spectroscopic data. The gamma-ray leakage spectrum of the Bulk Shielding Reactor has been measured because it is typical of the spectrum of gamma radiation incident upon a shield.

In addition, considerable fast-neutron spectral data were obtained on the present loading for the water-moderated reactor. The measurement of the energy spectrum of neutrons attenuated by various thicknesses of water was repeated and extended to a 50-cm distance from the face of the reactor. A measurement of the angular distribution of fast neutrons in water has been made, and the attenuated neutron spectrum through a shield mockup was measured.

SPECTRUM OF GAMMA RAYS EMITTED BY THE BSR[1]

Results of measurements of the gamma-ray energy spectra and angular distributions through lead and water were published previously.[2] In the following, the results of measurements of the gamma-ray spectrum of the Bulk Shielding Reactor without a shield are presented. These measurements may be considered as an extension of the earlier work.

The measurement of the spectrum from the unshielded reactor was necessarily delayed until the BSR was loaded with "cold" fuel elements, that is, elements which had not been used when the reactor power was higher than 3 watts. The low power level of the reactor was dictated by the counting-rate limitation of the spectrometer. With the reactor "hot," the power level from fission-product activity alone would have been too great.

For this particular experiment, a 6 by 5 fuel element arrangement was used in an unreflected reactor. The total power and the power distribution were determined with gold foils in the usual manner.

Spectrometer Arrangement. One end of an air-filled aluminum tube was placed against the face of the reactor, and the tube extended to the three-crystal gamma-ray spectrometer[3] (Fig. 11.1). For the first run, the air tube was only 5 in. long and was surrounded by a 5-in. thickness of lead which shielded the spectrometer proper from gamma radiation from other parts of the reactor. The results of this run showed that the neutron-induced background was so high as to make a meaningful interpretation of the data impractical.

In a second run, a 40-in. air column surrounded by water, except for the 5-in. thickness of lead at the end next to the spectrometer, served as a collimator. The additional water shielding reduced the neutron level sufficiently for the neutron-induced background to be negligibly small. The total background was measured by plugging the collimator within the spectrometer with lead. It was also found that the background from reactor fission products was small.

Results. The absolute photon (gamma-ray) flux obtained is plotted as a function of photon energy in Fig. 11.2. The flux values were determined from the known sensitivity of the spectrometer[3] and from the solid angle defined by the collimator shown in Fig. 11.1. Since the water surrounding the aluminum tube was not very effective in preventing gamma rays from entering the sides of the air column, the spectrum shown in Fig. 11.2 is too large by a small fraction, perhaps 20%.

[1] F. Maienschein and T. A. Love, *Spectrum of Gamma Rays Emitted by the Bulk Shielding Reactor*, ORNL CF 53-10-16 (to be published).

[2] F. C. Maienschein, *Gamma-Ray Spectral Measurements with the Divided Shield Mockup*, Part I, ORNL CF 52-3-1 (Mar. 3, 1952); Part II, ORNL CF 52-7-71 (July 8, 1952); Part III, ORNL CF 52-8-38 (Aug. 8, 1952); and T. A. Love, Part IV, ORNL CF 52-11-124 (Nov. 17, 1952).

[3] F. C. Maienschein, *Multiple-Crystal Gamma-Ray Spectrometer*, ORNL-1142 (July 3, 1952).

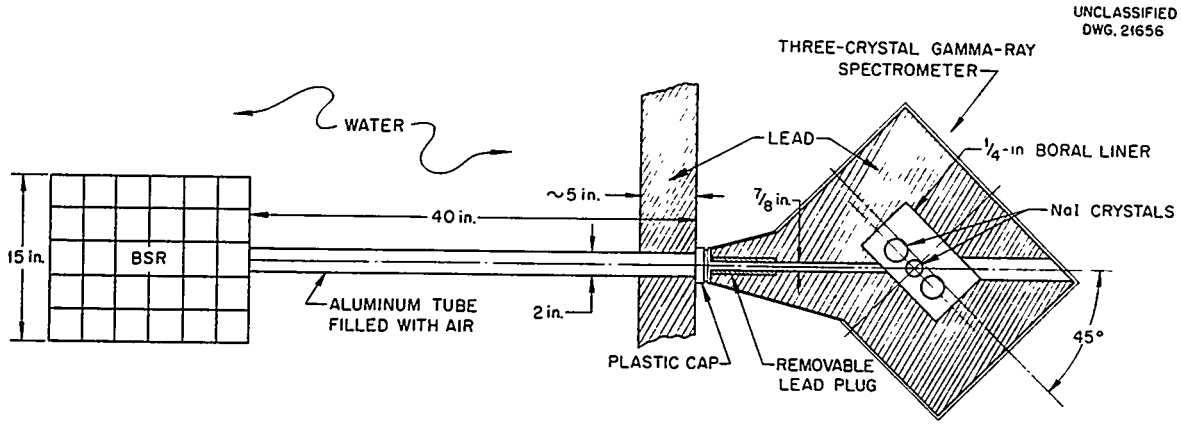

Fig. 11.1. Experimental Arrangement for Measurement of Bulk Shielding Reactor Gamma-Ray Spectrum.

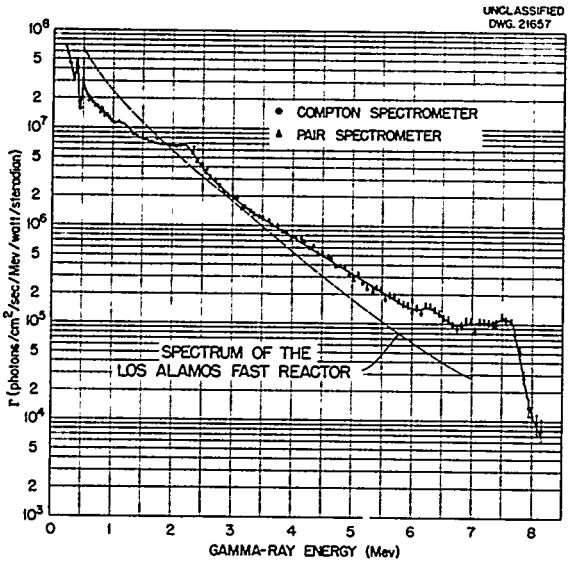

Fig. 11.2. Spectrum of Gamma Rays from the Bulk Shielding Reactor.

The spectrum shape shows the usual broad peaks at 2.2 Mev that are due to water capture and those at 7 to 8 Mev that are due to capture in aluminum and possibly other materials. The cause of the 0.4-Mev peak, which appears to be real, has not been found. The 0.49-Mev peak, however, may well be due to gamma rays from the 0.478-Mev level in the Li^7 formed by neutron capture in the boron liner of the spectrometer.

The smooth curve in Fig. 11.2 represents the spectral shape (not intensity) obtained by Motz[4] with a Compton-recoil magnetic spectrometer looking at a U^{235} slug in the center of the Los Alamos water boiler and one at the active core of the fast reactor. The curves cannot be expected to correspond closely because of the differences in neutron-capture gamma-ray sources and because the low resolution of the spectrometer used by Motz would smooth out any structure present. The general similarity in slopes, however, is interesting.

FAST-NEUTRON LEAKAGE SPECTRA OF THE BSR

The neutron spectrum of the BSR obtained with the reactor surrounded by cans of beryllium oxide as a reflector[5] was reported previously. For the data reported here, the previous spectral measurements were repeated and additional measurements were made; however, a water-reflected reactor (loading No. 22) was used.[6]

The measurements were made with the BSF proton-recoil fast-neutron spectrometer.[7] Except for the spectrum at the face of the reactor, the spectral measurements in water out to 30 cm from the fuel[8] are in agreement with the previous measurements. The spectrum at the face of the reactor

[4] J. W. Motz, *Phys. Rev.* 86, 753 (1952).

[5] R. G. Cochran and K. M. Henry, *Fast Neutron Spectrum of the Bulk Shielding Reactor*, Part I, ORNL CF 53-5-105 (to be published).

[6] R. G. Cochran *et al.*, *ANP Quar. Prog. Rep. Sept. 10, 1953*, ORNL-1609, Fig. 11.1, p. 127.

[7] R. G. Cochran and K. M. Henry, *A Proton Recoil Type Fast-Neutron Spectrometer*, ORNL-1479 (Apr. 2, 1953).

[8] R. G. Cochran and K. M. Henry, *Fast Neutron Spectrum of the Bulk Shielding Reactor*, Part II, ORNL CF 53-11-45 (to be published).

is shown in Fig. 11.3. In addition to the proton-recoil measurements, data obtained with the nuclear plate camera[9] have been used to extend the spectrometer data from 1.3 Mev down to 0.5 Mev.

Measurements were also made out to 50 cm from the reactor. The spectrum measured at 50 cm is shown in Fig. 11.4; the statistics on these data are quite poor, since the neutron intensity was approximately at the limit of sensitivity of the spectrometer.

An attempt was also made to measure the spectrum of neutrons emerging from the side of an aircraft divided-shield mockup.[10] The mockup consisted of a slab of lead 4¾ in. thick placed 16 in. from the reactor. The shield therefore extended out through the water to a position 113 cm from the reactor. Unfortunately, the neutron spectrometer was not sufficiently sensitive to detect neutrons at 113 cm; however, a spectral measurement was made at 70 cm, but the statistics (Fig. 11.5) were rather poor.

A measurement of the angular distribution of the fast neutrons in water was made during the quarter.[11] The experimental setup for this measurement is shown in Fig. 11.6, and the spectra vs. angle data are plotted in Fig. 11.7. At neutron energies above 8 Mev, the intensities at the various angles converge. This effect is probably due to neutrons which bypass part or all of the collimator. A distance greater than 10 cm from the reactor would be more desirable for this measurement, but then it would be difficult to obtain sufficient intensity. Figure 11.8 shows the variation of flux with direction for each of several neutron energies.

[9] M. P. Haydon, E. B. Johnson, and J. L. Meem, *Measurement of the Fast Neutron Spectrum of the Bulk Shielding Reactor Using Nuclear Plates*, ORNL CF 53-8-146 (to be published).

[10] *Report of the ANP Shielding Board for the Aircraft Nuclear Propulsion Program*, ANP-53 (Oct. 16, 1950).

[11] R. G. Cochran and K. M. Henry, *Angular Distribution of Fast Neutrons in Water*, ORNL CF 53-11-46 (to be published).

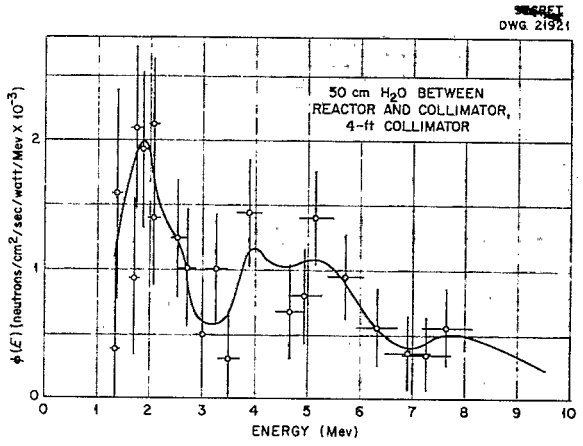

Fig. 11.4. Neutron Spectrum 50 cm from the BSR.

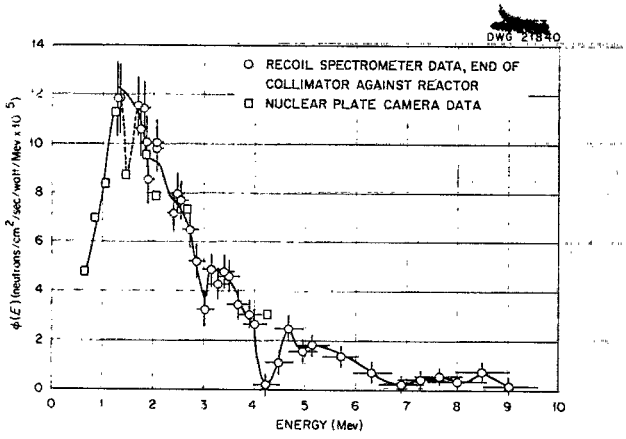

Fig. 11.3. Neutron Spectrum at the Face of the BSR.

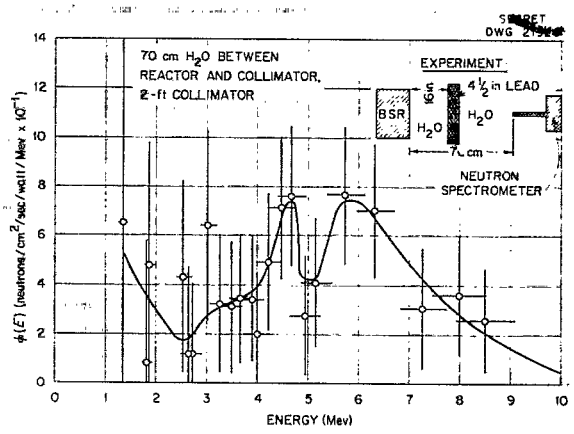

Fig. 11.5. Neutron Spectrum 70 cm from BSR.

DWG. 22199

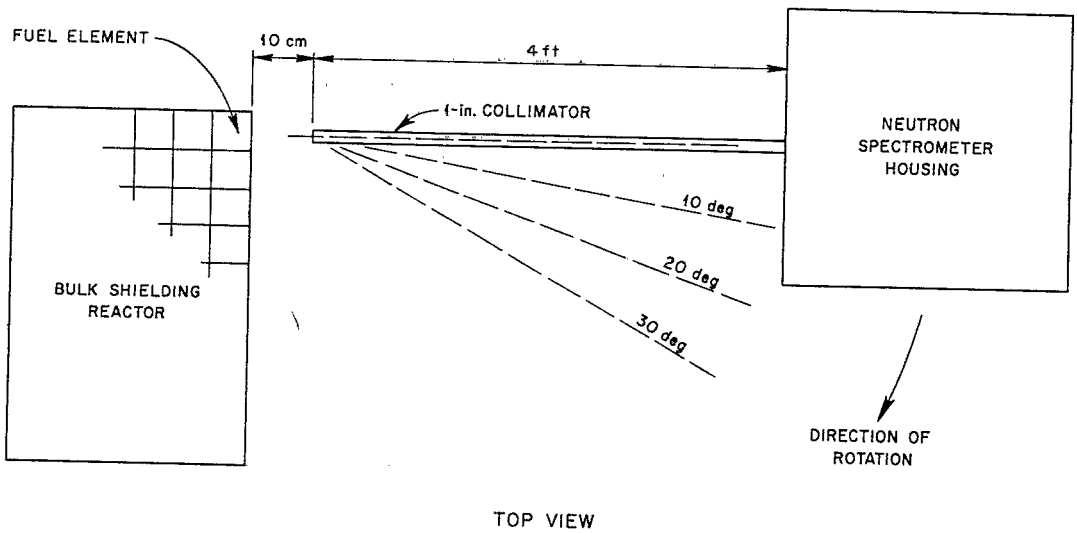

Fig. 11.6. Experimental Arrangement for Measurement of Angular Distribution of Neutrons from BSR in Water.

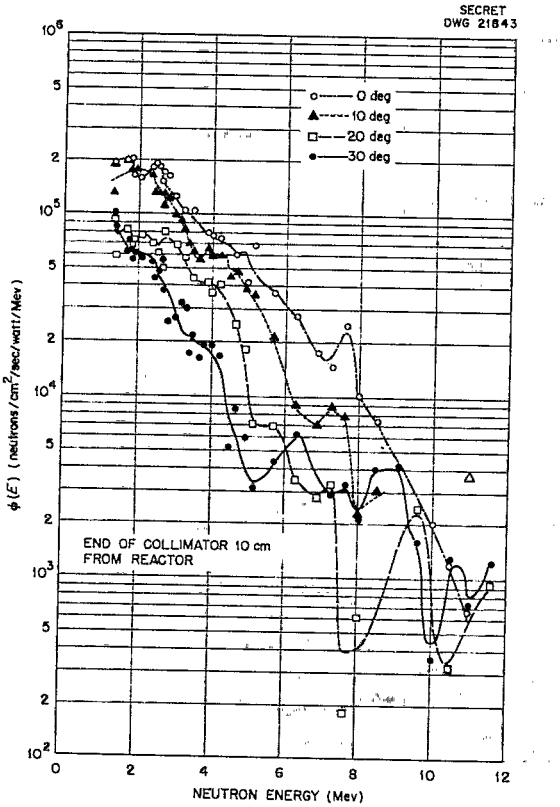

Fig. 11.7. Angular Distribution of Neutrons from BSR in Water.

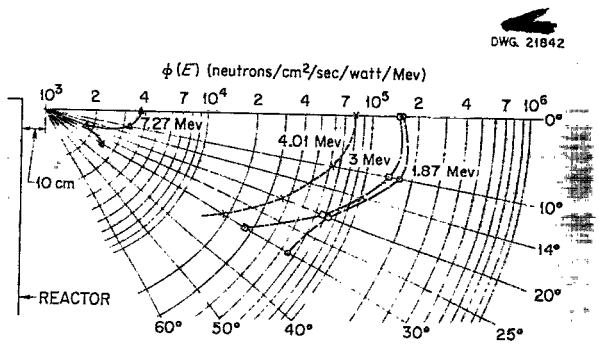

Fig. 11.8. Energy Angular Distribution of Neutrons from BSR in Water.

12. LID TANK FACILITY

C. L. Storrs
GE-ANP

G. T. Chapman D. K. Trubey
J. M. Miller F. N. Watson
Physics Division

Tentative results of a preliminary experiment performed at the Lid Tank indicate that most of the air-scattered neutrons that penetrate an aircraft crew shield follow the slant path. In another experiment, the study of neutron streaming through air ducts was resumed; data from the initial experiments have presented an important confirmation of the Simon-Clifford theory. A re-evaluation of all measurements for the determination of removal cross sections has improved some of the values. Reference to Lid Tank neutron and gamma data is facilitated by a recent survey of the first 50 experiments.

Approval has been received for the use of enriched uranium for a new Lid Tank source plate, and a design has been developed which will make possible a far more accurate power calibration. The source plate, as well as its appurtenant power-measuring equipment, is at present being constructed in the ORNL Research Shops. It is planned to install the source plate in January.

SLANT PENETRATION OF NEUTRONS THROUGH WATER

A preliminary experiment has been performed to determine the slant penetration of fission neutrons through water. An air-filled aluminum duct, 40 in. long and 2 in. in diameter, was used as a collimated "point" source of fast neutrons, and the fast-neutron dose was determined in the water around the end. The duct was tilted from the normal to the source plate to reduce background of fast neutrons from the ORNL Graphite Reactor. Since the fast neutrons are collimated in the outward direction, if not reduced they would overshadow the fission-plate neutrons which are, of course, isotropic. The data, plotted as isodoses around the duct, are shown in Fig. 12.1.

By integrating the dose along planes through the radiation field, the dose penetrating different thicknesses of water at various angles was determined (Fig. 12.2). This information must be regarded as tentative until the dose determinations have been repeated with more care, but the results obtained so far indicate that most of the dose comes from neutrons that penetrate the shield along the slant path. This indication is similar to that obtained for gamma rays for comparable attenuations.[1]

The observed relaxation lengths range from 4.9 to 6.3 cm. As would be expected, these values are smaller than those obtained with thick shields, since a fission spectrum was used as a source and the shields were quite thin.

[1] F. S. Kirn, R. J. Kennedy, and H. O. Wyckoff, *Oblique Attenuation of Gamma-Rays from Cobalt-60 and Cesium-137 in Polyethylene, Concrete and Lead*, NBS-2125 (Dec. 23, 1952).

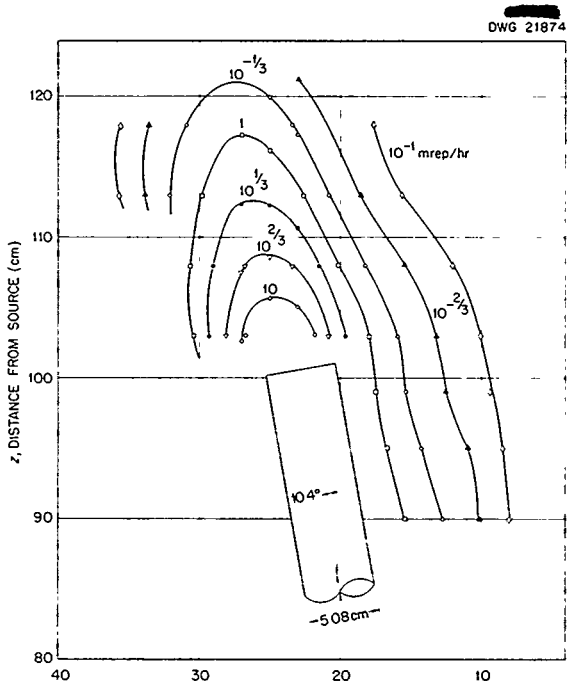

Fig. 12.1. Fast-Neutron Dose Distribution Off the End of a Duct 101.6 cm Long by 5.08 cm in Diameter.

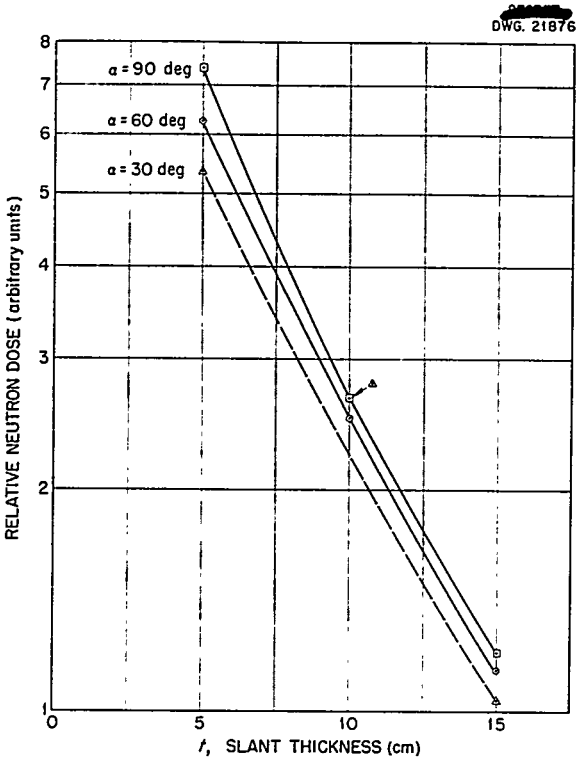

Fig. 12.2. Slant Penetration of Neutrons in Water.

To determine the total air-scattered dose in a divided shield, it is necessary to integrate over all angles. Such an integration would presumably give a straight-through relaxation length comparable to that observed in the BSR air-scattering experiment.[2] It would be desirable to extend the measurements to greater thicknesses of water and to harden the spectrum by putting water between the source and the duct entrance. Intensity problems limit the extent to which this can be accomplished, however.

AIR DUCT TESTS

The use of the Lid Tank Facility for the study of neutron streaming through air ducts has been resumed with emphasis on fast-neutron measurements. A flow-type dosimeter with somewhat greater sensitivity than that available heretofore was used to determine the dose around the ends of several ducts. One of these ducts was taken from the 19-duct array studied a year ago.[3] It had three sections, 22 in. long and $3\frac{15}{16}$ in. in diameter, joined at angles of 45 degrees. A second duct consisted of two such sections. The slant penetration experiment described in the preceding subsection provided a third measurement.

Putting the data from these three measurements into the Simon-Clifford formula[4] and solving for the reflection factor, α, gave values of 1.0 and 0.9, respectively, for the first and second bends. These values are in agreement with the value of about 1 obtained from the previous thermal measurements[5] made in water at a distance of 30 cm from the ends of the ducts (thus the emergent flux was filtered and was representative of the hard neutrons that determine the dose), and they constitute an important confirmation of those measurements. The value of 1 has been assumed in recent direct-cycle design studies. It is now felt that engineering designs based on the Simon-Clifford theory are on a sound basis when applied to a single duct, especially when the dimensions are similar to those studied.

Since it was observed that the peak values of dose measured at the end of the 19-duct array were a factor of approximately 10 higher than those observed with the single duct, a study of interference between adjacent ducts was indicated. This study has been started, with a single section and a three-section duct being used. In the first configuration, one of the possible streaming paths was reproduced in the array by placing the short duct parallel to the first section of the long duct and $12\frac{1}{2}$ in. from it. In this position, it lined up, approximately, with the last section. The result was an increase by a factor of 4.5 in the dose at the end of the long duct.

The short duct was then moved to a position that was again parallel to the first section but considerably closer (6 in.) and above it in a different plane so that there was no direct streaming path. The data (which must be considered tentative) showed no increase in the peak dose beyond the long duct but did show a broadening of the emergent neutron beam. The results obtained from these experiments are shown in Fig. 12.3.

[2] H. E. Hungerford, *The Skyshine Experiments at the Bulk Shielding Facility*, ORNL-1611 (to be published).

[3] J. D. Flynn and C. L. Storrs, *Radiation Measurements Around an Array of Cylindrical Ducts*, ORNL CF-52-12-187 (Dec. 15, 1952).

[4] A. Simon and C. E. Clifford, *The Attenuation of Neutrons by Air Ducts in Shields*, ORNL-1217 (Nov. 11, 1952).

[5] C. E. Clifford, private communication.

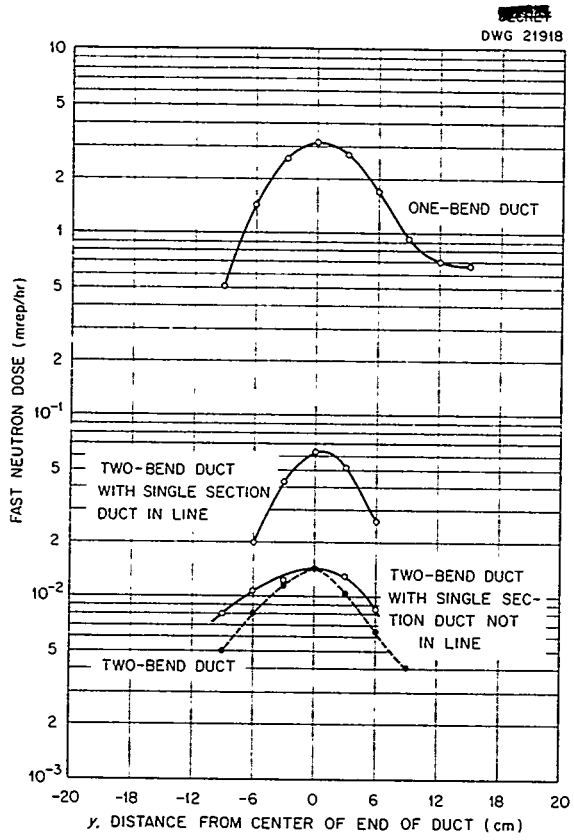

Fig. 12.3. Fast-Neutron Dose Beyond Various Configurations of Ducts with 45-deg Bends.

Further tests are planned to give more quantitative information on the interaction between neighboring ducts and possibly to improve the formula for streaming through ducts.

REMOVAL CROSS SECTIONS

The measurement of the effective fast-neutron removal cross section of C_7F_{16} has been repeated with the use of 15 in. of the liquid instead of 28 in. as in the previous measurement.[6] Despite this large difference in thickness, the measured values of the molecular removal cross section agreed to within 5%, which is within the experimental error, and thus they provide an interesting check on the validity of the geometrical corrections that were made. The revised value for carbon, 0.80 barn/atom instead of 0.84 barn/atom, when used with the current C_7F_{16} measurements, gives a removal cross section of 1.31 barns/atom for fluorine as compared with the value of 1.36 barns/atom reported in the previous report.

A re-examination of all the Lid Tank measurements for the determination of removal cross sections has improved some of the values. A summary of the presently accepted values obtained from direct measurements is given in Table 12.1. Additional values based on the direct measurements are given in Table 12.2.

TABLE 12.1. EFFECTIVE FAST-NEUTRON REMOVAL CROSS SECTION VALUES OBTAINED FROM LID TANK DIRECT MEASUREMENTS

MATERIAL	σ_R
Al	1.31 barns/atom
Be	1.05
Bi	3.43
C	0.80
Cu	2.08
Fe	1.95
Ni	1.85
W	2.6 + 0.2
C_7F_{16}	26.6 barns/molecule
C_2F_3Cl	6.50
B_4C	4.26
H_2O*	(2.90)
D_2O*	(2.78)

*Neither hydrogen nor deuterium has, properly, an effective removal cross section, since the total cross section is not nearly constant in the high-energy region. Rough values have been obtained for H_2O and D_2O based on 140-cm shields. These are reported in parentheses.

TABLE 12.2. EFFECTIVE FAST-NEUTRON REMOVAL CROSS SECTIONS BASED ON LID TANK DIRECT MEASUREMENTS

MATERIAL	σ_R (barns/atom)
B	0.87
D*	(0.92)
F	1.31
H*	(0.98)
O	0.94

*Cf., footnote to Table 12.1.

[6] C. L. Storrs *et al.*, *ANP Quar. Prog. Rep. Sept. 10, 1953*, ORNL-1609, p. 145-148.

SURVEY OF LID TANK EXPERIMENTS

Shielding experimentation at the ORNL Lid Tank Facility began in June 1949, and since that time approximately 60 major experiments have been performed. In view of the large role this facility has had in the development of various reactor shield designs and because of the constant need for reference to the data, it was felt that the experimental results should be compiled in one publication. Accordingly, a summary of the first 50 Lid Tank experiments will soon be presented by E. L. Czapek.[7,8]

As described in several previous reports, the Lid Tank Facility consists of a large water tank adjacent to an opening in the concrete shield of the ORNL Graphite Reactor (Fig. 12.4). A converter plate of uranium covers the opening between the water tank and the reactor shield. This plate absorbs most of the incident thermal neutrons emerging from the reactor and causes fission, which, in turn, produces the known uranium spectrum of neutrons, as well as gamma rays of various energies. Shielding samples are inserted in the tank, and the transmitted radiation is measured behind the shield. The geometry of the Lid Tank permits the use of very large samples, which, in turn, help to reduce uncertainties due to boundary conditions. The water in the tank protects personnel from radiation and allows easy positioning of test samples.

The Lid Tank Facility was built to test both compositions and geometries of shields. With the resulting experimental data, difficult attenuation problems could be quickly solved and shield thicknesses could be predicted (to within an accuracy of

[7]ORSORT student from Electric Boat Division of General Dynamics Corporation.

[8]E. L. Czapek, *General Survey of Lid Tank Experiments 1 Through 50*, ORNL-1636 (to be published).

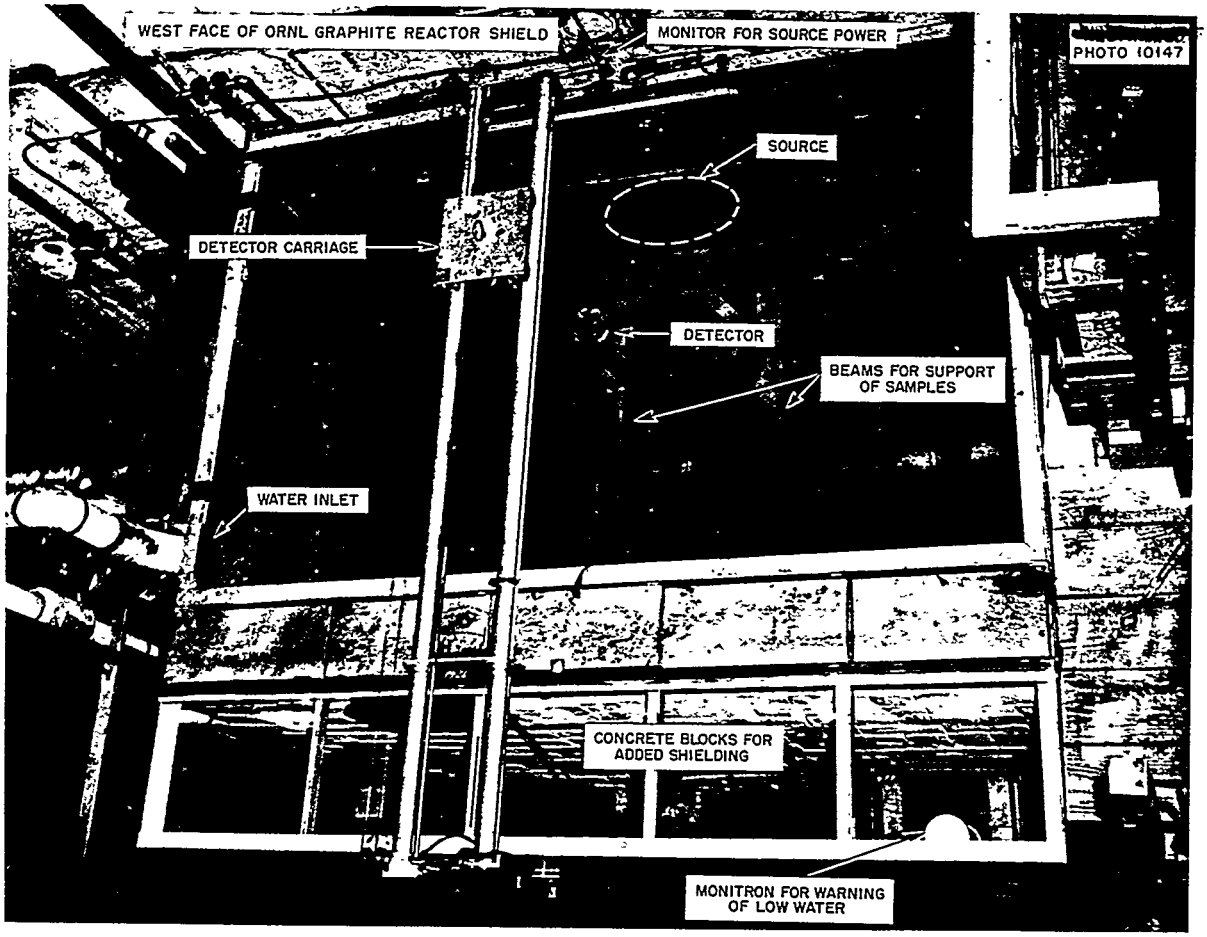

Fig. 12.4. View of Lid Tank Facility from Above.

±5%) without having to rely too much on a knowledge of the attenuation processes.

Experimentation at this facility has primarily been limited to investigations of the "unit shield" in which all material that functions primarily as shielding is located around the reactor. All the experiments covered in the survey can be grouped as follows:

1. Water Shield (experiments 1, 4, 10, 13)
2. Preliminary Investigations[9] (experiments 2, 3, 5, 6, 8, 10)
   a. Lead-water shield
   b. Iron-water shield
3. Boron Carbide Shields (experiments 11, 12)
4. Thermal Shields[9] (experiments 10, 20, 36)
   a. Lead-water shield
   b. Iron-water shield
5. Shield Mockups (experiments 7, 14, 15, 16, 17, 18, 29, 45)
   a. Submarine Thermal Reactor
   b. Submarine Intermediate Reactor
   c. Reflector-Moderated Reactor (ANP)
6. Shield Optimizations (experiments 9, 13, 24)
   a. Two-component shield of lead and borated water
   b. Suppression of capture gammas in lead-water shield
   c. Optimum position of a lead-iron gamma shield in relation to pressure shell
7. Shield Penetrations (experiments 19, 21, 22, 25, 26, 37, and 38 and special experiments)
   a. Cylindrical air ducts with or without bends
   b. Array of cylindrical air ducts with or without bends
   c. Annular duct (specialized mockups simulating GE-R1 air outlet and inlet sections)
   d. Structural members in shields (streaming effects)
   e. Instrument plug (modification in shield to improve control instrumentation)
8. Removal Cross Sections (experiments 23, 30, 31, 32, 33, 34, 35, 39, 40, 41, 42, 43, 46, 47, 49, 50)
9. Special Investigations
   a. Effects of boration of water (experiment 10)
   b. Effects of water and air gaps in shields (experiment 48)
   c. Induced radioactivity outside an air duct (experiment 27)
   d. Activation expected in a coolant (sodium) at various locations in a boron carbide shield (experiment 10)
   e. Gamma scattering around submarine bulkhead (sodium source) (special experiment)

The situation at present in regard to unit shields or reactor parts of divided shields appears to be that the basic mechanisms are understood and that, except for the very simplest problems, shield mockups are essential, although the effects of small changes in design can be quite well predicted. The Lid Tank method of mockup testing is highly developed, and large amounts of data can be collected in relatively short times.

[9] A small amount of boron was present in a majority of these shield mockups.

13. TOWER SHIELDING FACILITY

C. E. Clifford
T. V. Blosser L. B. Holland
Physics Division

The steel structure of the Tower Shielding Facility has been erected (Fig. 13.1), and the ground structures are approximately 75% complete. The underground building for the reactor controls and for personnel will be available for occupancy by December 10; access to the control area of the building was authorized in November.

The mechanical components of the reactor have been constructed and are now being assembled, and the reactor tank has been received. Construction of the crew-compartment tank is nearing completion. The last hoist is scheduled for delivery by January 1, 1954.

The optimistic date for completion of the facility is January 15, after which there will be a one-month period for critical experiments and shakedown operation. This will be followed by differential shielding measurements in the reactor and the crew-compartment water tanks.

A mockup of a GE air-cooled reactor shield design is scheduled for delivery by March 15 by the General Electric Company, and for testing in conjunction with this, a crew-shield mockup will be supplied by ORNL.

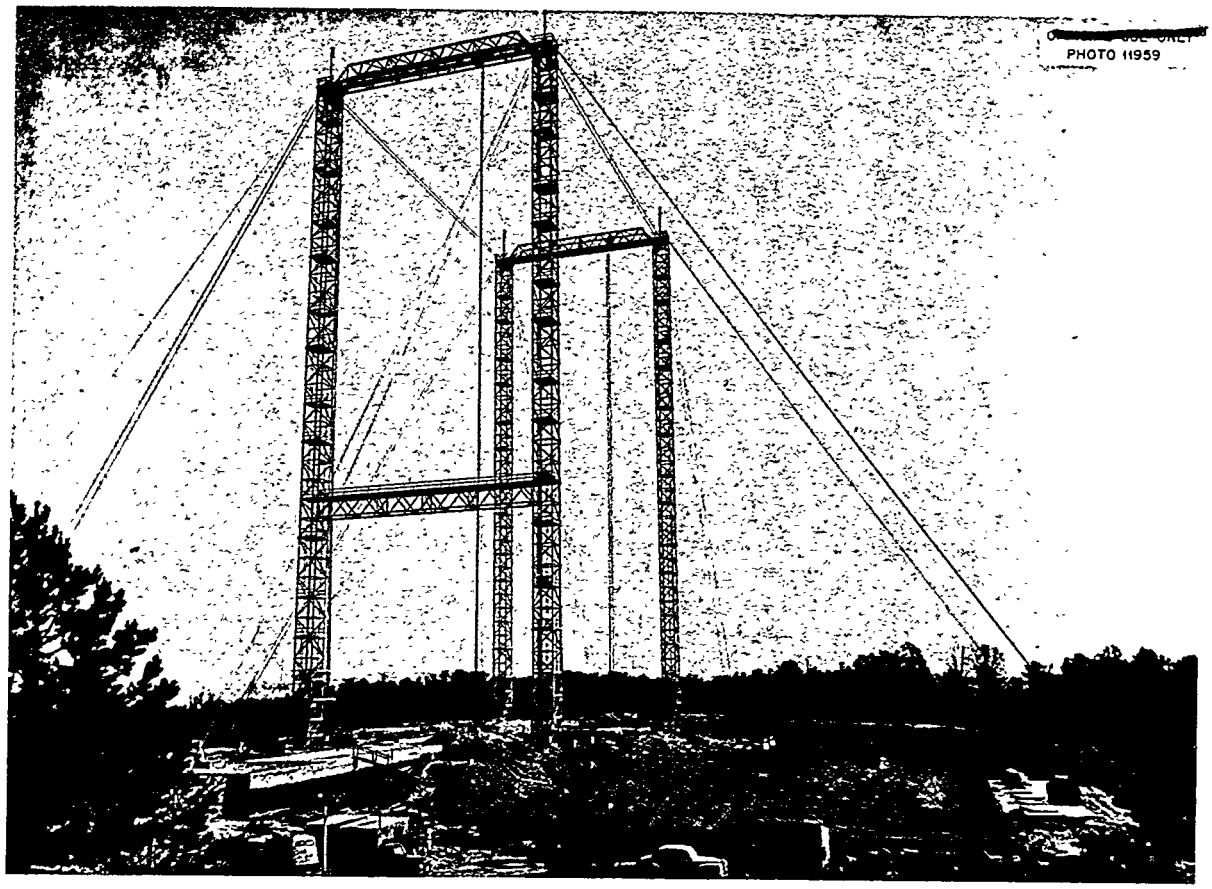

Fig. 13.1. Tower Shielding Facility, November 13, 1953.

14. SHIELDING ANALYSIS

E. P. Blizard M. K. Hullings
J. E. Faulkner F. H. Murray
Physics Division
H. E. Stern
Consolidated Vultee Aircraft Corporation

Much of the shielding analysis work for this quarter was reported in the Physics Division Semiannual Report[1] and is not repeated here. The work reported in the Division report included two treatments of geometrical transformations with methods of estimating reactor leakage. In addition, some calculational methods for obtaining neutron attenuation were presented. On comparison of the calculated attenuations with measured attenuations, it was possible to derive "effective removal cross sections" that when compared with other measurements showed reasonable agreement. In addition, gamma-ray absorption coefficients which have been measured for some elements have been used to interpolate the coefficients for other elements.

The visible light from an aircraft nuclear power plant has been estimated, and the calculations will be compared with measurements made on the BSR. The measurements of visible light are made in air and are not to be confused with the Cerenkov radiation (blue glow) which is so obvious in water. An estimate of neutron albedo was obtained to supply a simple model for ground and structure scattering problems.

VISIBLE LIGHT FROM A NUCLEAR POWER PLANT

The results of some experiments carried out at Los Alamos on the visible light from a polonium source[2] have been used in obtaining an estimate of the ionizing radiation that would have to be present around the aircraft reactor shield to just make it visible. If the airplane were approximately 200 ft from the observer, the ionizing radiation near the shield would have to be about 5×10^6 r/hr. If the airplane were very far from the observer, say 50,000 ft, the ionizing radiation would have to be about 10^9 r/hr. These estimates will be compared with measurements made on the BSR.

NEUTRON REFLECTION COEFFICIENT FOR WATER

An estimate of the neutron reflection coefficient for water has been obtained by using a simple model with a coincident source and a nondirectional receiver located above the water surface. If isotropic oxygen scatter and attenuation governed by the removal cross sections are assumed, the reflected flux F at height h for source strength N_0 is

$$F = \frac{N_0}{48\pi h^2}\left(\frac{\Sigma_{\text{scatter}}}{\Sigma_{\text{removal}}}\right).$$

The albedo approach gives

$$F = \frac{N_0 \alpha}{10\pi h^2}$$

for a re-emission distribution between isotropic and cosine, where α is the reflection coefficient. A value of $\alpha = 0.085$ is thus obtained which is in fair agreement with the experimental value of 0.08.

[1] E. P. Blizard *et al.*, *Phys. Div. Semiann. Prog. Rep. Sept. 10, 1953*, ORNL-1630 (in press).

[2] J. G. Hoffman, *Radiation Doses in the Pajarito Accident of May 21, 1946*, LA-687 (May 26, 1948).

Part IV

APPENDIXES

15. LIST OF REPORTS ISSUED DURING THE QUARTER

REPORT NO.	TITLE OF REPORT	AUTHOR(s)	DATE ISSUED
	I. Aircraft Reactor Experiment		
CF 53-9-15	Experimental Procedure on the ARE (Preliminary)	J. L. Meem	9-3-53
CF 53-9-53	Supplement to ARE Hazards Summary Report (ORNL-1407)	E. S. Bettis W. B. Cottrell	9-25-53
CF 53-10-62	ARE Fuel Recovery	F. N. Browder	10-5-53
CF 53-11-95	Report and Recommendations of Second ARE Cleaning Committee	G. A. Cristy L. A. Mann F. F. Blankenship G. M. Adamson	11-10-53
CF 53-12-9	ARE Design Data	W. B. Cottrell	to be issued
ORNL-1650	Stress Analysis of the ARE	R. L. Maxwell J. W. Walker	to be issued
	II. Experimental Engineering		
CF 53-9-32	ANP Experimental Engineering Quarterly Status Report	H. W. Savage	9-2-53
CF 53-9-102	Design Data and Proposed Test Schedule for Sodium-to-Air Radiators	H. J. Stumpf	9-8-53
CF 53-9-180	LITR Fluoride Fuel Test Loop	O. Sisman	9-25-53
CF 53-10-208	A Flat Plate Heat Exchanger for Reactor System Uses	R. W. Bussard	10-26-53
	III. Critical Experiments		
CF 53-9-19	Static Analysis of the ARE Criticality Experiment	C. B. Mills	9-1-53
ORNL-1615	Critical Experiments on Reactor	D. Callihan R. C. Keen	10-22-53
ORNL-1634	Preliminary Critical Assembly for the Aircraft Reactor Experiment	D. Callihan D. Scott	10-28-53
	IV. Shielding		
CF 53-5-239	Nuclear Dose Measurements on the Divided Shield Mockup at the Bulk Shielding Facility	H. E. Hungerford	5-20-53
CF 53-9-4	Lid Tank Shielding Test of the Reflector-Moderated Reactor	F. N. Watson	9-30-53
CF 53-9-16	Minimum Shield Weight Penalty for Air Ducts	E. P. Blizard	9-2-53
CF 53-8-146	Measurement of the Fast Neutron Spectrum of the Bulk Shielding Reactor Using Nuclear Plates	M. P. Haydon E. B. Johnson J. L. Meem	to be issued
CF 53-9-161	An Estimate of the Neutron Reflection Coefficient, Using the Concept of Removal Cross-Section	H. E. Stern	9-29-53
CF 53-10-1	Computation of Effective Removal Cross-Section Measured at ORNL Lid Tank	L. S. Abbott	no date
CF 53-10-16	Spectrum of Gamma Rays Emitted by the Bulk Shielding Reactor	F. C. Maienschein T. A. Love	to be issued
CF 53-11-2	The Shielding of Nuclear Radiations, Lecture I	E. P. Blizard	11-2-53
CF 53-11-45	Fast Neutron Spectrum of the Bulk Shielding Reactor, Part II	R. G. Cochran K. M. Henry	to be issued

REPORT NO.	TITLE OF REPORT	AUTHOR(s)	DATE ISSUED
	IV. Shielding (continued)		
CF 53-11-46	Angular Distribution of Fast Neutrons in Water	R. G. Cochran K. M. Henry	to be issued
CF 53-11-53	The Effect of Some Liquid Metal Ducts on Reactor Shields	M. K. Hullings	to be issued
CF 53-11-54	Gamma-Ray Spectrum of the Bulk Shielding Reactor	F. C. Maienschein	11-8-53
ORNL-1636	General Survey of Lid Tank Experiments 1 Through 50	E. L. Czapek	to be issued
	V. Metallurgy		
CF 53-10-117	Examination of LF Pump Loop	G. M. Adamson R. S. Crouse	10-6-53
CF 53-10-228	Metallographic Examination of Second Heat Exchanger from Bi-Fluid Pump Loop	G. M. Adamson R. S. Crouse	10-27-53
ORNL-1565	Scaling of Columbium in Air	H. Inouye	9-1-53
ORNL-1633	Fabrication of Spherical Particles	A. Levy	11-12-53
ORNL-1647	Interim Report on Static Liquid Metal Corrosion	W. D. Manly	to be issued
MM-147	Third Progress Report on the Flash Welding of Molybdenum. Part I – Temperature Distribution During the Flashing Cycle	Rensselaer Polytechnic Institute	9-30-53
MM-151	Redrawing of Special High Purity Inconel	Superior Tube Company	10-7-53
MM-157	Progress Report and Final Report to Carbide and Carbon Chemicals Company	Commonwealth Engineering Co. of Ohio	11-9-53
	VI. Chemistry		
CF 53-10-78	Fused Salt Compositions	C. J. Barton	10-9-53
ORNL-1626	Determination of Zirconium by the Chloranilic Acid Method	O. Menis	10-28-53
UA-PR-13	Progress Report for the Period April 1, 1953 Through June 30, 1953	University of Arkansas	7-30-53
BMI-852	Vapor Pressures of Beryllium Fluoride and Zirconium Fluoride	Battelle Memorial Institute	7-13-53
BMI-864	Potential Liquid Fuels for Nuclear Power Reactors	Battelle Memorial Institute	9-8-53
	VII. Heat Transfer and Physical Properties		
CF 53-8-106	Preliminary Results on Flinak Heat Transfer	H. W. Hoffman	8-18-53
CF 53-8-217	Preliminary Measurements of the Density and Viscosity of Fluoride Mixture No. 44	S. I. Cohen T. N. Jones	8-31-53
CF 53-9-98	Heat Capacity of Two Samples of 310 Stainless Steel and of a Brazing Compound	W. D. Powers G. C. Blalock	9-18-53
CF 53-10-86	Preliminary Measurement of the Density and Viscosity of Composition 43 (Na_2UF_6)	S. I. Cohen T. N. Jones	10-14-53
CF 53-11-128	Heat Capacity of Fuel Composition No. 33	W. D. Powers G. C. Blalock	11-23-53
ORNL-1624	The Nature of the Flow of Ordinary Fluids in a Thermal Convection Harp	D. C. Hamilton F. E. Lynch L. D. Palmer	to be issued

REPORT NO.	TITLE OF REPORT	AUTHOR(s)	DATE ISSUED
	VIII. Miscellaneous		
CF 53-9-8	The Small Hydrogen Moderated Reactor	C. B. Mills	9-2-53
CF 53-11-147	Directory of Active ANP Research Projects at ORNL	W. B. Cottrell	11-27-53
ORNL-1609	Aircraft Nuclear Propulsion Project Quarterly Progress Report for Period Ending September 10, 1953	W. B. Cottrell	10-15-53
ORNL-1632	ORNL Control Computer	J. J. Stone	to be issued

---

16. DIRECTORY OF ACTIVE ANP RESEARCH PROJECTS AT ORNL

NOVEMBER 27, 1953

I. REACTOR THEORY AND COMPONENT DESIGN		
A. Aircraft Reactor Design		
1. Reflector-Moderated Reactor Studies	9704-1	Fraas, LaVerne, Bussard
2. Fluid-Fuel Flow Studies	9704-1	Stumpf
3. Gamma Heating of the Moderator	9704-1	Bussard, Wilner
4. Design Consultants	9704-1	Wislicenus, JHU; Haines; Chambers, U.T.
B. ARE Design		
1. Building	1000	Browning
2. Electrical Power Circuits	1000	Walker
3. Fluid Circuit Design	7503	Cristy
4. Fuel Recovery Equipment	9201-3	Estabrook
C. ARE Installation		
1. Plumbing	7503	Webster *et al.*
2. Electrical System	7503	Packard *et al.*
3. Controls	7503	Epler, Mann
4. Instrumentation	7503	Affel
5. Expeditors	7503	Perrin, West
6. Coordinators	7503	Wischhusen, Watts
D. ARE Operations		
1. Staff	7503	Bettis, Meem, Cristy, Mann
2. Day Shift	7503	Whitman, Cottrell, Grindell, Croley, Schafer, Williams, Southern
3. Night Shift	7503	Affel, Perrin, Cobb, Leslie, Allen, Reid, Morrison, Huntley, Gregory, Addison
E. ARE Control Studies		
1. High-Temperature Fission Chamber	4500	Hanauer

2. Control System Design	4500	Epler, Ruble, Mann, Green, Hanauer
3. Control Studies on Simulator	4500	Oakes, Mann, Green
F. Reactor Physics		
1. Analysis of Critical Experiments	9704-1	Mills
2. Kinetics of Circulating-Fuel Reactors	9704-1	Ergen
3. Computation Techniques for ARE-Type Reactors	9704-1	Bengston, Ergen
4. Statics of Reflector-Moderated Reactors	9704-1	LaVerne, Burtnette, Spencer
5. Machine Computations	4500	Charpie, Coveyou, Sangren, Gerberich, Given, Atta
6. Interpretation of Critical Experiments	4500	Prohammer
G. Critical Experiments		
1. Reflector-Moderated Reactor Critical Assembly	9213	Callihan, Williams, Scott, Zimmerman, Lynn, Noakes (P&W)
2. Preliminary Assembly of Supercritical-Water Reactor (Pratt & Whitney)	9213	Callihan *et al.*
3. Preliminary Assembly of AC-1 (General Electric ANPP)	9213	Callihan *et al.*
H. Bearing, Seal, and Pump Development		
1. Mechanical Pumps for High-Temperature Fluids	9201-3	McDonald, Cobb, Huntley, Grindell
2. High-Temperature Seals for Rotary Shafts	9201-3	McDonald, Tunnell, Smith, Mason
3. Pump for Hydroxide Systems	BMI[1]	Dayton
4. Seals for Hydroxide Systems	BMI	Simons, Allen
5. Bearings for High-Temperature Application	9201-3	Stair, Tunnell, Smith, Mason
6. Canned-Rotor Pump Development	9201-3	McDonald, Stair, MacPherson, Grindell
7. Materials Compatibility in Molten Salts at High Temperatures	9201-3	Stair, Tunnell, Smith, Mason
I. Valve Development		
1. Valves for High-Temperature Fluid Systems	9201-3	McDonald
2. Valves for Hydroxide Systems	BMI	Simons, Allen *et al.*
J. Heat Exchanger and Radiator Development		
1. High-Temperature Fluid-to-Air Heat Exchange Test	9201-3	MacPherson, Salmon, Fraas, Stumpf
2. Fluoride-to-Liquid Metal Heat Exchange Test	9201-3	Salmon, Fraas, MacPherson, Bussard
3. Heat Exchanger Fabrication	9201-3	Petersen, Fraas
4. Boeing Turbojet with Sodium Radiator	9201-3	Fraas, Coughlen
5. Radiator and Heat Exchanger Design Studies	9201-3	Fraas, Stumpf, Bailey, U.T.
6. Full-Scale Test Facilities	9201-3	Coughlen
K. Fluid Dynamics of Liquid Fuel Reactors		
1. Pump-Core Shell Component Test	9201-3	Bussard, Gallagher
L. Instrumentation		
1. Pressure-Measuring Devices for High-Temperature Fluid Systems	9201-3	McDonald, Smith

[1]Battelle Memorial Institute.

2. Flow-Measuring Devices for High-Temperature Fluid Systems	9201-3	McDonald, Smith
3. High-Temperature Strain Gage	BLH[2]	
4. High-Temperature Calibration Gage	Cornell	
II. MATERIALS RESEARCH		
A. Phase Equilibrium Research		
1. Thermal Analysis of Fluoride Systems	9733-2	Insley, Barton, Bratcher, Truitt
2. Thermal Analysis of Chloride Systems	9733-2	Barton, Boyer
3. Phase Equilibria Among Fluorides by Quenching	9733-2	Insley, Moore, Metcalf, Truitt, Thoma, White
4. Equilibria in BeF_2-Bearing Systems by Quenching	Mound	Heik, Orban, Joy *et al.*
5. Differential Thermal Analysis of Fluorides	9733-2	Bolomey
6. Differential Thermal Analysis of BeF_2-Bearing Systems	Mound	Orban *et al.*
7. Equilibria Among Fluorides and Chlorides by Filtration	9733-2	Barton, Sheil
8. X-Ray Diffraction Studies of Complex Fluorides	4500	Bredig
	9766	Agron, Thoma
9. Phase Equilibria in Hydride-Hydroxide Systems	MHI[3]	Banus *et al.*
10. Phase Equilibria Consultant		McVay, U. Ala.
B. Chemistry of High-Temperature Liquids		
1. Equilibrium Pressures in Hydroxide-Metal Systems	U. Ark.	Smothers *et al.*
2. Equilibrium Pressures in Hydroxide-Metal Systems	9766	Knox, Kertesz
3. Equilibrium Pressure in Hydride-Halide Systems	Mound	Otto, Orban
4. Chemical Reactions in Fused Salts	9733-3	Overholser, Redman, Weaver
5. Solutions of Metals in Fused Salts	4500	Bredig, Johnson, Bronstein
6. Thermagalvanic Potentials in Fused Systems	9733-3	Cuneo
7. Decomposition Potentials in Fused Systems	9733-3	Topol, Overholser
8. Spectrophotometric Investigations of Fused Salts	9733-3	Friedmon, Blankenship
9. Preparation, Phase Behavior, and Reactions of UF_3	9733-2	Barton, Truitt, Blood, Watson, Blankenship
10. Rates of Reduction in Fused Salts	9733-2	Blood, Watson, Blankenship
11. Solubility of Uranium Compounds in Hydride-Hydroxide Systems	BMI[1]	Simons *et al.*
12. Free Energy of Fluorides	9201-3	Mann, Petersen, Cisar
13. Preparation of Pure Hydroxides	9733-3	Ketchen, Overholser
14. Preparation of Complex Fluorides	9733-3	Sturm, Overholser
15. Chemistry Consultants		Gibb, Tufts U. Hill, Duke U. Carter, Carter Lab.
C. Fluoride Production and Handling		
1. Pilot-Scale Production of Fluorides	9928	Nessle, Blakely, Eorgan, Croft, Didlake
2. Laboratory-Scale Fluoride Production	9733-2	Blood, Watson, Blankenship, Boody

[2]Baldwin-Lima Hamilton Corp.

[3]Metal Hydrides, Inc.

3. Preparation of Materials for Radiation Damage	9733-2	Blankenship, Boody
4. ARE Fuel Carrier Production	9201-3	Nessle, Eorgan, Blood, Thoma
5. ARE Fuel Concentrate Production	9212	Nessle, Eorgan
6. ARE Filling Operation	7503	Nessle, Eorgan
7. Sampling Techniques	9201-3	Mann, Blakely
8. Sampling Techniques	9766	Kertesz, Meadows, Didlake
D. ARE Fuel Reprocessing		
1. Fuel Recovery Process Development	4500	Ferguson, Cathers
2. Fuel Recovery Design Studies	4500	Goeller, Browder, Ruch
3. Unit Operations Studies	4505	Eister, Nurmi, Kackenmester
4. Pilot Plant Operations	3019	Jackson
	3505	Lewis, Matherne
5. Fuel Recovery Process Studies	7503	Nessle, Blakely, Croft, Eorgan
E. Corrosion by Liquid Metals		
1. Static Corrosion Tests	2000	Vreeland, Hoffman
2. Dynamic Corrosion Research in Convection Loops	9201-3	Adamson
3. Effect of Crystal Orientation on Corrosion	2000	Smith, Cathcart, Bridges
4. Effect of Carbides	2000	Vreeland, Hoffman
5. Dynamic Corrosion by Liquid Lead	2000	Cathcart
	9201-3	Adamson
6. Diffusion of Molten Media into Solid Metals	2000	Smith, Cathcart
7. Structures of Liquids by Diffraction Techniques	2000	Smith
8. Protective Coatings for Corrosion Resistance	2000	Vreeland, Hoffman
9. Corrosion Inhibitor Studies	9201-3	Adamson
10. Handling of Liquid Metal Samples	9201-3	Ketchen
11. Compatibility of Cermets in Liquid Metals	2000	Vreeland, Hoffman
12. Mechanism of Isothermal Mass Transfer	2000	Cathcart
F. Corrosion by Fluorides		
1. Static Corrosion of Metals	2000	Vreeland, Hoffman
2. Static Corrosion of Metals	9766	Kertesz, Buttram, Smith, Meadows
3. Corrosion in Small-Scale Dynamic Systems	2000	Vreeland, Trotter, Nicholson, Hoffman
4. Dynamic Corrosion Tests in Thermal-Convection Loops	9201-3	Adamson
5. Corrosion of Nonmetallic Materials	9766	Kertesz, Buttram, Meadows, Smith
6. Forced-Convection Corrosion Loop	9201-3	Salmon
G. Corrosion by Hydroxides		
1. Static Corrosion of Metals and Alloys	2000	Vreeland, Smith, Hoffman, Cathcart
2. Physical Chemistry of Hydroxide Corrosion	2000	Smith, Steidlitz, Boston
3. Static and Dynamic Corrosion	9766	Kertesz, Buttram, Smith
4. Static and Dynamic Corrosion by Hydroxides	BMI[1]	Simons *et al.*
H. Physical Properties of Materials		
1. Density of Liquids	9204-1	Jones, Cohen
2. Viscosity of Liquids	9204-1	Jones, Cohen
3. Thermal Conductivity of Solids	9204-1	Powers, Burnett
4. Thermal Conductivity of Liquids	9204-1	Claiborne, Powers, Burnett
5. Specific Heat of Solids and Liquids	9204-1	Powers, Blalock
6. Electrical Conductivity of Fluorides	9204-1	Greene
7. Surface Tension of Fluorides	9204-1	Cohen, Jones
8. Viscosity of Fused Salt Systems	9766	Kertesz, Knox

9. Vapor Pressure of Fluoride Systems	9733-2	Moore
10. Vapor Pressure of BeF_2-Bearing Systems	Mound	Orban *et al.*
11. Vapor Pressure of Fluid Systems	BMI[1]	Simons *et al.*
I. Heat Transfer		
1. Heat Transfer Coefficients of Fluoride and Hydroxide Systems	9204-1	Hoffman, Lones
2. Heat and Momentum Transfer in Convection Loops	9204-1	Hamilton, Palmer, Lynch
3. Heat Transfer in Circulating-Fuel Systems	9204-1	Poppendiek, Winn, Palmer
4. Forced Convection in Annuli	9204-1	Bradfute
5. Transient Boiling Research	9204-1	Rosenthal
6. Fluid-Flow Phenomena	9204-1	Palmer, Winn, Poppendiek
J. Metals Fabrication Methods		
1. Welding and Brazing Techniques for ARE	2000	Manly, Housley, Slaughter, Patriarca
2. Molybdenum Welding Research	BMI[1]	Russell
3. Molybdenum Welding Research	MIT[4]	Wulff
4. Resistance Welding for Molybdenum and Clad Metals	RPI[5]	Nippes, Savage
5. Welds in the Presence of Various Corrosion Media	2000	Vreeland, Slaughter Hoffman, Patriarca
6. Nondestructive Testing of Tube-to-Header Welds	2000	Slaughter, Patriarca
7. Basic Evaluation of Welds Metal Deposits in Thick Plates	2000	Slaughter, Gray, Patriarca
8. Development of High-Temperature Brazing Alloys	2000	Patriarca, Slaughter
9. Evaluation of the High-Temperature Brazing Alloys	2000	Slaughter, Patriarca
10. Application of Resistance-Welding Methods to ANP Materials	2000	Slaughter, Patriarca
K. New Metals Development		
1. Molybdenum and Columbium Alloy Studies	2000	Inouye
2. Heat Treatment of Alloys for Special Projects	2000	Bomar, Coobs
3. Alloy Development of New Container Materials	2000	Inouye
L. Solid Fuel Element Fabrication		
1. Solid Fuel Element Fabrication	2000	Bomar, Coobs
2. Diffusion-Corrosion in Solid Fuel Elements	2000	Bomar, Coobs
3. Determination of the Engineering Properties of Solid Fuel Elements	2000	Bomar, Coobs, Woods, Oliver, Douglas
4. Inspection Methods for Fuel Elements	2000	Bomar
M. Ceramics and Metals Ceramics		
1. Metal Cladding for Beryllium Oxide	Gerity Mich.	Graaf
2. Hot Pressing of Bearing Materials	2000	Bomar, Coobs
3. High-Temperature Firing of Uranium Oxide to Produce Selective Powder Sizes	2000	Bomar, Coobs
4. Development of Cermets for Reactor Components	9766	Johnson, Shevlin, Taylor, Hamner
5. Ceramic Coatings for ANP Radiators	9766	White, Griffin

[4]Massachusetts Institute of Technology.
[5]Rensselaer Polytechnic Institute.

6. Ceramic Valve Parts for Liquid Metals and Fluorides	9766	Shevlin, Johnson, Taylor
7. Ceramic Reflector	9766	Johnson, White
8. Ceramic Coatings for Shielding	9766	White, Shevlin
	U. Ala.	Handwerk
9. Fabrication of BeO Shapes	9766	Doney
10. Corrosion of Ceramics	9766	Curtis, Kertesz, Buttram
	2000	Vreeland, Hoffman
11. High-Density Graphite	9766	Doney, Corey
N. Strength of Materials		
1. Creep Tests in Fluoride Fuels	9201-3	Adamson
2. Creep and Stress Rupture Tests of Metals in Vacuum Gaseous Environments and in Fluid Media	2000	Oliver, Douglas
3. High-Temperature Cyclic Tensile Tests	2000	Oliver, Woods
4. Tube-Burst Tests	2000	Oliver, Douglas
5. Relaxation Tests of Reactor Materials	2000	Oliver *et al.*
6. Evaluation Testing for Other Development Groups	2000	Oliver, Woods, Reber
7. Fatigue Testing of Reactor Materials	2000	Oliver, Reber
O. Radiation Damage		
1. Fused Salt Fuels Irradiation in LITR	3550	Keilholtz, Morgan
	3005	Robertson, Webster, Robinson, Willis, Browning
2. Fused Salt Fuels Irradiation in MTR	3550	Keilholtz *et al.*
3. LITR Dynamic Corrosion Loop	3550	Keilholtz *et al.*
4. Fluoride Fuel Loops for LITR and MTR	3550	Sisman, Baumann,
	3005	Carroll, Brundage, Blacksher, Parkinson, Ellis, Olson, Morgan
5. Engineering Properties of Irradiated Metals	3550	Sisman, Parkinson, Baumann Carroll
6. Neutron Spectrum of LITR	3005	Trice, Sisman
7. Creep of Metals and Stress Corrosion in ORNL Graphite Reactor and LITR	3025	Wilson, Zukas
	3001	Davis
8. Creep of Metals in MTR	3025	Wilson, Hinkle
9. Thermal Conductivity of Metals in ORNL Graphite Reactor and LITR	3001	Cohen, Templeton
	3005	Weeks
10. Remote Metallography for GE-ANP, Pratt & Whitney, and In-Pile Corrosion Tests	3025	Feldman, Richt
	3001	Acton, Schwartz
11. Radiation Damage Consultants		Ruark, U. Ala.
		Smith, Cornell U.
P. Materials Analysis and Inspection Methods		
1. Determination of the Oxidation States of Metallic Corrosion Products	9733-4	White, Manning
2. Determination of Trivalent Uranium in Fuels	9733-4	White, Ross
3. Analysis of Reactor Fuels and Coolants	9733-4	White, Ross, Roemer, Manning
4. Determination of Reducing Power of Fuels and Coolants	9733-4	White, Manning
5. Determination of Oxides in Reactor Fuels	9733-4	White
6. High-Temperature Mass Spectrometry	9735	Baldock, Sites
7. X-Ray Study of Complex Fluorides	3500	Agron, Johnson, Bredig
	9766	Thoma

8. Petrographic Examination of Fuels	9766	McVay, White
9. Chemical Methods of Fluid Handling	9201-3	Mann, Blakely
10. Metallographic Examination	2000	Gray, Krouse, Roeche
11. Identification of Corrosion Products from Dynamic Loops	9733-3 2000	Blankenship Smith, Borie, Dyer
12. Assembly and Interpretation of Corrosion Data from Dynamic Loop Tests	9201-3 2000	Adamson, Blankenship Smith, Vreeland
13. Metallurgical Examination of Engineering Parts	9201-3	Adamson, Gray, Vreeland
14. Identification of Corrosion Products	2000	Yakel
15. Experimental Material Distribution	9766	Kertesz, Meadows, Didlake
III. SHIELDING RESEARCH		
A. Cross-Section Measurements		
1. Effective Removal Cross Sections	3001	Storrs, Trubey, Watson
B. Shielding Measurements		
1. Slant Penetration of Neutrons	3001	Storrs, Chapman
2. Air Duct Tests – Fast Neutrons	3001	Storrs, Miller
3. Unit Shield Optimization	3001	Storrs and crew
4. Mockup Tests for Shield Design	3001	Storrs and crew
5. Divided-Shield Mockup Tests (GE-ANPP)	3010	Cochran and crew
6. Duct Tests (GE-ANPP)	3010	Cochran, Flynn, Hull, Hungerford
7. Gamma Rays from Fission	3010	Maienschein, Love, Cochran, Henry
8. Full-Size Mockup Tests of Aircraft Shields	TSF[6]	Clifford, Blosser, Holland, Watson
9. Design Parameter Studies (Divided Shield)	TSF[6]	Clifford, Blosser, Holland, Watson
C. Shielding Instruments		
1. Gamma-Ray Spectroscopy and Calculations	3010	Maienschein, Love
2. Short-Period Fission-Product Gamma-Ray Spectra	3010 3001	Maienschein Campbell, Love
3. Fast-Neutron Dosimeter	4500	Blosser, Hurst
4. He^3 Counter for Neutron Spectrometry	3010	Cochran, Henry
5. Neutron Spectroscopy – Proportional Counter	3010	Cochran, Henry
6. Neutron Spectroscopy – Photographic Plates	3006	Haydon, Johnson, Cochran
D. Shielding Analysis		
1. Development of New Calculational Methods	4500	Murray
2. Application of Stochastic Methods	4500	Faulkner, Zerby
3. Calculation of Neutron Attenuations	NDA[7]	Goldstein, Aronson, Certaine
4. Calculations of Gamma-Ray Attenuation	NDA[7]	Goldstein, Wilkins
E. Experiments on Shielding Facility Reactors		
1. Miscellaneous Reactor Experiments (Temperature Coefficient, Xenon Poisoning, etc.)	3010	Cochran, Meem, Cole, Johnson, Flynn
2. Bulk Shielding Reactor Power Calibration	3010	Johnson, Cochran

[6]Tower Shielding Facility.

[7]Nuclear Development Associates, Inc.

CHART OF THE TECHNICAL ORGANIZATION AT THE OAK RID

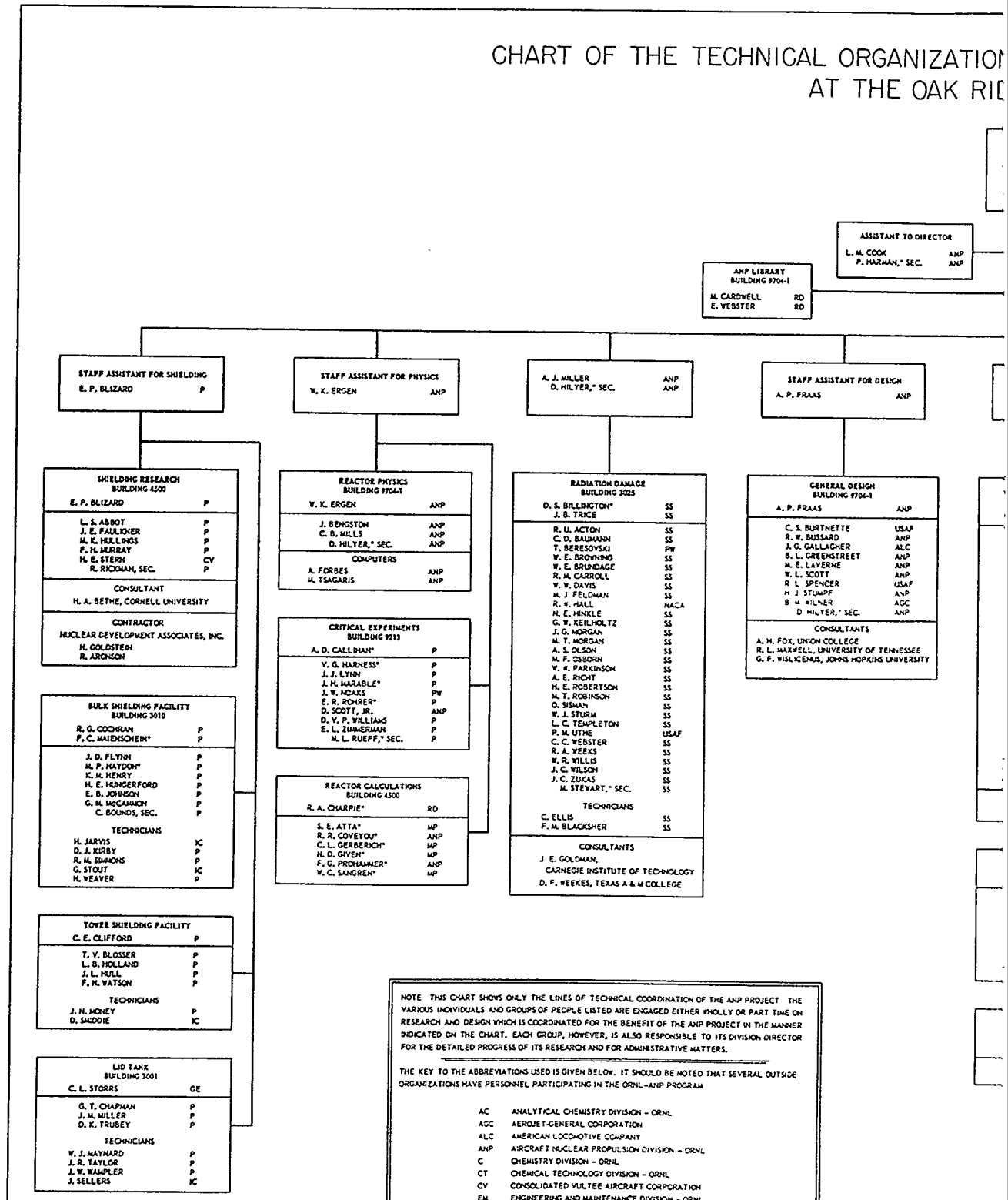

NOTE THIS CHART SHOWS ONLY THE LINES OF TECHNICAL COORDINATION OF THE ANP PROJECT THE VARIOUS INDIVIDUALS AND GROUPS OF PEOPLE LISTED ARE ENGAGED EITHER WHOLLY OR PART TIME ON RESEARCH AND DESIGN WHICH IS COORDINATED FOR THE BENEFIT OF THE ANP PROJECT IN THE MANNER INDICATED ON THE CHART. EACH GROUP, HOWEVER, IS ALSO RESPONSIBLE TO ITS DIVISION DIRECTOR FOR THE DETAILED PROGRESS OF ITS RESEARCH AND FOR ADMINISTRATIVE MATTERS.

THE KEY TO THE ABBREVIATIONS USED IS GIVEN BELOW. IT SHOULD BE NOTED THAT SEVERAL OUTSIDE ORGANIZATIONS HAVE PERSONNEL PARTICIPATING IN THE ORNL–ANP PROGRAM

AC	ANALYTICAL CHEMISTRY DIVISION – ORNL
AGC	AEROJET-GENERAL CORPORATION
ALC	AMERICAN LOCOMOTIVE COMPANY
ANP	AIRCRAFT NUCLEAR PROPULSION DIVISION – ORNL
C	CHEMISTRY DIVISION – ORNL
CT	CHEMICAL TECHNOLOGY DIVISION – ORNL
CV	CONSOLIDATED VULTEE AIRCRAFT CORPORATION
EM	ENGINEERING AND MAINTENANCE DIVISION – ORNL
GE	GENERAL ELECTRIC COMPANY
IC	INSTRUMENTATION AND CONTROLS DIVISION – ORNL
M	METALLURGY DIVISION – ORNL
MC	MATERIALS CHEMISTRY DIVISION – ORNL
MP	MATHEMATICS PANEL – ORNL
NACA	NATIONAL ADVISORY COMMITTEE FOR AERONAUTICS
P	PHYSICS DIVISION – ORNL
PW	PRATT AND WHITNEY AIRCRAFT DIVISION – UAC
RD	RESEARCH DIRECTOR'S DEPARTMENT – ORNL
REE	REACTOR EXPERIMENTAL ENGINEERING DIVISION – ORNL
SI	STABLE ISOTOPES DIVISION – ORNL
SS	SOLID-STATE DIVISION – ORNL
USAF	UNITED STATES AIR FORCE
Y-12	CARBIDE AND CARBON CHEMICALS COMPANY (Y-12 SITE)

*PART TIME

OF THE AIRCRAFT NUCLEAR PROPULSION PROJECT
E NATIONAL LABORATORY

DECEMBER 1, 1953

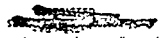

ANP PROJECT DIRECTOR

BRIANT — RD
HILYER * SEC — ANP

ASSISTANT DIRECTOR

MILLER — ANP

TECHNICAL ASSISTANT

W. B. COTTRELL — ANP
A. W. SAVOLAINEN — ANP
J. M. CISAR* — ANP
P. HARMAN, SEC. — ANP

ARE PROJECT ENGINEER

BETTIS* — ANP

R. C. BRIANT — RD

STAFF ASSISTANT FOR METALLURGY

W. D. MANLY — M

STAFF ASSISTANT FOR CHEMISTRY

W. R. GRIMES — MC

ARE OPERATIONS
BUILDING 7503

BETTIS — ANP
L. MEEM — ANP

G. AFFEL — ANP
W. ALLEN — ANP
G. COBB — ANP
B. COTTRELL* — ANP
A. CRISTY — EM
Y. ESTABROOK — ANP
G. GRANDELL — ANP
R. HUNTLEY — ANP
K. LESLIE — ANP
R. MANN* — IC
L. MORRISON — USAF
B. PERRIN — ANP
L. SOUTHERN — ANP
L. WATTS — REE
F. WEST — ANP
D. WHITMAN — ANP
WISHMEIER — EM
P. HARMAN,* SEC — ANP

TECHNICIANS

ADDISON — ANP
CRABTREE — ANP
CROLEY — ANP
GREGORY — ANP
ID — ANP
SCHAFER — ANP
WILLIAMS — ANP

CONSULTANT

H. BUCK, WELL SURVEYS, INC

REACTOR CONTROL
BUILDING 4500

EPLER* — IC

E. COLE* — IC
F. GREEN* — IC
C. GUNDLACH* — IC
H. HANAUER* — IC
R. MANN* — IC
B. RUBLE* — IC
C. OAKES* — IC
S. WALKER* — IC
P. GROOVER, SEC. — IC

FUEL REPROCESSING
BUILDING 4500

CULLER* — CT
R. BRUCE — CT

N. BROWDER — CT
I. CAMERS — CT

EXPERIMENTAL ENGINEERING
BUILDING 9201-3

H. W. SAVAGE — ANP

G. M. ADAMSON — M
J. P. BLAKELY — MC
C. P. COUGHLEN — ANP
J. E. EORGAN — MC
W. C. GEORGE — Y-12
R. HELTON — ANP
E. M. LEES — ANP
R. E. MacPHERSON — ANP
L. A. MANN — ANP
R. N. MASON — EM
W. B. McDONALD — ANP
G. J. NESSLE — MC
W. R. OSBORN — ANP
G. F. PETERSEN — ANP
O. F. SALMON — ANP
P. G. SEXTON — Y-12
P. G. SMITH — ANP
W. C. TUNNELL — ANP
D. R. WARD — ANP
D. ALEXANDER, SEC. — ANP
D. STOREY, REC. CL. — ANP
D. HARRIS, STENO. — ANP

TECHNICIANS

G. D. BRADY — M
G. S. CHILTON — ANP
J. M. COBURN — ANP
C. R. CROFT — MC
J. M. CUNNINGHAM — ANP
J. M. DIDLAKE — MC
F. A. DOSS — ANP
J. R. DUCKWORTH — ANP
F. M. GRIZZELL — ANP
R. A. HAMRICK — ANP
B. L. JOHNSON — ANP
J. W. KINGSLEY — ANP
D. E. McCARTY — ANP
G. E. MILLS — ANP
W. A. REDDEN — ANP
D. E. TOWELL — ANP
R. G. WILEY — ANP

CONSULTANTS

J. F. BAILEY, UNIVERSITY OF TENNESSEE
W. R. CHAMBERS, UNIVERSITY OF TENNESSEE
J. F. HAINES
W. K. STAIR, UNIVERSITY OF TENNESSEE

HEAT TRANSFER AND PHYSICAL PROPERTIES RESEARCH
BUILDING 9204-1

H. F. POPPENDIEK — REE

J. O. BRADFUTE — REE
S. I. COHEN — REE
N. D. GREENE — REE
D. C. HAMILTON — REE
H. W. HOFFMAN — REE
F. E. LYNCH — REE
L. D. PALMER — REE
W. D. POWERS — REE
M. ROSENTHAL — REE
T. SUTTON, SEC. — REE

TECHNICIANS

C. G. BLALOCK — REE
R. M. BURNETT — REE
S. J. CLAIBORNE — REE
T. N. JONES — REE
J. LONES — REE
G. W. WINN — REE

CERAMIC RESEARCH
BUILDING 9766

J. M. WARDE* — M

C. E. CURTIS* — M
L. M. DONEY* — M
S. D. FULKERSON* — M
R. L. HANNER* — M
M. P. HAYDON* — P
J. R. JOHNSON* — M
A. J. TAYLOR* — M
G. D. WHITE* — M
A. HOBBS,* SEC. — M

TECHNICIAN

J. A. GRIFFIN* — M

CONSULTANTS

T. N. McVAY, UNIVERSITY OF ALABAMA
T. S. SHEVLIN, OHIO STATE UNIVERSITY

METALLURGY
BUILDING 2000

W. D. MANLY — M

E. S. BOMAR — M
C. R. BOSTON — M
W. H. BRIDGES — M
J. V. CATHCART — M
J. M. CISAR* — ANP
J. H. COOBS — M
D. A. DOUGLAS — M
E. E. HOFFMAN — M
H. INOUYE — M
R. B. OLIVER — M
P. PATRIARCA — M
K. W. REBER — M
G. M. SLAUGHTER — M
G. P. SMITH — M
M. E. STEIDLITZ — M
D. C. VREELAND — M
J. W. WOODS — M
J. THOMAS, SEC. — M

TECHNICIANS

G. D. BRADY — M
J. T. EAST — M
G. M. GONZALEZ — M
L. L. HALL — M
J. D. HUDSON — M
R. W. JOHNSON — M
V. G. LANE — M
B. McNABB — M
J. E. POPE — M
C. E. SHUBERT — M
L. R. TROTTER — M
C. K. THOMAS — M

METALLOGRAPHY

R. J. GRAY* — M
R. S. CROUSE* — M
T. K. ROCHE* — M
T. M. KEGLEY* — M

TECHNICIANS

M. D. ALLEN* — M
N. M. ATCHLEY* — M
E. R. BOYD* — M
W. H. FARMER* — M
R. L. FITZGERALD* — M
J. C. GOWER* — M
E. P. GRIGGS* — M
R. M. WALLACE* — M
C. E. ZACHARY* — M

CONSULTANTS

N. CABRERA, UNIVERSITY OF VIRGINIA
N. J. GRANT, MASSACHUSETTS INSTITUTE OF TECHNOLOGY
J. L. GREGG, CORNELL UNIVERSITY
E. F. NIPPES, RENSSELAER POLYTECHNIC INSTITUTE
W. F. SAVAGE, RENSSELAER POLYTECHNIC INSTITUTE
E. C. WRIGHT, UNIVERSITY OF ALABAMA

CONTRACTORS

BALDWIN-[illegible]-HAMILTON CORPORATION
F. G. TATNALL AND OTHERS

BATTELLE MEMORIAL INSTITUTE (AEC CONTRACTOR)
T. M. PARKE
H. SALLEY
Z. SCHOFIELD
AND OTHERS

GERITY MICHIGAN COMPANY
G. GRAFF AND OTHERS

MASSACHUSETTS INSTITUTE OF TECHNOLOGY
J. WULFF AND OTHERS

RENSSELAER POLYTECHNIC INSTITUTE
E. F. NIPPES AND OTHERS

SUPERIOR TUBE COMPANY
HUGH COOPER

CHEMISTRY
BUILDING 9733-3

W. R. GRIMES — MC

P. A. AGRON — C
C. J. BARTON — MC
F. F. BLANKENSHIP — MC
C. M. BLOOD — MC
R. A. BOLGMEY — MC
F. P. BOODY — MC
S. A. BOYER — MC
L. M. BRATCHER — MC
D. R. CUNEO — MC
H. A. FRIEDMAN — MC
E. E. KETCHEN — MC
R. P. METCALF — MC
R. E. MOORE — MC
L. G. OVERHOLSER — MC
J. D. REDMAN — MC
R. J. SHEIL — MC
B. J. STURM — MC
R. E. THOMA, JR. — MC
L. E. TOPOL — MC
JACK TRUITT — MC
G. M. WATSON — MC
C. F. WEAVER — MC
D. E. CALDWELL, SEC — MC

CORROSION LABORATORY
BUILDING 9766

F. KERTESZ — MC
H. J. BUTTRAM — MC
F. A. KNOX — MC
R. E. MEADOWS — MC
N. V. SMITH — MC

CONSULTANTS

J. M. CARTER
T. R. P. GIBB, WILLIAMS COLLEGE
O. G. HILL, DUKE UNIVERSITY
H. INSLEY, BUREAU OF STANDARDS
T. N. McVAY, UNIVERSITY OF ALABAMA

CONTRACTORS

BATTELLE MEMORIAL INSTITUTE
J. W. CLEGG
R. W. DAYTON
R. I. JAFFEE
H. A. PRAY
AND OTHERS

CARTER LABORATORIES
J. M. CARTER

METAL HYDRIDES, INC.
M. D. BANUS AND OTHERS

MOUND LABORATORY
J. J. BURBAGE AND OTHERS

UNIVERSITY OF ARKANSAS
W. J. SMOTHERS AND OTHERS

ANALYTICAL CHEMISTRY
BUILDING 9733-4

C. D. SUSANO — AC
B. E. YOUNG,* SEC. — AC

R. L. McCUTCHEN* — AC
J. C. WHITE — AC
E. M. ZARZECKI,* SEC. — AC

BUILDING 9201-2

A. F. ROEMER, JR. — AC
C. R. WILLIAMS — AC
AND OTHERS

CONSULTANT

H. H. WILLARD, UNIVERSITY OF MICHIGAN

SPECTROGRAPHIC ANALYSIS
BUILDING 9734

J. R. McNALLY — SI
J. A. NORRIS* — SI
AND OTHERS

MASS SPECTROMETRY
BUILDING 9735

C. R. BALDOCK* — SI
J. R. SITES — SI